Palmitoylation of BK channels

Owen Jeffries B.Sc. (Hons)

Thesis Presented for the Degree of Doctor of Philosophy

The University of Edinburgh

August 2010

Declaration

The composition of this thesis and work described herein is my own, carried out at the Centre for Integrative Physiology, University of Edinburgh. No part of this thesis has been submitted for any other degree or qualification.

Owen Jeffries

August 2010

Acknowledgements

I'd like to begin by thanking Mike for all his guidance and advice throughout the four years of my PhD and thesis write-up. The countless redrafts, chats, brainstorming sessions and formulation of papers and conference posters have culminated in this piece of work and will no doubt formulate my attitude and character for the rest of my career. Your door was always open, thank you.

I'd like to thank Iain, without whom I would not be the patch clamper I am today .... of course that depends on whether my abilities at the rig are any good, but your teachings and patience to answer questions, discuss theories and new papers really helped to craft my critical and scientific mind, thanks.

To Heather, for I would not be a molecular biologist without her support, always open to incessant questions that befit the ever more complicated techniques in modern day biology, your patience amazes me, thank you.

Thanks to Lie Chen and Lijun Tian for educating me in imaging and biochemical assays, without your support I would not have the range of techniques I have acquired in my time in Edinburgh that has made these stories so complete.

Outside of the lab, I'd like to thank my parents Ray and Beryl and little sis Sian, for supporting me throughout my time here, even if just for a bit of a chat, the ocassional envelope filled with chocolate in the post to keep me going or the cash to buy some new fancy bike bits to keep me on the road. I'd also like to thank Nanny Magee for her kind thoughts and my Nanny Jeffries for reading my first scientific paper cover to cover, every single word, without even understanding it.

I'd thank my bike(s) .. but perhaps that's inappropriate...

And finally to Fozia, without whom, im not sure I could have done this, your emotional support, your strength and kindness not to mention your monthly care packages of foz food in my freezer to keep me going... a way to a man's heart and all that..... really means that a little piece of this work belongs to you too.

Abstract

Palmitoylation is a post-translational modification that has been implicated in the control of multiple proteins, including ion channels. S-Palmitoylation is a lipophilic modification that involves the attachment of palmitate through a thioester linkage to a cysteine residue in a target protein. By increasing the hydrophobicity of the target region, palmitoylation can promote membrane targeting. Here, palmitoylation is shown to play an important role in regulating large conductance calcium- and voltage- activated (BK) potassium channels.

The STREX splice variant of the BK channel contains a 58 amino acid insert at the splice site C2 within the intracellular C-terminal RCK1-RCK2 linker that confers increased calcium sensitivity to the channel and determines PKA inhibition of channel activity. The cysteine rich STREX domain was predicted to be palmitoylated, and using an imaging assay STREX was shown to act as a membrane targeting domain through palmitoylation of a di-cysteine motif (C645:C645). A membrane potential assay and electrophysiological analysis demonstrates that palmitoylation at the C645:C646 site in STREX is important in mediating the increased calcium sensitive properties inherent to the STREX channel. Palmitoylation is also shown to modulate PKA channel inhibition.

The stability of palmitoylation can often be reliant on the local environment within the protein. Generally in most proteins; lipidated regions, basic domains or transmembrane domains are found adjacent to a palmitoylation site. In STREX, a polybasic domain composed of 11 basic residues just upstream from the C645:C646 palmitoylation site, functions to control the palmitoylation status of the STREX insert. A site directed mutagenesis approach to disrupt the polybasic domain revealed an important role in controlling membrane targeting of the STREX C-terminus, mediating the increased calcium sensitivity inherent to STREX channels and controlling the palmitoylation status of the C645:C646 palmitoylation site using multiple techniques involving electrophysiology, fluorescent imaging and biochemical assays. Further to this, using imaging to examine the membrane association of fluorescently tagged C-terminal proteins, phosphorylation is shown to

function as a physiological electrostatic switch to regulate the polybasic region in controlling palmitoylation of the STREX insert.

Finally, an additional palmitoylation site that is constitutively expressed in all BK channels was identified to be located in the S0-S1 linker (C53:C54:C56). Mutation of the C53:C54:C56 palmitoylation site in the S0-S1 linker was shown to abolish all palmitoylation in BK channels that did not contain the STREX insert. Palmitoylation allows the S0-S1 linker to associate with the plasma membrane however the mutated de-palmitoylated channels did not affect channel conductance or the calcium/voltage sensitivity of the channel. Palmitoylation of the S0-S1 linker was shown to be a critical determinant of cell surface expression of BK channels, as steady state surface expression levels were reduced by ~55% in the C53:C54:C56 mutant. STREX channels that could not be palmitoylated in the S0-S1 linker also showed decreased surface expression even through STREX insert palmitoylation was unaffected.

Palmitoylation is rapidly emerging as an important post-translational mechanism to control ion channel behaviour. This work reveals that palmitoylation of the BK channel can control channel function of the STREX splice variant channel and can regulate cell surface expression in all other channel variants. Palmitoylation appears to be functionally independent at these two distinct sites expressed within the same channel protein.

Table of contents

Declaration..... ii

Acknowledgements..... iii

Abstract..... iv

List of Figures..... xv

List of Tables..... xix

Chapter 1 – Introduction 1

1.1 The evolution of the ion channel..... 2

1.2 The potassium channel family..... 5

1.2.1 Potassium channels with phenotypic behaviour..... 5

1.2.2 The potassium channel family 5

1.2.3 The identification of a calcium- and voltage- sensitive K^+ current..... 8

1.3 The BK channel..... 9

1.3.1 Characteristics of the BK channel..... 9

1.3.2 The physiological role of the BK channel 10

1.3.3 The BK channel knock-out mouse 11

1.3.4 BK channel pharmacology.....12

1.4 The structural composition of the BK channel 13

1.4.1 The core region 15

1.4.1.1 The voltage sensing domain 15

1.4.1.2 The S0 transmembrane domain 18
1.4.2 The pore region 19
1.4.3 The intracellular C-terminus 23
1.4.3.1 The RCK domains 24
1.4.3.2 The calcium bowl 25
1.4.3.3 The gating ring theory - the S6-RCK1 linker 26
1.4.3.4 The RCK1-RCK2 linker 28
1.4.3.5 The C-terminus, a necessary component? 29
1.5 The 3D structure of the BK channel 30
1.6 The dynamic regulation of BK channels 37
1.6.1 Regulatory β- subunits 37
1.6.2 Alternative splicing – diversifying channel function 39
1.6.2.1 Alternative splicing in the BK channel 41
1.6.2.2 The STREX splice variant 43
1.6.3 Post-translational modifications 46
1.6.3.1 Lipophilic modification of proteins 46
1.6.3.1.1 Palmitoylation 47
1.6.3.1.2 Palmitoyl Acyl Transferases 48
1.6.3.1.3 Palmitoylation - A diverse role in modulating ion channels 48
1.6.3.1.4 Palmitoylation and secondary membrane targeting motifs 49
1.6.4 Polybasic domains 50
1.6.4.1 The electrostatic switch 52
1.6.5 Phosphorylation 52

1.7 Outlining the primary aims of the thesis....53

Chapter 2 – Material & Methods....56

2.1 Molecular Biology Protocols....58

2.1.1 Channel Constructs....58

2.1.2 Standard PCR conditions....58

2.1.3 Site Directed Mutagenesis....60

2.1.4 Design of oligonucleotides for site directed mutagenesis....60

2.1.5 Transformation of chemically competent E.coli....62

2.1.6 PCR screening of bacterial colonies....63

2.1.7 Maxiprep alkaline lysis for plasmid DNA isolation....63

2.1.8 Miniprep alkaline lysis for plasmid DNA isolation....63

2.1.9 Quantitation of DNA....64

2.1.10 Preparation of DNA for sequencing....64

2.1.11 Double Restriction Digest....64

2.1.12 DNA agarose gel electrophoresis & gel purification....65

2.1.13 Ligation of plasmid vector and insert DNA....65

2.2 Mammalian cell culture protocols....66

2.2.1 Cell lines....66

2.2.2 Standard cell culture passage protocol....67

2.2.3 Transfection of cells using Lipofectamine2000....67

2.3 Electrophysiology & Membrane potential assays....68

2.3.1 Electrophysiology....68

2.3.2 Electrophysiological Assays....68
2.3.3 Fluorescent Membrane Potential (FMP) assay....71
2.4 Imaging protocols....72
2.4.1 Fixing and mounting of cells....72
2.4.2 Screening of fluorescently-labelled cells....72
2.4.3 Confocal Imaging of fluorescently-labelled cells....73
2.4.4 Immunofluorescent cell surface labelling....73
2.4.5 Immunofluorescent labelling....74
2.4.6 Quantification of Immunofluorescent labelling....74
2.5 Biochemical assays....75
2.5.1 ^{3}H-palmitic acid incorporation....75
2.5.2 Western Blotting and ^{3}H detection....76
2.6 Prediction Algorithms....76
2.6.1 CSS-palm - palmitoylation prediction....76
2.6.2 BH search – membrane binding prediction....77
2.7 Statistical analysis....78
2.8 Reagents....78

Chaper 3 – Palmitoylation of the STREX insert....80
3.1 Chapter 3 introduction....81
3.1.1 The STREX splice variant of the BK channel....81
3.1.2 Working hypothesis....84
3.1.3 Aims to be addressed in this chapter....84

3.1.3.1 Is STREX a membrane targeting domain? 84
3.1.3.2 Is membrane targeting of STREX palmitoylation-dependant? 84
3.1.3.3 What is the functional significance of palmitoylation? 85
3.1.3.4 Does phosphorylation regulate membrane targeting of STREX? 85
3.2 Results 86
3.2.1 STREX as a membrane targeting domain 86
3.2.2 STREX is a cysteine rich domain 86
3.2.3 Cysteine residues in STREX are predicted to be palmitoylated 87
3.2.4 C645-C646 residues are important for STREX C-terminus association at the plasma membrane 89
3.2.5 Palmitoylation controls the association of C-terminus constructs at the plasma membrane 91
3.2.6 STREX channel activation driven by increased calcium is diminished in C645A:C646A mutant channels 93
3.2.7 Single channel amplitude is unchanged in STREX, C645A:C646A and ZERO channels 96
3.2.8 C-terminal targeting to the plasma membrane mediates STREX channel properties 96
3.2.9 Voltage dependence is unchanged in mutant channels 101
3.2.10 Palmitoylation of the C-terminus is abolished by mutation of the C645:C646 residues in the STREX 101
3.2.11 The PKA phosphorylation motif in STREX mediates membrane targeting of the C-terminus 103
3.2.12 PKA phosphorylation dissociates the STREX C-terminus from the plasma membrane 105
3.3 Discussion 108

3.3.1 STREX insert is a membrane targeting domain 108

3.3.2 Palmitoylation controls membrane association of STREX.....109

3.3.3 Palmitoylation functionally affects STREX channels 109

3.3.4 Can STREX structurally interact with the plasma membrane? 110

3.3.5 Phosphorylation decreases membrane stability 114

3.3.6 How could membrane targeting of the RCK1-RCK2 change the properties of the BK channel 115

3.3.7 Challenges for the future 116

3.3.8 In Summary 116

Chapter 4 – The polybasic domain in STREX 117

4.1 Chapter 4 introduction 118

4.1.1 Polybasic domains.....118

4.1.2 What would the functional role of a polybasic domain be in the STREX channel?.....120

4.1.3 Working Hypothesis.....121

4.1.4 Aims to be addressed in this chapter 121

4.1.4.1 Is the polybasic domain a functional membrane association domain? 121

4.1.4.2 Does the polybasic domain influence channel properties? 121

4.1.4.3 How is palmitoylation of the STREX C-terminal influenced by the polybasic domain? 122

4.1.4.4 Does phosphorylation regulate the function of the polybasic domain? 122

4.1.4.5 What does the polybasic domain interact with? 122

4.2 Results 123

4.2.1 The polybasic domain is an evolutionary conserved region 123

4.2.2 Basic-Hydrophobicity analysis suggests that the polybasic domain could potentially interact with the plasma membrane 123

4.2.3 The polybasic domain is important for associating the STREX C-terminus at the plasma membrane 127

4.2.4 The polybasic domain is functionally important to the STREX channel ..129

4.2.5 Single channel amplitude does not mediate changes in channel activity with mutation of the polybasic domain 131

4.2.6 STREX channel activity can be modulated by the polybasic domain 133

4.2.7 Voltage dependence is unchanged in polybasic mutant channels.....135

4.2.8 Mutation of polybasic domain affects the activation and deactivation kinetics of the STREX channel 138

4.2.9 Does the polybasic domain work alone?.....142

4.2.10 The polybasic domain regulates the palmitoylation status of the C645:C646 site in the STREX channel 144

4.2.11 Phosphorylation within the polybasic domain destabilises the basic region abolishing palmitoylation.....144

4.2.12 Does the polybasic domain target $PI(4,5)P_2$ in the plasma membrane? 147

4.3 Discussion.....152

4.3.1 The polybasic domain is a functional membrane targeting domain 152

4.3.2 Disruption of the polybasic domain shifts STREX channel properties towards the ZERO channel phenotype 152

4.3.3 The polybasic domain controls palmitoylation of the STREX C645:C646 site.....154

4.3.4 The polybasic domain's non specific interaction with the plasma membrane 155

4.3.5 Control of membrane targeting by phosphorylation – an electrostatic switch 156

4.3.6 The structure of the polybasic domain and STREX insert 157

4.3.7 A polybasic domain as a nuclear localisation signal? 159

4.3.8 Challenges for the future 161

4.3.9 In Summary 162

Chapter 5 - Palmitoylation controls cell surface expression of BK 163

5.1 Chapter 5 introduction 164

5.1.1 Additional palmitoylation sites in the BK channel 164

5.1.2 Working hypothesis 165

5.1.3 Aims to be addressed in this chapter 165

5.1.3.1 Are there additional palmitoylation sites in the BK channel and do they target the plasma membrane? 165

5.1.3.2 What is the function of an additional palmitoylation site in BK channels? 167

5.1.3.3 Are palmitoylation sites functionally linked within a protein? 167

5.2 Results 168

5.2.1 A palmitoylation site in the S0-S1 linker of the BK channel 168

5.2.2 BK channels are palmitoylated at the S0-S1 linker 168

5.2.3 The S0-S1 targets the plasma membrane which is diminished by mutation of the C53:54:56A site 171

5.2.4 Palmitoylation of the S0-S1 linker is functionally important to the BK channel 174

5.2.5 Single channel amplitude is not affected in de-palmitoylated BK channels 176

5.2.6 S0-S1 palmitoylation has no effect on intrinsic channel activity.....178

5.2.7 Palmitoylation is an important determinant of BK channel cell surface expression. 182

5.2.8 STREX channels are still palmitoylated when the S0-S1 linker palmitoylation motif is mutated.....186

5.2.9 S0-S1 palmitoylation is functionally important in STREX channels that are also palmitoylated within STREX 186

5.2.10 Palmitoylation of the S0-S1 linker controls cell surface expression of STREX channels 188

5.3 Discussion.....191

5.3.1 BK channels are palmitoylated in the S0-S1 linker.....191

5.3.2 Palmitoylation at the S0-S1 linker controls cells surface expression but not channel activity 191

5.3.3 The importance of palmitoylation at the S0-S1 linker 192

5.3.4 How might palmitoylation of the S0-S1 linker control cell surface expression? 193

5.3.5 The local environment is important for palmitoylation.....194

5.3.6 The role of distinct palmitoylation sites in proteins 195

5.3.7 Challenges for the future 196

5.3.7.1 Are there extrinsic factors that regulate palmitoylation? 196

5.3.7.2 On what timescale does palmitate turnover occur? 196

5.3.7.3 The palmitoylation membrane trafficking pathway - from Golgi to membrane and back? 197

5.3.8 In summary.....199

Chapter 6 – General discussion 200

6.1 General discussion.....201

6.1.1 Aims of the thesis.....201

6.1.2 STREX is a membrane targeting domain controlled by palmitoylation ...201

6.1.2.1 Is palmitoylation the key to mediating the increased calcium sensitivity of STREX channels?.....202

6.1.2.2 Does phosphorylation within the polybasic domain act as an electrostatic switch controlling membrane targeting of the STREX domain?.....204

6.1.3 Palmitoylation in the S0-S1 linker of the BK channel regulates cell surface expression.....206

6.1.3.1 How does palmitoylation of the S0-S1 linker regulate cell surface expression?.....206

6.1.3.2 Two distinct palmitoylation sites with different functional properties ...207

6.1.4 Final overview.....207

References.....208

Appendices.....235

List of Figures

Chapter 1 - Introduction

Figure 1.1 The evolution of ion channels 3

Figure 1.2 The potassium channel family..... 6

Figure 1.3 Features of the BK channel.....14

Figure 1.4 Hydrophilicity profile for the mSlo BK channel sequence.....16

Figure 1.5 The crystal structure of the KcsA K+ channel pore and selectivity filter..20

Figure 1.6 Negatively charge residues line the entrance and exit to the pore.....22

Figure 1.7 Spring-based gating mechanism for BK channels.....27

Figure 1.8 Cryo-EM structure of the BK channel.....31

Figure 1.9 The positions of the transmembrane domains in the BK channel.....33

Figure1.10 The structure of the BK channel intracellular C-terminus domain and proposed arrangement of the calcium bowl.....34

Figure1.11 The proposed crystal structure of the BK channel.....36

Figure1.12 Overview of pre-mRNA alternative splicing.....40

Figure 1.13 Intron-exon structure map of murine BK channel and alternative splice sites.....42

Chapter 2 – Material & Methods

Figure 2.1 Schematic of channel constructs.....59

Chaper 3 – Palmitoylation of the STREX insert

Figure 3.1 Sequence alignment of the cysteine rich STREX insert 82

Figure 3.2 Cysteine residues are important for targeting of the STREX C-terminus (S6:STREX) to the plasma membrane.....90

Figure 3.3 Palmitoylation controls the association of C-terminus constructs at the plasma membrane.....92

Figure 3.4 STREX activation driven by calcium influx is diminished in C645A:C646A mutant channels 95

Figure 3.5 Single channel amplitude is unchanged in STREX, C645A:C646A mutant and insertless ZERO BK channels.....97

Figure 3.6 C645A:C646A mutation rightward shifts the V0.5MAX of the STREX channel towards the ZERO channel.....99

Figure 3.7 The voltage dependence of the mutant C645A:C646A channel is unaffected.....100

Figure 3.8 Palmitate incorporation into S6:STREX is abolished by mutation of cysteine residues C645A:C646A and is absent in ZERO channels.....102

Figure 3.9 Mutation of the S636 PKA phosphorylation site in STREX disrupts C-terminus association with the plasma membrane.....104

Figure 3.10 PKA phosphorylation of S6:STREX disrupts C-terminal association with the plasma membrane.....106

Figure 3.11 Model of RCK1-RCK2 linker interaction with the plasma membrane through the STREX domain.....113

Chapter 4 – The polybasic domain in STREX

Figure 4.1 Sequence alignment of basic residues in the intracellular C-terminus of the STREX channel.....119

Figure 4.2 Basic Hydrophobicity profiles of the STREX C-terminus with mutations in the putative polybasic domain.....125

Figure 4.3 The polybasic domain is important for targeting of the STREX C-terminus to the plasma membrane.....128

Figure 4.4 STREX channel activation driven by calcium influx is diminished when the polybasic domain is disrupted.....130

Figure 4.5 Single channel amplitude is not affected by disruption of polybasic domain.....132

Figure 4.6 Disruption of the polybasic domain shifts the activation of STREX channels.....134

Figure 4.7 The voltage dependence of STREX channel activation is not affected by disruption of the polybasic domain.....136

Figure 4.8 STREX channel activity in polybasic mutant channels is not shifted in zero calcium.....137

Figure 4.9 STREX channel activation rates in polybasic mutants.....139

Figure 4.10 STREX channel deactivation rates in polybasic mutants.....141

Figure 4.11 Palmitoylation of STREX is modulated by the polybasic domain.....145

Figure 4.12 Palmitate incorporation into S6:STREX is abolished by mutation of PKA phosphorylation site S636.....146

Figure 4.13 Phosphoinositides do not modulate the BK channel.....149

Figure 4.14 The STREX channel membrane targeting domain.....158

Chapter 5 - Palmitoylation controls cell surface expression of BK

Figure 5.1 Sequence alignment of conserved cysteine residues in the S0-S1 linker of the BK channel.....166

Figure 5.2 BK channels are palmitoylated in the intracellular S0-S1 linker.....170

Figure 5.3 Palmitoylation targets the S0-S1 linker to the plasma membrane.....172

Figure 5.4 Activation of BK channels by calcium influx is attenuated in S0-S1 mutant channels.....175

Figure 5.5 Single channel amplitude is not changed in de-palmitoylated BK channels 177

Figure 5.6 Calcium sensitivity is un-affected in de-palmitoylated channels 179

Figure 5.7 The voltage dependence of the ZERO C53A:C54A:C56A channel is unchanged.....180

Figure 5.8 Number of functional ZERO C53A:C54A:C56A channels appears reduced in membrane patches when compared to wild-type ZERO channels.....181

Figure 5.9 Palmitoylation of the S0-S1 linker regulates cell surface expression of BK channels.....183

Figure 5.10 Disruption of the S0-S1 palmitoylation motif in the STREX channel reduces palmitoylation.....185

Figure 5.11 Disruption of the S0-S1 linker palmitoylation site in STREX splice variant channels also attenuates the ionomycin driven channel activation.....187

Figure 5.12 The S0-S1 palmitoylation motif also controls cell surface expression of STREX channels.....189

Figure 5.13 The BK channel palmitoylation membrane trafficking pathway - from Golgi to membrane and back? 198

Chapter 6 – General discussion

Figure 6.1 Working model of palmitoylation of BK channels.....203

List of Tables

Table 2.1 Primers used for site directed mutagenesis in the BK channel..... 61

Table 3.1 Predicted palmitoylation scores for cysteine residues in the Intracellular C-terminus of the STREX splice variant of the BK channel..... 88

Table 4.1 Disruption of the polybasic domain by introduction of negative and neutral charges changes predicted palmitoylation scores for the STREX palmitoylation site C645:C646..... 143

Table 5.1 Predicted palmitoylation scores for cysteine residues in the ZERO channel

..... 169

CHAPTER ONE

INTRODUCTION

1.1 The evolution of the ion channel

Amongst the numerous proteins that are vital to life are the ion channels, membrane proteins that allow rapid movement of ions through a pore, across an otherwise impermeable lipid cell membrane. The movement of ions through channels that cross the cell membrane is at least three orders of magnitude faster than pumps or carrier proteins and eleven orders faster than simple diffusion (Moczydlowski, 1986), making ion channels extremely efficient at regulating physiological function.

Membrane ion channel proteins differ markedly from water soluble proteins by the presence of hydrophobic segments that are able to insert into the lipid membrane as transmembrane (TM) domains. These TM domains have evolved to be just long enough to span the lipid bilayer, being ~21 amino acids in length and comprised largely of hydrophobic residues (Stryer, 1997). If we step back in the evolutionary timescale to postulate what the primitive ion channels might have been like, we can look to the simple structure of the bacterial channels in the potassium channel family for clues. The bacterial potassium channel, KcsA, is composed of 2 transmembrane domains, which is considered to be the minimal structural requirement for a functioning ion channel (Doyle *et al.*, 1998; MacKinnon *et al.*, 1998). This 2-TM channel may not be too dissimilar to the very early ion channels, the ancestors of today's ion channels. Modern day mammalian 6-TM domain potassium channels may well have evolved from similar primitive 2-TM channels, whereby acquisitions of additional domains incorporating a voltage sensor and regulatory domains have developed over an evolutionary timescale.

It is fascinating to speculate how the ion channels may have arisen. Certainly the most basic ion channels are the 2-TM channels (such as KcsA), that form a tetramer of four individual α-subunits around a central conducting pore. The voltage-gated potassium channels are 6-TM polypeptides that also form symmetrically as a tetramer around a central pore. However, in contrast to the potassium channels, the genes that encode the calcium and sodium channels contain four internal repeats that include all four domains of the channel within one polypeptide (Figure 1.1). This illustrates beautifully the theory that the calcium ion channel genes and sodium ion

Figure 1.1
The evolution of ion channels

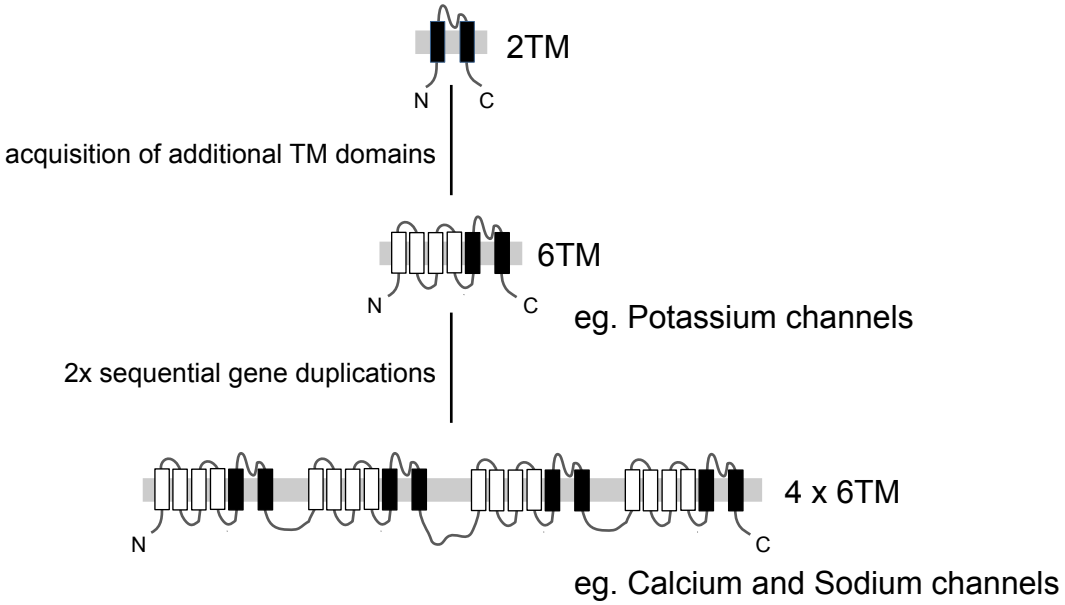

Figure 1.1. The evolution of ion channels. Schematic diagram illustrating the 2-transmembrane (TM) channels that form a tetramer of four individual α-subunits around a central conducting pore. 2-TM's are thought to be the basic requirement for a functional channel. Through evolution the 2-TM channels acquire additional domains such as a voltage sensing region characteristic of the 6-TM voltage gated K^+ channels that also form a tetramer around a central pore region. Through sequential gene duplications, channels with four subunit domains linked together in a single large polypeptide evolved, such as in Ca^{2+} and Na^+ channels. The pore regions are indicated by solid black shading.

channel genes most probably evolved from potassium channel genes through a process of two sequential gene duplication events (Ranganathan, 1994).

Additionally, it is postulated that sodium channels may have emerged from calcium channels after further random mutation as they are only found in higher organisms (Franciolini & Petris, 1989; Strong *et al.*, 1993). Indeed sodium channels have more sequence identity to corresponding calcium channel subunit domains (61%) than they do to subunits within the same polymer (50%) or to the single subunit domain of the potassium channels (27%) (Hille, 1989). It has been demonstrated that artificially linked subunits of voltage-gated potassium channels can form functional channels however there is no evidence of such potassium channels in existence (Liman *et al.*, 1992). It is all too possible considering the evidence we have seen in the genome, that potassium may have been the first charge carrier across the impermeable cell membrane. Since sodium channels appear later in the evolutionary timescale and calcium in high concentrations is toxic without intracellular chelation, it would seem that they would be unlikely candidates for the first ion to have been initially carried across the cell membrane. Indeed, the regulation of internal potassium milieu in primitive cells is known to be crucial to cell survival (Biggin *et al.*, 2000) and so it is plausible that the potassium channel may contain the remnants of the earliest ion channel.

Across the evolutionary lineage, the retention of specific amino acids within a protein's primary sequence can indicate regions of structural and functional importance to the higher vertebrates. Those regions retained under heavy evolutionary selection pressure conserve important motifs necessary for protein function whereby homology can be sought through alignment techniques across the vertebrate phylum. The subtle changes in the genome and the highly conserved nature of functional residues and motifs reveal the finite precision by which ion channels have advanced over billions of years.

It is only through the duplication and divergence of ion channel genes along with random mutation and splice variation that a diverse family of ion channels was born from that ancestral ion channel. Internal signalling, resetting of membrane and ionic potentials and communication between cells, drove the early channels by trial and error to achieve the diversity required for complex life. The modern day ion channels have survived several hundred million years of evolution (prokaryotes appeared

about 3500 million years ago) (Franciolini & Petris, 1989) and whilst they probably do not reflect the early ion channels, the remains of their earliest ancestors probably still lie buried as small sequences within the genetic code of each modern day ion channel.

1.2 The potassium channel family

1.2.1 Potassium channels with phenotypic behaviour

Seymour Benzer, one of the founders of neurogenetics in the late 1960's, proposed that mutant behavioural and neurological phenotypes might reflect defects in the genome (Benzer, 1967). He suggested that these defects may occur in ion channels that he correctly surmised would be conserved across metazoans (Benzer, 1971; Salkoff *et al.*, 2006).

The molecular nature of ion channels has only been elucidated in the last 25 years. The first potassium channel gene (a voltage-gated K^+ channel) was first cloned from the Drosophila Shaker locus (Kamb *et al.*, 1987; Papazian *et al.*, 1987; Pongs *et al.*, 1988), identified almost 20 years previously as an ether-induced leg shaking phenotype in mutant Drosophila melanogaster (Kaplan & Trout, 1969). Subsequently a large number of potassium channel genes have been cloned.

1.2.2 The potassium channel family

Potassium-selective (K^+) channels are the largest and most diverse group of ion channels represented by some 70 known loci in the mammalian genome (Gutman *et al.*, 2005). They have been observed in virtually all cell types and demonstrate an extensive structural diversity creating a wide heterogeneous functionality. Potassium channels are highly selective cation channels that have an equilibrium potential close to the cellular resting potential of many cells, making them important determinants in maintaining the resting membrane potential (Salkoff *et al.*, 2006).

Figure 1.2
The potassium channel family

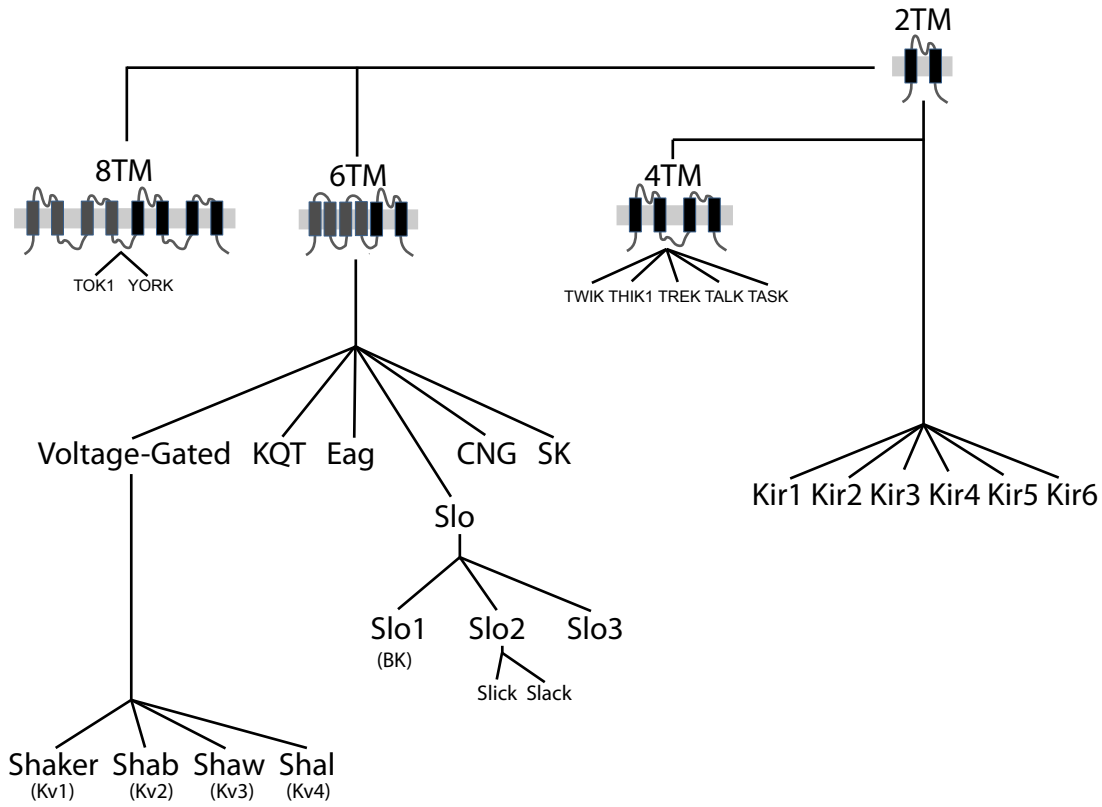

Figure 1.2. The potassium channel family. A hierarchical classification scheme for potassium channel genes. Potassium channels belong to the ion channel superfamily. They can be grouped into four main structural classes encoding 2 transmembrane (2TM), 4 transmembrane (4TM), 6 transmembrane (6TM) and 8 transmembrane (8TM) subunits. There are six families within the 6TM class, conserved between vertebrate and invertebrate species. These families can also be further subdivided into subfamilies. About 40% amino acid sequence identity is present between subfamilies. Significantly higher amino acid identity (50-70%) is shared within subfamilies.

The diverse array of K^+ channels can now be classified into four major structural classes; those processing two transmembrane domains (2TM) (eg. the inward rectifier channels Kir1-6) around a conserved pore domain, four transmembrane domains (4TM) associated with two pore domains (including TWIK, THIK1, TREK, TALK and TASK channels), the six transmembrane domains (6TM) associated with one pore domain (such as the voltage gated Kv channels) and the eight transmembrane domains (8TM) with two pore domains, which comprise a 6TM+2TM structure and have only been found in yeast cells (TOK1 and YORK channels) (Figure 1.2). Within structural classes are conserved gene families populated by subfamilies defined by common functional and structural features. Within the 6TM K^+ channel class is a subfamily of channels that are distinguished by an unusually large single-channel conductance and have been named as 'big' potassium (BK) channels (Blatz & Magleby, 1986), also known as maxi-K channels (Latorre *et al.*, 1983) or Slo1 channels (Atkinson *et al.*, 1991).

Isolation of the Slo multigene family by sequence analysis identified a module resembling a voltage-gated channel with an additional intracellular C-terminal domain that can respond to a host of intracellular and extracellular factors (Atkinson *et al.*, 1991; Salkoff *et al.*, 2006). Studies have identified four genes encoding the Slo family of channels in the mammalian genome that comprise: the Slo1 channel, two very similar Slo2 channels termed Slo2.1 (Slick) and Slo2.2 (Slack) and the Slo3 channel. All four genes independently form a homotetrameric channel, whereby each subunit that forms the functioning channel is identical and can conduct K^+ selective currents. SLO-1 channels are activated by voltage but are different to purely voltage-gated K^+ channels because they are also activated by intracellular Ca^{2+} (Atkinson *et al.*, 1991). SLO-2 channels are sensitive to a host of intracellular factors including Cl^- and Ca^{2+} in C.elegans (Yuan *et al.*, 2000) and Cl^- and Na^+ in mammalian orthologues (Yuan *et al.*, 2003) with evidence of negative regulation by ATP in Slo2.1 channels (Bhattacharjee *et al.*, 2002). SLO-3 channels have only been identified in spermatocytes and mature spermatozoa and are sensitive to pH (Schreiber *et al.*, 1998; Salkoff *et al.*, 2006).

1.2.3 The identification of a calcium- and voltage- sensitive K^+ current

In 1958 George Gardos a Hungarian haematologist, described a potassium conductance across the plasma membrane that responded to minor increases in intracellular calcium (Gardos, 1958). By buffering extracellular free calcium with EDTA (a calcium chelator), potassium diffusion across the plasma membrane was substantially reduced. This was the first indication of the existence of a calcium activated potassium channel. The channel which was identified in human erthrocytes, has since been implicated in sickle cell anaemia (Maher & Kuchel, 2003) and has the distinction of being named after its discoverer, as the Gardos channel or in the nomenclature, SK4. However, it wasn't until 1970 that an actual ionic current activated by a rise in intracellular calcium was identified (Meech & Strumwasser, 1970) confirming the initial observations by Gardos. In the decades that followed, a calcium-dependant K^+ channel was isolated and characterised in chromaffin cells, with a reversal potential of lower than -60 mV in normal Ringers and a large unitary conductance (Marty, 1981). Further studies revealed that the channel could be uniquely regulated by calcium and membrane potential independently and that each could equally enhance the channel's open probability (Pallotta, 1985).

In the late 1980's and early 1990's with the development of neurogenetics and novel techniques to isolate and clone specific genes, the gene responsible for the calcium sensitive large potassium conductance was identified. Following on from the work which led to the molecular cloning of the first K^+ channel from the Shaker locus in Drosophila melanogaster, the gene responsible for the Slowpoke phenotype was isolated and cloned (Atkinson *et al.*, 1991). Slowpoke describes a mutation that confers behavioural lethargy in Drosophila and was found to be mediated by a calcium sensitive potassium current (Elkins *et al.*, 1986). It was subsequently named the Slo gene. The human homologue hSlo was later cloned from brain (Dworetzky *et al.*, 1994) and mouse mSlo was isolated from brain and skeletal muscle (Butler *et al.*, 1993). This gene encodes what we call today, the BK channel.

1.3 The BK channel

1.3.1 Characteristics of the BK channel

The BK channel is a large conductance potassium channel that is uniquely regulated by both voltage and intracellular calcium. The gene that codes the channel is located on human chromosome 10, 49% of the distance from the centromere to the telomere of the chromosome arm 10q, corresponding to a band, 10q22.3 (Tseng-Crank *et al.*, 1994). The open reading frame encodes for a single pore-forming subunit of approximately 125 kDa molecular weight and can range from between ~1154 to >1200 amino acids in length. The modular design of the BK channel in the evolutionary lineage suggests that the channel may have evolved from a core module representing a voltage-dependant channel which then acquired an additional C-terminal domain that is responsive to multiple intracellular and extracellular factors. The large conductance unique to the BK channel averages around 250 pS (Marty, 1981; Latorre *et al.*, 1982; Latorre *et al.*, 1983; Farley & Rudy, 1988) in equimolar K^+ gradients (~120 pS in physiological gradients, (Bielefeldt *et al.*, 1992)), markedly larger than other voltage-gated K^+ channels that average less than a tenth of that conductance. This would suggest that major structural rearrangements must also have occurred in the selectivity filter and pore region to accommodate an ionic flux an order of magnitude larger than its evolutionary ancestors.

BK channels can assemble from 2 distinct subunits that form a 1:1 stoichiometry (Knaus *et al.*, 1994a; Toro *et al.*, 1998), they are the pore forming α-subunits and regulatory β-subunits (Garcia-Calvo *et al.*, 1994; McManus *et al.*, 1995). The BK channel pore-forming α-subunit is uniquely encoded by a single gene, KCNMA1, and the regulatory β-subunits are encoded by a family of four genes, KCNMB1-4. The α-subunit is the single product of one gene and therefore tetramerisation of the channel is largely homogenous with each subunit being symmetrically identical in the conducting central pore region. Evolutionary pressure has perhaps maintained this quirk in response to retaining absolute symmetry within the conduction pore of the BK channel, a feature that could possibly underlie part of the large conductive properties of the channel in contrast to the other asymmetrical channel pores, for example in the Na^+ and Ca^{2+} channels (Salkoff & Jegla, 1995).

1.3.2 The physiological role of the BK channel

BK channels are expressed in all cells throughout the body largely with the exception of cardiac tissue. Although, as with all exceptions in science there is some evidence to suggest BK channels may also be present in cardiac tissue as well (Ko *et al.*, 2009; Imlach *et al.*, 2010).

BK channels sense and regulate membrane voltage and intracellular Ca^{2+} thereby linking cellular excitability with signalling and metabolism. With the reversal potential of potassium being close to the resting membrane potential in excitable cells, the BK channel acts as an effective modulator of the resting membrane potential. The channel's dynamic regulation by calcium also allow it additionally to function as a negative-feedback regulator for Ca^{2+} entry in many different cell types (Salkoff *et al.*, 2006).

In smooth muscle cells the BK channel has been shown to be dynamically regulated by vasodilators and vasoconstrictors that potently regulate contractile tone (Brenner *et al.*, 2000b; Sausbier *et al.*, 2005). The BK channel regulates contractility firstly, through activation by small local increases in calcium (Ca^{2+} sparks) released from ryanodine receptors in the intracellular sarcoplasmic reticulum, that appear to be responsive to circulating hormones (Jeffries *et al.*, 2010b), to induce vasodilation. Secondly, BK channels can be activated by influx of calcium across the plasma membrane through calcium channels activated during depolarisation (Nelson *et al.*, 1995; Jeffries *et al.*, 2010b), not to mention depolarisation itself, which activates the channels leading to dilation of the vessel. Hence calcium can indirectly lead to vasodilation through the activation of the BK channel. BK channels are also responsive to a host of other factors such as protein kinases (Schubert & Nelson, 2001), endothelial-derived relaxant substances (Tanaka *et al.*, 2004), growth factors (Weaver *et al.*, 2004), hypoxia [that includes three proposed mechanisms: i) the Hemoxygenase-2 mechanism (Williams *et al.*, 2004); ii) regulation via the STREX splice variant (McCartney *et al.*, 2005); and iii) the AMP kinase mechanism (Peers, 1990; Evans *et al.*, 2009; Peers *et al.*, 2010) and regulation by β-subunits (Brenner *et al.*, 2000b).

The BK channel's role in regulation of contractile tone in smooth muscle is evident in pathophysiologies such as cardiovascular disease, characterised by elevated blood

pressure whereby dysfunction of the BK channel fails to regulate the resting membrane potential or act as a 'brake' of calcium entry (Brenner *et al.*, 2000b; Sausbier *et al.*, 2005). In bladder smooth muscle, BK channel dysfunction leads to an overactive bladder and urinary incontinence (Meredith *et al.*, 2004), in the colon removal of regulatory β-subunits leads to differences in bowel structure and function, manifested by atypically loose fecal matter (Hagen *et al.*, 2003) and in penile arterial and corpus cavernosum smooth muscle, where the BK channel mediates relaxation important for penile erection, dysfunction leads to impaired erectile function (Christ *et al.*, 2004; Werner *et al.*, 2005).

BK channels also play an important role in the regulation of neuronal excitability (Raffaelli *et al.*, 2004; Sausbier *et al.*, 2004). The BK channel is particularly prevalent in the central nervous system (CNS) where it is localised to cell somas, dendrites and presynaptic terminals (Marrion & Tavalin, 1998; Gribkoff *et al.*, 2001a; Salkoff *et al.*, 2006). They have been implicated in controlling the frequency and duration of action potentials such as those generated in dendrites (Womack & Khodakhah, 2004). In the neuronal soma they contribute to the fast after-hyperpolarisation that determines the firing rate of the neuron (Faber & Sah, 2003). Presynaptically, BK channels have been identified in the modulation of neurotransmitter release and can act a braking mechanism under conditions of excessive depolarisation, maintaining homeostasis for regulating synaptic transmission (Raffaelli *et al.*, 2004). The importance of the BK channel in the CNS is highlighted by distinct channelopathies implicated in various pathophysiological conditions including epilepsy and paraoxysmal dyskinesia (Brenner *et al.*, 2005; Du *et al.*, 2005), deficient motor co-ordination (Sausbier *et al.*, 2004) and high frequency hearing loss (Ruttiger *et al.*, 2004). Additionally, the BK channel has been demonstrated to function in immunity (Ahluwalia *et al.*, 2004) and in the promotion of tumor cell proliferation (Weaver *et al.*, 2004; Bloch *et al.*, 2007).

1.3.3 The BK channel knock-out mouse

The ability to knockout genes in mice, developed in the 1980's (Goldstein, 2001), has led to a greater understanding of gene function. The challenge to create the BK (α-subunit) knockout mouse was completed only in the last six years by two

independent labs – Peter Ruth in Europe (Sausbier *et al.*, 2004) and Richard Aldrich in USA (Meredith *et al.*, 2004). Interestingly, despite the prevalence of the BK channel throughout the body and the important role it is believed to play, the BK knockout mice are viable and exhibit a spectrum of subtle abnormalities. The mice have been described with ataxia and abnormal gait (Sausbier *et al.*, 2004), high frequency hearing loss (Ruttiger *et al.*, 2004), vascular hypertension (Sausbier *et al.*, 2005), incontinence due to over active bladder function (Meredith *et al.*, 2004) and erectile dysfunction (Werner *et al.*, 2005) consistent with defects in brain and smooth muscle excitability. The mutant mice have a normal life expectancy, are able to produce offspring and when compared to wild-type mice do not show gross morphological differences in young or adult mutant brains (Sausbier *et al.*, 2004). The apparent non-lethal phenotype of the knockout animals suggest that there may be compensatory mechanisms (Sprossmann *et al.*, 2009) or that the channel may play more important roles under conditions of stress and in deleterious conditions (Sausbier *et al.*, 2004; Chatterjee *et al.*, 2009).

1.3.4 BK channel pharmacology

Indeed, the diversity of BK channels across many different cell types has made them attractive therapeutic targets. However the widespread expression of the BK channel, as previously described, has hampered the specificity with which targeting of this protein could be made possible for pharmacological intervention.

BK channel activators have been proposed in potential treatments for hypertension, pre-term labour and ischaemic stroke (Liu *et al.*, 1998; Song *et al.*, 1999; Brenner *et al.*, 2000b; Gribkoff *et al.*, 2001b; Sobey, 2001) whereby they increase potassium efflux leading to hyperpolarisation of the cell limiting excitability. Activators can modulate calcium binding, strengthen the role of β-subunit modulation or may bind directly to sites within the channel. They can modulate BK channel properties by increasing mean channel open time or by shifting the voltage- and/or calcium-sensing properties. Two examples of BK channel activators are the NS1619 and NS004 drugs which are benzimidazolone derivatives and are α-subunit selective (Olesen *et al.*, 1994).

BK channel blockers are valuable pharmacological tools for examining the structural and functional properties of BK channels (Ghatta *et al.*, 2006). These include peptide pore blockers iberiotoxin and charybdotoxin (Candia *et al.*, 1992) from spider venoms, quaternary ammonium compounds eg TEA (Li & Aldrich, 2004) and non-peptide fungal alkaloids e.g. paxilline isolated from the fungus *Penicillium paxilli* (Knaus *et al.*, 1994e). Their mechanisms of action are different and have been informative of the nature of the channel. TEA operates by a flickery-block that sits in the pore and hastens deactivation (Li & Aldrich, 2004). The toxins, charybdotoxin (all K^+ channels) and iberiotoxin (highly selective) (Candia *et al.*, 1992) bind to the external vestibule blocking the channel pore (Giangiacomo *et al.*, 1992). Tremorgenic mycotoxins such as paxilline verruculogen and penitrem A, reversibly block the channel (Knaus *et al.*, 1994e) inhibiting conductance by an allosteric mechanism inside the pore. Blockers although a useful tool, have been limited in their therapeutic application largely due to depression or memory impairment (Olesen *et al.*, 1994).

Interestingly, sulphatides, a group of glycosphingolipids located in the plasma membrane have been suggested to activate BK channels through possible lipid-membrane interactions. Moreover, it has been proposed that the STREX sequence (to be discussed later in section 1.6.2.2) may mediate part of this activation through the local membrane environment (Chi & Qi, 2006), postulating a role for STREX interaction with the lipid membrane.

1.4 The structural composition of the BK channel

The pore forming α-subunit of the BK channel consists of 7 transmembrane spanning domains (S0-S6) that make up the core region including a central pore between S5 and S6, and an extracellular amino (N) terminus at the S0 domain. The channel also contains a large intracellular carboxyl (C) terminus made up of four hydrophobic segments (S7-S10) (Meera *et al.*, 1997) (Figure 1.3).

The α-subunit forms a tetramer, whereby four α-subunits arrange around a central conducting pore. The tetrameric composition of the BK channel was initially

Figure 1.3
Features of the BK channel

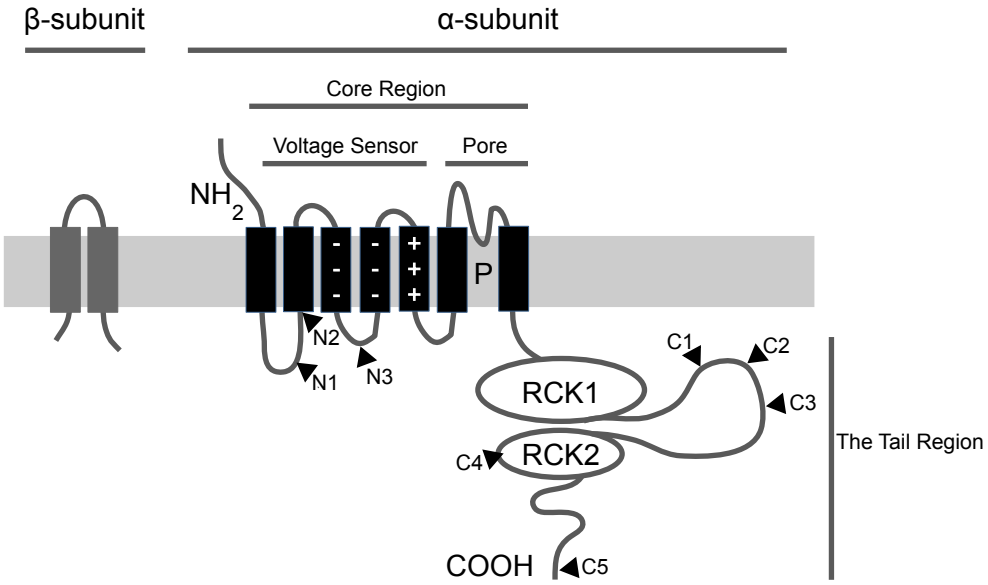

Figure 1.3. Features of the BK channel. Transmembrane topology of the pore forming α-subunit 7-TM core region (S0-S6), the extracellular amino (NH_2) terminus, large intracellular carboxyl (COOH or C-) terminus including regulators of K^+ conductance RCK1 & RCK2, are illustrated. The voltage sensing region is illustrated with positive and negative charges (+/- in white), along with the pore region and sites of alternative splicing within the channel (N1-N3 & C1-C5). The regulatory β-subunit is also illustrated in grey.

demonstrated in oocytes injected with a mixture of RNAs encoding wild-type BK channel subunits and TEA-insensitive BK channel subunits (Y308V) and showing unitary currents of four discrete amplitudes in the presence of 3 mM TEA (BK blocker) corresponding to inhibitions of approximately 80%, 55%, 25% and 10% (Shen *et al.*, 1994). Later, the biogenesis of tetrameric potassium channels was described involving a complex series of events. Initially, individual pore forming subunits are targeted to the ER membrane whereby compatible subunits can then assemble (Papazian, 1999). Tetramerisation is mediated by a conserved domain, which in voltage-gated K^+ channels is located in the amino terminus and in BK channels has been located just C-terminal to the channel pore. This association domain, in the region between the S6 transmembrane domain and the S7 hydrophobic C-terminal domain and RCK1, is called BK-TI (tetramerisation domain 1) and is required for functional channel expression (Quirk & Reinhart, 2001). This region alone is capable of tetramerisation and is the only region in the channel capable of doing so making it the likely candidate for functional channel assembly.

1.4.1 The core region

Alignment of the predicted primary sequence and hydrophilicity profiles of the Murine and Drosophila Slo (BK) gene sequence reveal a core domain that shares much homology with voltage-gated K^+ channels (Wei *et al.*, 1990; Jan & Jan, 1992; Salkoff *et al.*, 1992) (Figure 1.4). The core region of the BK channel contains 7 transmembrane domains incorporating a voltage sensor of conserved charged residues and a pore region. The S0 transmembrane domain later identified in the BK channel is additional to the 6-TM core of the voltage-gated K^+ channel and was demonstrated to have an extracellular amino terminus (Wallner *et al.*, 1996; Meera *et al.*, 1997).

1.4.1.1 The voltage sensing domain

The S1-S4 segments comprise the voltage sensing domain (VSD) of the BK channel that contain high density charged residues that can respond to changes in

Figure 1.4
Hydrophilicity profile for the mSlo BK channel sequence

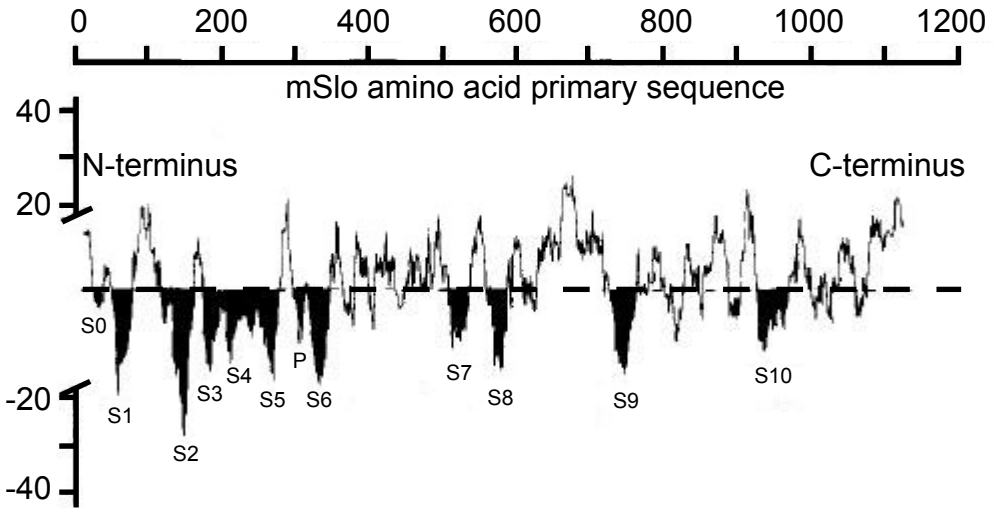

Figure 1.4. Hydrophilicity profile for the mSlo BK channel sequence. Schematic representation showing the primary sequence of the murine BK (mSlo) channel's predicted hydrophilicity profile. Evident are eleven hydrophobic domains (illustrated by solid black sections). Domains have been labelled (S0-S10). Adapted from a figure by Wei *et al*., 1994.

transmembrane potential (Figure 1.3). Almost 4 decades ago now, Armstrong and Bezanilla identified small gating currents in response to changes in membrane potential and proposed that these gating currents, first measured in sodium channels, signified opening of the channel pore (Armstrong & Bezanilla, 1974). Membrane proteins have learnt to sense these changes in transmembrane potential, whereby charged residues are able re-orientate in response to changes in the electric field, leading to conformational changes in the protein. Much of our recent understanding of voltage-sensing domains has been advanced by the development of the crystal structure of the voltage-gated K^+ channel and through optical investigations examining the movement of the voltage sensing domains (Bezanilla, 2008a).

In contrast to voltage-gated K^+ channels, BK channels have a relatively weak voltage dependence corresponding to a fivefold smaller gating charge (Ma *et al.*, 2006). In the absence of Ca^{2+}, the voltage required to half maximally activate the channel is estimated to be around +200 mV (Horrigan & Aldrich, 1999; Horrigan *et al.*, 1999). It is relatively unclear as to why this difference exists, however limitations in voltage sensor movement or a reduced contribution of residues to gating charge have been proposed. The pattern of charged residues in the BK channel is similar to voltage-gated K^+ channels, with the S2 and S3 domains containing acidic residues alongside a series of three regularly spaced basic (arginine) residues in S4 (Ma *et al.*, 2006).

Recent studies indicate that perhaps only 4 residues in the BK channel contribute to the voltage-sensing component of the channel and that only one of these residues is located in S4 (Diaz *et al.*, 1998; Ma *et al.*, 2006). Therefore it would seem that charged residues outside of S4 make significant contributions to gating charge, unlike the voltage-gated channels where the major component of gating charge movement is through S4 (Papazian *et al.*, 1995). Indeed it has been suggested that there may in fact be mechanical and functional coupling of S2 to S4 in gating movements, suggesting that both domains can influence each other's voltage-sensing ability (Pantazis *et al.*, 2010).

Much speculation underlies the mechanism of voltage sensor activation in both the BK channel and in the voltage-gated K^+ channels. It has been proposed by Roderick MacKinnon's group that in voltage-gated K^+ channels the S4 segment undergoes a

large movement in what is known as the paddle model. This model proposes that the S4 domain undertakes a large 15-20 Å perpendicular movement across the lipid bilayer during voltage sensing (Jiang *et al.*, 2003b; Lee *et al.*, 2009b; Tao *et al.*, 2010), to put this into perspective the membrane bilayer is between 10-40 Å in diameter (Mackinnon, 2004b; Bezanilla, 2008b). However, Francisco Bezanilla's group have controversially argued using FRET (fluorescence resonance energy transfer) technologies to examine fluorophores in the S4 segment, that movement of the S4 segment is limited (Chanda *et al.*, 2005; Posson *et al.*, 2005), but that there is significant rotation and tilting of the S4 segment, but by no more than ~2 Å perpendicular movement (Bezanilla, 2008a).

Fundamental differences in the structure and the contribution of charge residues to voltage sensor activation may exist between the voltage-gated K^+ channels and the BK channel. In the BK channel the voltage sensor would appear to be a more dynamic structure whose activation involves changes in position and a greater interaction with adjacent S1-S3 transmembrane domains (Ma *et al.*, 2006). It will be interesting to see how developments in future techniques help explain the differences of voltage dependence between BK channels and the rest of the voltage-gated K^+ channel family.

1.4.1.2 The S0 transmembrane domain

BK channels share much of the topological design conserved across the voltage-gated potassium channel family. However, they carry an additional hydrophobic transmembrane region (S0) and an extracellular N-terminus (Wallner *et al.*, 1996; Meera *et al.*, 1997)(Figure 1.3). Sequence conservation of several residues in the S0 transmembrane domain among BK channel orthologues suggest that it may have an important role in channel structure and function (Koval *et al.*, 2007). Interestingly, channels lacking the S0 domain appear to be neither functional (Wallner *et al.*, 1996; Morrow *et al.*, 2006) nor biochemically detectable on the cell surface (Liu *et al.*, 2008). Additionally, mutations of key residues in the S0 domain have been shown to shift the activation curves of the channel when compared to the wild-type channel, suggesting it may also play a role in voltage-dependant gating of the BK channel (Koval *et al.*, 2007). Recent structural studies have identified that the

S0 domain is located outside of the S1-S4 domains (Liu *et al.*, 2008; Liu *et al.*, 2010) (Figure 1.9) and can form a major contact with the transmembrane domain 2 (TM2) of the regulatory β1 subunits (Liu *et al.*, 2008) and β4 subunits (Wu *et al.*, 2009). The proximity of the S0 domain to the β-subunits correlates well with other studies that suggest that the proposed role of the S0 domain is in facilitating the regulatory effects of β-subunits (Wallner *et al.*, 1996; Meera *et al.*, 1997) (this will be discussed in section 1.6.1). It has also been shown that alternative splicing within the S0-S1 loop can regulate cell surface expression, suggesting that this region may be important for trafficking and that alternative splicing may generate novel trafficking motifs by inclusion of new sites or the uncovering of sites important for channel expression at the plasma membrane (Korovkina *et al.*, 2001; Zarei *et al.*, 2004). It is apparent that the S0 domain is important in facilitating the influence of the β-subunits, controlling cell surface expression and even in regulating voltage-dependence of the channels and therefore it has a unique role to play in modulating the BK channel.

1.4.2 The pore region

The pore region is located at the centre of the four α-subunits of the BK channel, with the narrowest part incorporating the selectivity filter. In each α-subunit the pore forming motif consists of the P-loop and the S5 and S6 domains which line the conductance pore.

The BK channel is able to carry a large selective K^+ current with a slope conductance in the range of 250 pS in symmetrical potassium gradients (Marty, 1981; Latorre *et al.*, 1983; Farley & Rudy, 1988) an order of magnitude greater than other K^+ channels. It is thought that major structural rearrangements within the pore must have occurred to allow the BK channel to carry such a large and yet highly selective current and yet the pore architecture of the BK channel has been suggested to be similar to other K^+ conducting channels (MacKinnon *et al.*, 1998; Jiang *et al.*, 2002b). However, studies with quaternary ammonium and sugars of different sizes suggest that the inner vestibule is likely to be much larger, which may contribute to the large current carried by the channel (Li & Aldrich, 2004; Brelidze & Magleby, 2005). The channel pore, described from the intracellular to extracellular

Figure 1.5
The crystal structure of the KcsA K^+ channel pore and selectivity filter

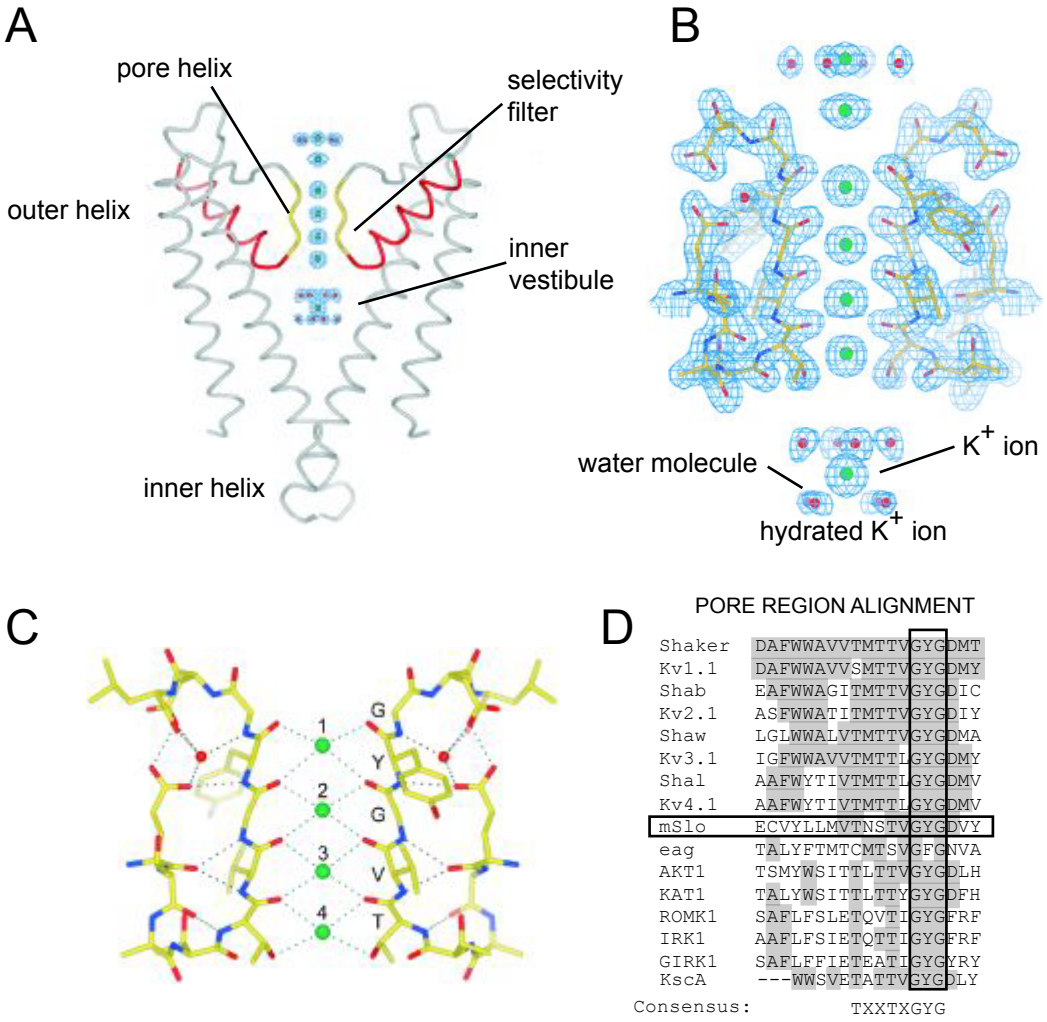

Adapted from R. MacKinnon's Nobel Lecture 2004

Figure 1.5. The crystal structure of the K^+ channel pore and selectivity filter. (A) Ribbon representation of KcsA K^+ channel showing the pore lining S5 and S6 domains. The pore helices are shown in red with the selectivity filter in yellow. Hydrated K^+ ions are seen in the large inner vestibule, K^+ ions are dehydrated in the narrow selectivity filter. (B) Electron density derived from high-resolution (2Å) structure of the KcsA K^+ channel. Features the selectivity filter with K^+ ions and water along the ionic pathway. K^+ ions could be visualised in the grasp of the selectivity filter protein atoms. (C) Detailed structure of the K^+ selectivity filter (two subunits). Oxygen atoms (red) coordinate K^+ ions (green spheres) at positions 1 to 4. Single amino acid code identifies signature sequence unique to all potassium selective channels. Green and grey dashed lines show O---K^+ and hydrogen-bonding interactions respectively. (D) Channel sequences are aligned to the Drosophila Shaker voltage gated K^+ channel (top) across the K^+ channel family with the KscA pore sequence at the bottom. BK (mSlo) is highlighted by a box.

aspect, is comprised of the channel mouth controlled by the inner helices of the S6 transmembrane domains, a large inner vestibule, the selectivity filter which is the narrowest part of the pore, before opening up to the external vestibule and exit of the channel (Figure 1.5).

The universal feature amongst all potassium selective channels is a hyperconserved signature sequence, GY/FG, which forms the K^+ selective filter of the pore (Heginbotham & MacKinnon, 1992; Heginbotham *et al.*, 1994). The pore region is so highly conserved that all potassium channels can be aligned based on the sequence homology of the pore lining selectivity filter, TXXTXGYG motif (Figure 1.5D). Mutagenesis of residues in the signature sequence, have identified it as key to controlling the channel's selectivity to K^+ (Heginbotham *et al.*, 1994). The seminal work of Nobel Prize laureate, Roderick MacKinnon, in mapping for the first time at high resolution the crystal structure of the selectivity filter in bacterial KcsA K^+ channels, revealed the mechanism of selectivity for potassium ions over smaller ions (MacKinnon, 2004a)(Figure 1.5). Sequence conservation of the pore region and additional structural studies from the MacKinnon laboratory, reveal that the architecture is retained in different types of K^+ channels and would probably reflect a similar structural arrangement in the BK channel (Doyle *et al.*, 1998; Jiang *et al.*, 2002a; Jiang *et al.*, 2003a; Kuo *et al.*, 2003). The MacKinnon lab have produced incredible images at 2Å resolution, visualising K^+ ions in the "grasp of the selectivity filter protein atoms" (MacKinnon, 2004a) illustrating how hydrated K^+ ions gather in the large internal vestibule (Figure 1.5A & B), held in place by negative charges at the base of the pore helixes before entering the selectivity filter where oxygen atoms (each binding site is a cage formed by eight oxygen atoms) compensate for the energetic cost of dehydration of the K^+ ions and therefore providing the selectivity required for the passing of K^+ ions (for example, Na^+ ions are too small and the dehydration energy is not compensated) (Figure 1.5C).

When looking elsewhere in the BK channel for unique structural differences in the pore region, two negatively charged rings at the intracellular entrance to the pore vestibule are visible (Brelidze *et al.*, 2003) (Figure 1.6). This ring of 8 negatively charged glutamate residues at the entrance to the inner vestibule is absent in lower conductance K^+ channels and may increase the concentration of permeating ions in the vestibules through an electrostatic mechanism, leading to an increased

Figure 1.6
Negatively charge residues line the entrance and exit to the pore

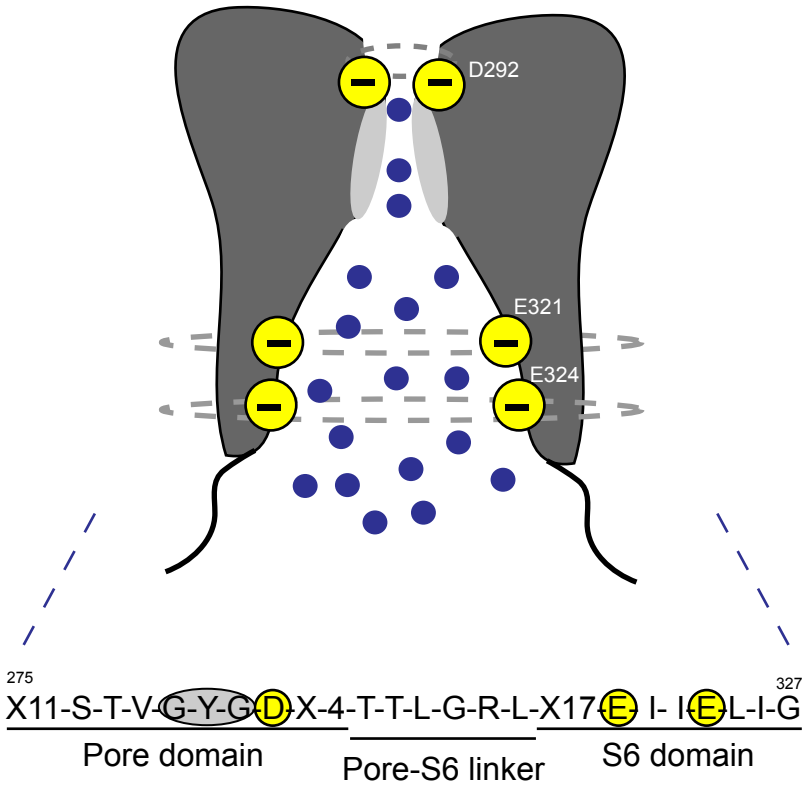

Figure 1.6. Negatively charge residues line the entrance and exit to the pore. The BK channel contains 8 negatively charged glutamate residues at the entrance to the inner vestibule of the pore, making two negatively charged rings that are absent in K^+ channels with smaller conductance. Additionally, on the extracellular aspect the BK channel there is a single ring of negative charge thought to enhance the entry rate of K^+ ions into the pore. Negative charges are illustrated in the pore model and amino acid sequence in yellow. The GYG selectivity filter is shown by the grey circle and potassium ions are shown as blue filled circles.

availability of ions to transit the selectivity filter which could increase single channel conductance (Brelidze *et al.*, 2003). Mutagenesis of the inner negative ring from +8 to -8 has been shown to systematically alter the single-channel conductance, reducing it by half (Brelidze *et al.*, 2003). Additionally, on the extracellular aspect of the BK channel there is a single ring of negative charge thought to enhance the entry rate of K^+ ions into the pore (Li & Aldrich, 2004). Mutations of the negative ring on extracellular vestibule, that decrease the external surface charge density have been shown to also reduce conductance substantially and reduce inward rectification at negative potentials (Haug *et al.*, 2004) (Figure 1.6). Even within the intracellular vestibule, disruption of aromatic residues have been shown to affect single channel conductance (Lippiat *et al.*, 2000). It would appear therefore that the environment within and around the inner vestibule is very important for maintaining the high unitary conductance associated with the BK channel and that several factors may indeed contribute to mediating this large conductance.

1.4.3 The intracellular C-terminus

The BK channel contains a large intracellular carboxyl (C) terminus that encompasses two-thirds of the total length of the channel protein (Toro *et al.*, 1998). It has four additional hydrophobic regions (S7-S10), although the hydrophobicity is lower than the S0-S6 core/pore domains and do not appear to be membrane spanning (Meera *et al.*, 1997) (Figure 1.3). Crystal structural studies have since confirmed that the C-terminus resides intracellularly (Wang & Sigworth, 2009; Wu *et al.*, 2010; Yuan *et al.*, 2010). The channel's structural organisation with a core region homologous to voltage-gated channels, suggest that the subsequent addition of the C-terminal domain may mediate many of the attributes of the channel that are unique to BK channels. The crystal structure of the C-terminus of the BK channel will be discussed in the next section (see section 1.5 and Figure 1.10).

It is now understood that the C-terminus consists of 2 regulators of potassium conductance (RCK 1&2) on each subunit, connected to the pore region by a short linker. Between each RCK domain is a non conserved linker that contains multiple sites of alternative splicing (Tseng-Crank *et al.*, 1994; Toro *et al.*, 1998; Chen *et al.*, 2005) with the remaining portion of the C-terminus represented by the highly

conserved calcium bowl that may or may not reside within RCK2 (Kim *et al.*, 2006; Yusifov *et al.*, 2008) and an additional region of extensive splicing (Wei *et al.*, 1994; Kim *et al.*, 2007a; Chiu *et al.*, 2010). The C-terminus contains multiple regulatory sites including the calcium bowl (Schreiber & Salkoff, 1997), several leuzine zipper domains (Tian *et al.*, 2003), multiple phosphorylation sites for cAMP- and cGMP-dependant protein kinases (Zhou *et al.*, 2001), haem binding domains (Tang *et al.*, 2003; Horrigan *et al.*, 2005) and protein kinase C and tyrosine kinase sites (Schubert & Nelson, 2001; Tian *et al.*, 2008b).

The C-terminal region has also been proposed to have an important role in channel tetramerization, whereby truncation of the C-terminus prevents correct assembly of functional channels (Quirk & Reinhart, 2001) (see section 1.4). However to directly contradict the important role the C-terminus is thought to play, there is evidence that the core region of the BK channel (amino acids 1-343) is sufficient for channel tetramerisation (Schmalhofer *et al.*, 2005). Further to this, there is controversial evidence that suggests that truncation of C-terminus does not even affect normal channel function (Piskorowski & Aldrich, 2002). Despite these studies a wealth of information reinforces the importance of the C-terminus particularly in controlling trafficking to the plasma membrane, the control of cell surface expression and modulating the calcium sensitivity of the channel (Kwon & Guggino, 2004).

1.4.3.1 The RCK domains

Two domains that regulate potassium conductance have been proposed in the BK channel, RCK1 and RCK2. The first RCK domain (RCK 1) encompasses a high affinity calcium sensor (D362/D367 and M513), which when mutated neutralises the calcium sensing affinity of the site (Bao *et al.*, 2002; Xia *et al.*, 2002; Zeng *et al.*, 2005). The RCK1 domain also contains an additional site sensitive to divalent cation binding, a low affinity site for calcium in the 10-100 µM range (Salkoff *et al.*, 2006). Recently a gain-of-function mutation causing an epileptic phenotype has been localised to this region (Du *et al.*, 2005).

A candidate RCK2 region of ~160 amino acids (Kim *et al.*, 2006) excluding the high affinity Ca^{2+} bowl and based on sequence alignment to RCK homologous regions,

has been put forward built upon comparisons to the bacterial MthK channels that have two RCK domains, despite the sequence identity between BK RCK domains and prokaryotic RCK domains being very low (<20%) (Yuan *et al.*, 2010). Considering this, the location boundaries are still fairly uncertain and several studies have included the high affinity Ca^{2+} bowl within RCK2 (Yusifov *et al.*, 2008; Wu *et al.*, 2010; Yuan *et al.*, 2010). RCK2 contains a similar predicted secondary structure to RCK1 despite being smaller and has conserved hydrophobic residues that form a dimeric interface between the two RCK domains. This interface is strong and highly specific and crucially important for regulation of the channel (Yuan *et al.*, 2010). Deletion studies involving the RCK2 domain demonstrate a failure to generate ionic current however this could be restored by co-transfecting separate core and tail regions and was not due to decreased cell surface expression (Kim *et al.*, 2006) therefore it would appear that the RCK2 domain is essential for a functioning channel but not necessarily important for channel assembly.

1.4.3.2 The calcium bowl

The BK channel is dynamically regulated by calcium binding which modulates the voltage required to activate the channel inducing a leftward shift to more negative potentials and into a more physiological range. These unique properties that make the voltage-sensitive component of the channel additionally sensitive to intracellular calcium have been attributed to the large intracellular C-terminus. Even though the entire channel α-subunit does not contain any established calcium binding motifs, the channel is still responsive to a few hundred nanomolar of calcium (Bao *et al.*, 2004). The tail region which comprises the last one-third portion of the C-terminus (S9-S10), shows the highest sequence conservation in the entire channel peptide among species (Wei *et al.*, 1994). This region has a series of highly conserved negatively charged aspartate (D) residues that determine the calcium sensitivity of the channel, hence this region has been termed, the calcium bowl (Schreiber & Salkoff, 1997). Mutations in the calcium bowl alter the high-affinity sensing of calcium by the channel by approximately half (Bian *et al.*, 2001; Bao *et al.*, 2002; Xia *et al.*, 2002). Experiments have demonstrated that transferring the portion of the C-terminus that contains the calcium bowl to a calcium insensitive channel, such as

SLO-3, confers calcium sensitivity to the channel (Schreiber *et al.*, 1999). Binding assays have additionally proven that calcium does indeed bind to the tail region of the BK channel, as mutation of the five calcium bowl aspartic acids inhibit binding (Bian *et al.*, 2001). It was proposed that a direct correlation was found between the biochemical measurement of Ca^{2+} binding to the tail domain and the Ca^{2+}-dependent activation of a BK channel. However, mutations in the calcium bowl revealed that the BK channel must contain a second calcium binding site, which was subsequently identified to be located in the RCK1 domain (Bao *et al.*, 2002; Xia *et al.*, 2002; Zeng *et al.*, 2005). Mutations in both high affinity calcium sites (residue M513 in RCK1 and D895 and D897 in the calcium bowl) eliminate all high affinity Ca^{2+} binding (Bao *et al.*, 2004; Yuan *et al.*, 2010). Physiologically, the high affinity calcium sites can be saturated over a range of 70 – 100 µM intracellular free calcium and once this calcium-dependant component determined by the tail domain is saturated, the channel gating behaviour is determined solely by the core domain (Wei *et al.*, 1994). Additional to the high affinity sites in the BK channel, concentrations of calcium or other divalent cations in the 100 µM to 100 mM range, produce distinct effects on channel gating that have been attributed to non-selective, low affinity binding sites (Horrigan & Aldrich, 2002). Crystallographic structural studies have since indicate that the Ca^{2+} bowl is located within the RCK2 domain and may have evolved from a helix in the RCK2 domain. These studies have also suggested that Ca^{2+} binding occurs at the assembly interface deep within the RCK1 and RCK2 dimer (Yuan *et al.*, 2010). The proposed structure of the BK channel calcium bowl is illustrated in the next section (see section 1.5 and Figure 1.10B).

1.4.3.3 The gating ring theory - the S6-RCK1 linker

In BK channels, it is proposed that the two RCK domains on each α-subunit create an octameric complex forming a gating ring similar to that described in bacterial MthK channels (Jiang *et al.*, 2001; Jiang *et al.*, 2002b). The gating domain is physically coupled to the pore by the S6-RCK1 linker and mechanically alters the conformation between the channel's open and closed state (Figure 1.7A). Activation of the voltage-sensing domain in the BK channel will change the conformation of the channel to open the pore. This will decrease the length of the linker-gating ring

Figure 1.7
Spring-based gating mechanism for BK channels

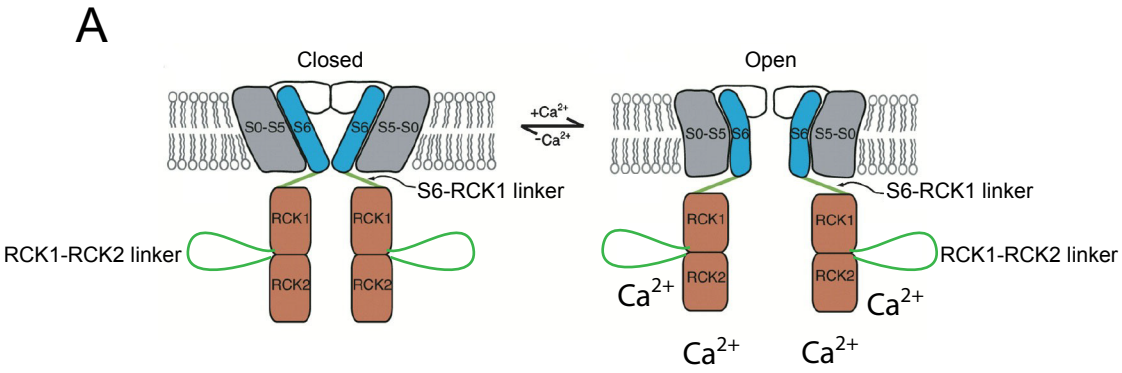

Jiang *et al.*, 2002 Nature

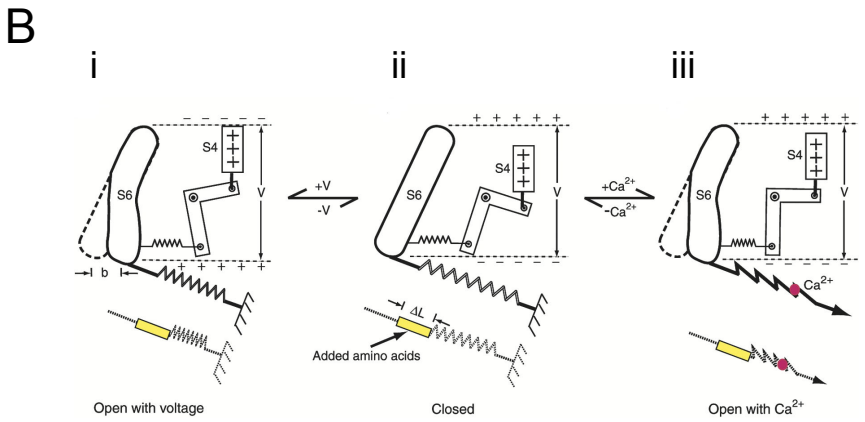

Niu *et al.*, 2004 Neuron

Figure 1.7. Spring-based gating mechanism for BK channels. (A) The proposed gating mechanism of a voltage- and calcium- activated K+ channel. The addition of Ca^{2+} expands the gating ring, pulling on the linker that tethers the RCK1/RCK2 gating ring to the S6 domain, pulling the inner helices apart to open the pore (Jiang *et al.*, 2002). (B) In the drawing, the S6 gate and S4 voltage sensor from a single subunit are shown. The linker-gating ring complex is represented by an intracellular spring that is directly attached to the S6 gate. The charged S4 voltage sensor is indirectly connected to the S6 gate through a spring. (i) Depolarization moves the charge on the S4 voltage sensor outward, opening the S6 gate, (ii) Increasing the linker length would decrease the opening forces. (iii) Ca^{2+} opens the channel by turning the passive spring of the linker-gating ring complex into an active force-generating machine (Niu *et al.*, 2004).

complex (Figure 1.7Bi). In the absence of calcium and voltage, the linker-gating ring complex forms a passive spring (Figure 1.7Bii). The spring is not expected to be slack as small changes in length have been shown to dramatically change channel activity, presumably directly changing the 'spring' tension in this region. Binding of calcium expands the gating ring, pulling on the linker that tethers the RCK1 ring to the S6 domain and pulling the inner helices apart to open the pore (Jiang *et al.*, 2001; Dong *et al.*, 2005) (Figure 1.7Biii). It is probable that the free energy from calcium binding to the channel is converted in to mechanical work changing the passive spring into a force-generating machine to open the pore (Yusifov *et al.*, 2008).

This model couples both the voltage sensing ability of the channel and the calcium sensing domain through the S6 gate allowing both independent and synergistic activation of the channel by voltage and calcium, the properties synonymous with the BK channel.

1.4.3.4 The RCK1-RCK2 linker

The linker between the RCK domains, the RCK1-RCK2 linker (see Figure 1.3), has also been implicated in the gating kinetics of the BK channel. It varies in length from sea urchin to human by ~100 to 240 amino acids taking into account multiple splice variants generated in this region and may be of structural importance despite poor evolutionary conservation (Lee *et al.*, 2009a). However, studies have predicted that the RCK1-RCK2 linker has no regular secondary structure (NORS). In crystallisation studies the RCK1–RCK2 linker could not be detected by electron density which was suggested as consistent with the region being unstructured (Wang & Sigworth, 2009; Wu et al; 2010; Yuan *et al.*, 2010).

In a study examining the length of the RCK1-RCK2 linker it was found that linker length rather than the specific amino acid sequence of the linker was important for functionality of the channel. Shortening of the RCK1-RCK2 linker reduced channel activity possibly by increasing the strain on the gating machinery or altering the dynamics of the interface between the two RCK domains. Lengthening the RCK1-RCK2 linker apparently did not have any effect on channel function. Hence it would

appear that the RCK1-RCK2 linker may play an important role in the dynamics of the interaction between the two RCK domains and the role they play on channel gating (Lee *et al.*, 2009a). Interestingly, the crystal structure explains why length of the linker may be important; the end of RCK1 using crystal structural analysis is a long distance away from the beginning of RCK2 (this is illustrated later in Figure 1.10) (Yuan *et al.*, 2010).

The RCK1-RCK2 linker is known to contain at least 3 sites of alternative splicing (Tseng-Crank *et al.*, 1994). In the light of the linker length theory in gating kinetics, it would be interesting to examine how splice insertion of, for example the 58 amino acid STREX insert at splice site C2 might affect the gating mechanism. It is conceivable that evolutionary retained splice sites may enforce a structural change, perhaps creating secondary structure in this region that could change the gating properties of the channel, perhaps changing the assembly interface between the two RCK domains. A study looking at the effect of stretch activation of the BK channel containing the alternatively spliced STREX insert in the RCK1-RCK2 linker, demonstrated that mechanical forces generated by membrane stretch can be detected via the STREX motif, leading to an open conformation of the channel (Naruse *et al.*, 2009) suggesting the possibility of some sort of interaction with the plasma membrane, but more importantly a possible role for the linker in controlling channel activity.

1.4.3.5 The C-terminus, a necessary component?

In the previous sections it has become clear that the C-terminus of the BK channel is important for normal channel function. Studies involving truncation of the entire C-terminus, three residues after the S6 transmembrane domain, show no evidence of channel tetramerization, cell surface expression or functional channels (Schmalhofer *et al.*, 2005). It appears that there is a crucial component to the functioning core region of the BK channel that necessitates the inclusion of the S0-S8 region (amino acids 1-652 as described by (Schmalhofer *et al.*, 2005)). When the tail region is functionally expressed as a separate domain and expressed in oocytes, patches that contain the S0-S8 core of the channel can be “cross-crammed” into these oocytes creating functional channels within minutes and suggesting that the C-

terminal domain must be cytosolic (Meera *et al.*, 1997). Experiments involving murine and Drosophila BK channels that have different affinities for calcium, also suggest that functional channels can be produced, even if the core and tail regions expressed are from different species (Wei *et al.*, 1994). This is consistent with the proposed role of the RCK1 domain as part of a linker-gating ring that must be attached to the pore S6-linker to be able to transmit the energy necessary for channel opening (Schmalhofer *et al.*, 2005).

Controversially, it has been suggested that BK channels truncated at the base of the S6 domain can form functional channels and also retain their calcium-sensing ability (Piskorowski & Aldrich, 2002). It remains to be seen whether this finding can be replicated, as it may be that there was some endogenous expression of BK channel that may have rescued the truncated channel, or indeed if this finding does hold true then it is possible that perhaps calcium binding sites are not present solely in the C-terminus but may also exist within the core region of the channel, perhaps masked by the normal folding of the protein and only revealed upon truncation, although this does seem very unlikely.

1.5 The 3D structure of the BK channel

So far I have described the topological aspects and functional domains of the BK channel with a little information on the structure of the inner pore based on studies from bacterial K^+ channels (MacKinnon, 2004a). In the following section I would like to discuss some of the seminal structural studies that have aided our recent understanding of the BK channel. In the last year or so there has been three or four key studies that have defined the BK channel structure. Studies from Fred Sigworth's lab using electron cryomicroscopy, demonstrated the first structural insight to the BK channel at a resolution of ~1.7-2.0 nm (Wang & Sigworth, 2009). These structural observations correlated well with studies that used disulphide cross-linking to identify the positions of the transmembrane domains in the BK channel (Liu *et al.*, 2010). Subsequent to Fred Sigworth's cryo-EM model, Roderick MacKinnon who won the Nobel prize for his work on the structure of ion channels, turned his attention to the BK channel describing the gating apparatus of the human

Figure 1.8
Cryo-EM structure of the BK channel

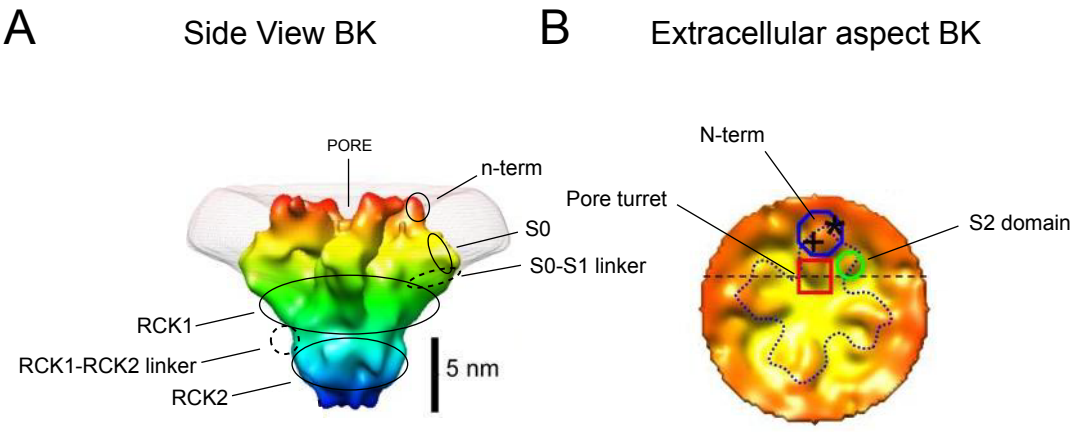

Wang & Sigworth, 2009 Nature

Figure 1.8. Cryo-EM structure of the BK channel. (A) Side view surface rendering of the membrane-subtracted BK channel map, obtained from 3,400 images of particles in large vesicles. Superimposed is the membrane density (mesh). The colour indicate the various predicted regions in accordance with comparisons with known crystal structures of Kv and MlotiK channels. For illustrative purposes dashed circles represent the probable position of S0-S1 linker and the RCK1-RCK2 linker with solid circles indicating the probable location of the identified domains. Scale bar illustrates size of the C-terminus and the approxiamate distance of the RCK1-RCK2 interface from the plasma membrane (B) Extracellular aspect of the membrane-restored reconstruction of BK. Protrusions are identified corresponding to the pore domain (red box), S2 voltage sensing domain (green circle) and S0-N terminus region (blue circle).

BK channel at a much higher resolution of 3.0 Å (Yuan *et al.*, 2010), with a parallel study from one of MacKinnon's previous colleagues Youxing Jiang confirming the structural arrangement of the C-terminus also at 3.1 Å (Wu et al; 2010).

Prior to Fred Sigworth's model of BK (Wang & Sigworth, 2009), the only information on the BK channel structure was through indirect studies on homologous prokaryotic K^+ channel structure through sequence alignment despite a very low sequence identity (<20%). Using a novel technique called electron cryomicroscopy (cryo-EM) (Frank, 2006) Wang & Sigworth expressed channels in lipid vesicles frozen in vitreous ice and imaged by electron microscope. They then summated images from around 8,400 individual protein particles, analysed them and created a 3D reconstruction of the BK channel at a resolution of 1.7-2.0 nm (Figure 1.8A). In their "membrane restored" cryo-EM map of the extracellular face of BK (Figure 1.8B) they identified protrusions corresponding to the turret region of the pore domain (red square), the S2 helix of the voltage sensor (green circle) which concurs with crystal structural analysis of both Kv1.2 and MlotiK1 X-ray structures (Long *et al.*, 2005; Clayton *et al.*, 2008) and a much larger protrusion not present in voltage gated K^+ channel structures at the periphery of the voltage sensing domain, the S0 domain with its extracellular N terminus of ~40 residues. They suggested that the S0 domain appeared to be in contact with the S2 and S3 domains, consistent with a recently revised cross linking study (Liu *et al.*, 2008; Liu *et al.*, 2010).

The position of the transmembrane domains of the BK channel has also recently been identified by Guoxia Liu *et al*, (Figure 1.9) using disulphide cross-linking to identify the proximities of cysteine substitutions in the extracellular flanks of the transmembrane domains. They have shown that the S0 domain is located outside of the S1-S4 bundle and is more closely associated with the S3 and S4 domains (see Figure 1.9) (Liu *et al.*, 2010), which they identified as inconsistent with their previous inference that the extracellular end of the S0 domain is between the S2 and S3 domains (Liu *et al.*, 2008). Using the Kv1.1/Kv2.1 channel structure they superimposed the extracellular ends of the S0-S6 domains to illustrate the proximities of each transmembrane domain in the BK channel (Figure 1.9A). A side view of the voltage-gated K^+ channel illustrates the position of transmembrane domains in the membrane which would be a similar arrangement in the BK channel however with an additional S0 domain (Figure 1.9B).

Figure 1.9
The positions of the transmembrane domains in the BK channel

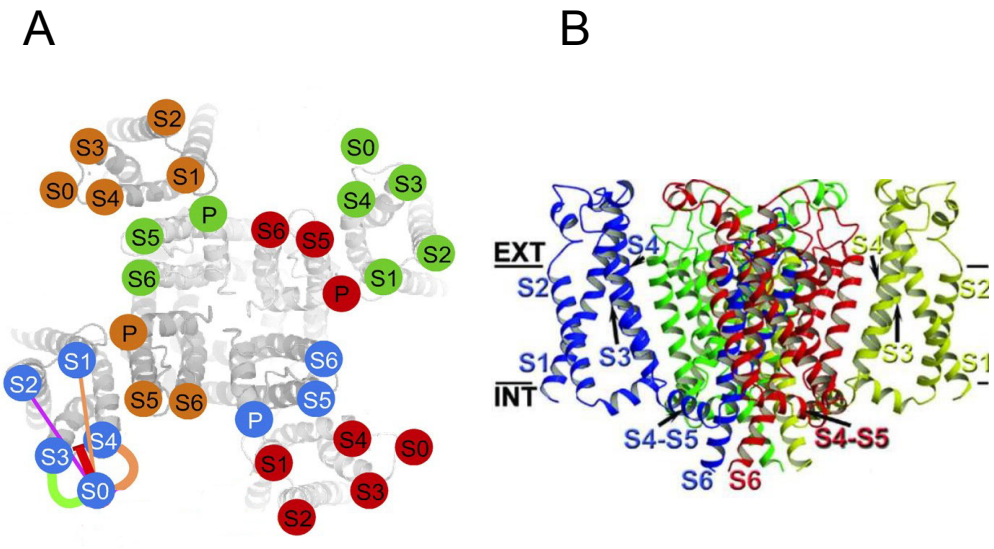

BK channel extracellular view
Liu *et al*, 2010. J. Gen. Physiol.

K^+ channel structure side view
Yarovoy *et al*, 2006. PNAS.

Figure 1.9. The positions of the transmembrane domains in the BK channel. (A) Extracellular view of the Kv1.2/Kv2.1 channel crystal structure with superimposed labelled circles uniquely coloured for each BK α-subunit, representing the approximate locations of the extracellular ends of S0-S6. Circles are based on the extent of cross-linking between cysteine residues in the extracellular loop linking transmembrane domains. Adapted from Liu *et al*., 2010. (B) View of the model in A from the side of the membrane (colours are not comparable). The model represents a Kv1.2 voltage-gated K^+ channel that is proposed to be similar in structure to the core region of the BK channel (Wang & Sigworth., 2009). The side profile demonstrates how the transmembrane domains position in the membrane around the central pore region. Adapted from Yarovoy *et al*., 2006.

Figure1.10
The structure of the BK channel intracellular C-terminus domain and proposed arrangement of the calcium bowl

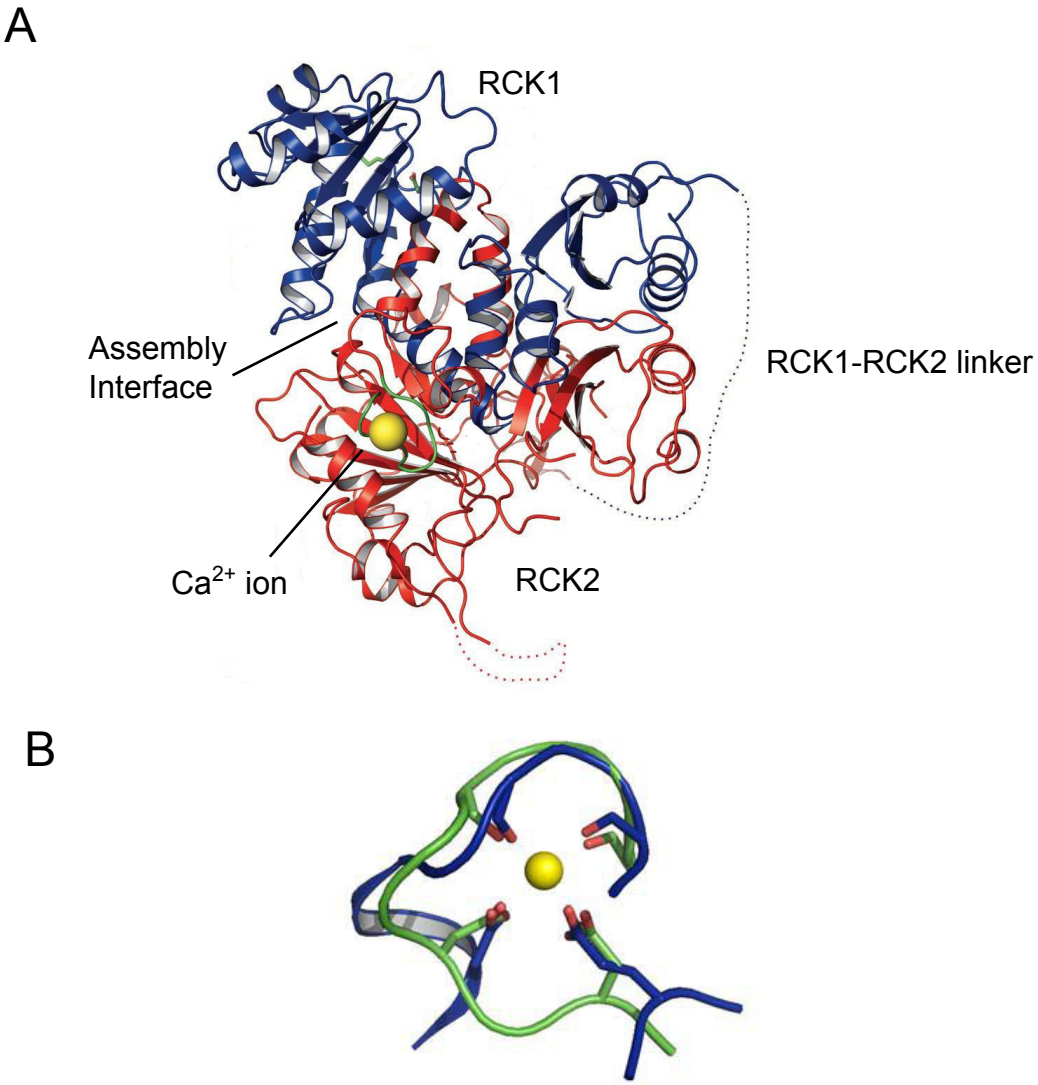

Yuan *et al*., 2010 Science

Figure 1.10. The structure of the C-terminus Domain. (A) Secondary structure of the human BK C-terminus from the crystal structure in ligand bound state (50 mM calcium) illustrating RCK1 (in blue) and RCK2 (in red) with unresolved segments indicated by dashed lines. The position of the RCK1-RCK2 linked is indicated. The Ca^{2+} bowl is indicated by a green line with a Ca^{2+} ion illustrated by a yellow sphere. (B) Superposition of the Ca^{2+} bowl from the human BK C-terminus (green) and the Ca^{2+} binding site from the calpain-1 catalytic subunit (blue) that has been previously defined, illustrating the modelled shape of the BK channel Ca^{2+} bowl.

To go back to the model of Wang and Sigworth, they were able to conclude that the pore and voltage sensing regions of the BK channel were similar to that seen in the crystal structures of the 6-TM voltage-gated K^+ channels (Long *et al.*, 2005; Long *et al.*, 2007). They then described the large C-terminal domain which composes the gating ring and the tail region which would contain the calcium bowl (Figure 1.8A) and suggested that the smaller second RCK domain (RCK2) in the BK channel can be seen in the lower mass of the gating ring, illustrated by the tapered channel structure (Figure 1.8A) (Wang & Sigworth, 2009).

Building upon the Wang and Sigworth model, the recent study from Roderick Mackinnon's lab described the crystal structure of the C-terminus of the BK channel by expressing residues 341-1056 in insect cells (*Spodoptera Frugiperda*), at much higher resolution of 3.0 Å (Yuan *et al.*, 2010)(Figure 1.10) in 50 mM calcium (ligand bound). In their model Yuan *et al*, describe the tandem RCK domains folded tightly against one another forming a more extensive interface than their prokaryotic counterparts. As previously mentioned (see section 1.4.3.4) the inability to define the electron density for the long linker connecting RCK1 and RCK2 is consistent with this region being unstructured, but they identify that length would be important as the end of RCK1 is located a long distance from the beginning of RCK2 (Figure 1.10A). Crucially it was suggested that the calcium bowl is not distal to the RCK2 domain, but an integral structural element of it and located at the assembly interface between the RCK domains (Figure 1.10A & B) (Yuan *et al.*, 2010).

The second major structural study which came from Youxing Jiang's lab extensively detailed the BK C-terminal structure at the assembly interface in a calcium free state (ligand un-bound) suggesting that calcium binding could trigger conformational changes at the assembly interface leading to channel activation. They also identified the three Ca^{2+} binding sites in their model and by including the S6-RCK1 linker in the structural study were able to generate a model for the full channel by docking the C-terminal domain of the BK channel to the homologous crystal structure of a Kv1.2 S1-S6 channel (Figure 1.11) (Wu et al; 2010).

Figure1.11
The proposed crystal structure of the BK channel

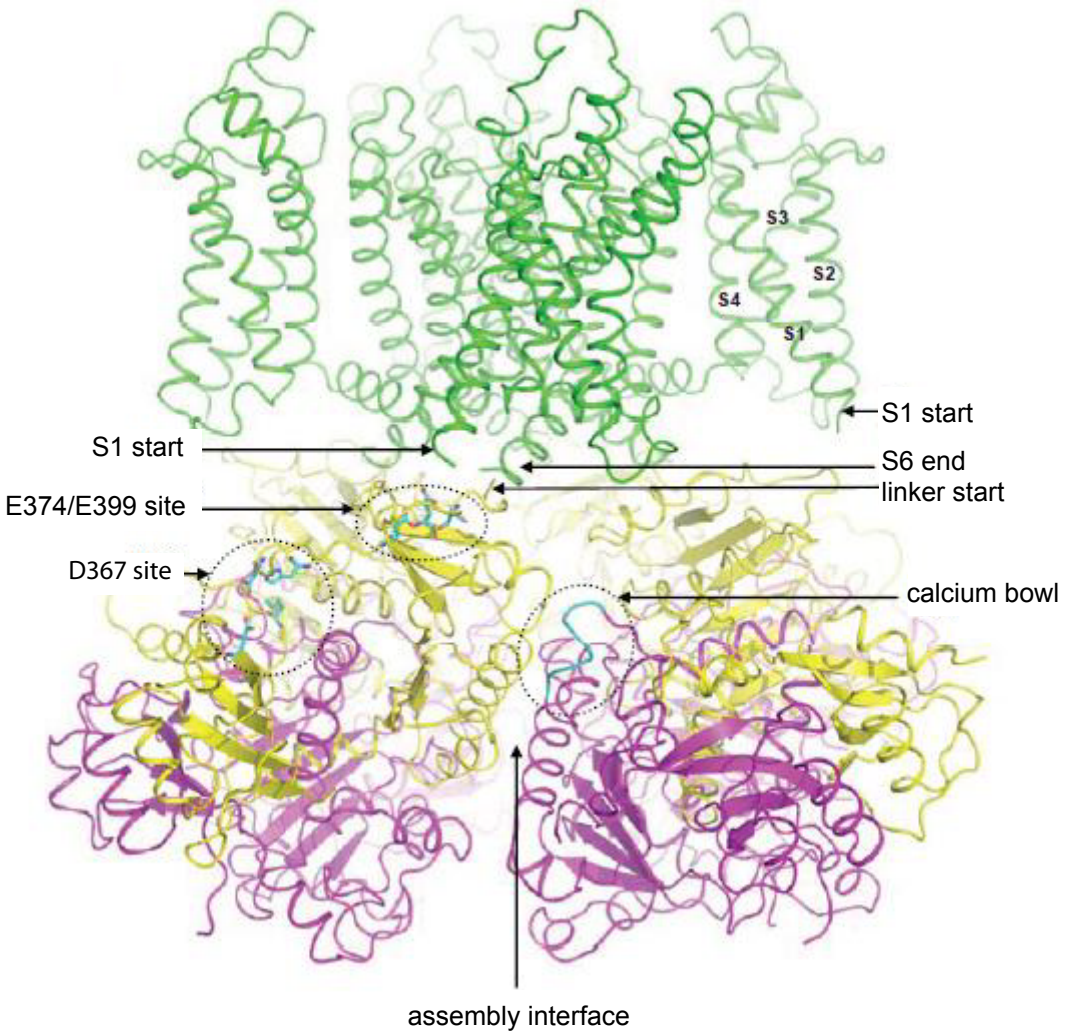

Wu *et al.*, 2010 Nature

Figure 1.11. The proposed crystal structure of the BK channel. A ribbon representation of the BK channel tetramer viewed from the side (Wu *et al*., 2010). The Kv1.2 S1-S6 crystal structure (green) is docked atop of the BK gating ring with the RCK1 and RCK2 domains coloured yellow and magenta, respectively. The C-terminus was resolved in a ligand un-bound state (calcium free). All three Ca^{2+} binding sites are circled. The Ca^{2+} bowl loop on RCK2 is coloured cyan.

1.6 The dynamic regulation of BK channels

The BK channel pore forming α-subunit is encoded only by a single gene (Slo, KCNMA1), forming a channel consisting of four α-subunits arranged around a central K^+ conducting pore. The α-subunit has high amino acid sequence identity (~98%) in mammals (Lu *et al.*, 2006) unlike other voltage-gated ion channels that have a variety of isoforms arising from multiple genes. Functional diversity of the BK channel can be achieved by a combinatorial association with regulatory β-subunits, variation in the usage of alternative splicing within the KCNMA1 gene, the formation of heterotetrameric channels composed of multiple splice variant α-subunits and co-translational as well as post-translational mechanisms. These additional mechanisms can influence channel activity through voltage sensitivity and calcium sensitivity, regulate the activation and deactivation rates that control cellular excitability and control trafficking of the channel protein to enable functional expression at the plasma membrane.

1.6.1 Regulatory β- subunits

The BK channel can achieve functional diversity through an association with auxiliary β-subunits (Brenner *et al.*, 2000b; Orio *et al.*, 2002; Lippiat *et al.*, 2003). The β-subunit was first cloned from bovine smooth muscle (Knaus *et al.*, 1994b; Knaus *et al.*, 1994c; Knaus *et al.*, 1994d) and subsequently named β1. Since then a family of four β-subunits have been identified each with a different tissue distribution and different effects on BK channel pharmacology and gating including the β2 subunit (Bentrop *et al.*, 2001), the β3 subunit (Xia *et al.*, 2000) and the β4 subunit (Brenner *et al.*, 2005). Moreover, β-subunits have also been implicated in trafficking of BK channels and expression at the cell surface (Toro *et al.*, 2006; Kim *et al.*, 2007b).

The β-subunits are membrane spanning proteins containing intracellular N- and C-terminal domains with two transmembrane domains, separated by a large extracellular loop (Jiang *et al.*, 1999)(Figure 1.3). The diversity required for tissue specific roles of the BK channel can in part be achieved by the tissue specific

expression of the regulatory β-subunits (Jiang *et al.*, 1999). Interestingly, it appears that BK β-subunits have not been identified in Drosophila or C.elegans (Orio *et al.*, 2002), suggesting that their expression may represent an adaption evolved to regulate BK channels in different tissues, in more complex vertebrate organisms.

In determining the region within the BK channel that is involved in β-subunit modulation, a Drosophila BK channel (*dSlo*) that is unresponsive to the β-subunit was studied with different chimeric regions of the human BK channel (*hSlo*) (Wallner *et al.*, 1996). Human BK channels purified from smooth muscle have been seen to be tightly associated with an accessory β-subunit that dramatically increases open probability (β1). It was found that the 31 amino acids at the N-terminus of the human BK channel, which include the S0 transmembrane domain, when explanted into the Drosophila BK channel, were critical for β-subunit modulation in BK channels (Wallner *et al.*, 1996). Therefore, it seems that the S0 domain of the pore-forming α-subunit of the BK channel is important for facilitating the regulatory effects of β-subunits (Wallner *et al.*, 1996; Meera *et al.*, 1997; Liu *et al.*, 2008; Wu *et al.*, 2009; Liu *et al.*, 2010). The additional S0 domain in the BK channel may represent part of the evolutionary adaptation within the α-subunit for effective regulation of the channel by these regulatory domains.

The β-subunits contribute greatly to the diverse phenotype associated with the BK channel through the control of calcium sensitivity, channel gating and pharmacology allowing the BK channel to play important physiological roles in different tissues with different β-subunit expression profiles around the body. Downregulation of the β1 subunit, primarily expressed in smooth muscle, is associated with elevated blood pressure (Brenner *et al.*, 2000a) and phasic contractions in bladder (Petkov *et al.*, 2001) with gain of function mutants suggested to be protective against diastolic hypertension (Fernandez-Fernandez *et al.*, 2004). The β2 subunit selectively expressed in chromaffin cells and the brain, demonstrates fast ‘ball and chain’ type channel inactivation (Bentrop *et al.*, 2001). The β3-subunit, structurally similar to β1 and β2 and mainly expressed in testis, pancreas and spleen, also confers rapid inactivation (Xia *et al.*, 2000). The β4 subunit is expressed predominantly in brain can effect BK channel regulation of neuronal excitability with dysfunction leading to temporal lobe seizures (Brenner *et al.*, 2005). The differing functions and locations of the β-subunits, illustrate how they can finely tune the gating properties of the BK

channel and modulate the functional diversity required of the channel around the body.

1.6.2 Alternative splicing – diversifying channel function

Functional complexity within the mammalian genome can be achieved by a process of alternative splicing. When the human genome project had finished mapping the human genome, surprisingly they identified far fewer genes (~30,000) than the earlier molecular predictions (of over 100,000 genes) that were expected to contribute to the higher complexities of the human organism (Claverie, 2001; Venter *et al.*, 2001). In fact by examining the number of genes, the human organism would appear to be only about five times as complex as a bacterium such as Pseudomonas aeruginosa (Claverie, 2001). With only about 1.5% of the human genome actually coding for functional proteins, non-coding “introns” that separate the coding sections called “exons” along with non-coding RNA and miscellaneously named “junk DNA”, make up the rest of the genome. However, alternative splicing accounts for the complexity required in the vertebrate genome.

The DNA sequence is represented by primary RNA transcripts which are then processed to remove non-coding introns so that the coding sections (exons) can be spliced together for generation of mature RNA which will then be transcribed into a functional protein (Figure 1.12). Alternative splicing can modify proteins by including or excluding specific coding sections within the gene creating distinct protein products. Alternative splicing is seen in nearly all metazoan organisms as a means for producing functionally diverse polypeptides from a single gene (Lopez, 1998). The diversity that splicing can create is exemplified in Drosophila, whereby alternative splicing of one gene (DSCAM) can produce nearly three times the number of proteins as would be encoded by the entire fly-genome (Black, 2000). This illustrates how splicing can effectively increase the coding capacity of a gene creating wide ranging functional diversity. Alternative splicing can also dynamically regulate the on-off gene expression switch by the introduction of premature stop codons within spliced exons (Smith & Valcarcel, 2000). Computer algorithms have predicted that splicing occurs in the genome far higher than expected and it would

Figure1.12
Overview of pre-mRNA alternative splicing

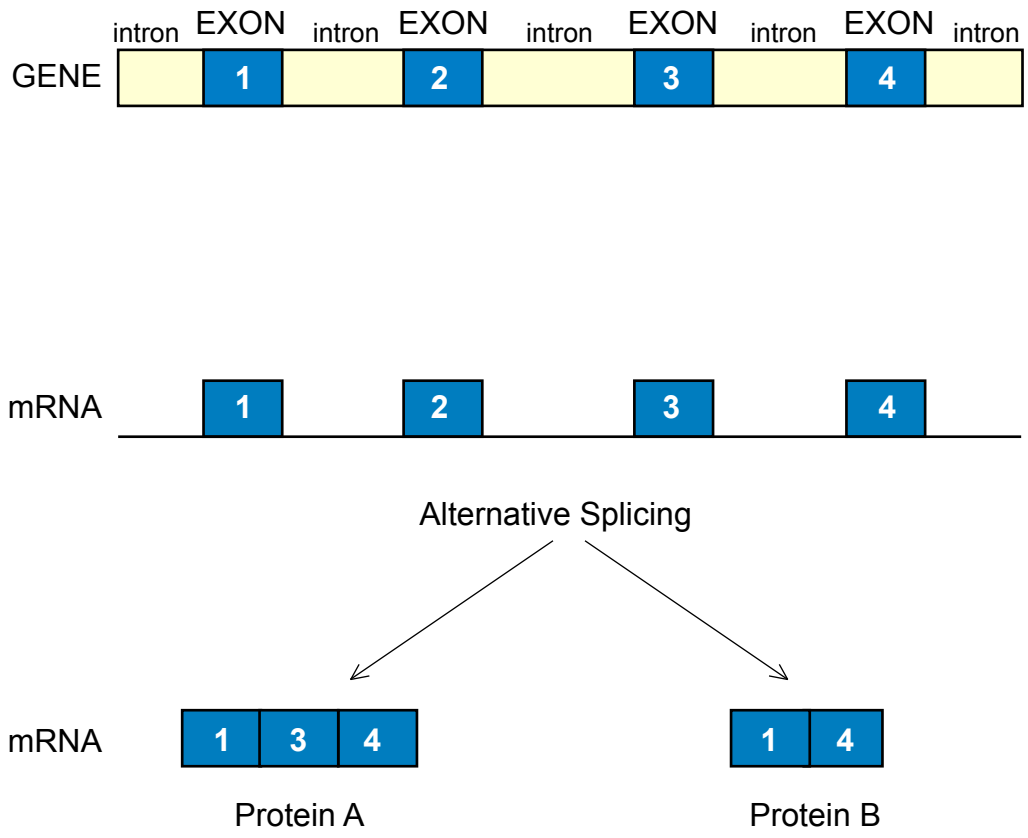

Figure 1.12. Overview of pre-mRNA splicing. A gene contains numerous exons and introns. Exons are the coding regions of the genome and can be spliced together in different ways. Exons 1-4 may be included or excluded from the mature mRNA generating different products. Alternative splicing allows selection of particular exons to generate functional diversity within a protein. The different forms of the mRNA are called transcript variants, splice variants, or isoforms.

appear that nearly every gene in the human genome may be spliced (Fodor & Aldrich, 2009).

Alternative splicing of ion channels has an important role in generating functional diversity. To pose an evolutionary question as to the function of splicing, it would appear that evolutionary progress has favourably retained the splicing mechanism for generating protein diversity over the evolution of new paralogues of ion channels. This crucially allows cells to directly regulate channel properties on a fast timescale and in a more precise manor than would be possible if transcription of one gene needed to be repressed and transcription of another initiated (Copley, 2004).

1.6.2.1 Alternative splicing in the BK channel

Differential splicing of BK channel RNA transcripts represents a mechanism for generating diversity from the single gene (KCNMA1) that codes the channel. Distinct phenotypes can be regulated by alternative splicing of the channel such as auditory tuning (Rosenblatt *et al.*, 1997; Beisel *et al.*, 2007) and neuronal excitability (Tseng-Crank *et al.*, 1994). Indeed numerous alternatively spliced variants of the BK channel have been identified (Lagrutta *et al.*, 1994; Xie & McCobb, 1998; Zarei *et al.*, 2001; Erxleben *et al.*, 2002b; Chen *et al.*, 2005; Fodor & Aldrich, 2009) that control multiple aspects of channel function. Generally the KCNMA1 gene is highly conserved consisting of around 35 exons, 27 of which are constitutive with the remainder being alternatively regulated (Figure 1.13). The entire coding region of the BK channel spans about 750 kb of the human genome (Lu *et al.*, 2006). Comparison of KCNMA1 cDNAs from a number of different vertebrate species suggest that there are up to 8 alternative sites of splicing that result in two or more changes of amino acid sequence, along with additional species-unique splice variants (Tseng-Crank *et al.*, 1994; Korovkina *et al.*, 2001; Zarei *et al.*, 2001; Zarei *et al.*, 2004; Beisel *et al.*, 2007). Some splice sites are found in the amino terminus (N1-N2) of the BK channel although the majority are located in the carboxy-terminus (C1-C5) (Tseng-Crank *et al.*, 1994).

In the BK channel alternative splicing has been demonstrated to play an important role in modifying channel function by altering calcium- and voltage- sensitivity

Figure 1.13
Intron-exon structure map of murine BK channel and alternative splice sites

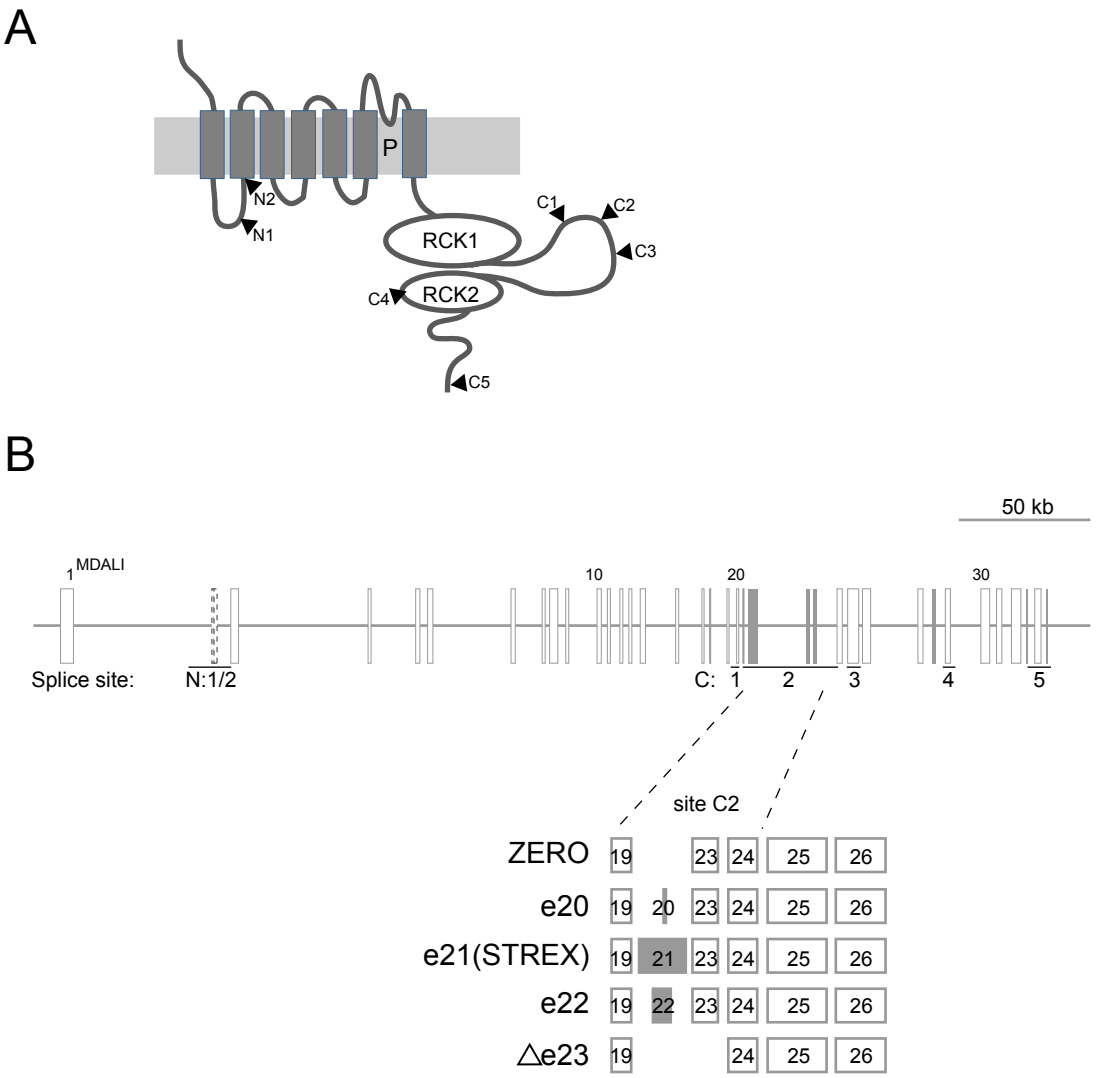

Figure 1.13. Intron-exon structure map of murine BK channel and alternative splice sites. (A) Topology of BK channel illustrating alternative splice sites in the N-terminus (N:1-2) and C-terminus (C:1-5). (B) Predicted intron-exon structure of mouse KCNMA1 gene. Constitutive exons are shown as open boxes and alternative spliced exons in splice site C2 are shaded grey. Exon 1 contains the initiator start methionine of MDALI.., Location of C-terminus splice sites are shown, numbered C1-5, N-terminal sites are shown, number N1-2. Expanded view across splice site C2 illustrates spliced exons for each of the five identified splice variants at this site. (Information summated from references: Tseng-Crank *et al*., 1994; Korovkina *et al*., 2001; Zarei *et al*., 2001; Chen *et al*., 2005; Beisel *et al*., 2006; Fodor & Aldrich, 2008). The approximate length of the genome is indicated.

(Adelman *et al.*, 1992; Lagrutta *et al.*, 1994; Tseng-Crank *et al.*, 1994; Saito *et al.*, 1997; Shipston *et al.*, 1999; Ha *et al.*, 2000), regulating protein phosphorylation (Tian *et al.*, 2001; Tian *et al.*, 2004) and other intracellular signalling cascades (Tian *et al.*, 2001; Erxleben *et al.*, 2002a) as well as controlling cell surface expression (Zarei *et al.*, 2001; Kwon & Guggino, 2004; Zarei *et al.*, 2004).

1.6.2.2 The STREX splice variant

In the BK channel, splice site C2 is located in the linker region between the RCK1 and RCK2 domains of the intracellular C-terminus (Figure 1.3) and has been shown to have five distinct splice variants that can be inserted at this site, some of which influence the channel phenotype. The insertless variant, referred to as the ZERO variant, results from splicing of exon 19 to exon 23, an e20 variant has a 3 amino acid 'IYF' insert includes exon 20 between exon 19 and exon 23. The e21 variant has a 58 amino acid insert from inclusion of exon 21 between exon 19 and 23 and the e22 variant has a 29 amino acid insert from inclusion of exon 22 between exon 19 and 23. The e23 variant skips exon 23 which results in splicing of exon 19 to 24 leading to a frameshift and a truncated channel that is not expressed at the plasma membrane (Chen *et al.*, 2005)(Figure 1.13). These splice variants can have a significant effect on the functional properties of the channel (Chen *et al.*, 2005; Saleem *et al.*, 2009).

The e21 variant, highly conserved from human to zebrafish, encodes a cysteine-rich domain of 58 amino acids that confers an apparent increased Ca^{2+} sensitivity to the BK channel and was first defined in 1997 (Saito *et al.*, 1997). Subsequently, it was identified that the number of channels containing this 58 amino acid splice insert, relative to channels without an insert at the C2 site, could be modulated by the hypothalamic-pituitary-adrenal (HPA) stress axis (Xie & McCobb, 1998). They henceforth named this exon, the STRess axis-regulated EXon, or STREX.

The STREX insert has been previously shown to contain a PKA phosphorylation serine site (S636) that mediates channel inhibition (Tian *et al.*, 2004) and a 'CSC' motif that confers hypoxic sensitivity to BK channels (McCartney *et al.*, 2005). Therefore the STREX insert has already been shown to have an important role in

tuning BK channel properties. However, the molecular basis for the apparent increased Ca^{2+} sensitivity is unknown. The cysteine rich composition of STREX when included in the RCK1- RCK2 linker within the C-terminus of the BK channel, generates a cysteine rich domain (CRD) that incorporates the upstream haem-binding domain (hbd) (see Figure 3.1), although the role of this domain is not known. STREX also introduces a series of basic residues to a region that already has an appreciable positive charge, although whether this region may also be a functional polybasic domain has also not been examined. Some of the additional features described that may underlie the mechanism that defines the STREX channel phenotype will be explored in this thesis.

The tissue distribution of the STREX channel variant suggests that it is mostly prevalent in endocrine tissues such as the chromaffin cells of the adrenal gland, the pancreas and pituitary as well as the cerebellum, uterine smooth muscle, and prostate (Tseng-Crank *et al.*, 1994; Ferrer *et al.*, 1996; Saito *et al.*, 1997; Xie & McCobb, 1998; Shipston *et al.*, 1999; Chen *et al.*, 2005; Zhu *et al.*, 2005). It is largely absent from spinal cord tissue, the majority of smooth muscle cells and skeletal muscle.

It is clear that extrinsic factors influence splicing of the BK channel gene at splice site C2. A hypophysectomy (ablation of the hypothalamus) was shown to trigger an abrupt decrease (by 50%) in the proportion of STREX channel variants in relation to insertless ZERO channels in adrenal chromaffin cells where the BK channel is thought to play an important role in cellular excitability (Xie & McCobb, 1998). This effect could be rescued by injection of ACTH, a stress hormone secreted from the pituitary under hypothalamic control, thus implicating the endocrine-stress axis in the regulation of STREX inclusion. However, in chronic stress models which would be predicted to have an opposing elevation in splice insertion of the STREX exon, a modest decrease (~25%) in the proportion of STREX channel variants has been observed in adrenal tissue (McCobb *et al.*, 2003). In a more recent study of chronic stress, no significant change was observed in the relative number of STREX channel transcripts despite an observed increase in the total number of BK channel transcripts under stress conditions in adrenal chromaffin cells and a decrease in STREX was actually noted in the pituitary gland (Chatterjee *et al.*, 2009). In another study, ablation of the pituitary gland shifted the firing properties of adrenal

chromaffin cells from a more STREX-like to a more ZERO-like phenotype (Lovell & McCobb, 2001) which would certainly implicate the HPA-axis in the splicing decisions of the BK channel gene. Intriguingly, both gonadal (sex) and adrenal (stress) hormones that respond to stress have been shown to regulate the splicing decision of the STREX exon, with glucocorticoids (stress hormones) negatively affecting inclusion of STREX and androgens (sex hormones) promoting STREX inclusion (Lai & McCobb, 2002) to act as a mechanism to fine-tune chromaffin cell excitability. Conversely, there is evidence for both positive and negative regulatory control of BK channel gene splicing by the stress hormone glucocorticoid (Lai & McCobb, 2002). These studies suggest that multiple steroid hormones (glucocorticoids and adrenal androgens) that are able to respond to elevation in stress levels can regulate STREX splicing (Lai & McCobb, 2002).

The antitheism seen in some of the hormonal studies described, may relate to the age of the animal studied and the distinct possibility that splicing is more plastic earlier in life (Lai & McCobb, 2002). Certainly, developmental changes have been described across the brain during which the proportion of STREX channels is highest in the early embryonic stage and then undergoes significant developmental downregulation, relative to increasing total BK expression, during postnatal stages (MacDonald *et al.*, 2006). This dynamic control of splicing decisions observed would be expected to have a significant role in the activity, plasticity and/or connectivity during neuronal development of the developing organism.

Speculatively, the downregulation of STREX channel transcripts may relate to a specific down-scaling of cell excitability perhaps linked to passive coping mechanisms in the developing organism as it proceeds into postnatal life (McCobb *et al.*, 2003). Whether splice regulation could contribute to coping mechanisms in response to stress in adult mammals would certainly be interesting to investigate.

Alternative splicing is a powerful mechanism to directly regulate BK channels precisely, inferring wide ranging functional properties on a fast timescale. Splicing allows the channel to be specifically modulated for specific cell types, at different developmental stages and in response to different physiological inputs.

1.6.3 Post-translational modifications

Proteins including ion channels are regulated by various post-translational modifications which tune protein function specific to the requirements of different cell types. They include lipid modifications such as palmitoylation and myristoylation (Resh, 2006a) and modulation by phosphorylation at serine, threonine or tyrosine residues (Levitan, 1994; Reinhart & Levitan, 1995; Shipston & Armstrong, 1996; Hall & Armstrong, 2000; Tian *et al.*, 2004; Tian *et al.*, 2008b; Zhou *et al.*, 2010).

1.6.3.1 Lipophilic modification of proteins

The covalent addition of lipid groups to proteins was first described for brain myelin by Folch and Lees in 1951 (Folch & Lees, 1951). It wasn't until nearly 30 years later that it was rediscovered that viral membrane glycoproteins contain covalently bound fatty acids (Schmidt *et al.*, 1979; Schmidt & Schlesinger, 1979). Indeed it has taken several more decades to understand the wide ranging significance of lipophilic modifications to proteins. Several hundred proteins have since been identified with covalently bound lipid groups. The three most common types of lipids to be attached to proteins are the fatty acids, isoprenoids and glycosylphosphatidylinositol anchors. These lipophilic additions regulate protein interaction with the plasma membrane and other proteins, as well as facilitating signalling and protein trafficking (Resh, 2006a). The addition of fatty acids to substrate proteins is a process called fatty acylation. The two most common forms of protein fatty acylation involve the covalent attachment of myristate (a 14-carbon saturated fatty acid) or palmitate (a 16-carbon saturated fatty acid). Myristoylation is a co-translational process and generally not reversible which occurs through amide linkages (*N*-acylation) to amino-terminal glycine residues. Palmitoylation, on the other hand, occurs by a post-translational mechanism through a thioester linkage (*S*-acylation) to specific cysteine residues. Palmitate, one of the most common fatty acid modifications, is unique in its ability to be dynamically regulated by reversible cycles of palmitoylation and de-palmitoylation.

1.6.3.1.1 Palmitoylation

Palmitoylation involves the attachment of palmitate through a thioester linkage to the sulfhydryl group of a cysteine residue in a target protein. This will increase the hydrophobicity of the protein and can therefore increase membrane association. Palmitoylated proteins can be classified into five general classes. 1) transmembrane proteins *S*-acylated on cysteines at or near the transmembrane domain. 2) Ras proteins where prior prenylation of the cysteine residue within the C-terminal is required for *S*-palmitoylation. 3) Proteins *S*-palmitoylated at one or more cysteines near the N- or C-terminus. 4) Members of the Src family of tyrosine protein kinases with a consensus sequence for dual acylation and 5) proteins including Hedgehog and the G-protein ($G_{\alpha s}$) subunit that contains palmitate covalently bound via an amide-linkage to an N- terminal cysteine residue (Resh, 1999, 2006a).

The diverse effects of palmitoylation on the modified protein are beginning to be understood more than just simply functioning to increase hydrophobicity and thereby membrane association, but also to regulate and specify membrane interactions, influence sorting, direct localisation to specific regions in the membrane (eg. lipid rafts), influence protein signalling, regulate protein trafficking and alter the functional properties of the protein (Resh, 1999; Bijlmakers & Marsh, 2003; Resh, 2006a). To examine the effect of pharmacological inhibition of protein palmitoylation, 2-bromopalmitate (2BP), a non-metabolizable palmitate analog is mainly used that blocks palmitate incorporation into proteins (Webb *et al.*, 2000). The mechanism responsible for 2BP mediated inhibition of protein palmitoylation is not known. It is possible that it binds to a palmitoyl transferase forming an inhibitor:enzyme complex. Alternatively, transfer of 2BP to the target cysteine may occur although the increased hydrophilicity of the bromine atom would reduce binding of the modified protein to the lipid bilayer (Resh, 2006c). It could also alter the lipid metabolism reducing the concentration of intracellular palmitoyl CoA pools. Despite the unknown nature of its actions it is an effective tool for studying the role of palmitoylation.

1.6.3.1.2 Palmitoyl Acyl Transferases

The enzymes responsible for the covalent addition of palmitate to target proteins have been elusive for a long time. Initially, genetic screening helped to identify the transferase enzymes in yeast that were involved in palmitoylation (Bartels *et al.*, 1999). These enzymes, referred to as palmitoyl acyl transferases or PATs, have a common topology and motif, comprising several transmembrane domains and an Asp-His-His-Cys (DHHC)-cysteine rich domain (CRD), hereafter referred to as a DHHC domain. The DHHC domain has been identified as the active palmitoyl transferase, as disruption of this motif by mutagenesis abolishes PAT activity (Fukata *et al.*, 2006). In mammalian genomes (human and mouse), 23 kinds of DHHC proteins are predicted (Fukata *et al.*, 2004; Ohno *et al.*, 2006). No DHHC domains have been identified in prokaryotes or archea, which coincides with the widespread occurrence of palmitoylation in eukaryotes and its apparent absence in prokaryotes (Mitchell *et al.*, 2006). To identify the PATs for a particular substrate, a systematic evaluation of all 23 DHHC proteins would be required. The prevalence of various pathological conditions in human, associated with mutations in DHHC proteins such as schizophrenia, Huntington's disease and X-linked mental retardation alongside various cancers make them attractive therapeutic targets of the future (Linder & Deschenes, 2007; Fukata & Fukata, 2010). The activity of palmitoylating enzymes (PATs) and de-palmitoylating enzymes called pamitoyl protein thioesterases (PPTs) are finely tuned and determine the palmitoylation status of the protein. In contrast to the large family of DHHC PATs, de-palmitoylating enzymes are limited and include acyl-protein thioesterase 1 (APT1), palmitoyl protein thioesterase 1 (PPT1) and PPT2 (Fukata & Fukata, 2010).

1.6.3.1.3 Palmitoylation - A diverse role in modulating ion channels

Recent studies have illustrated that ion channels can be reversibly modified by palmitoylation to regulate channel function, assembly, membrane targeting and steady state cell surface expression. Palmitoylation has been demonstrated to play a diverse role in the modulation of voltage sensing in the voltage-gated Kv1.1 channel by protein-membrane interaction (Gubitosi-Klug *et al.*, 2005) and the modulation of L-type Ca^{2+} channel (Chien *et al.*, 1996) and N- P/Q-type Ca^{2+}

channel (Hurley *et al.*, 2000) which function through the regulatory influence of β_{2a} subunit interaction. It has also been shown that palmitoylation has a wide role to play in channel trafficking such as in the regulation of cell surface stability and synaptic clustering of $GABA_A$ receptor ligand-gated channels (Rathenberg *et al.*, 2004), trafficking of the AMPA receptor and NMDA receptor ligand-gated ion channels (Hayashi *et al.*, 2005; Hayashi *et al.*, 2009) and targeting of the P2X7 receptor ATP-gated cationic channel to lipid microdomains, alongside additional roles in regulation of cell surface expression (Gonnord *et al.*, 2009). Palmitoylation has been implicated in mediating ion channel internalization in voltage-gated Kv1.5 ion channels (Jindal *et al.*, 2008) and has even been shown to regulate other post translational modifications such as the phosphorylation status of the glutamate receptor (GluR6) ligand-gated ion channel (Pickering *et al.*, 1995). Finally, another dimension in which palmitoylation has been demonstrated to play a significant role is in the structural assembly of sodium channels (Schmidt & Catterall, 1987) and the structural formation of aquaporin-4 channel arrays to mediate bidirectional water transport across the blood-brain interface (Suzuki *et al.*, 2008).

Palmitoylation is an integral process that is crucial not only for simple protein trafficking to the plasma membrane. Its dynamic controllable and versatile aspects are reasons why it may have been evolutionarily favoured as a post translational modification to fine tune protein and cellular function. Palmitoylation has emerged over the past decade as an important and dynamic mechanism to control ion channel proteins.

1.6.3.1.4 Palmitoylation and secondary membrane targeting motifs

Whilst there is no clear consensus sequence for palmitoylation, the common denominator is often an additional membrane-targeting sequence in the vicinity of the target cysteines that consists of either a region positive charges, adjacent lipid anchors or transmembrane domains (Bijlmakers & Marsh, 2003; Dietrich & Ungermann, 2004). This would suggest that the local environment of the target sequence is probably quite important in controlling the availability of certain cysteines for palmitoylation. In theory a single palmitoyl group should be sufficient for membrane association (Resh, 2006b) frequently however additional signals are

involved. A two-signal hypothesis for membrane binding was initially proposed for Ras proteins (Hancock *et al.*, 1990) which suggested that additional membrane binding signals for peripheral membrane proteins were required that may include the addition of lipid modifications such as myristoylation and prenylation or the presence of a polybasic domain. When palmitoylation is the second signal, the first signal may simply act as a targeting motif for interaction with the plasma membrane, whereby palmitoylation can occur and stabilize the association.

1.6.4 Polybasic domains

Clusters of hydrophobic and positively charged amino acids often precede and follow one or more palmitoylated cysteines. In G-protein signalling, the G_{α} subunit needs to be localised at the plasma membrane in order to couple to its effectors. Association of the G_{α} subunit with the plasma membrane is achieved through palmitoylation and as proposed by the two-signal hypothesis, a second targeting signal, which in this case is a cluster of basic residues (Crouthamel *et al.*, 2008). Disruption of the polybasic domain decreases membrane association and interestingly, also abolishes palmitoylation of the protein (Crouthamel *et al.*, 2008). Whether disruption of the polybasic domain abolishes targeting of the protein to the plasma membrane or whether the palmitoylation status was altered by the disruption of the surrounding basic environment is unknown. It is interesting to note that studies have suggested that multiple palmitoylated cysteine residues do actually decrease the relative importance of polybasic motifs (Crouthamel *et al.*, 2008), suggesting that stability may be an important function of the polybasic domain in proteins palmitoylated at a single site.

Regions of positive charge in a protein can function as membrane-binding signals through an enhanced affinity for the negatively charged headgroups of the lipid membrane, via an electrostatic interaction. Potential partners for these basic domains are the monovalent acidic phosphatidylserine (PS) (one negative charge) or the less abundant and more negatively charged phosphoinositides such as PIP_2 (four negative charges) and PIP_3. Additionally, these acidic lipids are more concentrated at the plasma membrane compared to intracellular membranes

(McLaughlin & Murray, 2005; Mulgrew-Nesbitt *et al.*, 2006), thus providing a good mechanism for guiding basic clusters to the plasma membrane.

The lipid composition of the plasma membrane largely comprises the zwitterionic, electrically neutral lipids of phosphatidylcholine (PC) and phosphatidylethanolamine (PE), constituting ~60%, with the charged monovalent acidic lipid phosphatidylserine (PS) constituting ~25% of the inner leaflet of the plasma membrane (McLaughlin *et al.*, 2002; Mulgrew-Nesbitt *et al.*, 2006). Compared to other phospholipids, phosphoinositides are present in very low levels of ~1-2%. Yet, despite their low concentration, phosphoinositides play an important role in nearly all aspects of cell physiology (Lemmon, 2003; McLaughlin & Murray, 2005; Di Paolo & De Camilli, 2006) and have a strong negative valency of -4 (McLaughlin *et al.*, 2002). Hence the cytosolic-membrane interface carries an appreciable negative charge, especially in comparison to other intracellular membranes that have less charge. Generally, targeting of polybasic clusters to the plasma membrane is fairly non-specific, however there is evidence of specific electrostatic sequestering of the strongly negative-charged phosphoinositdes (PIP_2 and PIP_3). Therefore, it is plausible that a protein with a cluster of four or more basic residues (Mulgrew-Nesbitt *et al.*, 2006) located at the membrane interface, would presumably be able to sequester a PIP_2 lipid molecule.

The specific role of a polybasic domain in either targeting of lipidated regions of protein to the plasma membrane or facilitating lipidation of regions of protein for stable attachment to the plasma membrane is not well understood. It is possible that polybasic regions are necessary signals to perhaps orientate protein segments towards the plasma membrane for palmitoylation (Kosloff *et al.*, 2002) because despite palmitoylation providing a strong anchor at the plasma membrane, it must first be targeted there to undergo this modification. Examples of proteins that are regulated by lipid and polybasic interaction with the plasma membrane include the PSD-95 and GAP-43 proteins (El-Husseini *et al.*, 2000), Ras proteins (Hancock *et al.*, 1989; Hancock *et al.*, 1991; Laude & Prior, 2008), and G protein alpha subunits (Pedone & Hepler, 2007). Indeed polybasic targeting motifs alone have also been shown to be sufficient for membrane targeting, such as in the small GTPases Rit and KRas (Heo *et al.*, 2006).

1.6.4.1 The electrostatic switch

Secondary signals necessary for palmitoylation can play an additional role in regulating cycles of de-palmitoylation and re-palmitoylation through myristol, farnesyl or electrostatic switches (Resh, 2006a). Electrostatic switches are physiological mechanisms that can function to disrupt positively charged polybasic regions, removing their functional significance. Phosphorylation could conceivably disrupt a polybasic domain by incorporation of a negatively charged phosphate group (Kim *et al.*, 1994a). For example, phosphorylation of K-Ras within its C-terminal polybasic region by PKC causes K-Ras to translocate from the plasma membrane to the mitochondria where it induces apoptosis (Bivona *et al.*, 2006). This mechanism is known as an electrostatic switch, whereby the function of the basic domain can be switched on or off by phosphorylation, decreasing the net positive charge in the region.

1.6.5 Phosphorylation

Protein phosphorylation has been identified as a mechanism whereby functional diversity can be generated in BK channels through post-translational modification. The phosphorylation state of a protein is an equilibrium between opposing protein kinase and phosphoprotein phosphatase activities (White *et al.*, 1991; Reinhart & Levitan, 1995). Several serine/threonine kinases have been shown to modulate BK channel activity, such as the cAMP dependant protein kinases (PKA) (Tian *et al.*, 2001; Tian *et al.*, 2004), cGMP dependant protein kinases (PKG) (White *et al.*, 2000; Zhou *et al.*, 2000) and protein kinase C (PKC) (Reinhart & Levitan, 1995; Shipston & Armstrong, 1996; Zhou *et al.*, 2010). Additionally, phosphatases can regulate the channel, such as, phosphoprotein phosphatase-1 (PP1) which has been implicated in modulating phosphorylation status (Reinhart & Levitan, 1995) and a calcium/calmodulin-dependant phosphatase has been shown to inhibit the channel (Loane *et al.*, 2006). PKA activation of BK channel can also be controlled by opposing endogenous type 2A-like protein phosphatases (PP2A) (Tian *et al.*, 1998; Tian & Shipston, 1998; Widmer *et al.*, 2003). These interactions can play an important role in tissue function by 'tuning' the apparent calcium and/or voltage sensitivity of the BK channel (Chung *et al.*, 1991; Schubert & Nelson, 2001).

Recent studies to come out of our lab have demonstrated that BK channels show functional heterogeneity in their response to protein kinase A (PKA) mediated phosphorylation. This heterogeneity is largely due to pre-mRNA splicing of the BK channel. PKA phosphorylation of a conserved serine phosphorylation motif S869 (or S927 numbered in STREX channels) in the C-terminus of the ZERO variant of the BK channel leads to channel activation (Tian *et al.*, 2001; Tian *et al.*, 2004). However, splice insertion of the STREX exon generates an additional PKA consensus motif (S636) that when phosphorylated, results in channel inhibition by PKA (Tian *et al.*, 2001; Tian *et al.*, 2004). In an elegant study examining the phosphorylation status of individual subunits that make up the functional channel, we determined that only 1 α-subunit within the BK channel tetramer is required to be phosphorylated by PKA at the S636 PKA-phosphorylation site, to lead to complete channel inhibition (Tian *et al.*, 2004). This single subunit rule of phosphorylation at the additional STREX phosphorylation site presumably induces a major change in the functional channel to mediate this inhibitory effect.

It is evident that protein kinases dynamically modulate the BK channel, largely by activating the channel via PKA and PKG and inhibiting the channel via PKC. Although recent studies have postulated multiple phosphorylation sites, suggesting the process may be more complex. Phosphorylation regulates the channel by shifting the voltage activation curve without effecting single channel conductance or voltage sensitivity. Alternative splicing is also able to switch channel activity in response to phosphorylation supporting data suggesting that it may be a more complex mechanism. Nevertheless, phosphorylation clearly plays an important role in tuning the BK channel in response to intracellular calcium and voltage sensitivity.

1.7 Outlining the primary aims of the thesis

Palmitoylation is increasingly emerging as a mechanism to regulate ion channels. It has recently been implicated in many diverse roles such as in the regulation of voltage sensing (Gubitosi-Klug *et al.*, 2005), membrane trafficking (Hayashi *et al.*, 2005; Hayashi *et al.*, 2009), channel assembly (Schmidt & Catterall, 1987) and protein phosphorylation (Pickering *et al.*, 1995). The ability of palmitoylation to

regulate proteins post-translationally endows the cell with control over various aspects of protein function through rapid cycles of palmitoylation and de-palmitoylation (Resh, 2006b).

In the BK channel, alternative splicing of the STREX insert at the multiple splice site C2 within the C-terminus, introduces features typically associated with (a) membrane targeting domains and (b) regions that could be regulated by palmitoylation.

Inclusion of STREX generates a cysteine rich region and a series of basic residues. Cysteine residues have been identified in many proteins as targets for post-translational modifications such as palmitoylation (Resh, 1999). Palmitoylation increases the hydrophobicity of a protein, which in turn facilitates membrane association. As previously discussed, whilst there appears to be no clear consensus sequences for palmitoylation sites, they often appear to be located near to additional membrane-targeting sequences in the vicinity of the target cysteines, such as polybasic domains (Bijlmakers & Marsh, 2003; Dietrich & Ungermann, 2004). Indeed, polybasic domains may function independently as membrane targeting domains for the negatively charged inner leaflet of the plasma membrane (McLaughlin & Murray, 2005; Mulgrew-Nesbitt *et al.*, 2006) or may be able to regulate the local environment within the protein to influence or regulate palmitoylation (Crouthamel *et al.*, 2008). Therefore, the cysteine rich STREX insert would appear to have characteristics similar to regions in other proteins that have been previously identified as being palmitoylated and function as membrane targeting domains.

Fundamentally, alternative splicing of the STREX insert alters the channel properties of the BK channel, increasing the calcium sensitivity of the channel and modulating the response of the channel to phosphorylation. Are these additional properties in STREX channels mediated by the cysteine rich domain and/or the putative polybasic domain generated by splicing of STREX? Does the STREX domain target an otherwise cytosolic C-terminus to the plasma membrane? Does palmitoylation regulate BK channel function? And, is it possible that other areas in the BK channel protein may be palmitoylated, outside of STREX?

In this thesis, I set out with the overall hypothesis that the BK channel is a palmitoylated protein and that palmitoylation controls channel function. I will investigate whether the STREX insert contains membrane targeting domains, whether this is reliant on palmitoylation and whether there are additional sites in the BK channel protein that are palmitoylated.

The focus of each chapter will involve determining:

1. Firstly in Chapter 3, whether the STREX insert functions as a palmitoylation-dependent membrane targeting domain and what the functional significance of this is.

2. Secondly in Chapter 4, whether the series of polybasic residues generated when STREX is alternatively spliced into the C-terminus may function as a functional polybasic domain in controlling membrane targeting and/or influencing the palmitoylation status of the channel.

3. And Finally in Chapter 5, I will examine the entire BK channel protein for additional sites that may be palmitoylated to determine if multiple sites act independently and what function palmitoylation may play in the channel.

CHAPTER TWO

MATERIALS & METHODS

'In the discovery of secret things, and in the investigation of hidden causes, stronger reasons are obtained from sure experiments and demonstrated arguments than from probable conjectures and the opinions of philosophical speculators'

William Gilbert (1601), De Magnete

2.1 Molecular Biology Protocols

2.1.1 Channel Constructs

The generation of full-length murine ZERO and STREX channels with epitope-tags in pcDNA3 vectors are described in (Shipston *et al.*, 1999). STREX channels have a 58 amino acid insert at splice site C2 located in the intracellular linker between the two RCK domains, whereas the ZERO channel has no insert (Figure 2.1A). C-terminal tagged –GFP and –HA fusion proteins were made as described in (Chen *et al.*, 2005). S0-S1 loop proteins were generated by PCR amplification from full length channel constructs using primers with overhanging XhoI and BamHI restriction sites and including a Kozak site to genetically enhance translation (Table 2.1). The PCR product was then restriction digested and subcloned in frame into a pEYFP-N1 vector backbone. To generate N-terminal Flag- epitope tagged full-length STREX and ZERO channel constructs, a synthetic double-stranded Flag- oligonucleotide was blunt end ligated in frame with the initiator methionine (MDALI..) codon using forward and reverse oligonucleotides as described in (Chen *et al.*, 2005)(Figure 2.1B).

2.1.2 Standard PCR conditions

Standard polymerase chain reactions (PCR) to amplify selected pieces of DNA, were carried out in 50 µl reactions, containing 1 U of Taq DNA polymerase (Fermentas), 10x reaction buffer (Fermentas), 0.2 mM each of dATP, dCTP, dTTP, and dGTP (NE BioLabs), 1.5 mM $MgCl_2$, and 125 ng of oligonucleotide sense and antisense primer. Reactions were generally run for 1 minute at 94 ^{O}C, through 25 cycles using annealing temperatures appropriate to the primers' calculated Tm using the Stratagene formula (see Equation 2.1), and 72 ^{O}C extension phases according to the length of the amplicon, approximately 1 minute per kb, followed by 7 minutes at 72 ^{O}C after the final cycle.

Figure 2.1
Schematic of channel constructs

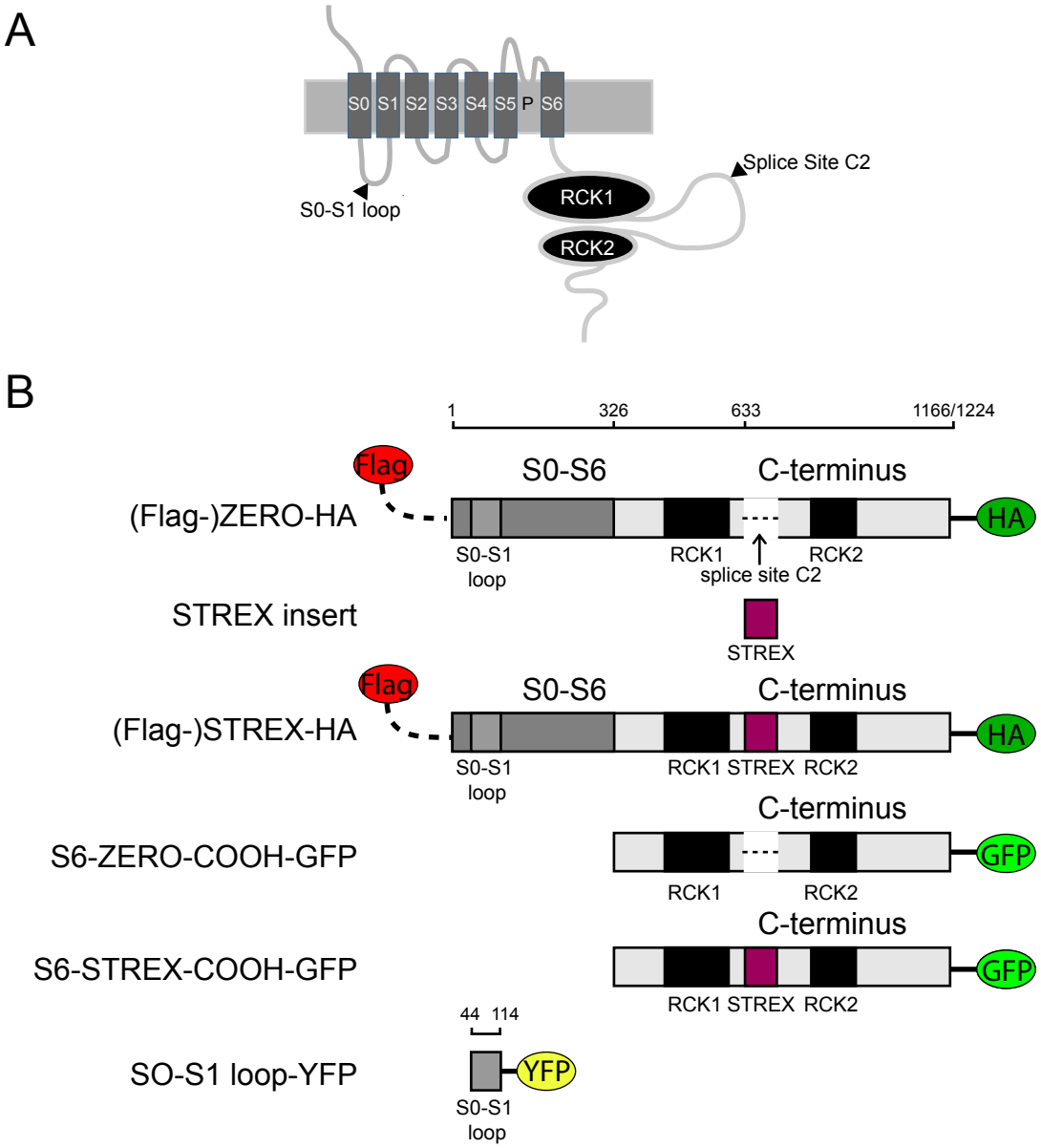

Figure 2.1. Schematic of channel constructs. (A) Topology of BK channel illustrating the full channel domain (light and dark grey) and C-terminal domain from the end of S6 (dark grey). (B) Schematic of expression constructs used in the study. Full length channels with C-terminal -HA tags and full length channels with N-terminal Flag-tagged (broken line illustrates constructs with or without Flag- tag) are illustrated (Flag-ZERO-HA and Flag-STREX-HA). C-terminal constructs (S6-COOH) represent the entire C-terminus from the end of the S6 transmembrane domain to the COOH end of the channel (S6:ZERO COOH-GFP and S6:STREX COOH-GFP). S0-S1 loop constructs only contain the intracellular loop between the S0 and S1 transmembrane domains (S0-S1 loop-YFP). The ZERO constructs have a dashed line which represents no insert at splice site C2. Numbering begins from MDALI..

Equation 2.1:

$$\mathrm{TM} = \frac{81.5 + 0.41\ (\%\mathrm{GC}) - \ 675}{\mathrm{N} - (\%\mathrm{mismatch})}$$

In equation 2.1, 'N' is the primer length as a number of base pairs.

2.1.3 Site Directed Mutagenesis

Site directed mutagenesis of a specific amino acid residue(s) was carried out using PCR in 50 µl reactions with the QuikChange XL Site-directed Mutagenesis Kit from Stratagene. The QuikChange method relies on linear amplification of template DNA by using high-fidelity DNA polymerase. Each reaction contained, 2.5 U/µl Pfu turbo polymerase, 1x reaction buffer, 3 µl Quiksolution (Stratagene), 0.2 mM each of dATP, dCTP, dTTP, and dGTP (NE BioLabs), 1.5 mM $MgCl_2$, 10 ng template DNA, 125 ng of oligonucleotide sense primer, 125 ng of oligonucleotide antisense primer, diluted in DEPC water. Reactions were generally run for 1 minute at 94 ^{O}C to denature the DNA template, then 18 cycles, using annealing temperatures appropriate to the primers' calculated Tm, assessed using the formula from Stratagene (see Equation 2.1) and 72 ^{O}C extension phases according to the length of the amplicon (approximately 1 minute per kb), followed by 10 minutes at 72 ^{O}C after the final cycle. The PCR product then underwent a DpnI (10 U/µl) digestion to eliminate any parental methylated DNA template, for 1 hour at 37 ^{O}C.

2.1.4 Design of oligonucleotides for site directed mutagenesis

When designing an oligonucleotide for site directed mutagenesis, a 17-20 base oligonucleotide with the mismatch located in the centre was sufficient for single base mutations (Table 2.1). This allows 8-10 perfectly matched nucleotides on either side of the mismatch. For mutations involving 2 or more mismatches, an oligonucleotide usually around 25 bases or longer was required to allow for 12-15 perfectly matched nucleotides on either side of the mismatch. Oligonucleotides were normally generated with between 40-60% G-C content, and with a higher G-C content at the

Table 2.1
Primers used for site directed mutagenesis in the BK channel

Mutation		Sequence 5' - 3'	
XhoI-Koz	FWD 5'-	CCG CTC GAG GGC CAC CAT GCG GAC GCT CAA GTA CCT G	-3'
BamHI	REV 5'-	GGT GGA TCC AAT CTG CCA GTC AGT GTC TG	-3'
C53A:C54A:C56A	FWD 5'-	CCT GTG GAC CGT TGC CTG CCA CGC CGG GGG CAA GAC G	-3'
	REV 5'-	CGT CTT GCC CCC GGC GTG GCA GGC AAC GGT CCA CAG G	-3'
C53A	FWD 5'-	AAG TAC CTG TGG ACC GTT GCC TGC CAC TGC GGG GGC AAG ACG AA	-3'
	REV 5'-	TTC GTC TTG CCC CCG CAG TGG CAG GCA ACG GTC CAC AGG TAC TT	-3'
C54A	FWD 5'-	AAG TAC CTG TGG ACC GTT TGC GCC CAC TGC GGG GGC AAG ACG AAG	-3'
	REV 5'-	CTT CGT CTT GCC CCC GCA GTG GGC GCA AAC GGT CCA CAG GTA CCT	-3'
C56A	FWD 5'-	CCG TTG CCG CCC ACG CCG GGG GCA AGA CGA AG	-3'
	REV 5'-	CTT CGT CTT GCC CCC GGC GTG GGC GGC AAC GG	-3'
C53A:C54A	FWD 5'-	GTA CCT GTG GAC CGT TGC CGC CCA CTG CGG GGG CAA	-3'
	REV 5'-	CTT GCC CCC GCA GTG GGC GGC AAC GGT CCA CAG GTA	-3'
C612A:C615A	FWD 5'-	AGG GCG TTT TTT TAC GCC AAG GCC GCT CAT GAT GAC GTC ACA GAT CC	-3'
	REV 5'-	GGA TCT GTG ACG TCA TCA TGA GCG GCC TTG GCG TAA AAA AAT GCC CT	-3'
C628A:C630A	FWD 5'-	AAA AGA ATT AAA AAA GCT GGC GCC AGG CGG CCC AAG ATG TCC	-3'
	REV 5'-	GGA CAT CTT GGG CCG CCT GGC GCC AGC TTT TTT AAT TCT TTT	-3'
K627E:R631E	FWD 5'-	GAT CCC AAA AGA ATT AAA GAA TGT GGC TGC GAG CGG CCC AAG ATG	-3'
	REV 5'-	CAT CTT GGG CCG CTC GCA GCC ACA TTC TTT AAT TCT TTT GGG ATC	-3'
K627A:R631A	FWD 5'-	GAT CCC AAA AGA ATT AAA GCA TGT GGC TGC GCG CGG CCC AAG ATG	-3'
	REV 5'-	CAT CTT GGG CCG CGC GCA GCC ACA TGC TTT ATT TCT TTT GGG ATC	-3'
R640E:R642E	FWD 5'-	GAT GTC CAT CTA CAA GGA AAT GGA ACG AGC ATG TTG TTT TG	-3'
	REV 5'-	CAA AAC AAC ATG CTC GTT CCA TTT CCT TGT AGA TGG ACA TC	-3'
R640A:R642A	FWD 5'-	GAT GTC CAT CTA CAA GGC AAT GGC ACG AGC ATG TTG TTT TG	-3'
	REV 5'-	CAA AAC AAC ATG CTC GTG CCA TTG CCT TGT AGA TGG ACA TC	-3'
S636E	FWD 5'-	GCA GGC GGC CCA AGA TGG AAA TCT ACA AGA GAA TGA GAC G	-3'
	REV 5'-	CGT CTC ATT CTC TTG TAG ATT TCC ATC TTG GGC CGC CTG C	-3'
S636A	FWD 5'-	GCA GGC GGC CCA AGA TGG CCA TCT ACA AGA GAA TGA GAC G	-3'
	REV 5'-	CGT CTC ATT CTC TTG TAG ATG GCC ATC TTG GGC CGC CTG C	-3'
C645A:C646A	FWD 5'-	CAA GAG ATT GAG ACGAGC AGC TGC TTT TGA TTG CGG ACG TTC TG	-3'
	REV 5'-	CAG AAC GTC CGC AAT CAA AAG CAG CTG CTC GTC TCA TTC TCT TG	-3'
C645A	FWD 5'-	GAG AAT GAG ACG AGC AGC TTG TTT TGA TTG CGG ACG	-3'
	REV 5'-	CCG CAA TCA AAA CAA GCT GCT CGT CTC ATT CTC TTG	-3'
C646A	FWD 5'-	GAA TGA GAC GAG CAT GTG CTT TTG ATT GCG GAC G	-3'
	REV 5'-	CGT CCG CAA TCA AAA GCA CAT GCT CGT CTC ATT	-3'
C649A	FWD 5'-	GCA TGT TGT TTT GAT GCC GGA CGT TCT GAG CGT G	-3'
	REV 5'-	CAC GCT CAG AAC GTC CGG CAT CAA AAC AAC ATG C	-3'
C656A:C658A	FWD 5'-	TCT GAG CGT GAC GCC TCG GCC ATG TCA GGC	-3'
	REV 5'-	GCC TGA CAT GGC CGA GGC GTC ACG CTC AGA	-3'
C684A	FWD 5'-	CTG TTA ATG ATG CCT CCA CCA GTT T	-3'
	REV 5'-	AAA CTG GTG GAG GCA TCA TTA ACA G	-3'
S927E	FWD 5'-	GGG ATG TTA CGC CAG CCG GAG ATC ACA ACT GGG GTC AAC	-3'
	REV 5'-	GTT GAC CCC AGT TGT GAT CTC CGG CTG GCG TAA CAT CCC	-3'
S927A	FWD 5'-	GAT GTT ACG CCA GCC GGC CAT CAC AAC TGG GGT CAA C	-3'
	REV 5'-	GTT GAC CCC AGT TGT GAT GGC CGG CTG GCG TAA CAT C	-3'

Table 2.1 Primers used for site directed mutagenesis in the BK channel. Numbering starts from initiator methionine MDALI.. in the murine BK channel (accession number NM_010610). Numbering after residue 632 includes the 58 amino acid STREX insert.

5’ prime end than the 3’ prime end. The T_M or melting temperature of the oligonucleotide reflecting base content, was calculated using an equation from Eurofins MWG Operon (equation 2.2 & 2.3) and was designed to be close to 70 ^{O}C, to coincide with the annealing temperatures of the polymerases used in the future PCR extension phase. Oligonucelotide sequences where ordered from Eurofins MWG Operon, Ebersberg, Germany.

Equation 2.2:

Sequences with 15 or less bases:

$$T_M\ [°C] = 2(n_A + n_T) + 4(n_G + n_C)$$

Equation 2.3:

Sequences with more than 15 bases:

$$T_M\ [°C] = 69.3 + [41(n_G + n_C) / s - (650 / s)]$$

Where, n = number of nucleotides of type X and, s = number of all nucleotides per sequence. The primer sequences designed for site directed mutagenesis carried out in this thesis are shown in Table 2.1.

2.1.5 Transformation of chemically competent E.coli

Transformation of newly synthesized plasmid DNA was carried out using chemically competent XL10-Gold® ultracompetent E.coli cells (Stratagene). 100 µl aliquots were stored at -80 ^{O}C and subsequently thawed on ice. They were then further split into 50 µL aliquots. 10 ng of plasmid DNA was added and the mixture was incubated on ice for 20 minutes. Subsequently, cells were heat-shocked at 42 ^{O}C for 45 seconds and 500 µL of LB medium was added. The mixture was incubated for 30 minutes to 1 hour at 37 ^{O}C in a shaking incubator, at 200 rpm and then 200 µl of cells were plated onto selective agar containing the appropriate antibiotic and incubated overnight at 37 ^{O}C.

2.1.6 PCR screening of bacterial colonies

Individual colonies grown on selective agar plates were picked using a sterile pipette tip, then dipped vigorously into a 50 µl PCR reaction tube containing primers specific to the region of interest. A standard PCR reaction amplified the region of interest, which could then be run out on an agarose gel. Those colonies that were shown by PCR screening to be the correct size (or if using double digest plasma DNA, if it contained the correct size of insert), were again picked from the same plate using a sterile pipette tip and inoculated into either 5 or 250 mls Luria Broth (LB) medium with the appropriate antibiotic. This was incubated overnight at 37 ^{O}C in a shaking incubator, at 200 rpm, in order to set up either a mini- or maxi- prep culture respectively.

2.1.7 Maxiprep alkaline lysis for plasmid DNA isolation

Maxiprep isolation of plasmid DNA required the 250 ml bacterial culture described in section 2.1.6 to be pelleted at 5000 x *g* for 5 minutes at 4 ^{O}C. The pellet was then homogeneously resuspended, harvested and lysed before clearing the bacterial lysate and precipitating the plasmid DNA using the QIAGEN Hispeed Plasmid Maxi Kit (QIAGEN) according to the manufacturer's instructions. Briefly, plasmid DNA binds to anion-exchange resin under low-salt and pH conditions. RNA, proteins, dyes and low molecular weight impurities are removed by a medium-salt wash. Plasmid DNA is then eluted in a high-salt buffer concentrated and desalted by isopropanol precipitation. The DNA is then washed filtered and eluted in QIAGEN Buffer TE or water.

2.1.8 Miniprep alkaline lysis for plasmid DNA isolation

Miniprep isolation of plasmid DNA for advanced screening of mutants required that individual bacterial colonies were seeded, using a sterile pipette tip, into 5 ml of LB medium, and then incubated overnight at 37 ^{O}C in a shaking incubator, at 200 rpm. 1.5 ml of each culture was transferred into a microcentrifuge tube, and centrifuged at 12000 x *g* for 1 minute. The LB broth was then aspirated from the pellet, which after

resuspension, followed the manual procedure (lyse, bind, wash and elute) using the QIAprep Spin Miniprep Kit (QIAGEN) according to the manufacturer's instructions.

2.1.9 Quantitation of DNA

A 1/100 dilution of the DNA sample in DEPC H_20 was prepared and its absorbance at 260 nm and 280 nm measured using a UV spectrophotometer. Purity was assessed using the ratio of A260/A280 with an ideal ratio of 1.8 indicating pure dsDNA, whilst lower ratios were indicative of contamination with other nucleic acids or protein. To calculate the concentration where an OD260 of 1 indicates DNA at a concentration of 50 µg/ml, the formula was applied as shown in Equation 2.4;

Equation 2.4:

$$\mathrm{OD260\ x\ 50\mu g/ml\ dilution\ factor} = \mathrm{[DNA]\ (\mu g/ml)}$$

2.1.10 Preparation of DNA for sequencing

DNA was sent for sequencing to Eurofins MWG Operon, Germany, as specified, in a total volume of 15 µl DEPC H_2O in 1.5 ml tubes. Purified plasmid DNA was sent at a concentration of 50-100 ng/µl as prepared previously (section 2.1.7 or 2.1.8). Primers were ordered from Eurofins MWG Operon for sequencing, or were sent at a concentration of 2 pmol/µl in a minimum volume of 15 µl (corresponding to an amount of 30 pmol). Sequencing covers an area of interest specific to the primers sent and not the whole plasmid. Sequencing results were analysed with vector NTI 10.1.1 (Invitrogen) and Chromas Lite 2.0 (Technelysium Pty Ltd).

2.1.11 Double Restriction Digest

On confirmation of the correct mutated sequence of DNA, double restriction digests of the sequenced region into a new vector were made to assure a clean vector backbone without possible additional erroneous mutations that would not have been

sequenced. Double restriction digests were prepared in 20 µl reactions, each containing 2-10 U (1 U being the amount of enzyme required to completely digest 1 µg substrate DNA in 60 minutes) of the respective restriction enzyme (NE BioLabs) in the appropriate buffer (NE BioLabs) diluted to 1x with DEPC water, and 0.2-1 µg of DNA sample. These reaction mixtures were then incubated at 37 ^{O}C for 1 hour.

2.1.12 DNA agarose gel electrophoresis & gel purification

Gel Electrophoresis, to separate the DNA by molecular weight to confirm sizes of digested fragments using an electric field, was carried out using a 1% agarose (w/v) gel, prepared in 50 ml or 100 ml of 1xTBE buffer (45 mM Tris-base, 45 mM Boric acid, 2 mM EDTA, pH 8.0), depending on the number of samples. If the expected size of the DNA fragment was less than 300 bp, the percentage of agarose was increased up to 4% to increase band definition when imaging under UV transillumination. SYBR Safe DNA gel stain (Invitrogen Molecular Probes) was added at a X1 final concentration and mixed by swirling. The gel was then poured onto a plate to set. DNA samples were mixed with 5 µL loading dye (10x recipe for 100 ml: 60% glycerol (v/v), 0.25% bromophenol blue (w/v), 33% 150 mM Tris (pH 7.6) (v/v) in H_20), loaded, and run for 20-30 minutes at 160 V using a Bio-Rad model 200/2.0 power supply and Bio-Rad wide min-sub cell GT gel electrophoresis apparatus. The appropriate DNA fragments could then be cut out and purified from the agarose gel using Zymoclean gel DNA recovery kit that utilises fast spin column technology to yield high-quality purified DNA.

2.1.13 Ligation of plasmid vector and insert DNA

Ligation of the vector backbone and the newly generated site directed mutant insert was carried out using T4 DNA ligase (Fermentas). Ligation catalyzes the formation of a phosphodiester bond between juxtaposed 5’ phosphate and 3’ hydroxyl termini in duplex DNA. The ligation enzyme joins blunt end and cohesive end termini as well as repairing single stranded nicks in duplex DNA. Reaction conditions were as follows – T4 DNA Ligase 5 U (Fermentas), 1x T4 DNA Ligase Reaction Buffer [50

mM Tris-HCL (pH 7.5), 10 mM $MgCl_2$, 10 mM dithiothreitol, 1 mM ATP, 25 ug/ml bovine serum albumin] (Fermentas). For vector:insert DNA ratios an equation (see equation 2.5) was used to find the optimum ratio for successful ligation. Generally a 1:3 and 1:7 ratio (vector:insert) was used.

Equation 2.5:

$$\frac{\text{ng of vector x kb size of insert}}{\text{kb size of insert}} \text{ x molar ratio of } \frac{\text{insert}}{\text{vector}} = \text{ng of insert}$$

This reaction was then carried out at 16 ^{O}C overnight, before proceeding to transformation of chemically competent E.coli as in 2.1.5 and Maxiprep in 2.1.7.

2.2 Mammalian cell culture protocols

2.2.1 Cell lines

The HEK 293 cell line, one of the most amenable and commonly used genetic expression systems in science, was used to transiently express cloned BK channels and splice variants of the BK channel. The HEK293 cell was initially derived from the human embryonic kidney (HEK) by Alex Van der Eb in the early 1970's and subsequently transformed by adenovirus in work carried out by Frank Graham (Graham *et al.*, 1977). Interestingly we call these "293" based on Graham's habit of numbering his experiments – the original HEK293 cell clone was simply his 293rd experiment. HEK 293 cells do not endogenously express BK channels but do retain their protein kinase and phosphatase pathways (Thomas & Smart, 2005). Manipulation of the HEK293 cell allows the study of isolated proteins in over-expression systems that hijack the cell's synthetic protein machinery and force efficient translation of the transfected gene. Transfection of the BK channel construct into the HEK 293 cell line provides a means to characterise and study the alternative splice variants and site directed mutants, in isolation of endogenous BK channels whilst in their native state.

2.2.2 Standard cell culture passage protocol

HEK 293 cells were used, over a passage range of 10-35 times. Cells were maintained in DMEM (Dulbecco's Modified Eagle Medium, 41965) + L-glutamine (GIBCO®, Invitrogen) with 10% (v/v) FCS (Fetal Calf Serum) no antibiotic (GIBCO®, Invitrogen), in 25 cm^2 flasks, at 37 ^{0}C in 95% (v/v) air, 5% (v/v) CO_2, and passaged every 3-4 days at 70-90% confluency. The medium was removed and discarded, and cells washed using 5 ml of HBSS (Hanks Balanced Salt Solution) (GIBCO®, Invitrogen). This was removed, then 0.5 ml of Trypsin-EDTA X1, 25300 (GIBCO®, Invitrogen) was added and cells incubated at 37 ^{O}C for 1-2 minutes. The flask was gently tapped to detach cells, which were then resuspended in 1 ml of DMEM + 10% FCS by triturating up and down slowly using a sterile p1000 pipette. Once cells were fully resuspended, 13 ml of DMEM+10%FCS were added to each 0.5 ml of cell suspension. Cells were triturated and 5 ml was then transferred into a new sterile 25 cm^2 tissue culture flask.

2.2.3 Transfection of cells using Lipofectamine2000

Cells were cultured on coverslips in sterile 6 well tissue culture plates in 2 ml DMEM + L-glutamine with 10% (v/v) FCS (no antibiotic), at 37 ^{O}C, in 95% (v/v) air, 5% (v/v) CO_2, until 40% confluent, normally after 24 hours. For each transfection reaction, 1.5 µg DNA and 5 µl Lipofectamine™ 2000 11668-019 (Invitrogen) were diluted separately in 100 µl DMEM + L-glutamine without serum, and incubated for 20 minutes. Following this incubation, 200 µl of the DNA-lipofectamine2000 complex in DMEM was added directly into the culture medium in the well. Cells were subsequently incubated for 24-48 hours at 37 ^{O}C in 95% (v/v) air, 5% (v/v) CO_2, in preparation for experimental study.

2.3 Electrophysiology & Membrane potential assays

2.3.1 Electrophysiology

The true birth of electrophysiology can be attributed to Luigi Galvani whose prophetic understanding described the propagation of neuromuscular electrical excitability at the turn of the eighteenth century. Intriguingly, for an ion channel electrophysiologist such as myself, Galvani's delicate work enabled him to first postulate the existence of water-filled channels which would penetrate the surface of muscle fibres to allow the spread of electrical excitability (Galvani, 1794; Verkhratsky *et al.*, 2006), the first concept of the ion channel (Verkhratsky *et al.*, 2006).

2.3.2 Electrophysiological Assays

The electrophysiological techniques used were single-channel and macro-patch current recordings, performed in the inside-out configuration of the patch clamp technique, at room temperature (20-24 °C). Channel constructs were studied in isolated HEK 293 cells normally 24-48 hours after transient transfection as described in section 2.2.3. Glass coverslips were placed in a perfusion recording chamber attached to an inverted microscope (Nikon Diaphot, Japan). The cells and patch pipettes were observed using x40 phase contrast objective. Mechanical and hydraulic manipulators (Narishige International, Japan, model MHW-3) mounted on the microscope stage, provided the control of coarse and fine manipulation required for patch clamping of isolated cells. Channel activity was recorded using an Axopatch-200 patch clamp amplifier (Axon Instruments, USA), an AD converter in the interface board (Digidata 1200, Axon Instruments, USA) and a computer for display and analysis. Borosilicate glass capillaries GC150F-7.5 (Harvard Apparatus, Kent) were pulled and fire polished to resistances of 5-10MΩ each day and subsequently attached to the mechanical and hydraulic manipulator.

All recordings were carried out in equimolar potassium gradients. The bath solution (intracellular) contained: 140 mM KCl, 5 mM NaCl, 1 mM $MgCl_2$, 30 mM glucose, 10

mM Hepes with free calcium $[Ca^{2+}]_i$ buffered with 1 mM BAPTA, (pH 7.3). The appropriate free calcium concentration is as described in the figure legends. The pipette solution (extracellular) contained the same solute composition as the bath solution with a standard 0.1µM $CaCl_2$. Channel activity was determined in a range of extracellular calcium (0 – 10 µM) after being allowed to stabilize for 10 minutes after patch excision.

To determine the single channel conductance (in pS) of BK channels, single channel amplitude (i) was measured over a range of voltage potentials (v) (-80 mV to + 80 mV) and plotted as a straight line. Conductance (G) was taken as the slope of the line as described by the Ohms law relationship as shown in equation 2.6;

Equation 2.6

$$V = IR \quad \text{or} \quad R = \frac{V}{I} \quad \text{which is equal to,} \quad \frac{1}{R} = \frac{I}{V} \quad \text{and,} \quad \frac{1}{R} = G$$

Macropatch recordings were made to determine channel activity, excised inside-out patches were held at a -80mV holding potential and pulsed for 100ms over a voltage range from -120mV to +120mV in 20mV increments. Tail currents were measured after the pulse potential as the tail current is proportional to the channel open probability at the end of the preceding depolarisation (Islas & Sigworth, 1999). The tail currents were then normalised to the peak tail current which was expressed as 100% when examined in high intracellular calcium (1 µM Ca^{2+}), and plotted as G/G_{MAX} versus the respective test potential. Each voltage step was stepped back to -80 mV and final values were expressed as a percentage, therefore these values reflect conductance (G), (each value was not divided by the -80 mV holding potential to give an absolute conductance value but because values were expressed as a percentage they yield the same results). The curves generated were then fitted to a Boltzmann equation using graphpad prism software using equation 2.6, whereby the voltage for half activation ($V_{0.5MAX}$) could be determined.

Equation 2.6:

$$Y = \text{Bottom} + \frac{(\text{Top} - \text{Bottom})}{1 + \exp\left(\frac{V50 - X}{\text{Slope}}\right)}$$

To determine the voltage dependence of the channel, a logarithmic transformation to linearize the activating component of the normalised (G/G_{MAX}) curve plotted against the depolarised potentials of 0 mV to +120 mV was made using equation 2.7. The voltage dependence was derived from the slope of the line.

Equation 2.7:

$$\mathrm{In}((G/G_{MAX})/(1\text{-}G/G_{MAX}))$$

To define the activation and deactivation kinetics of the channels, activation curves were best fitted by a single exponential function (as shown in equation 2.7) from the beginning of channel activation to the peak plateau current and deactivation curves were fitted from the peak tail current to the baseline.

Equation 2.7

$$f(t) = \sum_{i=1}^{n} A_i e^{-t/\tau_i} + C$$

The standard exponential was fitted using the Clampfit software which is a basic function used to fit changes in current or voltage that are controlled by one or more first-order processes. The fit solves for the amplitude A, the time constant τ, and the constant y-offset C for each component i. The simplex method was used which uses the least squares, mean absolute, maximum likelyhood and minimax minimization method.

By calculating the time constant (tau) at which the channel's activating or deactivating kinetics reached (tau = 1-1/*e),* differences between the channel variants could be examined. All kinetic analysis was carried out using Clampfit v 10.0.1.10. Data acquisition and voltage protocols were controlled by pCLAMP9 software (Axon Instruments). All recordings were sampled at 10 kHz and filtered at 2 kHz. Single-channel conductance measurements were derived by examining traces using WINEDR (Version 2.3.9, J. Dempster, University of Strathclyde, U.K.).

2.3.3 Fluorescent Membrane Potential (FMP) assay

Membrane potential assays were performed in transfected HEK293 cells using FLIPR® Membrane Potential Blue dye (Molecular Devices, Sunnyvale, California) as previously described (Saleem *et al.*, 2009). Cells were seeded onto black clear bottom Poly-D-Lysine coated 96-well plates (Greiner Bio-One Ltd, Gloucestershire UK) 48 hours prior to experiments. The fluorescent membrane potential (FMP) blue dye (Molecular Devices) was prepared as described by the manufacturer's instructions in normal saline solution containing in mM: 140 NaCl, 5 KCl, 2 $CaCl_2$, 1 $MgCl_2$, 20 glucose, 10 HEPES, (pH 7.4). Once the cells reached 90-100% confluency the culture medium was removed and cells were incubated with the FMP dye for 30 minutes at 37 ^{O}C to allow dye loading into the cell membrane. Assays were performed at 22 ^{O}C using a FlexStation® II (Molecular Devices) and channels activated by applying 1 µM of the calcium-ionophore, ionomycin (0.01% DMSO). The automated liquid-handling function of the Flexstation ® II administered 50 µl ionomycin (1 µM) to each individual well to a final volume of 250 µl, 16 seconds after the experiment began. The fluorescence changes were read at high sensitivity for 180 seconds at intervals of 1.52 seconds with excitation/emission wavelengths of 530/565nm respectively.

A decrease in relative fluorescent units (RFU) reflects membrane hyperpolarisation (BK channel activation). Non-transfected HEK 293 cells elicited a depolarisation in response to the influx of calcium ions and some calcium driven activity, this was reported as an increase in fluorescence. Blocking of the BK channel by Paxilline, a selective inhibitor of BK channels (Knaus *et al.*, 1994a), showed a response similar to untransfected HEK 293 cells with an increase in fluorescence. This indicated that the hyperpolarising decrease in fluorescence was indeed mediated by the transfected BK channel (Saleem *et al.*, 2009). Data was analysed using SoftMax Pro, Microsoft excel and GraphPad Prism. Raw data was displayed over the time course to illustrate the response of transfected cells to ionomycin. Average data was obtained at the peak ionomycin-induced hyperpolarising response within each assay plate corresponding to the control channel (either STREX or ZERO) response (the peak response was recorded at either T=70 seconds or T=100 seconds as stated in the figure legends). To examine the isolated channel current, the untransfected HEK response in each assay plate could be subtracted from each transiently transfected

channel variant and the peak value of the control STREX or ZERO channel response could then be normalised to 100% whereby mutant channels could be compared. Only assay plates that passed a 'Z' parameter statistical test (Zhang *et al.*, 1999) that examines the reliability of the data well to well, were used in these studies (Saleem *et al.*, 2009).

2.4 Imaging protocols

2.4.1 Fixing and mounting of cells

Transiently transfected HEK 293 cells as described in section 2.2.3 were typically fixed 48 hours post transfection. The medium was aspirated and the cells washed 3 times with 1 ml HBSS containing 2 mM $CaCl_2$ and 1 mM $MgCl_2$. The cells were then incubated in 1 ml 4% (w/v) paraformaldehyde in PBS (Phosphate Buffered Saline) for 15 minutes. The paraformaldehyde was aspirated and cells washed 3 times in HBSS containing 2 mM $CaCl_2$ and 1 mM $MgCl_2$, then quenched for 10 minutes in 1 ml PBS containing 50 mM NH_4Cl_2, prepared freshly. After quenching, the cells were washed a further 3 times in HBSS containing 2 mM $CaCl_2$ and 1 mM $MgCl_2$. Coverslips were dipped in distilled H_2O, drained briefly to remove excess H_2O, then mounted onto slides using Mowiol, a high quality anti-fade medium and left to dry overnight before imaging.

2.4.2 Screening of fluorescently-labelled cells

A Standard epi-fluorescent Nikon ECLIPSE TE200 microscope was used to screen the HEK 293 transfected fluorescently-labelled cells. Cells were examined under a 100x/1.3 Planar Fluor lens. Cells where studied under white light to ascertain reasonable confluency in a randomly selected field of view, before switching to fluorescence. All cells in each field of view were recorded according to fluorescence in the cellular membrane, cytosol, nucleus or a combination of all three. These tally results could then be calculated as a percentage of the total cell count (small 'n')

which would reflect 1 experiment or larger 'N'. Results could then be presented as mean percentage with the standard error about the mean.

2.4.3 Confocal Imaging of fluorescently-labelled cells

Confocal images were acquired with a Zeiss Axioscope confocal laser scanning microscope (LSM510) operating with a 25 mW argon laser tuned to lines at 458, 488 and 514 nm. Cells were examined with a Zeiss plan-apochromat 1.4 NA x63 oil immersion objective lens. Images through single confocal planes were taken at the middle of the z-axis of the cell. To image eGFP (and Alexa 488 antibody), 488 nm excitation was used and emission was collected using a 500-530 nm band pass filter and for eYFP, 514 nm excitation and a 530 nm long pass filter was used. The multi-track function was used to image two or more fluorophores in the same cell in order to minimise cross-talk between fluorophores. Texas red (excitation 595-605 nm) was used to detect the Alexa fluor 594 antibody labeled Flag-tagged constructs with emission at 617 nm.

2.4.4 Immunofluorescent cell surface labelling

To study cell surface expression of BK channels, constructs were made with an extracellular N-terminal Flag- tag to record channel expression on the cell surface and with -HA tags on the C-terminus to study total BK expression inside the cell (constructs were made as described in section 2.1.1). 48-72 hours after transfection of Flag tag constructs, the medium was aspirated and the cells washed once with DMEM + L-glutamine +10% (v/v) FCS (no antibiotic) at room temperature. The Anti-flag M2 mouse monoclonal antibody (Sigma) was diluted 1:100 in DMEM + L-glutamine +10% (v/v) FCS. Cells were incubated for 2 hours on ice, to block channel endocytosis, with the primary antibody. The cells were then washed in DMEM + L-glutamine +10% (v/v) FCS (no antibiotic) once. The secondary antibody, Alexa fluor 594 conjugated anti-mouse IgG antibody (Invitrogen / Molecular Probes) was diluted 1:1000 in DMEM + L-glutamine +10% (v/v) FCS. The cells were then incubated with the secondary antibody for 1hr on ice. Subsequently the cells were then fixed in 1ml

4% (w/v) paraformaldehyde in PBS, for 30 minutes at room temperature. The paraformaldehyde was aspirated and cells washed 3 times with PBS. Coverslips could then be mounted by dipping in distilled H_2O, drained briefly to remove excess H_2O, then mounted onto slides using Mowiol, and left to dry overnight at room temperature in the dark, then stored at 4 ^{O}C, before imaging.

2.4.5 Immunofluorescent labelling

Channel constructs labelled with a C-terminal -HA tag required permeabilisation for immuno-labelling. The protocol described in section 2.4.4 was followed until fixing of cells by paraformaldehyde at which point cells were washed 3 times with PBS before preceeding to the permeabilization of the cells. Cells were permeabilized with 0.3% Triton X-100 in PBS for 10 minutes at room temperature, then washed three times in PBS. To block further permeabilization of cells a blocking solution of 3%BSA in PBS and 0.05% Triton X-100 was incubated for 30 minutes. To label the HA tag, cells were incubated with an anti-HA rabbit polyclonal antibody (Zymed) (1:500) in the blocking solution as before. This was then left overnight at 4^{O}C or incubated at room temperature for 1 hour. Cells were washed three times in PBS and then incubated with a secondary antibody Alexa 488 conjugated anti-Rabbit IgG (1:1000) in blocking solution, for 1 hour at room temperature. An additional wash in PBS three times preceeded two washes in distilled H_2O before mounting of the coverslips. For mounting, coverslips were dipped in distilled H_2O, drained briefly to remove excess H_2O, then mounted onto slides using Mowiol, and left to dry overnight at room temperature in the dark, then stored at 4 ^{O}C, before imaging.

2.4.6 Quantification of Immunofluorescent labelling

Confocal images were acquired on a Zeiss LSM510 laser scanning microscope, using a 63x oil Plan Apochromat (NA =1.4) objective lens, in multi-tracking mode. Quantification of Flag surface expression was done in two ways: 1) Using confocal microscopy, transfected cells were examined for total protein expression, identified by the intracellular C-terminal -HA tag that was labelled with the secondary antibody Alexa 488 (at wavelength ~520 nm) and counted. In the same field of view, cells

were then examined under a different fluorescent wavelength (~620 nm) to detect the extracellular Flag- tagged secondary antibody Alexa fluor 594, on channels that would only be on the surface of the cell. The gain intensity set to detect Flag- tagged channels on the control cells was used at the same intensity when examining mutant channel constructs so that comparative analysis by counting could be made. These values could then be expressed as a percentage of total channels transfected and subsequently as a percentage of control which is illustrated in the figures in this thesis. 2) Confocal images of random single cells or small clusters of cells taken at wavelengths to detect both Flag- and -HA were examined using Image J. 1.42q (Wayne Rasband. National Institutes of Health USA) software. Absolute measures could be made by highlighting a particular cell, switiching to greyscale and quantifying total fluorescent protein expression. A ratio of surface Flag- (extracellular) fluorescence to intracellular signal (-HA) was taken and normalised to the corresponding control group (100%) as indicated in the respective figure legends. In these experimental paradigms the data obtained for relative surface expression using the threshold method was quantitatively the same as using absolute ratio measures.

2.5 Biochemical assays

2.5.1 ^{3}H-palmitic acid incorporation

HEK 293 cells were transiently transfected in 12-well cluster dishes ($\approx 3 \times 10^{6}$ cells per well) using Fugene HD transfection agent (Roche) in a 6:2 ratio to cDNA. The intracellular C-terminal or full length constructs used are indicated in the respective figure legend and all contained a C-terminal –HA epitope tag. Forty-eight hours after transfection, cells were washed with pre-warmed (room temperature) PBS, then 1 ml of fresh DMEM containing 10 mg/ml fatty acid-free BSA was added for 30 minutes at 37 °C. Cells were incubated in DMEM/BSA containing 0.5-0.8 mCi/ml ^{3}H-palmitic acid (Perkin Elmer, USA) for 4 hours at 37 °C, and then the medium containing the free label was removed. Cells were then lysed in 150 mM NaCl, 50 mM Tris-Cl, 1% Triton X-100 (pH 8.0), and channel fusion proteins were captured by

using magnetic microbeads coupled to the HA antibody (μMACS epitope tag isolation kits, Miltenyi Biotec) overnight at 4 °C. After washing columns with 150 mM NaCl, 1% Nonidet P-40, 0.5% deoxycholate, 0.1% SDS, 50 mM Tris-Cl (pH 8.0), followed by washes with 50 mM Tris-Cl (pH 7.5) captured proteins were eluted in SDS/PAGE sample buffer [50 mM Tris-Cl (pH 6.8), 5 mM DTT, 1% SDS, 1 mM EDTA, 0.005% bromophenol blue, 10% glycerol] prewarmed to 95 °C.

2.5.2 Western Blotting and ^{3}H detection

Duplicate samples were run on separate SDS-PAGE gels for subsequent Western Blotting to detect total –HA tagged channel construct and for fluorography of ^{3}H-palmitate incorporation. SDS-PAGE was used to separate proteins according to their electrophoretic mobility. SDS (sodium dodecyl sulphate), is an anionic detergent which denatures secondary and non-disulfide-linked tertiary structures and applies a negative charge to each protein in proportion to its mass. The SDS-PAGE gel was run at 170 V for one hour to separate the proteins. Proteins were transferred to nitrocellulose membranes and probed with a polyclonal α-HA antibody (1:1,000; Zymed) with subsequent application of a secondary antibody conjugated to horseradish peroxidise (HRP) and detection by enhanced chemi-luminescene (ECL) using a GeneGnome imaging system. To detect ^{3}H-palmitate incorporation the nitrocellulose membrane was dried, sprayed with En^{3}hance fluorographic spray (PerkinElmer–Cetus) and exposed to light-sensitive film at −80 °C by using a Kodak Biomax transcreen LE (Amersham) for 1-4 weeks at -80 °C.

2.6 Prediction Algorithms

2.6.1 CSS-palm - palmitoylation prediction

We exploited the published CSS-palm palmitoylation algorithm (Zhou *et al.*, 2006; Ren *et al.*, 2008) to predict cysteine residues within the entire coding sequence of

the murine BK channel α-subunit as well as the STREX C-terminus alone. Palmitoylation prediction was set to the highest cutoff in the algorithm at 0.9. Scores indicate CSS-palm prediction; a higher number represents a higher probability, with a score above 1.0 demonstrating a strong prediction. Mutagenesis of key residues was also examined to determine the affect on palmitoylation status of the already identified palmitoylated residues. CSS-palm scores were determined with the published and recently revised CSS-palm v2.0 algorithm at http://bioinformatics.lcd-ustc.org/css_palm/prediction.php by inputting the full-length coding sequence of the murine STREX channel, start methionine MDALI.., accession number: NM_010610.2 and AF156674 for STREX.

2.6.2 BH search – membrane binding prediction

A Basic Hydrophobicity (BH)-scale algorithm recently developed (Brzeska *et al.*, 2010) was used to identify potential membrane binding sites in less structured regions of proteins. It is a modified version of the EMBOSS Pepinfo program, designed to be more convenient for scoring basic residues and their interaction with the plasma membrane. The algorithm can be found at http://helixweb.nih.gov/bhsearch/. The program examines the hydrophilic nature of basic residues in a protein and their electrostatic interaction with the negatively charged plasma membrane. Using a scoring system, the program averages values in a previously determined and newly adapted Wimley and White hydrophobicity scale (Wimley & White, 1996) called the Basic Hydrophobicity (BH) scale. Each amino acid in a segment of a selected length, called the window size, is scored according to the scale and a value given to the amino acid in the middle of the window. To discriminate between segments from soluble proteins and membrane spanning sequences, a window length of 19 was determined to best identify membrane-spanning sequences. It was proposed that a larger window length of 19 was more suitable because protein-spanning sequences passing through the interior of the protein are usually shorter than membrane spanning sequences (Kyte & Doolittle, 1982). Thus, for a window of 19, the first score, which is the average of the values for residues 1-19, is given to residue 10. The program then averages the values for residues 2-20 and gives that score to residue 11, continuing in this

manner until the end of the sequence with the last residue scored being 10 residues from the C terminus. Residues at the start or end of protein sequences are therefore not accurate scores. A threshold value of 0.6 was identified as the optimal parameter for identifying lipid-binding sites in proteins (Brzeska *et al.*, 2010).

2.7 Statistical analysis

Data was analysed and presented using GraphPad Prism v4.03 (GraphPad Software, Inc). All statistical analysis was carried out using one-way Anova with tukey post-hoc test comparison test, with significant differences indicated by p values of less than 0.05*, 0.01** and 0.001***.

2.8 Reagents

2-Bromohexadecanoic Acid (2BP) - Sigma-Aldrich Co Ltd. Palmitate inhibitor. Made up as a fresh 100 mM stock in 100% ethanol and applied at a final concentration 100µM.

2-Hydroxytetradecanoic acid (2HM) – Sigma-Aldrich Co Ltd. Myristate inhibitor. Dissolved in DMSO. Used at a final concentration of 0.1-1 mM.

Neomycin trisulfate salt hydrate – Sigma-Aldrich Co Ltd. Used to inhibit actions of PIP_2. Soluble in H_2O and made up as a 1 M stock stored at -4 ^{0}C. Used as a final concentration of 5 mM.

Poly-L-Lysine Hydrochloride – Sigma-Aldrich Co Ltd. Used to inhibit actions of PIP_2. Made up in PBS and sonicated for 10 minutes at stock concentration of 25 µg/ml, stored at -20 ^{0}C. Used at final concentration of 5 µg/ml.

$PI(4,5)P_2$ – L-a-Phosphatidylinositiol-4,5-bisphophate (Brain, Porcine-Triammonium Salt) Avanti Polar Lipids, Inc. Made up in de-ionised H_2O and sonicated on ice for 10-30 minutes (to replicate conditions as in (Vaithianathan *et al.*, 2008) and stored in -20 ^{0}C. Used as a final concentration of 10 µM.

$PI(4,5)P_2$ [diC16, synthetic] – Triphosphoinositide sodium salt, 1,2-Diacyl-*sn*-glycero-3-phospho-(1-D-*myo*-inositol 4,5-bisphosphate) sodium salt - Sigma-Aldrich. Made up in de-ionised H_2O and sonicated on ice for 10-30 minutes (to replicate conditions as in (Vaithianathan *et al.*, 2008) and stored in -20 ^{0}C. Used as a final concentration of 10 µM.

PIP_2 (Phosphatidylinositol-4,5-Biphosphate) Monoclonal Antibody – Assay Designs. Made up in PBS at 40 µg/µl stock and stored in -20 ^{0}C. Used as a final concentration of 10-15 µg/µl injected directly into the bath.

8-CPT-cAMP - Merck-Calbiochem. PKA activator. Soluble in H_2O and stored at -20 ^{0}C. Used at final concentration of 0.1 mM, application for 10-30 minutes.

8-CPT-cGMP - Merck-Calbiochem. PKG activator. Soluble in DMSO and stored at -20 ^{0}C. Used at a final concentration of 0.1 mM application for 10-30 minutes.

Okadaic acid – Merck-Calbiochem. Inhibits protein phosphatases (PP1 & PP2) and some serine/threonine protein phosphatases. Soluble in ethanol made up as stock concentration of 1 mg/ml stored at -20 ^{0}C and used as a final concentration of 10 nM.

H89 – Assay Designs - PKA inhibitor. Soluble in DMSO stored at -20 ^{0}C. Used at a final concentration of 1 µM.

CHAPTER THREE

PALMITOYLATION of the STREX insert

3.1 Chapter 3 introduction

3.1.1 The STREX splice variant of the BK channel

The C-terminus of the BK channel, despite the presence of hydrophobic domains, is predicted to be a cytosolic component of the BK channel (Meera *et al.*, 1997). In studies that used immunolabelling of the linking regions between the hydrophobic domains in the C-terminus under non-permeabilised conditions, the C-terminus was identified as cytosolic (Meera *et al.*, 1997). This work supported evidence gathered from investigations examining core and tail domains expressed separately (Wei *et al.*, 1994; Meera *et al.*, 1997) and recent crystal structural analysis that has modelled the C-terminal domain as an entirely cytosolic component of the BK channel (Wang & Sigworth, 2009; Wu *et al.*, 2010; Yuan *et al.*, 2010).

Alternative splicing within the BK channel C-terminus has been shown to dramatically change the properties of the channel. Insertion of the 58 amino acid STREX insert at the C2 splice site (Figure 3.1A), leftward shifts the calcium- and voltage- sensitivity of the channel (Saito *et al.*, 1997; Shipston *et al.*, 1999; Chen *et al.*, 2005; Saleem *et al.*, 2009) and generates an additional PKA phosphorylation site (S636) that results in channel inhibition (Tian *et al.*, 2001; Tian *et al.*, 2004). However, the molecular basis for the change in BK channel phenotype with STREX inclusion is unknown.

Features contained within the sequence of the alternatively spliced STREX exon may help to identify the mechanisms that underlie the different channel properties associated with the STREX channel. The STREX insert, upon inspection, is a cysteine-rich domain, with 6 out of 58 amino acids being cysteine residues (Figure 3.1B). Cysteine residues are known targets for post-translational lipid modifications, with palmitoylation being one of the most common forms. Palmitoylation can modify protein function by increasing the hydrophobicity of the target protein facilitating membrane targeting and adhesion (Resh, 1999). Using a prediction algorithm (Zhou *et al.*, 2006; Ren *et al.*, 2008) to determine potential palmitoylation sites in proteins, the STREX insert was identified as a target for palmitoylation (Table 3.1). Palmitoylation sites have been previously identified in other proteins to be located in

Figure 3.1
Sequence alignment of the cysteine rich STREX insert

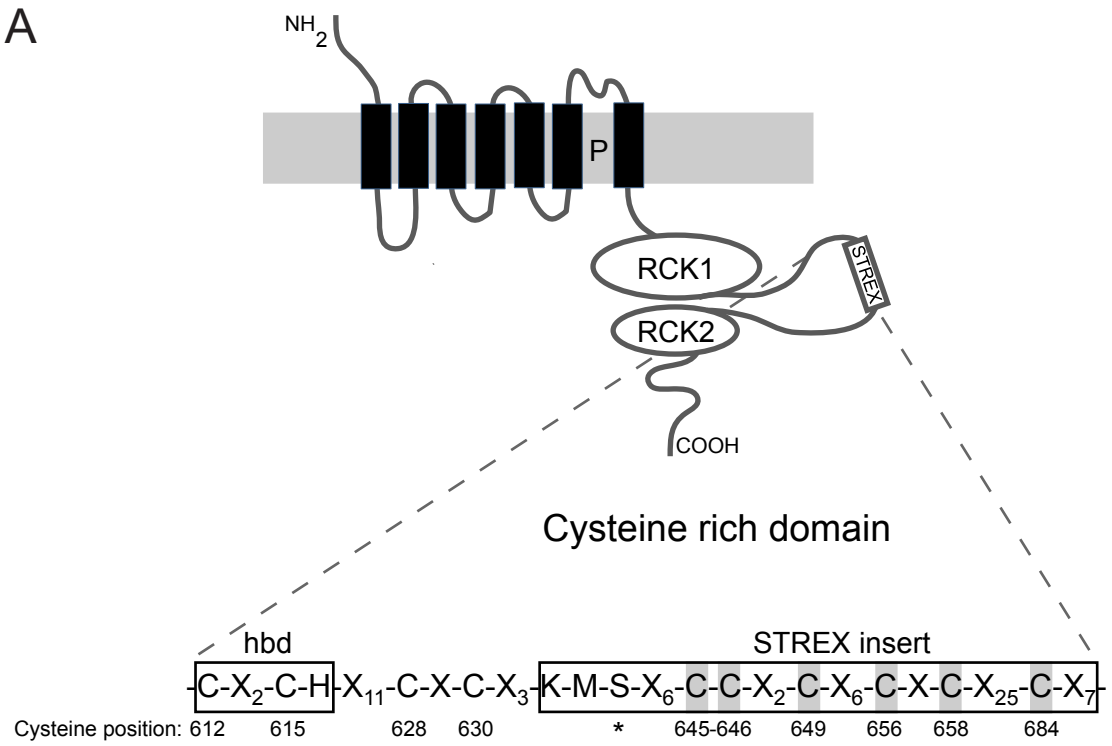

Figure 3.1. Sequence alignment of cysteine rich STREX insert. (A) Schematic illustrating the topology of the BK channel pore forming α-subunit. The STREX insert at the C2 site of splicing is located within the RCK1-RCK2 linker region, in the intracellular C-terminus. Inclusion of STREX introduces a cysteine rich domain (CRD) encompassing the haem-binding domain (hbd) and the STREX insert. Cysteine residues within the STREX insert are highlighted in grey, with all cysteine residues that make up the CRD numbered (from C612 – C684) and the PKA phosphorylation serine residue (highlighted by an asterisk, *). (B) Sequence alignment of the STREX insert illustrates the evolutionarily conserved cysteine residues highlighted in grey, across vertebrates. Channel sequence of the mouse is numbered from MDALI start site (accession number NM_010610).

C-terminal domains (Resh, 1999), such as in the ionotropic glutamate receptor GluR6 that contains two palmitoylation cysteine sites within in the C-terminus (Pickering *et al.*, 1995). Membrane targeting domains often use combinations of palmitoylation and other lipid modifications or polybasic domains to carry out specific functions (Bijlmakers & Marsh, 2003; Dietrich & Ungermann, 2004). The local environment around a palmitoylation site often appears to be quite indicative of its ability to be palmitoylated and function as a membrane targeting domain. Therefore, the additional presence of a series of basic residues around the C2 splice site and STREX domain may well be characteristic of a palmitoylated functional membrane targeting region.

One possible explanation for the dramatic shift in channel gating seen with splicing of the STREX insert is that STREX itself may act as a membrane targeting domain that may change the configuration of the channel through the process of palmitoylation. The C2 splice site is located in the linker (RCK1-RCK2 linker) that joins the two RCK domains that form the gating domain of the BK channel. The RCK1-RCK2 linker has recently been modelled on the periphery of the gating domain and hence does not appear to be buried within the channel structure (Yuan *et al.*, 2010) (Figure 1.10). This suggests that it is possible that the linker region could freely interact with the plasma membrane. Additional studies have identified that the RCK1-RCK2 linker, which has poor evolutionary conservation across different species, is predicted to have no regular secondary structure (NORS) (Lee *et al.*, 2009a) and in crystal structural studies of the channel, this region cannot be defined (Wang & Sigworth, 2009; Yuan *et al.*, 2010). It has also been shown that the length of the RCK1-RCK2 linker rather than the specific amino acid sequence is more important in manifesting changes in channel activity (Lee *et al.*, 2009a). Therefore the linker would appear not to be constrained by specific arrangements within the channel and may be able to adopt a conformational change upon splice inclusion of the STREX insert.

The STREX insert also brings a previously identified phosphorylation site that has been implicated in the functional heterogeneity to PKA regulation seen in the BK channel. Specifically it was found that PKA phosphorylation at the S927 site, outside of STREX, activates the channel whereas inclusion of the STREX insert which contains an additional PKA phosphorylation site, S636, results in channel inhibition

(Tian *et al.*, 2001; Tian *et al.*, 2004). Phosphorylation therefore plays an important role in the properties attributed to the STREX channel by PKA regulation and may have additional roles influencing how the STREX domain operates in the channel.

3.1.2 Working hypothesis

In this chapter, the hypothesis that STREX is a membrane targeting domain independent of the N-terminal transmembrane domains and is controlled by palmitoylation will be tested.

3.1.3 Aims to be addressed in this chapter

3.1.3.1 Is STREX a membrane targeting domain?

In order to examine whether STREX functions as a membrane targeting domain, the cellular location of C-terminal constructs generated without N-terminal transmembrane domains, with and without the STREX insert (see methods section 2.1.1), was examined by a fluorescent imaging strategy. These fluorescent fusion proteins were expressed in HEK293 cells that are amenable expression systems for studying the BK channel which is not native to this cell line. It would be predicted that the insertless 'ZERO' C-terminal domain which has been largely cited as a cytosolic domain, would be present in the cytoplasm of the cell. Therefore if the STREX insert is able to function as a membrane targeting domain, then the 'STREX' C-terminal domain, which is the same as ZERO except for an additional 58 amino acid insert at splice site C2, would locate at the plasma membrane.

3.1.3.2 Is membrane targeting of STREX palmitoylation-dependant?

To study palmitoylation as a mechanism for targeting STREX to the plasma membrane a fourfold approach was made. Firstly, a prediction algorithm allowed identification of potential palmitoylation sites within the BK C-terminus. Secondly, a site directed mutagenesis strategy mutating key cysteine residues that are predicted

to be palmitoylated in STREX, allowed the location of fluorescently tagged C-terminal constructs to be determined therefore identifying key residues involved in membrane targeting. Thirdly, by using pharmacological approaches to inhibit lipid modification the mechanism responsible for membrane association was identified. And fourthly, to directly assess palmitoylation of the STREX C-terminus, incorporation of radiolabelled ^{3}H-palmitate into C-terminal channel proteins identified the key cysteine residues in the C-terminus that are important for palmitoylation.

3.1.3.3 What is the functional significance of palmitoylation?

To examine the functional significance of palmitoylation, successful mutant cysteine residues identified in the imaging and radiolabelling assays were substituted into full length channels and screened using a membrane potential assay that can discriminate different channel phenotypes based on altered voltage- and calcium-sensitivity or changes in cell surface expression. Channels with differing responses dissected out by the membrane potential assay were then taken forward and examined by electrophysiological patch clamp techniques to isolate the kinetics of the mutant channels with relation to the wild-type STREX channel.

3.1.3.4 Does phosphorylation regulate membrane targeting of STREX?

To identify whether phosphorylation of the S636 site within the STREX insert that mediates channel inhibition by PKA is involved in the regulation of the membrane targeting properties of the STREX insert, a similar imaging strategy was used to examine cellular location of C-terminal STREX fluorescently tagged fusion protein by mutating the S636 phosphorylation site and introducing phospho-mimetic substitutions to simulate the phosphorylated channel.

3.2 Results

3.2.1 STREX as a membrane targeting domain

To examine whether the STREX insert may act as a membrane targeting domain, an imaging approach was taken to examine where the C-terminal domain localises in HEK293 cells. C-terminal constructs of the insertless ZERO channel and the STREX channel, that is the same as ZERO except for an additional 58 amino acid insert, were created by subcloning the murine intracellular carboxyl (C-) terminus (from residue G328 to residue C1226) of the BK α-subunit. A fluorescent protein tag (GFP) was fused to carboxyl end of the C-terminal protein to allow detection of the expressed protein (see section 2.1.1 & Figure 2.1). Constructs were then expressed in mammalian HEK293 cells (Figure 3.2A).

Expression of the insertless ZERO C-terminus construct (S6:ZERO), demonstrated a diffuse cytoplasmic presence (17%) and strong nuclear localisation (99%). There was no evidence of plasma membrane expression (N= 3, n= >500 cells counted) (Figure 3.2B, left panel). Conversely, expression of the STREX C-terminus construct (S6:STREX) resulted in robust plasma membrane expression, with 73% of all cells transfected showing clear fluorescence at the plasma membrane in the absence of transmembrane segments and a strong nuclear fluorescence in over 90% of all cells (N= >4 n= >1000 cells counted) (Figure 3.2B, centre panel).

Therefore, alternative splicing of the STREX insert does influence the cellular location of the largely cytosolic/nuclear C-terminus and acts as a membrane targeting domain.

3.2.2 STREX is a cysteine rich domain

Alternative splicing of the STREX insert at splice site C2 generates a cysteine rich domain (CRD) (Figure 3.1A). Within the CRD 10 cysteine residues make up the 78 amino acid residues in the region that incorporates the CRD (from C612 – F691) (Figure 3.1A). The CRD comprises the STREX insert and an upstream hame-binding domain (hbd). Sequence alignment of the murine coding region of the CRD

suggests strong evolutionary conservation of cysteine residues across the vertebrate phyla, indicating that these residues may have structural or functional importance (Figure 3.1B).

Cysteine residues can be modified by post-translational modifications such as palmitoylation which will enhance a protein's ability to be targeted to the plasma membrane (Resh, 1999). Therefore it is possible that membrane targeting of the STREX domain may be mediated through palmitoylation of cysteine(s) residues within STREX.

3.2.3 Cysteine residues in STREX are predicted to be palmitoylated

To investigate whether the cysteine rich domain may promote targeting of the STREX insert to the plasma membrane via palmitoylation, a recently developed computer algorithm (CSS-Palm v2.0) (Zhou *et al.*, 2006; Ren *et al.*, 2008), was used to screen for potential sites of palmitoylation within the STREX C-terminus.

The CSS-Palm algorithm predicts cysteine residues or cysteine motifs that may be palmitoylated. The algorithm is based on data from 263 experimentally verified palmitoylation sites from 109 distinct proteins (published prior to November 2006) which groups them into subsets based on sequence similarity and identifiable palmitoylation motifs. Each cysteine is given a final score for potential palmitoylation based on a defined similarity score. The higher the score of a cysteine residue within a sequence, the more confidence there is that the peptide may be palmitoylated above the high threshold cut off value of 0.9. A value above 2.0 indicates a very high score as a potential palmitoylation site. The most recent version of the algorithm (CSS-palm v2.0) was used in this study. The CSS-palm v2.0 algorithm can be found at http://bioinformatics.lcd-ustc.org/css_palm.

The murine STREX splice variant of the BK channel sequence (accession number NM_010610) spanning the intracellular C-terminus from the end of the S6 transmembrane domain to the end of the intracellular carboxyl tail (G328 - C1226), was examined by inputting the amino acid sequence, in FASTA format, into the CSS-Palm platform to retrieve prediction results.

Table 3.1
Predicted palmitoylation scores for cysteine residues in the intracellular C-terminus of the STREX splice variant of the BK channel

A

	Position	Peptide	CSS-palm v2.0 score	
	422	ADA**C**LIL	0.2	
	430	NKY**C**ADP	0.1	
	485	DAI**C**LAE	0.3	
	498	AQS**C**LAQ	0.6	
	554	PTV**C**ELC	0.6	
	557	CEL**C**FVK	0.9	
	612	FFY**C**KAC	0.7	
	615	CKA**C**HDD	0.8	
	628	IKK**C**GCR	0.0	
	630	KCG**C**RRP	0.1	
STREX	645	RRA**C**CFD	2.5	
STREX	646	RAC**C**FDC	0.6	
STREX	649	CFD**C**GRS	1.1	
STREX	656	ERD**C**SCM	0.2	
STREX	658	DCS**C**MSG	0.3	
STREX	684	VND**C**STS	0.3	
	753	FHW**C**APK	0.1	
	780	VVV**C**IFG	0.3	
	855	INL**C**DMC	0.8	
	858	CDM**C**VIL	0.8	
	878	DKE**C**ILA	0.4	
	969	PFA**C**GTA	0.2	
	1033	RDR**C**RVA	0.2	
	1053	DGG**C**YGD	0.3	
	1224	EDEC***	1.7	*

B

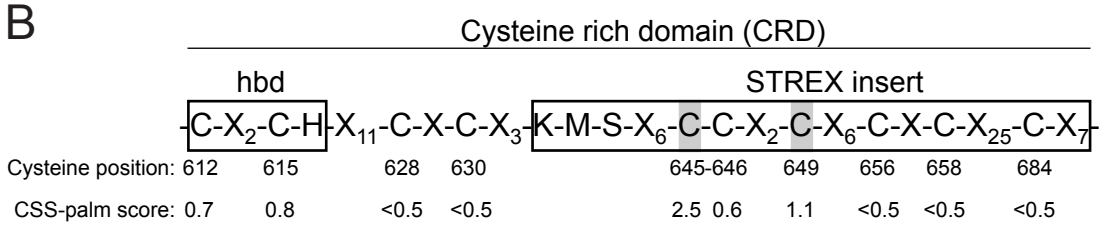

Table 3.1. Predicted palmitoylation scores for cysteine residues in the intracellular C-terminus of the STREX splice variant of the BK channel. (A) Scores indicate CSS-palm prediction; a higher score represents higher probability. CSS-palm scores were determined with the published CSS-palm v2.0 at http://bioinformatics.lcd-ustc.org/css_palm by inputing the protein sequence of the entire intracellular C-terminus of the STREX variant of the BK channel (starting at glycine residue G328 and spanning until cysteine residue C1226). Highest scoring residues for palmitoylation are shown in grey. (B) Sequence diagram illustrating the position of cysteine residues in the CRD with prediction scores >0.5. * cysteine score at end of peptide is not reliable.

The algorithm calculated the predicted palmitoylation score for all cysteine residues in the C-terminus of the BK channel (Table 3.1A). Using a high threshold cut-off score (above 0.9), the two residues with the highest predicted scores were located within the STREX insert, C645 - CSS-Palm score 2.5 and C649 - CSS-Palm score 1.1 (indicated by grey boxes) (Table 3.1A).

Therefore the algorithm suggests that cysteine residues within the STREX insert may be palmitoylated which would enable the STREX domain to function as a membrane targeting domain.

3.2.4 C645-C646 residues are important for STREX C-terminus association at the plasma membrane

The S6:ZERO construct did not show evidence of plasma membrane association, therefore it would be assumed that if cysteine residues are important for localisation at the plasma membrane, then any cysteine residues outside of the STREX region would appear not to have a functional role in plasma membrane targeting of the C-terminus. To examine the potential of cysteine residues within the STREX domain to anchor the C-terminus at the plasma membrane via palmitoylation, a site directed mutagenesis approach was taken by mutating cysteines to neutral alanine (A) residues. Cysteine residues within the identified CRD incorporating STREX were also examined. C-terminal constructs were designed with individual cysteine mutations and dual cysteine mutations and transfected into HEK293 cells to examine C-terminal association with the plasma membrane.

The total plasma membrane expression of the S6:STREX -GFP fusion construct was normalised to 100% therefore allowing direct comparison of mutated cysteine constructs to S6:STREX (black bars) (Figure 3.2C). Mutation of cysteine residues in the N-terminal end of the CRD upstream of the STREX insert that includes cysteine residues within the hbd (C612A:C615A) and (C628A:C630A), had no effect on the association of the C-terminal fusion proteins at the plasma membrane (C612A:C615A, 97 ± 9 %, and C628A:C630A, 98 ± 5 % of S6:STREX. N= >4, n= >350 cells counted).

Figure 3.2
Cysteine residues are important for targeting of the STREX C-terminus (S6:STREX) to the plasma membrane

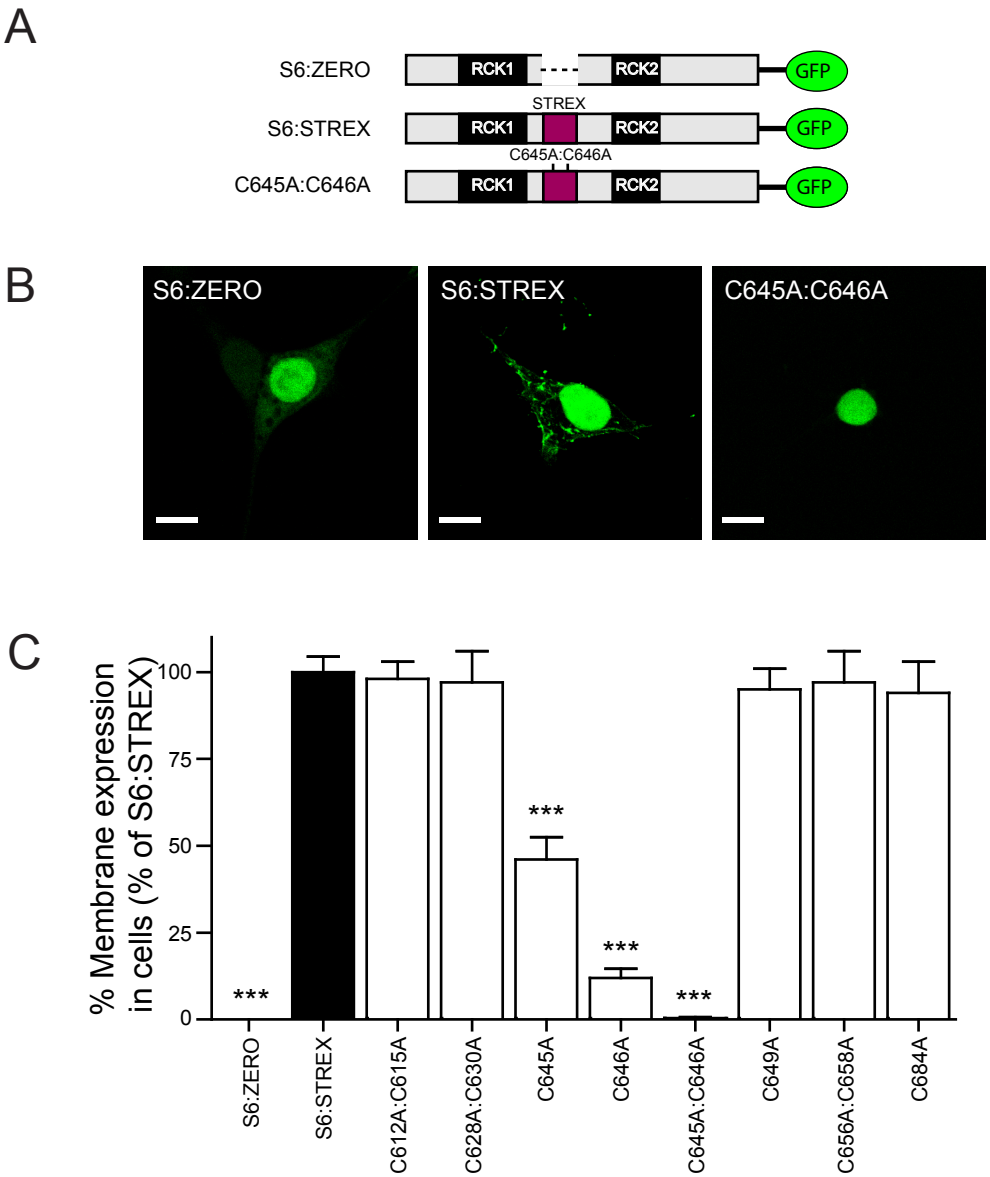

Figure 3.2. Cysteine residues are important for targeting of the STREX C-terminus (S6:STREX) to the plasma membrane. (A) Schematic of C-terminal -GFP fusion constructs. (B) Representative single confocal images of C-terminal STREX (S6:STREX), dicysteine mutant (C645A:C646A) and the insertless C-terminal ZERO (S6:ZERO) construct, expressed in HEK293 cells. (Scale bars: 10 µm). (C) Summary bar graph of the respective C-terminal cysteine point mutation constructs expressed at the plasma membrane as a percentage of S6:STREX (where S6:STREX is 100%). *** $p<0.001$ compared with S6:STREX (ANOVA with tukey post hoc test).

Within the STREX insert, mutation of C645A reduced plasma membrane expression to 46 ± 6 % with mutation of the adjacent cysteine residue, C646A, having a greater effect reducing plasma membrane expression to 12 ± 3 % (N= >4, n= >600 cells counted). The double mutant (C645A:C646A) almost completely abolished plasma membrane association of the C-terminal fusion proteins to 0.5 ± 0.3 % plasma membrane expression of S6:STREX (N= >4, n= >1600 cells counted) (Figure 3.2B, right panel). Subsequent cysteine residues in the C-terminal end of STREX had no significant effects in reducing association at the plasma membrane, (C649A 95 ± 6%, C656A:C658A 97 ± 9 % and C684A 94 ± 9 % of S6:STREX. N= >4, n= >350 cells counted).

The data would suggest that the C645 or C646 cysteine residues must be crucial for targeting of the STREX C-terminal constructs to the plasma membrane. Therefore palmitoylation at these cysteine residues may be important for membrane targeting of the STREX insert.

3.2.5 Palmitoylation controls the association of C-terminus constructs at the plasma membrane

To identify whether palmitoylation does play an important role in association of the STREX C-terminus at the plasma membrane an inhibitor of palmitoylation, 2-bromopalmitate (2-BP, 100 µM) was pre-incubated for various time periods in transiently transfected HEK293 cells (Fig 3.3). 2-bromopalmitate (2BP) is a non-metabolizable palmitate analog that blocks palmitate incorporation into proteins (Webb *et al.*, 2000). Pre-incubation with 2-BP for 6 hours had no significant effect on plasma membrane association of S6:STREX constructs (104 ± 7 %, N=>4, n= >500 cells counted), however longer incubation periods of 24 and 48 hours had a significant effect in nearly completely abolishing membrane association of the STREX C-terminus (Figure 3.3B, right panel & C). 24 hours incubation with 2-BP decreased the association of STREX at the plasma membrane to 21 ± 4 % whereas a longer incubation time of 48 hours essentially abolished plasma membrane expression to 1 ± 0.7 % (N= >4, n= >1000 cells counted). As a control for general effects of post-translational lipid modification a myristoylation inhibitor, 2-

Figure 3.3
Palmitoylation controls the association of C-terminus constructs at the plasma membrane

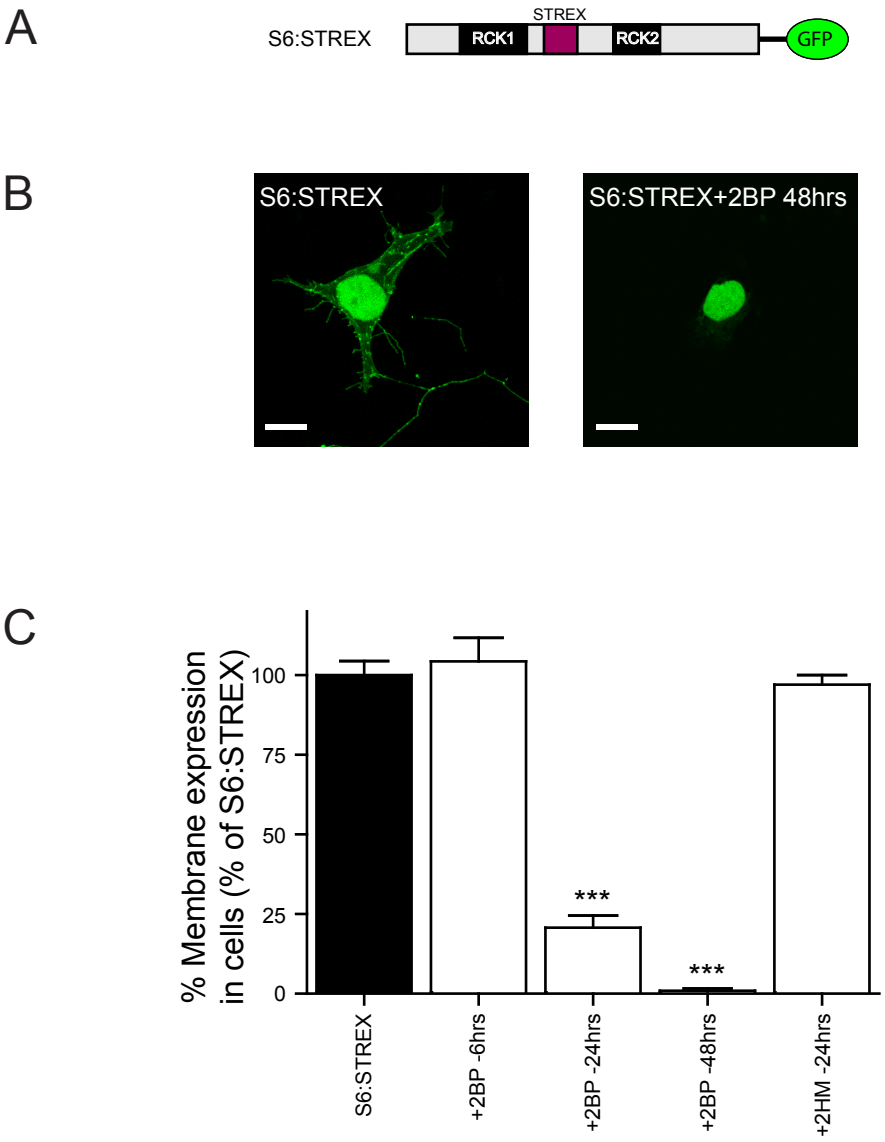

Figure 3.3. Palmitoylation controls the association of C-terminus constructs at the plasma membrane. (A) Schematic of the STREX C-terminal -GFP fusion construct. (B) Representative single confocal images of S6:STREX, and S6:STREX after 48hr incubation with palmitoyltransferase inhibitor 2BP (100 μM) (Scale bars: 10 μm). (C) Summary bar graph of the respective C-terminal construct localization at the plasma membrane after 6, 24 and 48 hours incubation with 2BP, expressed as a percentage of S6:STREX (where S6:STREX is 100%) and 24 hour incubation with myristate inhibitor 2HM (0.1 nm). *** $p<0.001$ compared with S6:STREX (ANOVA with tukey post hoc test).

hydroxymyristate (2-HM, 0.1-1 mM), was found to have no significant effect on C-terminal association at the plasma membrane (97 ± 3 %, N=>4, n= >350 cells counted), (Figure 3.3C). The vehicle for 2-BP, 0.1% DMSO also had no effect on C-terminal targeting to the plasma membrane (102 ± 3 %, N=>4, n= >350 cells counted).

The data suggests that palmitoylation plays a key role in the STREX domain associating at the plasma membrane. The decreased expression seen at the plasma membrane with 48 hours pre-incubation of 2-BP was similar to the decreased expression seen with mutation in the double cysteine motif (C645A:C646A) in STREX. This would suggest that endogenous palmitoylation may regulate the C645:C646 motif in STREX, to promote the C-terminus of the STREX channel to associate with the plasma membrane independent of transmembrane domains.

3.2.6 STREX channel activation driven by increased calcium is diminished in C645A:C646A mutant channels

To examine the functional effect of palmitoylation, cysteine residues were mutated in full length STREX channels and examined in a membrane potential assay that has been previously used as a preliminary screen of recombinant BK channels (Saleem *et al.*, 2009) with good correlation to patch clamp electrophysiology.

The membrane potential assay is a high-throughput assay that uses voltage sensitive fluorescent reporter dyes (FLIPR-blue bis-oxonol dye, Molecular Devices) with rapid sensitivity to report ion channel activity to a stimulus. Using Ionomycin (1 µM) to stimulate calcium entry into cells, the calcium sensitive component of the BK channel could be driven, activating the channels. Upon stimulation of the BK channel, potassium ion efflux would hyperpolarise the cell membrane which would result in a decrease in relative fluorescence as the FLIPR dye moves out of the cell membrane and is quenched by the extracellular medium. In un-transfected cells calcium entry would cause a depolarisation which resulted in an increase in relative fluorescence as the FLIPR dye moved into the cytoplasm of the cell.

Full length STREX channels, STREX channels with mutation of the C645A:C646A and ZERO channels were transiently transfected into HEK293 cells and seeded into 96 well assay plates. Cells were loaded with FLIPR-blue dye (Molecular Devices) and the assay was then run in the Flexstation ® II during which cells were stimulated by 1 µM Ionomycin to activate the BK channel. Ionomycin was delivered by the automated liquid-handing function of the Flexstation ® II which administered 50 µl of Ionomycin to a total well volume of 200 µl, 16 seconds after the Flexstation ® II began reading to allow a measure of baseline fluorescence. Changes in fluorescence were then measured over a time course of 180 seconds.

Changes in absolute relative fluorescence could be detected (units = relative fluorescent units, RFU) and illustrated in a graph against time (seconds) or expressed as the isolated channel current by subtracting the control HEK response from the transiently transfected channel response within the assay plate. Using the full length STREX channel as a control response, the peak hyperpolarisation was normalised to 100% (at t=70 seconds) and channel variants and mutants could then be compared to the STREX channel.

A representative trace illustrates the activation of the STREX channel (black circle) showing a decrease in fluorescence that peaks at around the 70 second time point corresponding to hyperpolarisation of the cells (Figure 3.4A). Un-transfected HEK293 cells (open circle) show an increase in fluorescence corresponding to depolarisation due to calcium influx (Figure 3.4A). Comparing the insertless ZERO (grey circles) channel to the more calcium sensitive STREX channel (black circles), the hyperpolarising response in the same assay is largely attenuated at t=70s to 42 ± 10% when compared to STREX at 100% (N= 3, n= >20). Mutation of the key dicysteine residues (C645A:C646A) identified as important for targeting the C-terminus to the plasma membrane (inverted triangles) shows a reduced hyperpolarising response of 68.3 ± 4% when compared to STREX at 100% at t=70s (N= 3, n= >20) midway between the STREX and ZERO channel phenotype (Figure 3.4B). The discrimination of STREX and ZERO correlate well with the calcium and voltage sensitivities previously identified (Saleem *et al.*, 2009).

The data suggests that the C645A:C646A mutant channel displays an intermediate phenotype between the increased calcium sensitive STREX channel and the less sensitive ZERO channel. It may be that palmitoylation of the dicysteine motif

Figure 3.4
STREX activation driven by calcium influx is diminished in C645A:C646A mutant channels

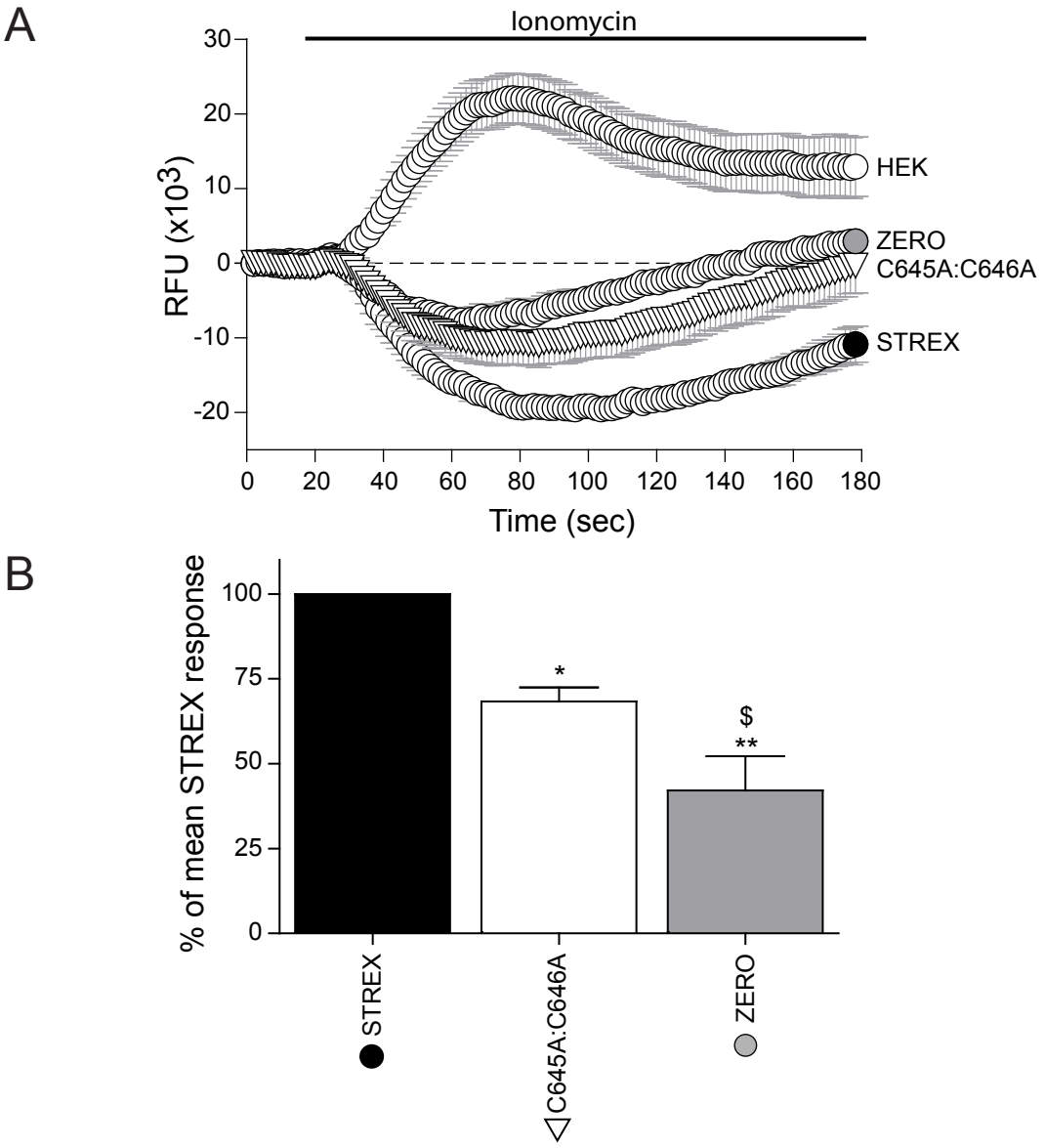

Figure 3.4. STREX activation driven by calcium influx is diminished in C645A:C646A mutant channels. (A) Representative time course plots of mean change in relative fluorescence units (RFU) of the FLIPR-blue membrane potential dye in HEK293 cells expressing STREX (black circles, ●), C645A:C646A (inverted triangles,▽), ZERO (grey circles,◍), and mock-transfected HEK293 (open circles, ○), in response to calcium influx induced by 1 µM Ionomycin. (B) Summary bar chart of the peak hyperpolarisation at t=70s for each variant expressed as a percentage of the STREX response (where STREX is 100%). Data was determined at the maximum hyperpolarising response in STREX (t=70s) in the time course plots in (A). All data are Means ± S.E.M (N=3, n= >30), * $p<0.05$, ** $p<0.01$, compared to STREX. ($) ZERO is not significantly different from C645A:C646A (ANOVA with tukey post hoc test).

mediates the different properties that STREX insertion confers to the channel. Whether the dicysteine mutant channel has decreased calcium sensitivity becoming more “ZERO-like” or whether channel conductance has changed by disruption of channel structure requires full electrophysiological investigation. The membrane potential assay cannot directly discriminate between shifts in the calcium or voltage sensitivity of the channel, changes in single channel amplitude, nor would it resolve absolute cell surface expression of functional channels at the plasma membrane.

3.2.7 Single channel amplitude is unchanged in STREX, C645A:C646A and ZERO channels

To investigate whether differences in single channel amplitude of the mutant C645A:C646A channels may mediate the attenuated response described in the membrane potential assay, it was necessary to examine isolated channels electrophysiologically.

Single channel amplitude was measured at a range of membrane potentials (-80 mV to +80 mV) in excised inside-out patches in symmetrical potassium gradients (140 mM $[K^+]_i$ / 140 mM $[K^+]_o$) and 0.33 µM $[Ca^{2+}]_i$ (Figure 3.5A). Single channel slope conductance of the STREX channel was 233 ± 2.5 pS. There was no significant difference in single channel slope conductance in the C645A:C646A mutant channel at 230 ± 2.5 pS and the insertless ZERO channel at 231 ± 2.5 pS. Single channel openings are shown at +40 mV for each channel variant in Figure 3.5B.

This suggests that the differences in channel activity described in the membrane potential assay are not mediated by changes in single channel amplitude.

3.2.8 C-terminal targeting to the plasma membrane mediates STREX channel properties

To examine BK channel activation in mutant channels, macroscopic currents were recorded by inside-out patch clamp analysis in symmetrical potassium gradients (140 mM $[K^+]_i$ / 140 mM $[K^+]_o$), as before, to examine the calcium- and

Figure 3.5
Single channel amplitude is unchanged in STREX, C645A:C646A mutant and insertless ZERO BK channels

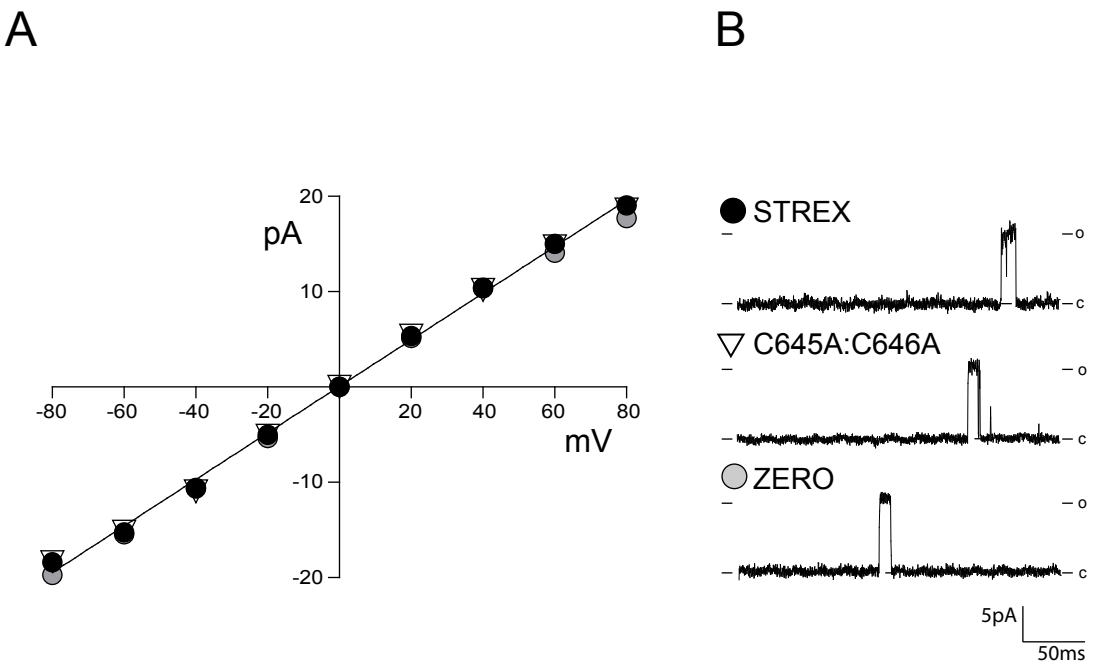

Figure 3.5. Single channel amplitude is unchanged in STREX, C645A:C646A mutant and insertless ZERO BK channels. (A) Current voltage plot for STREX channels (closed circles, ●) dicysteine mutant C645A:C646A channels (inverted triangles ▽) and insertless ZERO channels (grey circles, ○), illustrating that single channel conductance is unaffected in 0.33 μM free Ca^{2+} and 140 mM equimolar potassium gradients (N=3). Single channel conductance derived from the slope of the line. The conductance of STREX is 233.7 ± 0.2 pS, C645A:C646A is 230.4 ± 0.2 pS and for ZERO was 231.0 ± 0.2 pS. SEM is shown within the symbols. (B) Representative single channel recordings of excised inside-out patches at +40 mV.

voltage- sensitivity in the channel (Figure 3.6). An equimolar potassium gradient was used to remove the chemical gradient, therefore isolating the electrical driving force of the channels. Representative macropatch currents illustrate the typical outward component of the BK channel response to a depolarising voltage step protocol (-120 to +120 mV) from a holding potential of -80 mV (Figure 3.6A). Activation (G/G_{MAX}) curves were obtained by plotting normalised tail current amplitudes versus the respective test potential. These curves were fitted to a Boltzmann equation whereby the voltage for half activation ($V_{0.5MAX}$) could be determined (Figure 3.6B). Tail currents were examined because the amplitude of the tail current is proportional to the channel open probability at the end of the preceding depolarisation (Islas & Sigworth, 1999). Previous functional studies of the STREX splice variant have demonstrated a dramatic shift in the apparent calcium sensitivity of the STREX channel compared to the insertless ZERO variant (Saito *et al.*, 1997; Shipston *et al.*, 1999; Chen *et al.*, 2005). In particular the difference in half maximal voltage for activation is most apparent at sub-micromolar free calcium concentrations whereas above 1 µM free calcium the voltage for half maximal activation of STREX channels begin to converge with the ZERO channel. Therefore the STREX variant is more potently activated within the physiological calcium and voltage range than ZERO (Chen *et al.*, 2005).

Measurement of channel activity was made in 0.33 µM Ca^{2+} at the midpoint of the physiological range for STREX to allow discrimination of differences in channel activity. The half maximal voltage for activation of normalised (G/G_{MAX}) curves was determined in relation to STREX (Figure 3.6C). The voltage for half maximal activation of the STREX channel was 34.9 ± 1.6 mV. The C645A:C646A mutation significantly rightward shifted the voltage for half activation by ~18 mV to 52.8 ± 2.5 mV ($p<0.001$ compared to STREX. N=>3), with the insertless ZERO channel showing the largest rightward shift to 68.2 ± 3 mV ($p<0.001$ compared to STREX. N=>3), in accordance with previous studies (Saito *et al.*, 1997; Shipston *et al.*, 1999; Chen *et al.*, 2005).

This data would appear to suggest that the C645:C646 dicysteine residues in STREX that target the C-terminus to the plasma membrane may mediate part of the shift in the half maximal activation of the STREX splice variant of the BK channel in relation to the insertless ZERO channel. The shift in channel activity recorded in the

Figure 3.6
C645A:C646A mutation rightward shifts the $V_{0.5MAX}$ of the STREX channel towards the ZERO channel

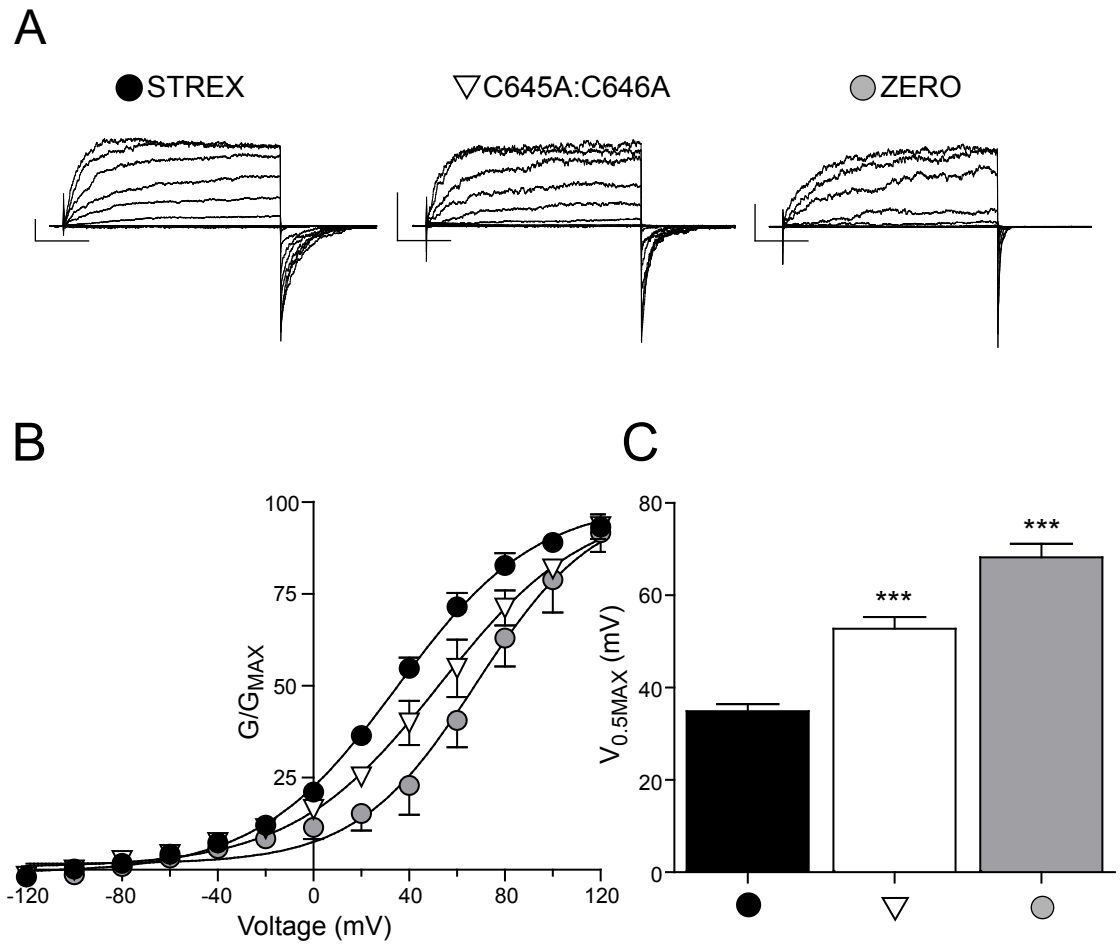

Figure 3.6. C645A:C646A mutation rightward shifts the $V_{0.5MAX}$ of the STREX channel towards the ZERO channel. (A) Representative traces showing outward currents at depolarized potentials from HEK293 cells expressing STREX (black circles, ●), C645A:C646A (inverted triangles, ▽), and ZERO (grey circles, ◍), from excised inside-out patch recordings in equimolar (140 mM) potassium gradients and 0.33 µM free Ca^{2+}. Outward currents were elicited by 100 ms depolarising voltage steps from -120 to +120 mV in 20 mV increments from a holding potential of -80 mV. (Scale bars: 1 nA / 25 ms) (B) G/G_{MAX} conductance curves from tail currents. (C) Summary bar graph showing $V_{0.5MAX}$ for STREX, cysteine mutant C645A:C646A and ZERO channels. All data are Means ± S.E.M (n= >3), *** p<0.001, compared to STREX (ANOVA with tukey post hoc test).

Figure 3.7
The voltage dependence of the mutant C645A:C646A channel is un-affected

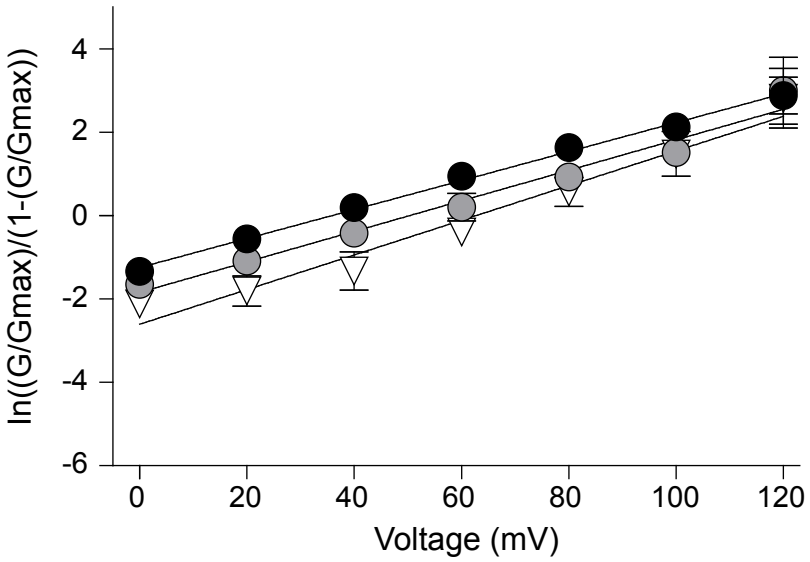

Figure 3.7. The voltage dependence of the mutant C645A:C646A channel is un-affected. A logarithmic transformation of the G/G_{MAX} activation curves over depolarised potentials of 0 to +120 mV as described in the macropatch recordings in Figure 3.6B. STREX (closed circles, ●), C645A:C646A (inverted triangles,▽), and ZERO (grey circles, □). The voltage dependence was derived from the slope of the line.

dicysteine mutant channel using electrophysiology correlates well with the shift in the channel response described by the membrane potential assay.

3.2.9 Voltage dependence is unchanged in mutant channels

To determine whether the voltage sensitivity of the C645A:C646A mutant channels has changed when compared to STREX or ZERO channels, a logarithmic transformation to linearize the activating component of the normalised (G/G_{MAX}) curves in Figure 3.6B were plotted against the depolarised potentials from 0 mV to +120 mV (Figure 3.7). Disruption of the C645:C646 cysteine residues has no effect on the voltage dependence of the channels when compared to STREX and ZERO. Therefore the changes in activity described for the STREX C645A:C646A and ZERO channels appear not to be mediated by an altered voltage sensitivity of the channels.

3.2.10 Palmitoylation of the C-terminus is abolished by mutation of the C645:C646 residues in the STREX

To directly address whether the STREX channels are indeed palmitoylated and to investigate if mutation of the key cysteine residues within STREX (C645A:C646A) could disrupt the palmitoylation status of the channel, ^{3}H-palmitate incorporation into C-terminal fusion proteins was examined in HEK293 cells (Figure 3.8).

Transfected –HA tagged C-terminal constructs expressed in HEK293 cells were incubated with DMEM/BSA containing 0.5mCi/ml 3H-palmitic acid for 4 hours at 37 ^{0}C and then lysed to collect the channel fusion proteins. The recovered samples could then be separated by SDS/PAGE and probed with polyclonal HA antibodies. A duplicate membrane was dried and sprayed with En^{3}hance fluorographic spray and exposed to a light sensitive film at -80 ^{0}C for 1-3 weeks to detect palmitate incorporation as described (see methods section, 2.5.1).

The representative fluorographs (Figure 3.8) show that the STREX C-terminal construct (S6:STREX) is robustly palmitoylated in HEK293 cells by endogenous

Figure 3.8
Palmitate incorporation into S6:STREX is abolished by mutation of cysteine residues C645A:C646A and is absent in ZERO channels

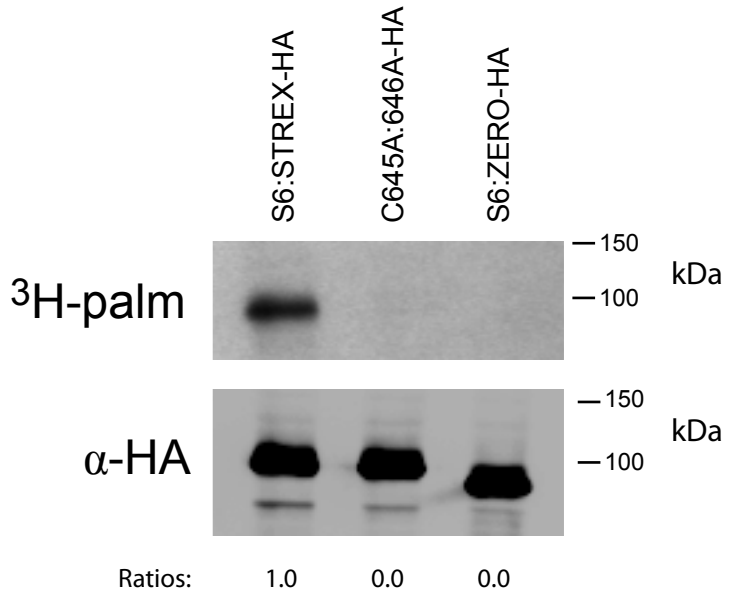

Figure 3.8. Palmitate incorporation into S6:STREX is abolished by mutation of cysteine residues C645A:C646A and is absent in ZERO channels. Representative fluorographs (Upper) and Western blots (Lower) of S6:STREX-HA, double cysteine mutant C645A:C646A-HA, and S6:ZERO-HA, expressed in HEK293 cells. Constructs were labelled with ^{3}H-palmitate for 4 hours and the respective constructs immunoprecipitated (IP) using α-HA magnetic microbeads, subjected to SDS-PAGE and probed by a polyclonal HA antibody and detected by fluorography. Ratios of palmitate detection in comparison to total protein expression are included (normalised to S6:STREX).

palmitoyl tranfererases. In the insertless ZERO C-terminal construct, there is no detectable ^{3}H-palmitate incorporation suggesting that the STREX insert contains the only palmitoylation site within the entire C-terminus of the BK channel. ^{3}H-palmitate incorporation was also abolished in the C645A:C646A mutant, suggesting that these residues are the major site of palmitoylation within the STREX insert and within the C-terminus of the STREX splice variant of the BK channel (Fig 3.8). Western blot analysis showed that total protein expression was essentially unchanged in the assays (n=3). Therefore this data identifies a novel palmitoylation site within the STREX C-terminus of the BK channel, (C645:C646), that is regulated by endogenous palmitoylation. The data also supports the hypothesis that the STREX insert is important for targeting of the C-terminus to the plasma membrane through a mechanism of palmitoylation.

Regulation of the palmitoylation status at this site in the STREX insert may be influenced by the local environment or by other important motifs close to the palmitoylation site. In palmitoylated proteins it has been shown that the local environment adjacent to a palmitoylation site is important for stability at the plasma membrane (Bijlmakers & Marsh, 2003; Dietrich & Ungermann, 2004). Therefore, the PKA phosphorylation site just upstream of the STREX palmitoylation site could potentially influence palmitoylation and hence the conformation of the STREX channel.

3.2.11 The PKA phosphorylation motif in STREX mediates membrane targeting of the C-terminus

It has been previously shown that BK channels are differentially regulated by PKA mediated phosphorylation. PKA activates ZERO channels at a conserved C-terminal phosphorylation site (S927), downstream of the splice site C2. Conversely splicing of the STREX insert generates an additional PKA consensus motif in STREX, S636, just upstream of the palmitoylation site (C645:C646), that results in channel inhibition by PKA, that conforms to a single subunit rule (Tian *et al.*, 2004) (Figure 3.9A).

Figure 3.9
Mutation of the S636 PKA phosphorylation site in STREX disrupts C-terminus association with the plasma membrane

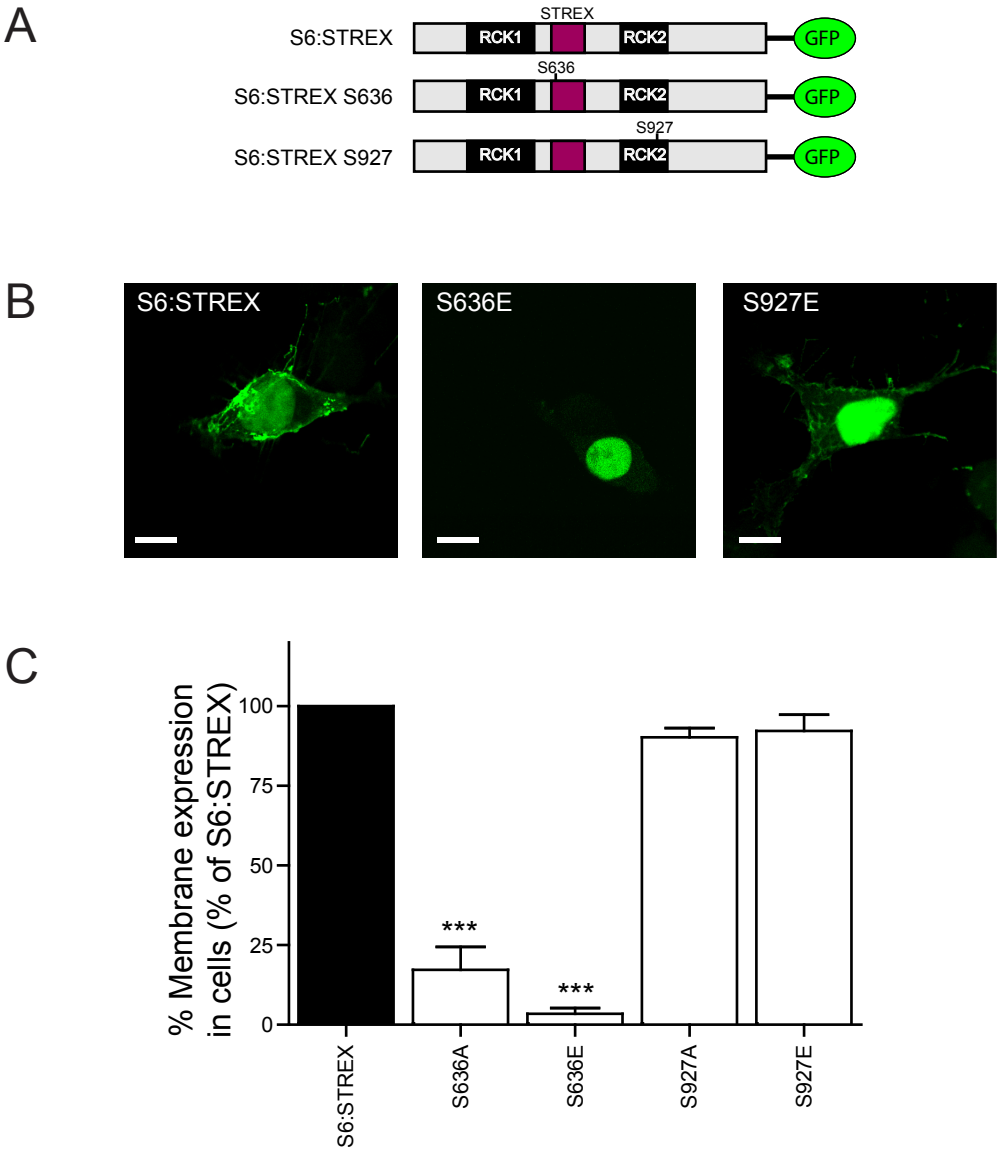

Figure 3.9. Mutation of the S636 PKA phosphorylation site in STREX with a phosphomimetic residue disrupts C-terminus association with the plasma membrane. (A) Schematic of C-terminal -GFP fusion constructs. (B) Representative single cell confocal images of C-terminal S6:STREX, S636E and S927E, in HEK293 cells (Scale bars: 10 µm). (C) Summary bar graph of the respective mutant serine C-terminal constructs localization at the plasma membrane expressed as a percentage of S6:STREX (where S6:STREX is 100%). *** $p<0.001$ compared with S6:STREX (ANOVA with tukey post hoc test).

To determine whether palmitoylation and phosphorylation might together mediate a conformational change in STREX that controls the different channel properties in the channel through membrane targeting, phosphomimetic mutant constructs were created to examine membrane association of C-terminal domains. Substitution of the PKA consensus serine residue with a phosphomimetic glutamic acid (E) residue (S636E) in STREX, essentially abolished C-terminal localisation at the plasma membrane to 3.5 ± 1.7% in comparison to STREX at 100%. Substitution with a neutral alanine (A) residue also reduced plasma membrane association of C-terminal constructs to 17.2 ± 7% (N= >4, n= >600 cells counted) (Figure 3.9C). To examine whether these effects were unique to phosphorylation at the PKA consensus site in STREX, the same mutations were made at the conserved PKA motif downstream of the C2 splice site (S927), which is the major site for PKA activation. Substitution of serine-927 with glutamic acid and alanine residues had no significant effect on STREX C-terminal association with the plasma membrane (S899E was 92.2 ± 5% of S6:STREX, S899A was 90.3 ± 2.9% of S6:STREX. N= >4, n= >500 cells counted), (Figure 3.9C).

Therefore mimicking phosphorylation at the PKA motif in STREX (S636) decreases membrane targeting of the STREX C-terminus. However, to directly investigate PKA mediated regulation of C-terminal association at the plasma membrane, PKA was activated using a cell-permeable cAMP analogue 8-CPT-cAMP, to study the effect.

3.2.12 PKA phosphorylation dissociates the STREX C-terminus from the plasma membrane

In this set of experiments HEK293 cells expressing the STREX C-terminal construct were incubated with the membrane-permeable cAMP analogue 8-CPT-cAMP (0.1 mM) for 10-30 minutes, to establish whether constructs at the plasma membrane could be dissociated by PKA phosphorylation. Pretreatment with 8-CPT-cAMP (0.1 mM), significantly reduced membrane association of the STREX C-terminal constructs to 38 ± 3% when compared to STREX at 100% (N= >4, n= >350 cells counted) (Fig 3.10). The effect of cAMP could be abolished with PKA inhibitor H89 (1 µM) (96 ± 5% of S6:STREX) (N= >4, n= >350 cells counted) (Fig 3.10). Okadaic acid (10 nM) a potent inhibitor of protein phosphatases 1 and 2A that has been

Figure 3.10
PKA phosphorylation of S6:STREX disrupts C-terminal association with the plasma membrane

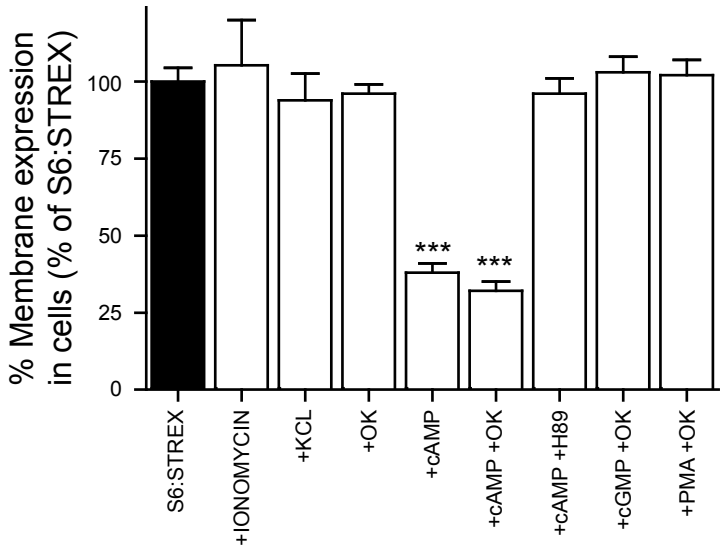

Figure 3.10. PKA phosphorylation of S6:STREX disrupts C-terminal association with the plasma membrane. Summary bar graph illustrating the effect of kinase activity on association of the S6:STREX -GFP tagged construct at the plasma membrane expressed as a percentage of S6:STREX (where S6:STREX is 100%). Ionomycin (1 μM) and KCL (25 mM) were used as activators of the BK channel. Okadaic acid (10 nM) inhibits phophatase activity which has also been shown to modulate BK channel activity. cAMP (0.1 mM) activates PKA-dependant phosphorylation and H89 (1 μM) is an inhibitor of PKA phosphorylation. cGMP (0.1 mM) activates PKG-dependant phosphorylation and PKC was activated with the phorbol ester PMA (100 nM) both in the presence of okadaic acid. *** $p<0.001$ compared with S6:STREX (ANOVA with tukey post hoc test).

shown to modulate the BK channel (White *et al.*, 1991; Reinhart & Levitan, 1995; Loane *et al.*, 2006) had no effect on membrane association of the C-terminal STREX constructs (96 ± 3%) and did not affect the cAMP response (32.1 ± 3%).

To examine the effect of other protein kinases to exclude non-specific phosphorylation of BK channels at different sites, cells were activated by protein kinase G (PKG) or C (PKC) analogues that have been shown to modulate BK channel activity independent of STREX (White *et al.*, 2000; Zhou *et al.*, 2000). Activation of PKG with the cell permeant cGMP analogue 8-CPT-cGMP (0.1 mM) in the presence of okadaic acid had no effect of STREX localisation at the plasma membrane (103 ± 5%). Similarly, PKC activation with the phorbol ester PMA (100 nM) in the presence of okadaic acid had no effect (102 ± 5%) (N= >4, n= >350 cells counted). Therefore PKG and PKC phosphorylation of BK channels does not affect membrane association of the STREX domain.

As a further control for general activation of the BK channel and membrane association of the C-terminal constructs, ionomycin (a calcium ionophore) (1 µM) was used to elevate intracellular calcium and high KCL (25 mM) was used to depolarise the cell membrane. There was no significant effect on the plasma membrane localisation of STREX (ionomycin, 105.2 ± 14.7% and KCl, 93.8 ± 8.7%. N= >4, n= >350 cells counted) (Fig 3.10).

Together, this data supports a model in which PKA phosphorylation of STREX results in dissociation of the STREX domain from the plasma membrane. This may represent the configurative changes that may underlie the dramatic changes in channel activity seen with PKA inhibition in STREX channels.

3.3 Discussion

Here for the first time, the alternatively spliced STREX insert within the RCK1-RCK2 C-terminal linker of the BK channel has been shown to function as a membrane targeting domain. This ability of STREX to associate with the plasma membrane is regulated by palmitoylation and may be modulated by phosphorylation. Palmitoylation may also contribute to the increased calcium sensitivity inherent to the STREX splice variant of the BK channel. Aspects of this work have been published in PNAS (see appendix #1; (Tian *et al.*, 2008a)).

3.3.1 STREX insert is a membrane targeting domain

By determining the cellular location of fluorescently tagged C-terminal constructs of the BK channel, the ZERO C-terminal construct as expected for a cytosolic protein, was located diffusely in the cell's cytoplasm, however, unexpectedly it was also found in the nucleus (this will be discussed later in chapter 4 section 4.3.7) when expressed in HEK293 cells. STREX C-terminal constructs, that have an additional 58 amino acid insert within the RCK1-RCK2 linker, demonstrated strong plasma membrane expression in up to 73% of cells expressing the C-terminal fusion protein and also a strong nuclear expression. Identical results were seen in cells that endogenously express STREX channels including murine anterior pituitary corticotrophe (AtT20) cells, rat pheochromocytoma PC12 cells, and human insulinoma INS-1 cells (see appendix #1; (Tian *et al.*, 2008a)). Therefore, alternative splicing of the STREX insert, which is dynamically regulated by stress hormones (Xie & McCobb, 1998), introduces a membrane targeting domain to the cytosolic C-terminus of the BK channel.

To examine the mechanism underlying membrane association of STREX, a strategy to mutate cysteine residues identified as potential sites for palmitoylation within the STREX cysteine rich domain (CRD) was used. Two evolutionary conserved cysteine residues C645:C646 were found to be important for the membrane targeting ability of STREX C-terminus constructs. Mutation of these cysteine residues decreased membrane association of STREX C-terminal constructs by ~99%, no other cysteine

residue in the CRD had any effect. Application of a palmitoylation inhibitor, 2-BP reduced membrane association of the STREX C-terminal constructs by ~99%, as seen with the double cysteine mutant. Interaction of the STREX domain with the plasma membrane was not disrupted by an inhibitor of myristoylation (2-HM) suggesting that the effect of palmitoylation is not mediated by the general properties of lipidation of proteins.

3.3.2 Palmitoylation controls membrane association of STREX

To directly address whether the STREX C-terminus is palmitoylated, a radiolabelled assay examining ^{3}H-palmitate incorporation into C-terminal STREX, the insertless C-terminal ZERO and mutant cysteine C645A:C646A STREX C-terminal constructs was examined. The ZERO C-terminus was not palmitoylated suggesting that the insertless C-terminus does not have any additional palmitoylation sites. The STREX C-terminus was robustly palmitoylated and importantly, mutation of the identified cysteine residues, C645A:C646A, totally abolished palmitoylation within the STREX C-terminal construct. This suggests that the C645:C646 cysteine residues are the key palmitoylation sites within the STREX splice variant C-terminus of the BK channel.

^{3}H-palmitate incorporation was also studied in full length STREX channel constructs which were also robustly palmitoylated, however in full length channel constructs that did not have the 58 amino acid STREX insert, (ZERO channels), ^{3}H-palmitate incorporation was diminished but not abolished (see appendix #1; (Tian *et al.*, 2008a)). Hence the C645:C646 site in STREX is the major palmitoylation site in the BK C-terminus, however the channel may be palmitoylated at additional sites outside of the C-terminus (this will be discussed further in chapter 5).

3.3.3 Palmitoylation functionally affects STREX channels

So does palmitoylation have a functional role in the BK channel? To examine this, channels with mutation of the key cysteine residues identified as being palmitoylated were studied electrophysiologically. Double cysteine mutation in the STREX channel

rightward-shifted the voltage for half-maximal activation by ~33 mV, back towards the less calcium sensitive insertless ZERO channel phenotype. Therefore, it would appear that palmitoylation is able to regulate channel activity perhaps mediating the increased calcium sensitivity of the STREX channel over the ZERO channel. This suggests that the properties associated with STREX may be controlled by dynamic post-translational modification through palmitoylation of the STREX domain. Whether palmitoylation *per se* controls the changes in channel properties directly through the voltage or calcium sensor or whether the RCK1-RCK2 interaction with the plasma membrane mediates a shift in channel properties through a conformational change in the gating domain, is unknown.

In additional experiments following on from this work it was demonstrated that inhibition of palmitoylation by 2-BP also rightward-shifted the voltage for half-maximal activation of the STREX channel by ~15 mV (see appendix #1; (Tian *et al.*, 2008a)). The smaller shift in channel activity in comparison to that seen in the cysteine mutant channel could possibly be due to channels that are still palmitoylated, although the right-ward shift is consistent with a role for palmitoylation in contributing to STREX channel's increased calcium sensitivity.

3.3.4 Can STREX structurally interact with the plasma membrane?

Upon alternative splicing of STREX at splice site C2, the STREX insert is located within the RCK1-RCK2 linker of the cytosolic C-terminal domain of the BK channel. Crystal structural studies described recently by the Sigworth, MacKinnon and Jiang labs have illustrated the RCK1-RCK2 linker as located peripherally to the channel's gating domain (see Figure 1.10)(Wang & Sigworth, 2009; Wu *et al.*, 2010; Yuan *et al.*, 2010). Therefore the region appears not to be buried within the globular structure of the functioning RCK domains, but would potentially be able to interact with different regions of the cell including possibly the plasma membrane.

Cryo-EM studies examining the BK channel structure in its lipid environment, suggest that the distance from the RCK1-RCK2 interface to the plasma membrane would be ~5 nm (see Figure 1.8)(Wang & Sigworth, 2009). Recent crystal structural analysis examining the tandem RCK domains within each C-terminal subunit of the

human BK channel, describe a long unstructured linker connecting RCK1 to RCK2. The end boundary of the RCK1 domain (in murine STREX channel) is defined at F610, based on the unstructured region in the channel sequence that links the two RCK domains (Yuan *et al.*, 2010). This recent crystal structure builds upon comparative studies by the same group in 2001 which aligned the BK channel sequence to the crystal structure of prokaryotic K^+ channels despite low sequence homology at less than 20% (Jiang *et al.*, 2001). Studies have identified the boundary of the second RCK2 domain using alignment techniques against several bacterial K^+ channels and based on some of the preliminary work by Jiang *et al*, (in murine STREX channel) to start at H776 (Yusifov *et al.*, 2008) which was confirmed by the recent BK crystal structure studies (Wu *et al.*, 2010; Yuan *et al.*, 2010). This means that the linker between the RCK domains (RCK1-RCK2 linker) is 166 amino acids in length (it would be 108 amino acids in length for the insertless ZERO channel linker).

The RCK1-RCK2 linker region is predicted to have no regular secondary structure (NORS) (Lee *et al.*, 2009a) so it is difficult to assess firstly, the structure the linker may adopt and secondly, what the linear length of the polymer would be. To identify whether the STREX domain would be capable of interaction with the plasma membrane, simple assumptions can be made to predict the potential length of the RCK1-RCK2 linker.

In the literature, a cited value for the average length of an amino acid within a polypeptide varies. Estimates examining protein folding and unfolding, cite a contour length of ~4 Å per amino acid (Carrion-Vazquez *et al.*, 1999; Ainavarapu *et al.*, 2007). Using this value and for the purposes of the model assuming the RCK1-RCK2 linker has very little secondary structure and conforms to a linear string, the length would be (166 amino acids x 4 Å) ~64 nm. Of course amino acid chains would not be expected to form linear strings and there would probably be some structural component within the linker. However, it is wholly feasible using these assumptions that the linker could reach the plasma membrane potentially by unravelling from whatever structure the linker may have or even if unstructured, it may be able to freely move within the cell cytoplasm to reach the plasma membrane which is 5 nm from the RCK1-RCK2 interface.

Alternatively, if we consider that the plasma membrane of a cell is ~10 nm in thickness and requires ~21 amino acids in an α-helical conformation to cross the lipid bilayer (Stryer, 1997), then by asking the question of what is the easiest way to get to the plasma membrane and back using simple α-helices, less than ~30 amino acids (5nm distance = 11 amino acids x2 = 22) is all that would be required. Although we do not know how the RCK1-RCK2 linker folds, it realistically could reach across the relatively small 5 nm distance to interact with the plasma membrane (Figure 3.11).

Whether palmitoylation targets this region to the plasma membrane, or whether palmitoylation occurs at the plasma membrane, whereby the region may have been targeted through some other mechanism was examined in a follow up study recently published from our lab (Tian *et al.*, 2010). In the study we were able to identify the enzymes responsible (DHHC's) for palmitoylating the STREX palmitoylation site. The DHHC's involved were mostly thought to be localised in the Golgi/ER (see appendix #3; (Tian *et al.*, 2010)) and despite one of the DHHC's involved being a membrane bound enzyme, it is possible that the STREX domain could be palmitoylated in the Golgi before export to the plasma membrane whereby the palmitoylated STREX RCK1-RCK2 linker can then target the plasma membrane. This proposes that palmitoylation itself may act as a membrane targeting signal.

It is also unknown in the full length functional channel, in its native environment, whether the C-terminus would actually interact with the plasma membrane. A feasible experiment to test this could involve a protease digestion site at the S6-RCK1 linker whereby the C-terminal, fluorescently tagged, could be removed from the transmembrane core and then examined for stable cell surface expression.

Together, the data in this chapter suggests that the STREX domain can interact with the plasma membrane to contribute to the altered features inherent to the STREX channel. Future experiments could focus on the properties of membrane binding through palmitoylation by examining binding of recombinant proteins to liposomes.

Figure 3.11
Model of RCK1-RCK2 linker interaction with the plasma membrane through the STREX domain

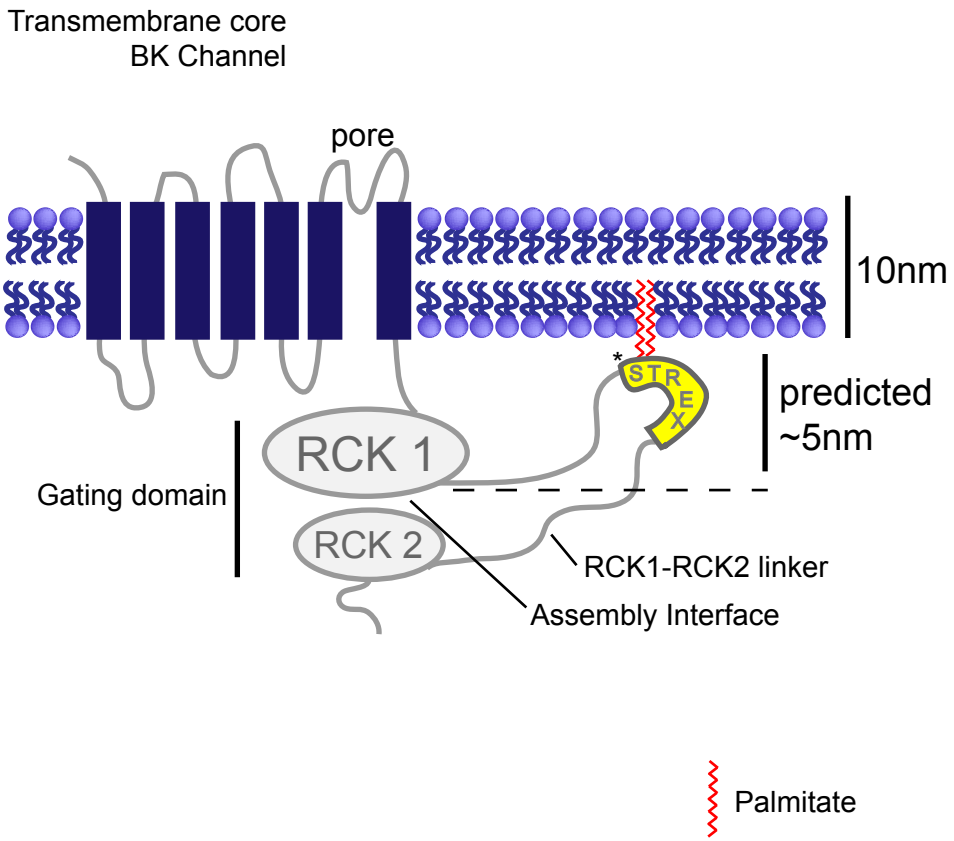

Figure 3.11. Model of RCK1-RCK2 linker interaction with the plasma membrane through the STREX domain. Model illustrating how palmitoylation may anchor the STREX domain at the plasma membrane. Distances of plasma membrane and distance from RCK1-RCK2 interface to the plasma membrane are shown (not to scale). The RCK1-RCK2 linker is 166 amino acids in length, predictions suggest a minimum of 30 amino acids are required to reach the plasma membrane and back using a simple structure. Palmitate residues that insert into the lipid membrane are illustrated in red at the dual cysteine C645-C646 palmitoylation site. The phosphorylation site in STREX, S636 is indicated by a (*). The STREX insert is indicated in yellow.

3.3.5 Phosphorylation decreases membrane stability

BK channels are differentially regulated by PKA mediated phosphorylation that leads to activation in ZERO channels, and inhibition in STREX channels. PKA regulation of channel inhibition in STREX channels was also found to conform to a single subunit rule (Tian *et al.*, 2004). It is probable that the opposing inhibitory effects described with PKA phosphorylation in STREX are the result of major conformational rearrangements in the C-terminus of the BK channel. It has been shown that palmitoylation of STREX mediates membrane targeting and therefore this could be a mechanism whereby phosphorylation of a single subunit could result in channel inhibition by destabilisation of the STREX domain.

The STREX phosphorylation site is just 9 amino acids upstream from the C645:C646 palmitoylation site in STREX. Mutation of S636 to a phosphomimetic (glutamic acid - E) residue in fluorescently tagged STREX C-terminal constructs resulted in a decreased membrane association of STREX by ~96%. Substitution with a neutral (alanine – A) residue at S636 also decreased membrane association of the C-terminal STREX construct by ~83%, suggesting that this area may be functionally important in regulating how the STREX domain interacts with the plasma membrane or it may be structurally important for stability of STREX at the plasma membrane. Using cAMP, to activate PKA-dependant phosphorylation of C-terminal STREX constructs already at the plasma membrane, also decreased association by ~62%. This effect could not be mimicked by PKG or PKC analogues or protein phosphatase inhibitors, but importantly was blocked by a PKA inhibitor, H89.

These studies using site directed mutagenesis to disrupt the STREX PKA-phosphorylation site do not reveal the mechanism underlying phosphorylation and membrane association of the STREX domain. Additionally we do not understand the cycles of phosphorylation or dephosphorylation that may be involved in regulating channel trafficking and recycling from the membrane. Nor do we understand how phosphorylation may regulate palmitoylation at the site just immediately downstream, that is if palmitoylation is the key regulator of membrane association of the STREX domain. However, the data suggests that PKA-dependant phosphorylation in STREX can regulate destabilisation of the membrane association

of the STREX domain. Interestingly, the STREX phosphorylation site is located in a region of basic charge, the introduction of a strongly negative charge as a result of palmitoylation may be significant in disrupting the basic environment just upstream from the palmitoylation site. Basic domains as seen in STREX, have been shown to be important for palmitoylation, for example in G-protein signalling the G_{α} subunit associates with the plasma membrane through palmitoylation. However, disruption of a region of basic residues close to the palmitoylation site decreases membrane association and abolishes palmitoylation of the protein (Crouthamel *et al.*, 2008). Therefore, one of the major questions is whether this basic domain is important for palmitoylation or stability of STREX at the plasma membrane and does phosphorylation regulate this?

The role of the basic domain and whether phosphorylation could potentially control membrane stability and palmitoylation within STREX will be discussed further in chapter 4.

3.3.6 How could membrane targeting of the RCK1-RCK2 change the properties of the BK channel

A study examining the length of the RCK1-RCK2 linker suggests that the length rather than amino acid composition is more important in conferring mechanical constraints on the BK channel's gating domain (Lee *et al.*, 2009a). They suggest that changing the length of the linker could affect channel activity by increasing the strain on the gating machinery or by altering the dynamics of the interface between the RCK domains. If the RCK1-RCK2 linker were to act almost like a spring that could influence the gating domain of the channel, it is conceivable that STREX could induce a conformational change in the RCK1-RCK2 linker that might alter the interface between the RCK domains. In the crystal structure of the C-terminal domain, the calcium binding site is proposed to be located on the RCK assembly interface (Yuan *et al.*, 2010) which is different to the much studied MthK channel where calcium binds on the flexible interface (see Figure 1.11). Therefore if structural changes or changes in tension are able to influence the assembly interface between the RCK domains where calcium binds in the BK channel, then these changes conceivably could also alter calcium binding or calcium affinity and

therefore change the characteristics of the insertless ZERO BK channel to those inherent to the STREX BK channel. If the RCK1-RCK2 linker is capable of interacting with the plasma membrane through the STREX domain, then it would certainly support the theory that STREX can mediate stretch sensitivity by modulating BK channel activity through interaction with the plasma membrane (Naruse *et al.*, 2009).

3.3.7 Challenges for the future

Challenges for the future will be to examine (i) the functional relevance of palmitoylation in native cells (ii) what controls palmitoylation within the cell (iii) What palmitoyl acyl transferases (PATs) and or pamitoyl protein thioesterases (PPTs) are involved in controlling palmitoylation of the channel (iv) and how do the PATs and PPTs regulate the channel (v) could palmitoylation regulate other properties in the channel for example protein interaction of specific membrane targeting to specialist regions (vi) is the basic domain near to the palmitoylation site important – this will be addressed in chaper 4 (vii) are their additional palmitoylation sites in the BK channel – this will be addressed in chapter 5 (viii) were does palmitoylation of STREX occur and is this specific – partly addressed in (appendix #3; (Tian *et al.*, 2010)) (ix) do extracellular signals regulate palmitoylation of STREX?

3.3.8 In Summary

This data reveals that the STREX splice variant of the BK channel is regulated by palmitoylation, controlling membrane targeting of the STREX domain. Palmitoylation and membrane targeting of the RCK1-RCK2 linker may be the mechanism responsible for the increased calcium sensitivity associated with STREX channels over insertless ZERO channels and in regulating PKA-dependant channel inhibition.

CHAPTER FOUR

The POLYBASIC DOMAIN in STREX

4.1 Chapter 4 introduction

4.1.1 Polybasic domains

Palmitoylation sites appear to have no canonical consensus sequence that can identify a target cysteine residue(s) within a protein. Target cysteines are usually located near to transmembrane domains where they are able to interact with the plasma membrane (Bijlmakers & Marsh, 2003; Dietrich & Ungermann, 2004) or in intracellular domains close to additional membrane targeting sequences. Regions of basic charge or adjacent lipid anchors (Bijlmakers & Marsh, 2003; Dietrich & Ungermann, 2004) are often identified in the vicinity of palmitoylated cysteine residues located in intracellular domains.

In STREX channels, the C645:C646 cysteine residues are palmitoylated within the STREX insert located in the C-terminus, as previously discussed (see chapter 3). Alternative splicing of the 58 amino acid STREX insert also introduces a series of basic charges to a region just upstream of the C645:C646 palmitoylation site. This region incorporates 11 basic amino acid residues out of a total of 21 amino acids in close proximity to the STREX channel palmitoylation site. It is possible that this series of basic residues upon splice insertion of STREX may form a functional polybasic domain (Figure 4.1).

Polybasic domains are clusters of basic residues in proteins that can function as membrane targeting signals (Heo *et al.*, 2006). They enhance a protein's affinity for the negatively charged inner leaflet of the plasma membrane through an electrostatic mechanism whereby basic residues interact with acidic lipids. Indeed, it is well established that many proteins require non-specific electrostatic interactions for their activity and regulation (Mulgrew-Nesbitt *et al.*, 2006). However, generally simple electrostatics are not enough to strongly associate proteins at the plasma membrane (Mulgrew-Nesbitt *et al.*, 2006) and therefore many basic domains function in conjunction with additional hydrophobic regions within the same region of the protein (Ben-Tal *et al.*, 1996). Polybasic domains are also considered to influence palmitoylation of peripheral proteins in stabilising membrane localisation, such as in the G-protein subunit family (Crouthamel *et al.*, 2008).

Figure 4.1
Sequence alignment of basic residues in the intracellular C-terminus of the STREX channel

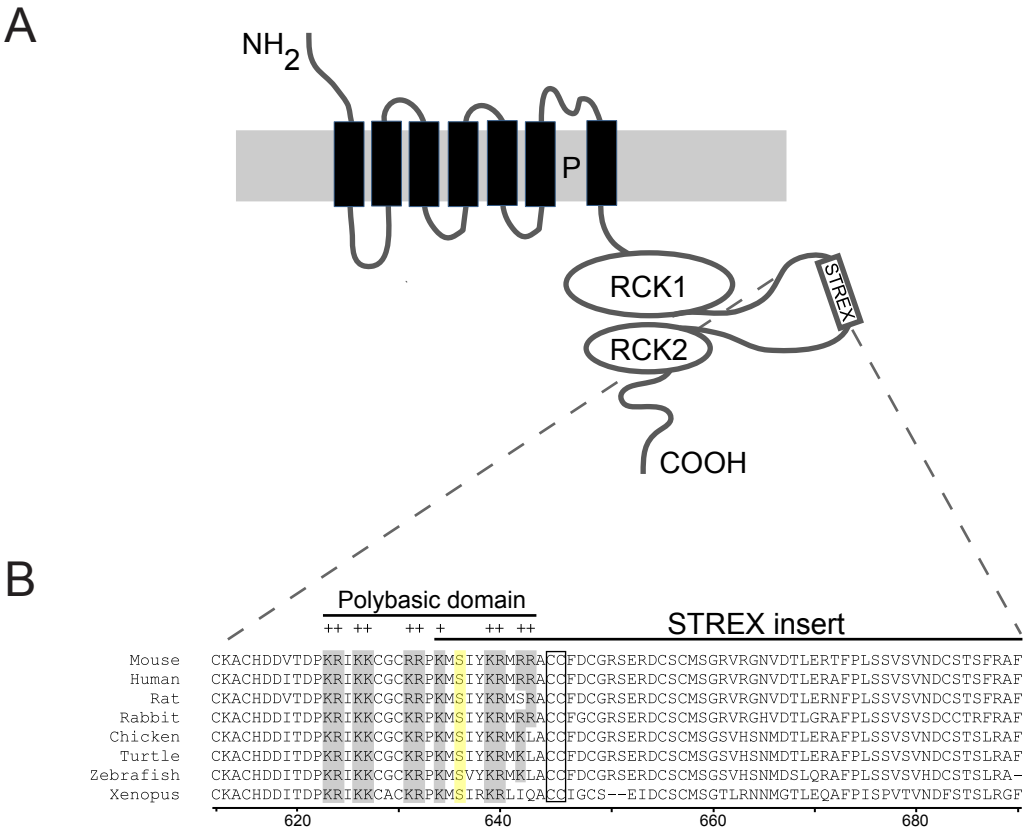

Figure 4.1. Sequence alignment of basic residues in the intracellular C-terminus of the STREX channel. (A) Schematic illustrating the topology of the BK channel pore forming α-subunit. Splicing of the STREX insert is at splice site C2 within the RCK1-RCK2 linker region, in the intracellular C-terminus. (B) Inclusion of STREX introduces a series of basic residues (+) (basic charge conservation highlighted by grey box) that form a putative polybasic domain (indicated by labelled black line). Sequence alignment of the region preceding and including the STREX insert (indicated by labelled black line) illustrates the highly conserved positively charged residues in the polybasic domain across vertebrates and the palmitoylated cysteine residues in STREX (indicated by black box outline). S636 PKA-phosphorylation site in STREX is indicated in yellow. Channel sequence of the mouse is numbered from MDALI start site (accession number NM_010610) and illustrated beginning at cysteine residue 612.

The lipid membrane carries an appreciable negative charge in comparison to other intracellular membranes which have less charge (Stryer, 1997). Hence, polybasic clusters generally bind to the plasma membrane through non-specific electrostatic interactions, although there is evidence that they may also specifically sequester phosphoinositides that have greater negative valences (McLaughlin *et al.*, 2002; Mulgrew-Nesbitt *et al.*, 2006). The local environment around a palmitoylation site in many proteins appears to be important (Crouthamel *et al.*, 2008) and therefore the question is whether this basic region might function as a polybasic domain that may influence membrane association or regulate the palmitoylation status of the C645:C646 site in STREX.

Preliminary screening of the STREX channel using an algorithm to examine basic regions that may potentially interact with the plasma membrane (Brzeska *et al.*, 2010), identified the polybasic domain just upstream of the STREX palmitoylation site as a possible plasma membrane targeting motif (Figure 4.2).

4.1.2 What would the functional role of a polybasic domain be in the STREX channel?

Polybasic domains play a dual role in facilitating targeting and stabilization of lipidated regions of proteins to the plasma membrane. Disruption of these polybasic domains in regions with lipid modifications can often decrease membrane association of the protein (Crouthamel *et al.*, 2008).

In the previous chapter it was identified that phosphorylation within the STREX insert at serine-S636, could influence membrane association of the STREX C-terminus. Phosphorylation at this serine has been previously identified as being important in mediating the STREX channel's inhibitory effect on channel activity mediated by PKA phosphorylation (Tian *et al.*, 2004). Using a site directed mutagenesis strategy, the introduction of a phosphomimetic residue with a negatively charged side chain (glutamic acid) appeared to decrease membrane association of the STREX C-terminus despite the region presumably still being capable of palmitoylation at the C645:C646 site. A reduced membrane association of the STREX C-terminus was also induced using a cAMP analogue to establish the effect of PKA phosphorylation. The presence of basic charges in the vicinity of the

phosphorylation site was postulated to be significant in exerting this effect (see section 3.3.6). It is possible that this basic region may have a potential role as a putative polybasic domain. The serine phosphorylation site, S636, is located in the mid-point of the identified polybasic domain (Figure 4.1) and phosphorylation would presumably introduce a strong negative charge that would disrupt the basic charge of this region. Therefore, it is important to establish the role of the polybasic domain in membrane targeting through palmitoylation of the STREX C-terminus and what the mechanism is that mediates membrane dissociation by PKA phosphorylation.

4.1.3 Working Hypothesis

In this chapter, the hypothesis that splicing of the STREX insert introduces a functional polybasic domain that may control the ability of palmitoylation to anchor STREX at the plasma membrane will be tested.

4.1.4 Aims to be addressed in this chapter

4.1.4.1 Is the polybasic domain a functional membrane association domain?

In order to examine whether the polybasic domain identified just upstream of the STREX palmitoylation site is functional in controlling membrane association, firstly a basic-hydrophobic prediction algorithm was used to identify whether the putative polybasic domain was indicative of a membrane association domain. Secondly, by deliberately disrupting the polybasic domain, neutralising positive charges in the region with neutral amino acids or negatively charged amino acids for maximum disruption by site directed mutagenesis, membrane association of fluorescently tagged STREX C-terminal constructs was assessed by an imaging strategy.

4.1.4.2 Does the polybasic domain influence channel properties?

To examine the functional significance of the polybasic domain, mutated residues within the polybasic domain were screened in full length channels using a

membrane potential assay that can discriminate different channel phenotypes based on activation driven by calcium. Polybasic mutant channels were then examined more closely by electrophysiological patch clamp techniques to determine the calcium- and voltage- sensitivity of the mutant channels and isolate the differing kinetics in relation to the wild-type STREX channel.

4.1.4.3 How is palmitoylation of the STREX C-terminal influenced by the polybasic domain?

To determine whether disruption of the polybasic domain only affects membrane targeting of the STREX C-terminus or whether disruption of the local environment around the palmitoylation site may affect the palmitoylation status within STREX, incorporation of radiolabelled ^{3}H-palmitate into STREX C-terminal channel proteins was examined to identify palmitoylation at the C645:C646 site when the overall basic charge of the polybasic domain is disrupted.

4.1.4.4 Does phosphorylation regulate the function of the polybasic domain?

To examine whether phosphorylation may function as a physiological switch to control the overall basic charge of the polybasic domain, the PKA phosphorylation site was mutated in the STREX C-terminal constructs and examined to identify radiolabelled ^{3}H-palmitate incorporation to determine whether the palmitoylation of the C645:C646 site is modified.

4.1.4.5 What does the polybasic domain interact with?

Finally, to assess whether the polybasic domain has a specific lipid-binding partner such as $PI(4,5)P_2$ in the plasma membrane or whether binding is non-specific, full length STREX channels were examined electrophysiologically to assess the effect of depletion of phosphoinositides on channel activity in accordance with mutagenesis studies within the polybasic domain.

4.2 Results

4.2.1 The polybasic domain is an evolutionary conserved region

Sequence alignment of the series of basic charged amino acids that make up the putative polybasic domain identified in the region upstream of the C645:C646 palmitoylation site in STREX, suggests that these basic residues are largely evolutionary conserved across the vertebrate phyla (Figure 4.1B). Alternative splicing of the STREX insert at splice site C2, bring an additional 5 basic charges to a region immediately upstream that already contains 6 basic residues. This generates a series of 11 basic amino acid residues out of 21 (K623 – R642) in close proximity to form a cluster that could operate as a functional polybasic domain. In this polybasic domain evolutionary retention across vertebrates appears to favour conservation of basic charge rather than the specific amino acid, which is apparent when examining the alignment of the Murinae (mice and rat) amino acid sequence against all other vertebrates. The basic arginine residue (R631) in the Murinae genome is substituted for a basic Lysine (K) residue in the same position across other vertebrates. Therefore it would seem that the charged nature of this region, and not necessarily the amino acid sequence, may be of significant functional importance.

4.2.2 Basic-Hydrophobicity analysis suggests that the polybasic domain could potentially interact with the plasma membrane

To determine whether the polybasic domain identified in the C-terminus of the STREX splice variant of the BK channel would be able to function independently as a membrane interaction domain, a computer algorithm (Brzeska *et al.*, 2010) that utilises basic and hydrophobic parameters was used to calculate potential membrane interaction sites within the C-terminus.

Hydrophobicity scales are useful for determining regions of proteins that may penetrate into the plasma membrane, however many do not take into account the

effect of basic residues and their electrostatic interaction with negatively charged regions of the plasma membrane. A Basic Hydrophobicity (BH)-scale algorithm recently developed (Brzeska *et al.*, 2010) identifies potential membrane binding sites in less structured regions of proteins. It takes into account the role of a hydrophilic basic residue's electrostatic interaction with the negatively charged plasma membrane, as well as the significance of hydrophobic residues in membrane attachment. Using a scoring system, the program averages values in a previously determined and newly adapted Wimley and White hydrophobicity scale (Wimley & White, 1996) called the Basic Hydrophobicity (BH) scale. Each amino acid in a segment of a selected length, called the window size, is scored according to the scale and a value given to the amino acid in the middle of the window. To discriminate between segments from soluble proteins and membrane spanning sequences, a window length of 19 was determined to best identify membrane-spanning sequences. It was proposed that a larger window length of 19 was more suitable because protein-spanning sequences passing through the interior of the protein are usually shorter than membrane spanning sequences (Kyte & Doolittle, 1982). A threshold value of 0.6 (dashed line) (Figure 4.2) was identified as the optimal parameter for identifying lipid-binding sites in proteins (Brzeska *et al.*, 2010).

The mouse STREX splice variant of the BK channel sequence (accession number NM_010610) spanning the intracellular C-terminus from the end of the S6 transmembrane domain (beginning at glycine residue 328, ..GNRKK..) to the end of the intracellular carboxyl tail (ending at cysteine residue 1226, ..VEDEC), was examined using the BH algorithm. Inputting the STREX C-terminus channel sequence (S6:STREX), the identified polybasic domain exceeded the probability threshold of 0.6 for a potential membrane interaction site, with maximum values recorded between residues 626-646 (Figure 4.2A) with a peak score of 1.05. The STREX insert is highlighted by a grey box in all respective algorithm plots illustrated in Figure 4.2. The insertless ZERO channel C-terminus sequence (S6:ZERO) that does not have the 58 amino acid STREX insert at splice site C2 and was previously shown not to associate with the plasma membrane in an imaging assay (see chapter 3, Figure 3.2) did not exceed the threshold for interaction with the plasma membrane despite 6 remaining basic residues (Figure 4.2D). This suggests that according to the algorithm, inclusion of the STREX insert is crucial for association of

Figure 4.2
Basic Hydrophobicity profiles of the STREX C-terminus with mutations in the putative polybasic domain

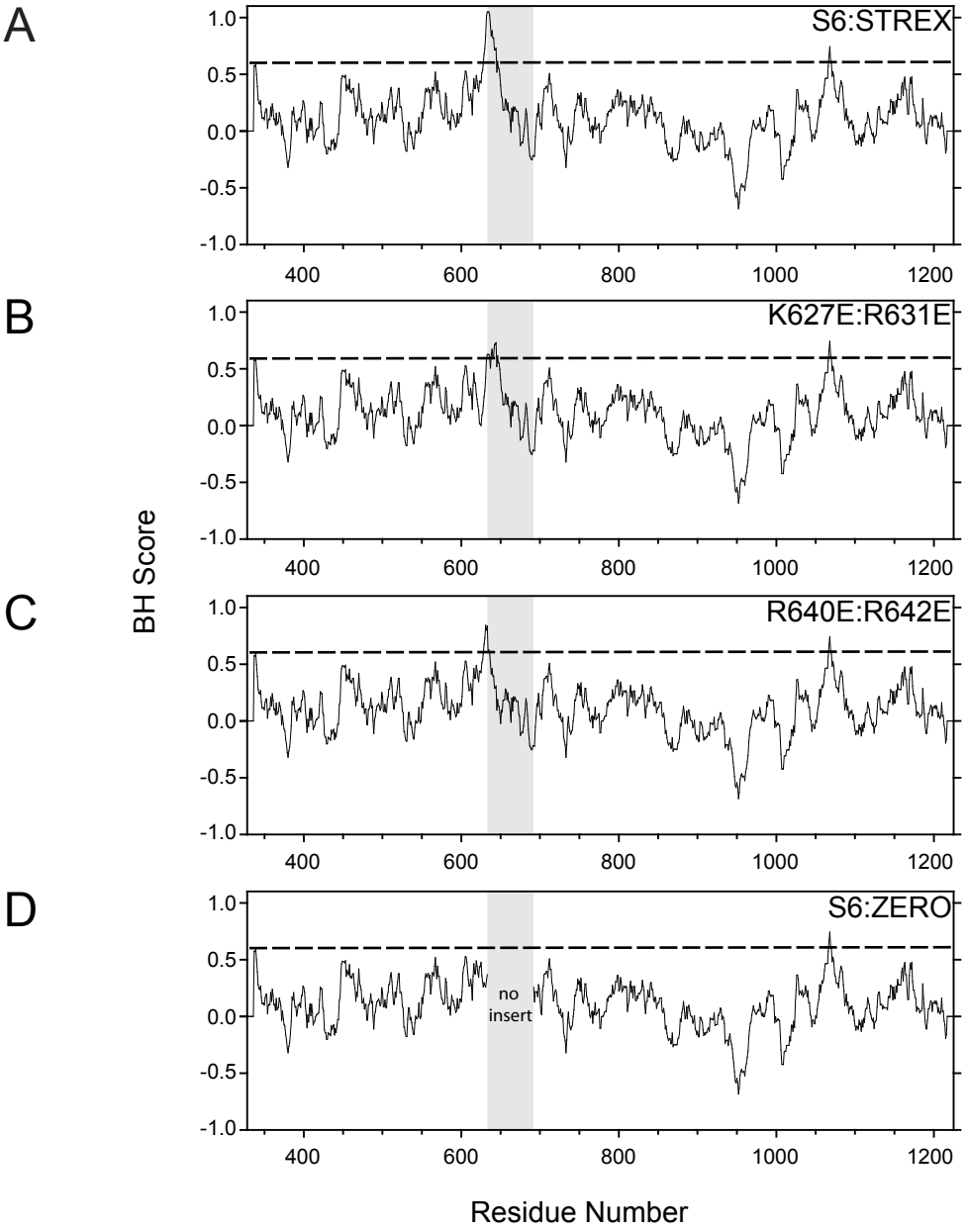

Figure 4.2. Basic Hydrophobicity profiles of the STREX C-terminus with mutations in the putative polybasic domain. (A) The C-terminus of the BK channel containing a STREX insert (indicated by grey box) contains a predicted membrane binding site in the identified polybasic domain (peak residues 633-635). (B) Mutation of positive residues to negative in the region immediately upstream of STREX (K627E:R631E). (C) Mutation of positive residues to negative in the region inside the STREX insert (R640E:R642E). (D) The ZERO insertless C-terminus predicts no major membrane binding sites.

this region with the plasma membrane via a polybasic domain and that greater than 6 basic residues are required to generate a region with a strong enough membrane binding energy to form a functional polybasic domain. By disrupting the polybasic domain, the importance of a series of basic residues for plasma membrane interaction was assessed using a site-directed mutagenesis strategy. Firstly, to neutralise the influence of positive charge in the polybasic domain, a neutral alanine (A) amino acid residue was substituted for basic residues in two independent regions of the polybasic domain inside and outside of the STREX insert. Secondly, to maximally disrupt the influence of the polybasic domain, negatively charged glutamic acid (E) amino acid residues were substituted for basic residues in the same two independent regions of the polybasic domain.

Mutation of the polybasic domain followed a two-fold approach firstly, targeting the basic region immediately upstream of the STREX insert by identifying K627 and R631 as potential key residues close to the centre of this region that would disrupt the polybasic domain and then secondly, targeting the downstream basic region inside STREX, identifying R640 and R642 as potential key residues that would disrupt the centre of this region of basic charge and therefore the influence the role of the polybasic domain.

Disruption of the polybasic domain by inserting negatively charged glutamic acid (E) residues at K627E:R631E, immediately upstream of the STREX insert (Figure 4.2B) and at R640E:R642E, within the STREX insert (Figure 4.2C) decreased the BH probability score for potential plasma membrane interaction to 0.63 and 0.84 respectively. Neutralising basic residues in the polybasic domain did not have such a profound influence on disrupting membrane interaction (probability score: K627A:R631A 0.82, R640A:R642A 0.91), suggesting that substitution with negative residues has the most significant effect in disrupting the ability of the polybasic domain to associate with the plasma membrane.

The palmitoylation deficient C-terminus of the STREX channel (C645A:C646A) which has previously been shown to decrease targeting of the C-terminus to the plasma membrane (see chapter 3, Figure 3.2), did not affect the BH probability score of 1.05 for plasma membrane interaction seen with the wild-type STREX channel C-terminal sequence (data not shown).

This data suggests that the polybasic domain may act independently of palmitoylation as a plasma membrane targeting motif through a conserved series of basic charges.

4.2.3 The polybasic domain is important for associating the STREX C-terminus at the plasma membrane

Previously, the STREX insert was identified as a plasma membrane targeting domain for the C-terminus of the BK channel (see chapter 3). Identification and removal of a key palmitoylation motif in the STREX insert, abolished membrane targeting of fluorescently labelled STREX C-terminal fusion proteins (Figure 3.2). Considering that the polybasic domain may be able to act independently of palmitoylation to associate with the plasma membrane, the role of the polybasic domain in membrane association was examined using a similar imaging strategy (Figure 4.3).

Fluorescently labelled STREX C-terminal constructs were developed as previously described (see section 2.1.1 & Figure 2.1) using the carboxyl terminus without N-terminal or transmembrane domains of the BK α-subunit and attaching a green fluorescent protein tag to the carboxyl end of the fusion protein (Figure 4.3A). Expression of the STREX C-terminus construct (S6:STREX) resulted in robust plasma membrane expression (Figure 4.3B, upper left panel), with 60% of cells transfected showing fluorescence at the plasma membrane in the absence of transmembrane segments (n=650 cells counted) in HEK293 cells. Total plasma membrane expression in S6:STREX was normalised to 100% allowing comparison of mutated constructs to STREX (Figure 4.3C). The S6:STREX construct also showed strong expression in the nucleus with 91% of cells transfected also showing nuclear localisation.

Using site directed mutagenesis to neutralise or disrupt the function of the polybasic domain, the affect on localisation at the plasma membrane could be examined. Mutation of the basic region immediately upstream of the STREX insert to neutral alanine (A) residues (K627A:R631A) and negative glutamic acid (E) residues (K627E:R631E), abolished membrane targeting to 26.5% and 6.3% respectively (n= 491 and 636 cells counted) (Figure 4.3C), with the fluorescent fusion proteins

Figure 4.3
The polybasic domain is important for targeting of the STREX C-terminus to the plasma membrane

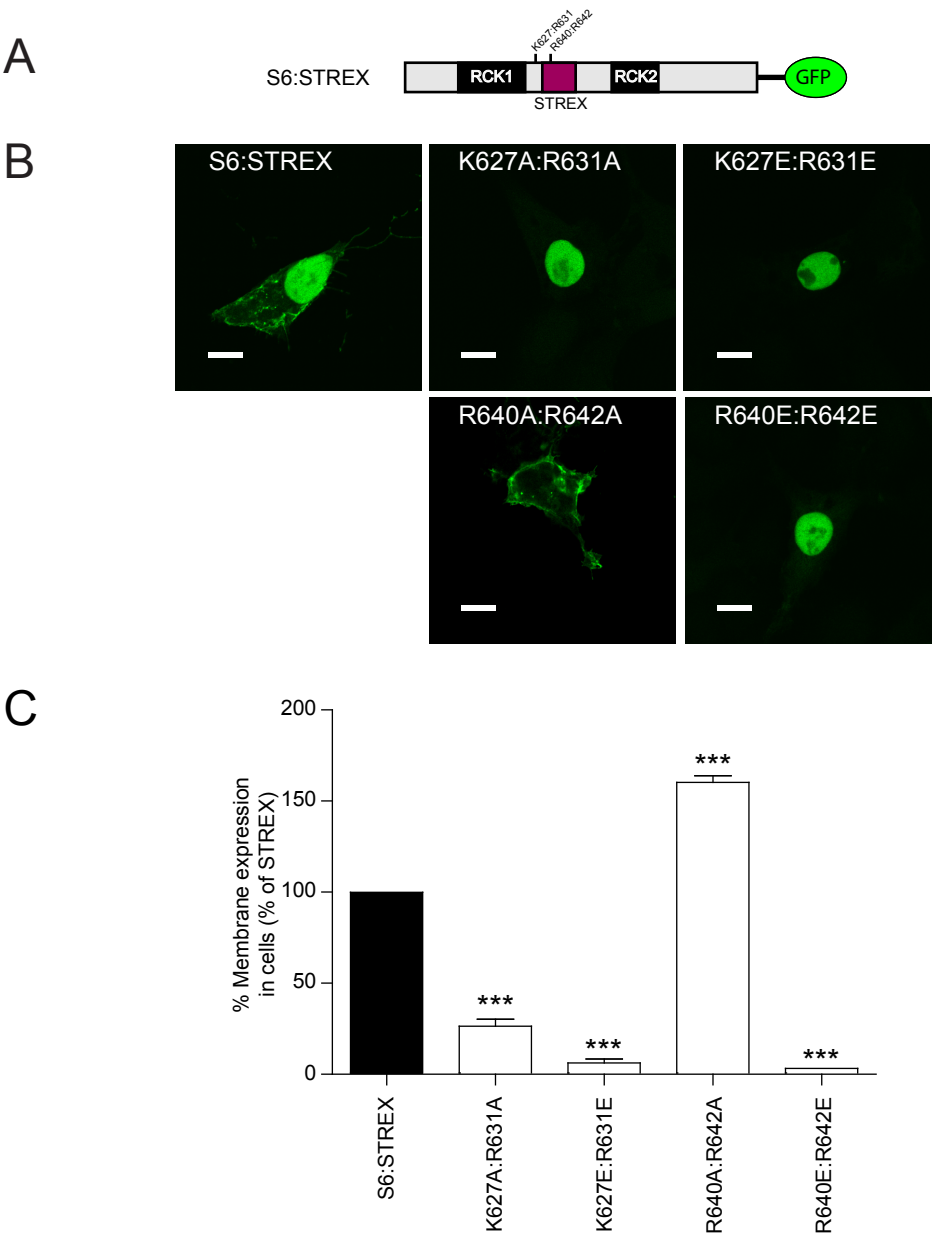

Figure 4.3. The polybasic domain is important for targeting of the STREX C-terminus to the plasma membrane. (A) Schematic of C-terminal -GFP fusion construct with mutation sites indicated relative to STREX. (B) Representative single cell confocal images of C-terminal STREX (S6:STREX) and C-terminal STREX polybasic mutants K627A:R631A, K627E:R631E, R640A:R642A and R640E:R642E, expressed in HEK293 cells. (Scale bars: 10 μM). (C) Summary bar graph of the respective C-terminal construct localization at the plasma membrane expressed as a percentage of S6:STREX (where STREX is 100%). *** $p<0.001$ compared with STREX (ANOVA with tukey post hoc test).

appearing to be targeted to the nucleus (99% and 100% respectively). Mutation of the basic region inside the STREX insert to negative glutamic acid (E) residues (R640E:R642E), also abolished membrane targeting to 3.3%, with targeting directly to the nucleus (100%) (n= 1031 cells counted). Surprisingly, when the same approach was taken to neutralise the basic region inside the STREX insert with alanine (A) residues (R640A:R642A) fluorescence at the plasma membrane actually increased to 160% when compared to S6:STREX (n=760 cells counted) (Figure 4.3C). Nuclear localisation was also almost totally abolished in the (R640A:R642A) mutant, with only 11.5% of cells showing fluorescence in the nucleus compared to 91% in the S6:STREX control construct.

4.2.4 The polybasic domain is functionally important to the STREX channel

The functional effect of disruption of the polybasic domain in the normal full length STREX channel was first examined using a membrane potential assay (Saleem *et al.*, 2009). As before, mutated channels were transiently transfected into HEK293 cells and seeded into 96 well assay plates. The FLIPR-blue dye (Molecular Devices) was administered to the cells to allow the dye to load into the cell membrane. The assay was then run in the Flexstation ® II during which cells were stimulated by 1 µM Ionomycin, a calcium ionophore, to activate the BK channel. Changes in fluorescence were then measured over a time course of 180 seconds.

Using the full length STREX channel as a control response, the peak hyperpolarisation was taken at t=100s and these values could then be expressed as the isolated channel current by subtracting the control HEK response from the transiently transfected channel response within the assay plate and then normalised to 100%. All polybasic mutants could then be compared to the STREX channel phenotype (Figure 4.4). A representative trace illustrates the raw data for the different channel responses to activation driven by calcium influx in the polybasic mutant channels with respect to the STREX channel response and the un-transfected HEK293 response (Figure 4.4A). Disruption of the polybasic domain by introducing negatively charged amino acids to both previously identified basic regions (K627E:R631E & R640E:R642E) significantly attenuated channel activation to calcium influx to 85.9 ± 3.3 % and 71.9 ± 3.7 respectively (n= >25), in relation to

Figure 4.4
STREX channel activation driven by calcium influx is diminished when the polybasic domain is disrupted

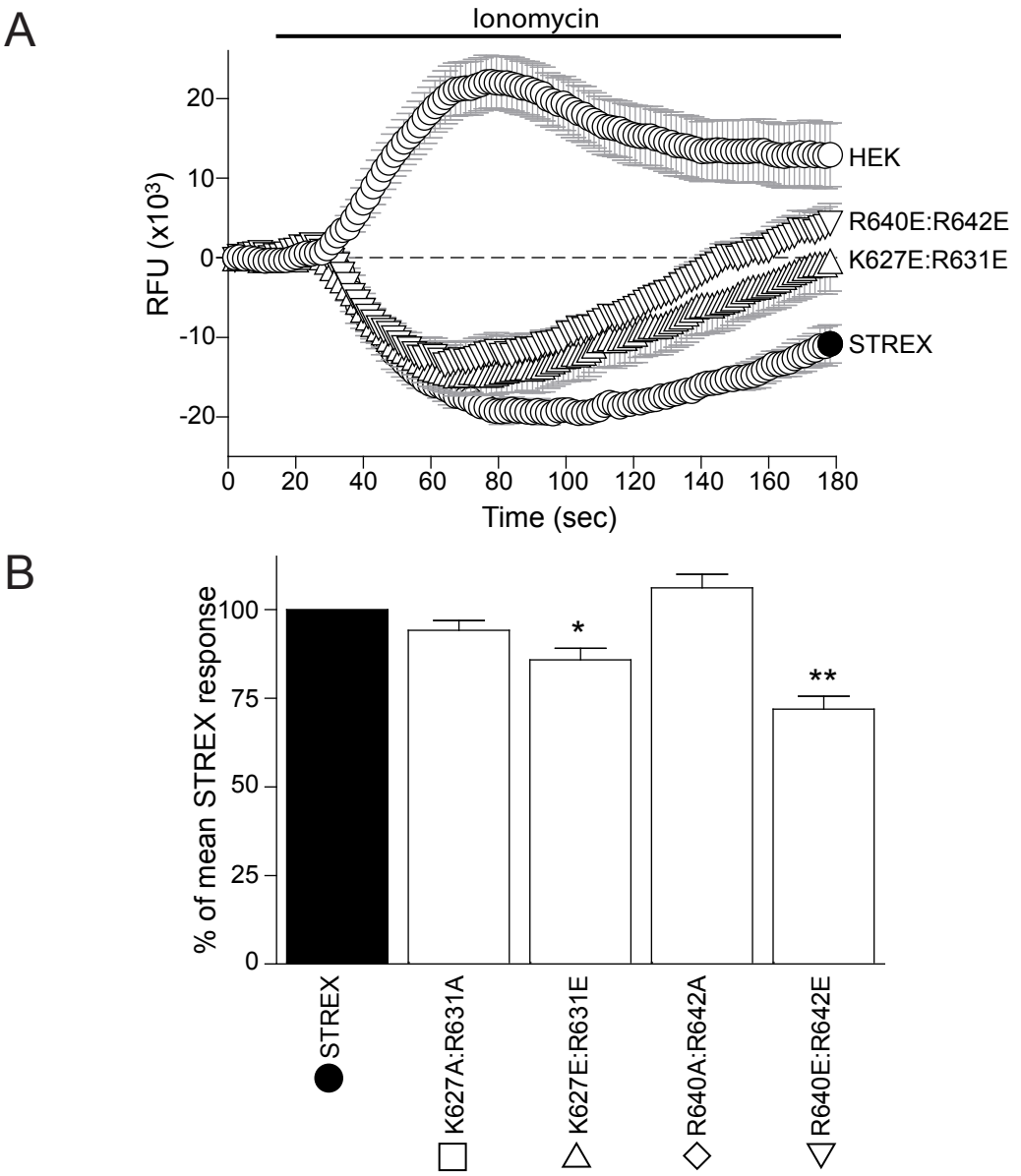

Figure 4.4. STREX channel activation driven by calcium influx is diminished when the polybasic domain is disrupted. (A) Representative time course plots of mean change in relative fluorescence units (RFU) of the FLIPR-blue membrane potential dye in HEK293 cells expressing STREX (closed circles, ●), K627E:R631E (upright triangles, △), R640E:R642E (inverted triangles, ▽), and mock-transfected HEK293 (open circles, ○), in response to calcium influx induced by 1 μM Ionomycin. (B) Summary bar chart of the membrane potential change for each construct expressed as a percentage of the maximal hyperpolarisation with the untransfected HEK293 response subtracted and STREX expressed as 100%. Data was determined at the maximum hyperpolarising response in BK-STREX (t=100s) in the time course plots in (A). All data are Means ± S.E.M (N=4, n=48), * $p<0.05$, ** $p<0.01$, compared to STREX (ANOVA with tukey post hoc test).

STREX (Figure 4.4B). This data suggests that the channel's sensitivity to increased intracellular calcium has significantly decreased in polybasic mutant channels. Mutation of the polybasic domain by substituting neutral alanine (A) residues for basic charge did not have any statistically significant effect on the ionomycin-induced hyperpolarising response of the channel (K627A:R631A, 94.2 ± 2.8 and R640A:R642A, 106.1 ± 3.9, n = >25) (Figure 4.4B).

4.2.5 Single channel amplitude does not mediate changes in channel activity with mutation of the polybasic domain

The membrane potential assay described in the previous section, examines the general ionomycin-induced hyperpolarising responses of the BK channel and various mutants by driving activation of the channel in a well of transfected HEK293 cells. However, the assay cannot discriminate between the calcium- or voltage-sensitivity of the channel, nor can it assess changes in single channel amplitude and it cannot indicate changes in cell surface expression of functional channels at the plasma membrane. Therefore, to investigate the properties of the mutant channels that may mediate the altered sensitivities described in the membrane potential assay, it was necessary to examine isolated channels electrophysiologically.

To determine the single channel amplitude of STREX and investigate whether a decrease in single channel amplitude might mediate the decreased sensitivity of the polybasic mutants as described in the membrane potential assay, measurements were made at a range of voltage potentials (-80 mV to +80 mV) in equimolar (140 mM) potassium gradients. Channels were examined at 0.33 µM [Ca^{2+}] in excised inside-out patches (Figure 4.5). The slope conductance of the STREX channel was 244 +/- 4.4 pS. There was no significant difference in single channel slope conductance across the polybasic mutants in comparison to STREX under these recording conditions (Figure 4.5A). Mean single channel amplitude under the same conditions and examined at +40 mV (Figure 4.5B) was as follows; STREX 10.4 ± 0.2, K627A:R631A 10.1 ± 0.34, K627E:R631E 9.9 ± 0.3, R640A:R642A 10.3 ± 0.2, & R640E:R642E 10.9 ± 0.03 (n=3). This suggests that changes in the sensitivity of the polybasic mutant channels described in the membrane potential assay are not mediated by changes in single channel amplitude.

Figure 4.5
Single channel amplitude is not affected by disruption of polybasic domain

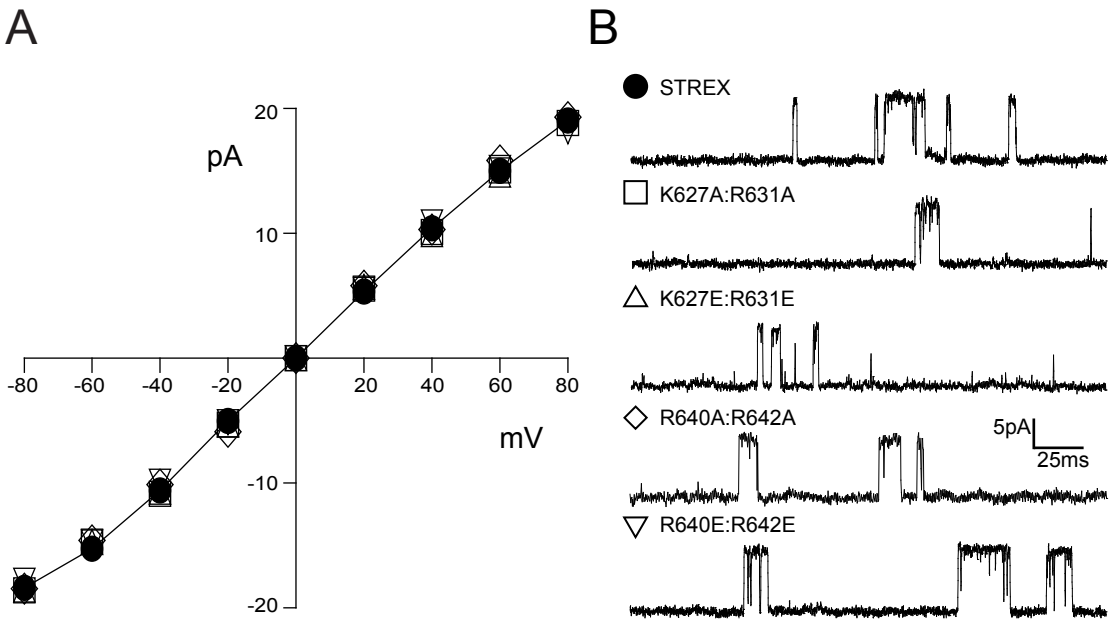

Figure 4.5. Single channel amplitude is not affected by disruption of polybasic domain. (A) Current voltage plot for STREX channels and STREX channels with mutations in the polybasic domain. Recordings were made in excised inside-out patches in equimolar 140 mM K^+ gradients, 0.33 μM free Ca^{2+} and at +40 mV. STREX (closed circles, ●), K627A:R631A (squares, □), K627E:R631E (upright triangles,△), R640A:R642A (diamonds, ◇), and R640:R642 E (inverted triangles, ▽) (N=3) Single channel conductance was derived from the slope of the line.(B) Representative single channel recordings of excised inside-out patches recorded in same conditions as before and at +40 mV.

4.2.6 STREX channel activity can be modulated by the polybasic domain

To investigate if disruption of the polybasic domain might have an effect on channel activity, macroscopic BK currents were recorded in equimolar potassium gradients by inside-out patch clamp analysis (Figure 4.6). Representative currents illustrate the typical outward component of the BK response to a depolarising voltage step protocol (-120 to +120 mV) from a holding potential of -80 mV (Figure 4.6A).

Activation (G/G_{MAX}) curves, as before, were obtained by plotting tail current amplitude against test potential and fitting to a Boltzmann equation allowing determination of the voltage for half activation ($V_{0.5MAX}$)(Figure 4.6B). Previous functional studies of the STREX splice variant of the BK channel have demonstrated a dramatic shift in the apparent calcium sensitivity of the STREX channel compared to the insertless ZERO variant (Saito *et al.*, 1997; Shipston *et al.*, 1999; Chen *et al.*, 2005). The STREX channel is more calcium sensitive over a range of 0 to 1.0 µM Ca^{2+} whereby beyond 1 µM Ca^{2+} it becomes difficult to distinguish the sensitivity of STREX from ZERO, as the calcium binding sites in the channel become saturated (Chen *et al.*, 2005). All further analysis of the STREX channel and the polybasic mutants were therefore carried out in 0.33 µM Ca^{2+} where the apparent calcium sensitivity is much greater than the insertless ZERO channel.

Measurement of channel activity in 0.33 µM Ca^{2+} meant that mutational disruption of the polybasic domain could be directly compared to wild type STREX channel activity. The half maximal voltage for activation of normalised (G/G_{MAX}) curves was determined for each polybasic mutant in relation to STREX (Figure 4.6C). The voltage for half activation of the STREX channel was 40.6 ± 2.5 mV (n=8).

Mutation of the basic region with negative residues immediately upstream of the STREX insert to disrupt the polybasic domain (K627E:R631E), caused a significant (~ +30 mV) rightward shift in the half maximal voltage for activation of the channel to 71.9 ± 7.8 mV, with channels beginning to activate at -20 mV. Substitution of neutral residues in this region (K627A:R631A) had no significant effect, (54.3 ± 10.5), although there was a trend to a rightward shift in channel activity (see Figure 4.6B & C), perhaps suggesting that neutral substitution of basic residues may not fully disrupt the polybasic domain but may begin to decrease the influence of the charged domain. Disruption of the downstream basic region inside STREX with negative

Figure 4.6
Disruption of the polybasic domain shifts the activation of STREX channels

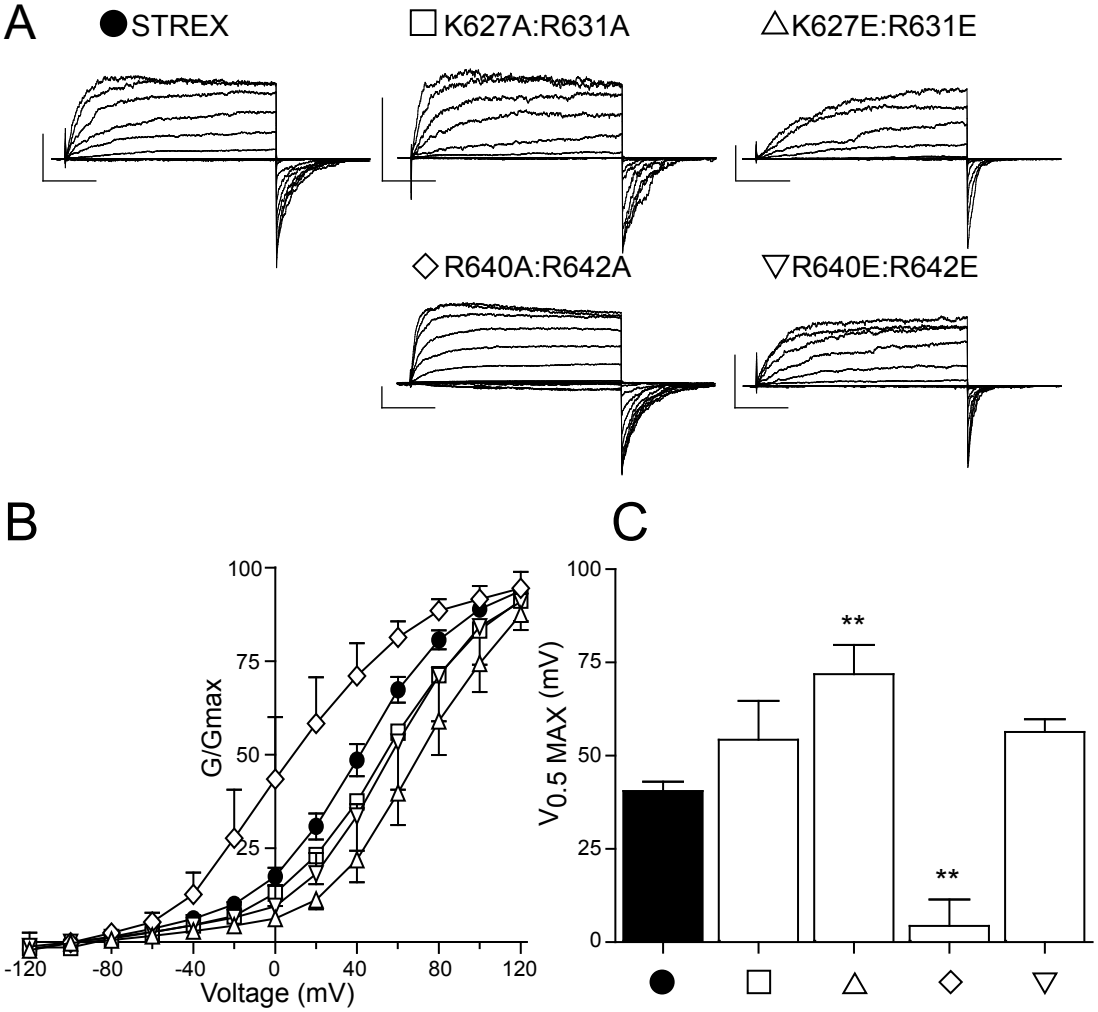

Figure 4.6. Disruption of the polybasic domain shifts the activation of STREX channels. (A) Representative traces showing outward currents at depolarized potentials from HEK293 cells expressing STREX (closed circles, ●), K627A:R631A (squares, □), K627E:R631E (upright triangles, △), R640A:R642A (diamonds, ◇) and R640E:R642E (inverted triangles,▽) from excised inside-out patch recordings in equimolar (140 mM) K^+ gradients and 0.33 µM free Ca^{2+}. Outward currents were elicited by 100 ms depolarising voltage steps from -120 to +120 mV in 20 mV increments from a holding potential of -80 mV. (Scale bars: 1 nA / 25 ms) (B) G/G_{MAX} conductance curves showing STREX channel activity over a range of voltage potentials and variants with mutations in the polybasic domain. (C) Summary bar graph showing $V_{0.5MAX}$ of the STREX channel and each polybasic mutant expressed in HEK293 cells. All data are Means ± S.E.M (n=3-7), ** p<0.01, compared to STREX (ANOVA with tukey post hoc test).

residues (R640E:R642E), did not have a significant functional effect on half maximal voltage for activation, (56.4 ± 3.4 mV). Again this was an intermediate rightward shift (of ~ +16 mV) between STREX and the K627E:R631E channel mutant suggesting that perhaps only partial disruption of the polybasic domain occurs by mutating this downstream region of the polybasic domain (Figure 4.6B & C). Interestingly, mutation of the same downstream basic region inside STREX with neutral alanine (A) residues, (R640A:R642A), caused a large leftward shift (of ~ -35 mV) in the channel activation, with the channel activating at much more negative potentials close to -60 mV. The half maximal voltage for activation of the channel R640A:R642A was 4.4 ± 7.1 mV (Figure 4.6B & C), which suggests that the mechanism that mediates this effect may be different to mutations made in the region immediately upstream of the STREX insert and different to mutation in the same region with negatively charged residues.

4.2.7 Voltage dependence is unchanged in polybasic mutant channels

Disruption of the polybasic domain is functionally significant to channel activity (Figure 4.6), but what is not clear is whether the voltage sensitivity has changed or whether the calcium sensitivity of the channel has been changed.

To determine whether the voltage sensitivity of the polybasic mutant channels has changed in relation to the wild type STREX channel, a logarithmic transformation to linearize the activating component of the normalised (G/G_{MAX}) curves in Figure 4.6B was plotted against the depolarised potentials of 0 mV to +120 mV (Figure 4.7). Disruption of the polybasic domain has little or no effect on voltage dependence of the channels when compared to STREX. Therefore, disruption of the polybasic domain does not alter the voltage dependence of the mutated polybasic channels.

To further analyse the inherent voltage sensing properties of the polybasic mutant channels, the voltage sensing component of channel activation was isolated by examining channels in an extracellular solution containing zero calcium (<10 nM Ca^{2+}) (Figure 4.8). As described before, normalised (G/G_{MAX}) curves were constructed by measuring tail currents, this time in zero calcium (Figure 4.8A). The half maximal voltage for activation of normalised (G/G_{MAX}) curves was again determined for each polybasic mutant in relation to STREX (Figure 4.8B). The

Figure 4.7
The voltage dependence of STREX channel activation is not affected by disruption of the polybasic domain

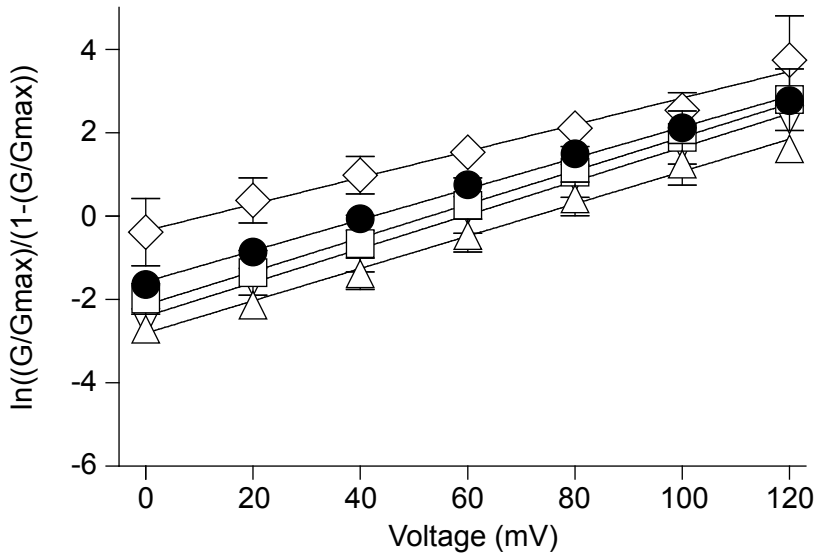

Figure 4.7. The voltage dependence of STREX channel activation is not affected by disruption of the polybasic domain. A logarithmic transformation of the G/G_{MAX} activation curves over depolarised potentials of 0 to +120 mV as described in the macropatch recordings in Figure 4.6B. STREX (closed circles, ●), K627A:R631A (squares, □), K627E:R631E (upright triangles, △), R640A:R642A (diamonds, ◇), and R640E:R642E (inverted triangles, ▽), illustrate that mutation of the polybasic domain does not significantly affect the voltage sensitivity of the channels. The voltage dependence was derived from the slope of the line.

Figure 4.8
STREX channel activity in polybasic mutant channels is not shifted in zero calcium

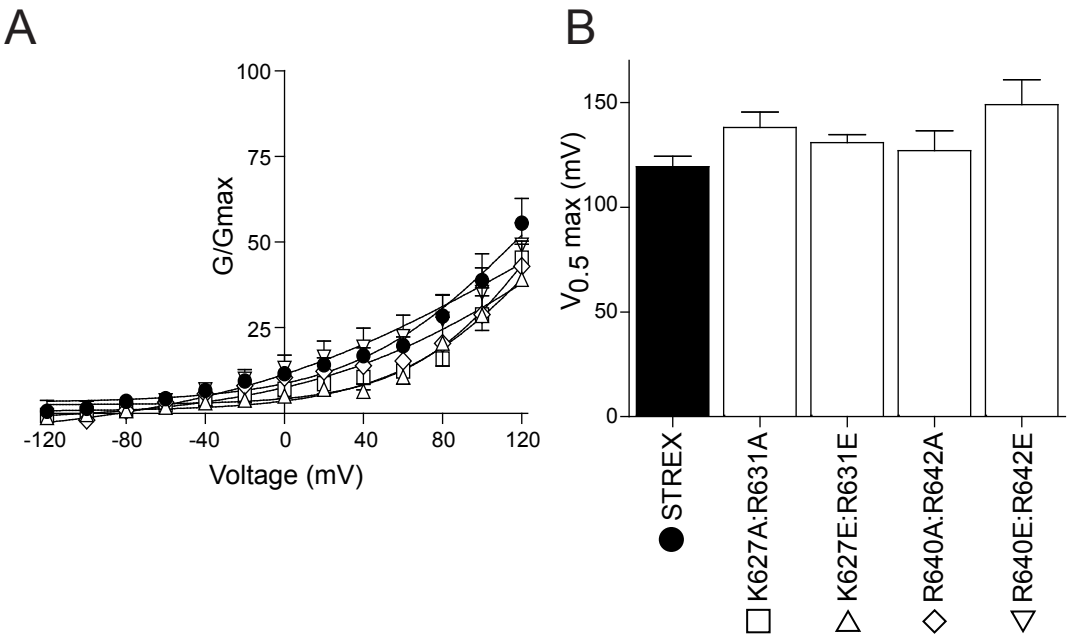

Fig 4.8 STREX channel activity in polybasic mutant channels is not shifted in zero calcium. (A) G/G_{MAX} conductance curves of STREX channel activation over a range of transmembrane voltage potentials (-120 to +120 mV) from excised inside-out macropatch recordings in in equimolar (140 mM) K^+ gradients and zero calcium (<10 nM) and variants with mutations in the polybasic domain. STREX (closed circles, ●), K627A:R631A (squares, □), K627E:R631E (upright triangles, △), R640A:R642A (diamonds, ◇), and R640E:R642E (inverted triangles, ▽). (C) Summary bar graph showing $V_{0.5MAX}$ of the STREX channel and each polybasic mutant expressed in HEK293 cells in zero calcium.

voltage for half activation of the STREX channel this time was 119.3 ± 5.0 mV. However, neutral or negative mutation of the polybasic domain in the region upstream of the STREX insert or in the region within the STREX insert had no significant effect on the half maximal voltage for activation of the channel. The voltage for half maximal activation of the polybasic mutant channels were as follows; K627A:R631A, 130 ± 3.7 mV; K627E:R631E, 138 ± 7.5 mV; R640A:R642A, 148.9 ± 12.0 mV and R640E:R642E, 130.9 ± 3.7 mV. Therefore it is possible to conclude that any changes seen in the activity of the polybasic mutant channels in relation to wild type STREX must be due to the effects on the calcium sensitive component of the STREX splice variant of the BK channel.

4.2.8 Mutation of polybasic domain affects the activation and deactivation kinetics of the STREX channel

It has been previously described that the STREX channel has considerably slower deactivating kinetics when compared to the ZERO channel (Chen *et al.*, 2005). In 0.33 µM Ca^{2+} it was shown that channel activity was rightward shifted in polybasic mutants that had negatively charged residues substituted in the basic region. The rightward shift in channel activity is moving towards the ZERO channel phenotype and so it is plausible to hypothesize that the activation and deactivation kinetics in the polybasic mutants may also shift towards a more ZERO-like channel phenotype, therefore this was studied next.

The representative macroscopic currents examined previously (Figure 4.6A) comparing STREX with channels that had mutations in their polybasic domain, demonstrated visible shifts in channel kinetics. To define the activation kinetics of the various polybasic mutants, activation curves were best fitted by a single exponential function from the beginning of channel activation to the peak plateau current. By plotting tau (tau = 1-1/*e)* the activation kinetics of the channel and various mutant channels could be examined (Figure 4.9).

The STREX channel showed a half activation time constant of 19.6 ± 3.01 ms (n=7) at +60 mV in 0.33 µM Ca^{2+} and equimolar (140 mM) potassium gradients (Figure 4.9A & C). The only mutant that showed significantly faster activation kinetics than

Figure 4.9
STREX channel activation rates in polybasic mutants

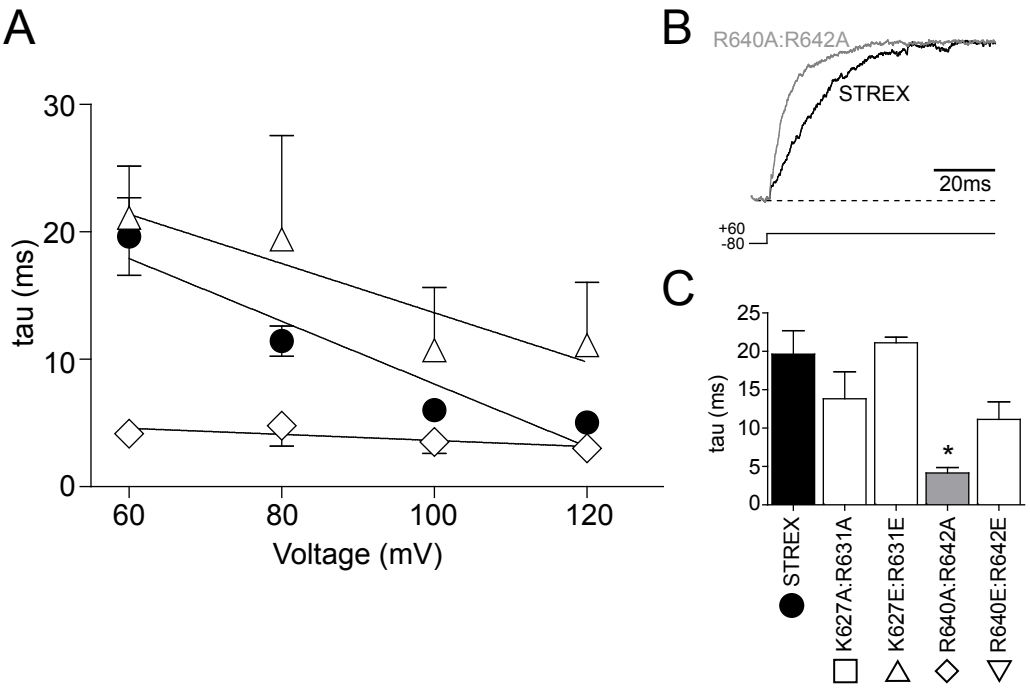

Figure 4.9. STREX channel activation rates in polybasic mutants. Recordings are from excised inside-out patch recordings in equimolar (140 mM) K^+ gradients and 0.33 µM Ca^{2+} in HEK293 cells. (A) Data recorded shows a depolarising voltage pulse from a holding potential of -80 mV to the indicated voltages in STREX (closed circles, ●), K627E:R631E (upright triangles,△), R640A:R642A (diamonds,◇). (B) A typical example of the activating kinetics of STREX (black) and the R640A:R642A (grey) mutant upon a voltage pulse to +60 mV and expressed relative to the plateau current as 100%. (C) Summary bar graph showing the time constant for activation of STREX and the mutated polybasic channels. All data are Means ± S.E.M (n=3-7), * $p<0.05$, compared to STREX (ANOVA with tukey post hoc test).

STREX was R640A:R642A with a time constant of 4.16 ± 0.71 ms (n=3). A representative trace shows the activating kinetic of a STREX channel (black) in Figure 4.9B, in which the R640A:R642A (grey) mutant is overlain to illustrate the differences in activation rates of the two channel constructs. The other polybasic mutant channels did not show any statistically significant change in channel activation (Figure 4.9C). To define the deactivating kinetics of the various polybasic mutants, deactivation curves were fitted in the same way by a standard exponential function from the peak tail current to the baseline. By deriving the time constant the deactivation kinetics of the channel and various polybasic mutant channels could be compared (Figure 4.10).

The STREX channel showed a tau of 10.22 ± 1.64 ms (n=7) at +120 mV in 0.33 µM Ca^{2+} and equimolar (140 mM) potassium gradients (Figure 4.10A & C). This time the K627E:R631E mutant channel which has previously been shown to disrupt the polybasic domain causing a significant rightward shift in channel activity and $V_{0.5MAX}$, had a tau value that was significantly faster at 3.9 ± 0.6 ms at +120 mV. A representative trace illustrates the different kinetics in deactivation between STREX (black) and K627E:R631E (grey), the mutant is overlain to illustrate the difference in deactivation rates of the two channel constructs (Figure 4.10B). The other polybasic mutant channels did not show any statistically significant change in deactivation kinetics.

It is clear from the evidence presented so far, that the polybasic domain does play a functional role in mediating the channel properties that give the STREX splice variant of the BK channel its phenotype. Disruption of the polybasic domain with negatively charged amino acids thought to oppose the influence of the large basic charge inherent to the domain, rightward shifts the activity of the channel back towards the insertless ZERO BK channel without affecting single channel amplitude. Disruption of the polybasic domain was also shown to increase deactivating kinetics of the channel, typical of what would be expected of a channel that behaves more like the ZERO channel. However what has been suggested is that these effects are most likely to be mediated through a calcium sensitive component of the channel, since voltage dependence of activation was unchanged and no differences could be seen between the mutant channels in zero calcium. Surprisingly, mutation of the basic region inside STREX with neutral residues suggested that the channel was

Figure 4.10
STREX channel deactivation rates in polybasic mutants

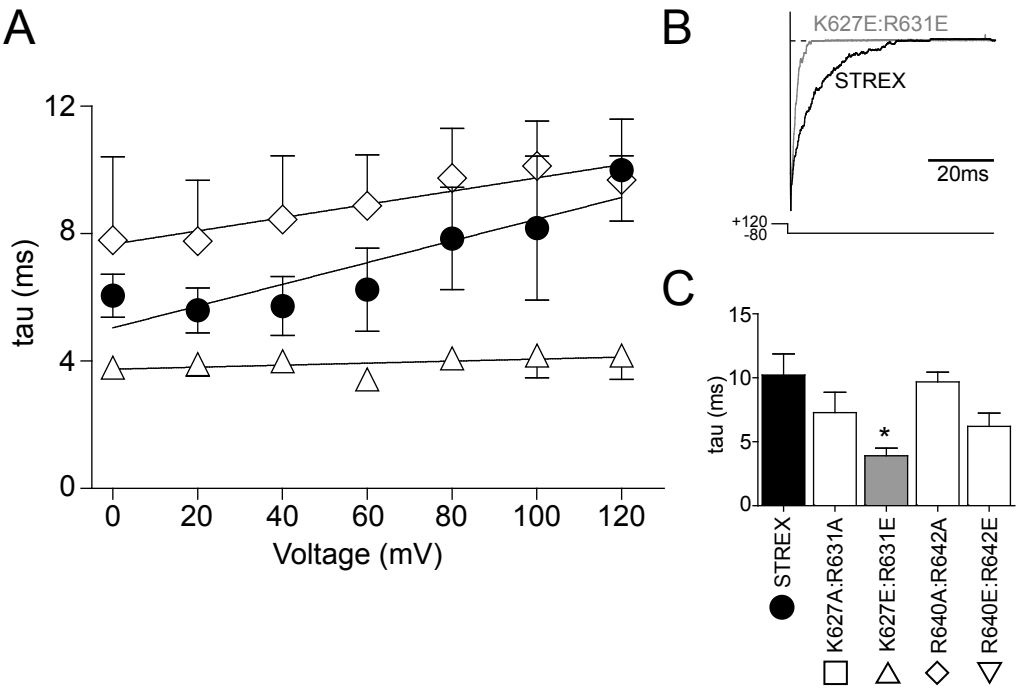

Figure 4.10. STREX channel deactivation rates in polybasic mutants. Tail currents were measured from excised inside-out patch recordings in equimolar (140 mM) K^+ gradients and 0.33 μM Ca^{2+} in HEK293 cells. (A) Data recorded following 100 ms voltage pulses to the indicated voltages and repolarisation to a holding potential of -80 mV in STREX (closed circles, ●), K627E:R631E (upright triangles, △), R640A:R642A (diamonds, ◇). (B) A typical example of the deactivating tail current kinetics of STREX (black) and the K627E:R631E (grey) mutant channel following a 100ms voltage pulse from +120mV to -80mV and expressed relative to the peak tail current as 100%. (C) Summary bar graph showing the time constant for deactivation of STREX and the mutated polybasic channels. All data are Means ± S.E.M (n=3-7), * $p<0.05$, compared to STREX (ANOVA with tukey post hoc test).

activated more than STREX, illustrated by increased activity over the voltage range examined and faster activating kinetics. As with the other mutants this was not mediated through altered voltage dependence or changes in single channel amplitude.

4.2.9 Does the polybasic domain work alone?

It is interesting to speculate on how the polybasic domain may exert its control on the STREX channel. In the previous chapter, palmitoylation was shown to play an important role in membrane targeting of the intracellular C-terminus of the STREX BK channel. Many palmitoylated proteins have been shown to operate alongside other additional signalling mechanisms such as a polybasic domain (Bijlmakers & Marsh, 2003; Dietrich & Ungermann, 2004). Therefore, it is important to ascertain whether the polybasic domain in STREX does operate independently of the palmitoylation motif as suggested by the membrane association prediction algorithm (Figure 4.2). Does this polybasic domain act alongside palmitoylation as a requirement for stability at the plasma membrane? Or does the polybasic domain influence the palmitoylation status of the STREX channel?

Using the CSS-palm algorithm that was used to predict the key cysteine residues involved in palmitoylation of the STREX channel, disruption of the polybasic domain was examined in relation to predictive scores for palmitoylation of cysteine residues in the STREX palmitoylation motif, C645, C646 and C649 (Table 4.1). The algorithm predicted that the CSS-palm score for palmitoylation of C645 (the cysteine with the highest predicted palmitoylation score in BK) would be very slightly lowered when mutations were made in the nearby polybasic domain. STREX 2.48 versus K627A:R631A 2.38, K627E:R631E 2.42 and R640E:R640E 2.39 (Table 4.1). Interestingly the R640A:R642A mutant that was more active than the STREX channel and showed increased presence at the plasma membrane when expressed as a C-terminal protein in imaging assays, actually showed an increased probability score for palmitoylation at 2.70 (Table 4.1). This analysis suggests that it is possible that the polybasic domain may be involved in regulating the palmitoylation status of the STREX palmitoylation motif and membrane targeting of the domain. Therefore it was important to directly examine the palmitoylation status of the intracellular C-

Table 4.1
Disruption of the polybasic domain by introduction of negative and neutral charges changes predicted palmitoylation scores for the STREX palmitoylation site C645:C646

	Position	Peptide	CSS-palm v2.0 score
S6:STREX	645	RRA**C**CFD	2.484
	646	RAC**C**FDC	0.571
	649	CFD**C**GRS	1.083
K627A:R631A	645	RRA**C**CFD	2.422
	646	RAC**C**FDC	0.56
	649	CFD**C**GRS	0.905
K627E:R631E	645	RRA**C**CFD	2.375
	646	RAC**C**FDC	0.726
	649	CFD**C**GRS	1.048
R640A:R642A	645	ERA**C**CFD	2.391
	646	RAC**C**FDC	0.167
	649	CFD**C**GRS	0.429
R640E:R642E	645	ARA**C**CFD	2.703
	646	RAC**C**FDC	0.417
	649	CFD**C**GRS	0.81

Table 4.1. Disruption of the polybasic domain by introduction of negative and neutral charges changes predicted palmitoylation scores for the STREX palmitoylation site C645:C646. Scores indicate CSS-palm prediction; a higher score represents higher probability. CSS-palm scores were determined with the published CSS-palm v2.0 at http://bioinformatics.lcd-ustc.org/css_palm by inputing the protein sequence of the entire intracellular C-terminus of the STREX variant of the BK channel (starting at glycine residue G328 and spanning until cysteine residue C1226) and then polybasic mutant sequences. Negative substitution generally lowers the score however, neutral substitution at the R640A:R642A site unexpectantly increases the predicted palmiotylation score.

terminus of the channel with mutations in the polybasic domain in order to ascertain the role of the polybasic domain in palmitoylation of STREX channels.

4.2.10 The polybasic domain regulates the palmitoylation status of the C645:C646 site in the STREX channel

To address whether disruption of the polybasic domain would affect the palmitoylation status of the STREX C-terminus as previously described (see Chapter 3), radiolabeled ^{3}H-palmitate incorporation into C-terminus fusion proteins were examined in HEK293 cells (Figure 4.11). The representative fluorographs show that in the polybasic mutants K627A:R631A, K627E:R631E and R640E:R640E, ^{3}H-palmitate incorporation was essentially abolished, suggesting that the polybasic domain must play an important role in regulating the palmitoylation status of the C645A:C646A palmitoylation motif. Interestingly, the R640A:R642A C-terminal mutant showed an increased level of palmitoylation suggesting that neutral substitution of basic residues with alanine (A) residues close to the identified palmitoylation motif can increase palmitoylation status of the C-terminal constructs. This finding was very much unexpected however it may explain the differences seen with this mutant channel in previous experiments. Western blot analysis showed that total protein expression was unchanged in the assays and data was quantified by expressing detectable levels of ^{3}H-palmitate over detectable levels of protein expression and then comparing to STREX as 100% (n=3). Quantification showed that there was a 300% increase in palmitoylation of C-terminus constructs when the channel was mutated at R640A:R642A and that the K627A:R631A mutation could reduce (to 10%) but not abolish palmitoylation of the C-terminus constructs.

4.2.11 Phosphorylation within the polybasic domain destabilises the basic region abolishing palmitoylation

If disruption of the polybasic domain by neutralisation of basic charge or introduction of two negatively charged amino acid residues can abolish palmitoylation then it was hypothesized that phosphorylation of the S636 PKA site, which would also introduce

Figure 4.11
Palmitoylation of STREX is modulated by the polybasic domain

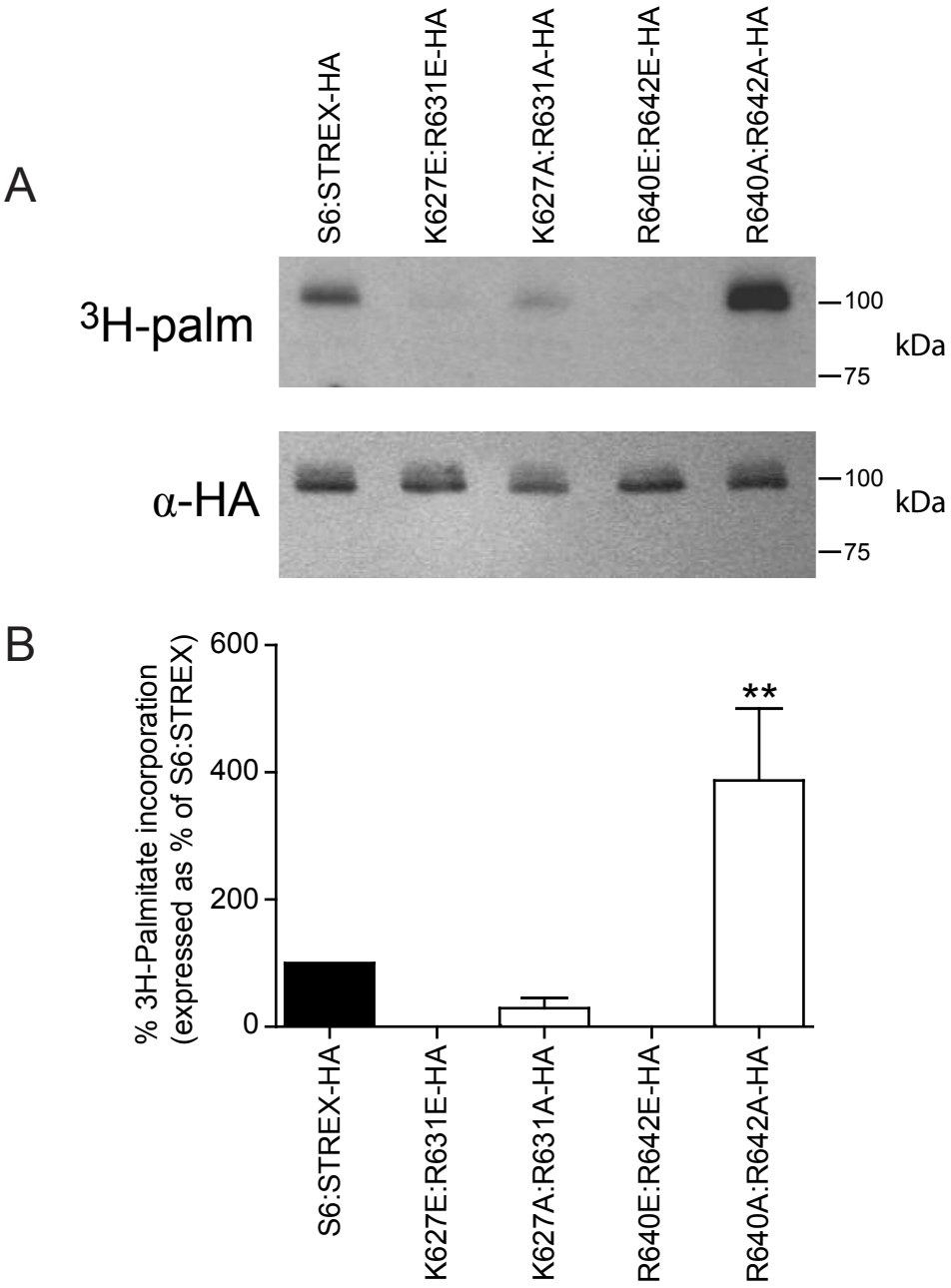

Figure 4.11. Palmitoylation of STREX is modulated by the polybasic domain. (A) Representative fluorographs (upper) and western blots (lower) of -HA tagged C-terminal S6:STREX-HA, and polybasic mutant C-terminal channels K627A:R631A-HA, K627E:R631E-HA, R640A:R642A-HA, R640E:R642E-HA expressed in HEK293 cells. Constructs were labelled with ^{3}H-palmitate for 4 hours and immunoprecipitated (IP) by using α-HA magnetic microbeads and detected by fluorography. (B) Quantative data of detectable levels of palmitoylation expressed as a ratio in comparison to total protein expression and relative to S6:STREX as 100%. (N=3) ** $p<0.01$, compared to S6:STREX (ANOVA with tukey post hoc test).

Figure 4.12
Palmitate incorporation into S6:STREX is abolished by mutation of PKA phosphorylation site S636

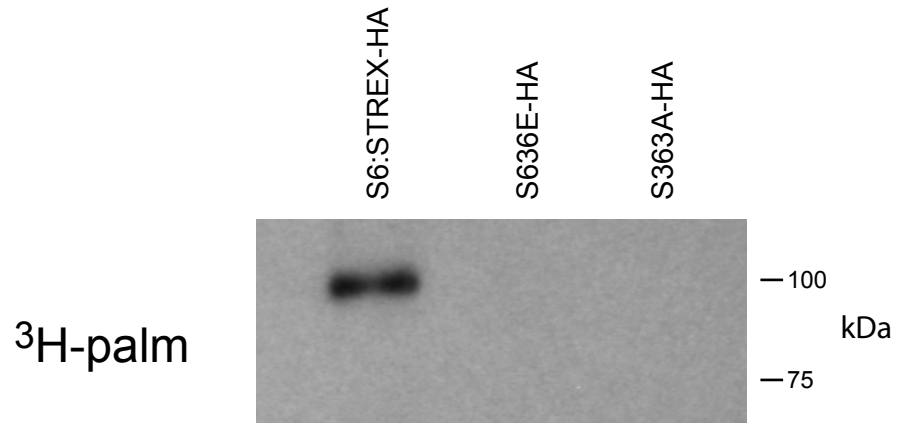

Figure 4.12. Palmitate incorporation into S6:STREX is abolished by mutation of PKA phophorylation site S636. Representative fluorographs of S6:STREX-HA, phosphomimetic S3363E-HA, and phosphonull S363A-HA, expressed in HEK293 cells. Constructs were labelled with ^{3}H-palmitate for 4 hours and the respective constructs immunoprecipitated (IP) using α-HA magnetic microbeads, subjected to SDS-PAGE and probed by a polyclonal HA antibody and detected by fluorography.

2 negative charges, within STREX and the middle of the basic domain may also have the same affect. In chapter 3, phosphorylation at the PKA phosphorylation site within STREX, S636, was shown to disrupt the STREX C-terminal construct's association at the plasma membrane (see Figure 3.9). Therefore radiolabeled ^{3}H-palmitate incorporation into C-terminal fusion proteins that had phosphonull alanine (A) mutations and phosphomimetic glutamic acid (E) mutations at the PKA phosphorylation site were examined in HEK293 cells (Figure 4.12). The representative fluorographs demonstrate that mutation of the PKA phosphorylation site with either a negatively charged glutamic acid amino acid to mimic phosphorylation or a neutral amino acid which would remove the phosphorylation site, totally abolished palmitoylation in the STREX C-terminus. Whilst introduction of a negative glutamic acid residue abolished palmitoylation as would be predicted, neutral substitution also had the same effect suggesting that maybe the phosphorylation motif is important in the region for effective palmitoylation.

4.2.12 Does the polybasic domain target PI(4,5)P_2 in the plasma membrane?

Polybasic domains facilitate interactions with the negatively charged plasma membrane through electrostatic interactions. Many proteins such as Src, K-Ras, and MARCKS, with basic domains bind non-specifically to the overall negatively charged inner leaflet of the plasma membrane that is composed of the charged monovalent acidic lipid phosphatidylserine (~25%) that has one negative charge (McLaughlin *et al.*, 2002; Mulgrew-Nesbitt *et al.*, 2006). However, there is also strong evidence that other proteins such as small guanosine triphosphatases (GTPases), with a cluster of four or more basic residues can laterally sequester phosphoinositides in the plasma membrane such as PI(4,5)P_2 which has a stronger negative valency of four negative charges (McLaughlin & Murray, 2005; Heo *et al.*, 2006).

To test whether the polybasic domain in STREX is anchored to the plasma membrane by binding to PI(4,5)P_2, the strategy was to examine the role of PI(4,5)P_2 in the plasma membrane and its effect on channel function (Figure 4.13).

Recently studies have demonstrated that PI(4,5)P_2, independent of PI(4,5)P_2 metabolites and downstream signalling can activate BK channels (Vaithianathan *et al.*, 2008). Therefore to replicate these findings and determine the effect of PI(4,5)P_2

on the channel and the role that the polybasic domain might play in affecting channel activity, $PI(4,5)P_2$ (Avanti Polar Lipids, Inc) was added directly to the intracellular face of excised patches in the inside-out configuration (Figure 4.13A). All subsequent patches were examined in equimolar potassium gradients (140 mM) and 0.33 µM Ca^{2+}. However, $PI(4,5)P_2$ did not appear to have any effect on channel activity or single channel amplitude in the conditions examined (Figure 4.13A,E & F). $PI(4,5)P_2$ was made up as described in the methods section (see section 2.7) and applied as described by Vaithianathan *et al*. It is interesting that in their methods Vaithianathan *et al*, report sonicating the $PI(4,5)P_2$ (although sourced from a different company – Sigma-Aldrich) in a working stock solution for 30 minutes on ice (Vaithianathan *et al.*, 2008). However, Avanti polar lipids, the leading suppliers in lipid compounds, specifically highlight that $PI(4,5)P_2$ is more difficult to work with than more conventional lipids and recommend caution when sonicating the $PI(4,5)P_2$ vesicles as $PI(4,5)P_2$ will break down more easily than conventional lipids (Avanti Polar Lipids, Inc). Following on from this advice I also tried to apply $PI(4,5)P_2$ dissolved in de-ionised H_2O without sonication, but again did not see any change in channel activity (data not shown). Repeating the same experiment but with $PI(4,5)P_2$ from Sigma-Aldrich and sonicating for 30 minutes on ice also did not have any effect on channel activity (data not shown).

In their study, the BK channel variant used would not have the STREX insert, therefore I also examined the affect of $PI(4,5)P_2$ upon the ZERO insertless variant of the BK channel but again did not see any change in channel activity (data not shown). Therefore under the conditions used in this thesis the effect of $PI(4,5)P_2$ reported by Vaithianathan *et al* could not be replicated. The reason for this discrepancy is not clear, however, this may perhaps be a secondary effect of prolonged sonication and destruction of $PI(4,5)P_2$.

Alternatively, if $PI(4,5)P_2$ was to have specific role in anchoring the STREX domain linker at the plasma membrane via the polybasic domain, then depletion of $PI(4,5)P_2$ should have a measurable effect on channel activity (Figure 4.13B). In the same study, Vaithianathan *et al*, reported that $PI(4,5)P_2$ monoclonal antibodies applied to the cytosolic side of the plasma membrane decreased NPo (channel activity) in BK channels to <35% of channels that had been previously activated by lipid kinases (activated by Mg-ATP) in the absence of protein phosphatases (Okadaic acid) to increase $PI(4,5)P_2$ levels in the patch. This was carried out after a 30 minute

Figure 4.13
Phosphoinositides do not modulate the BK channel

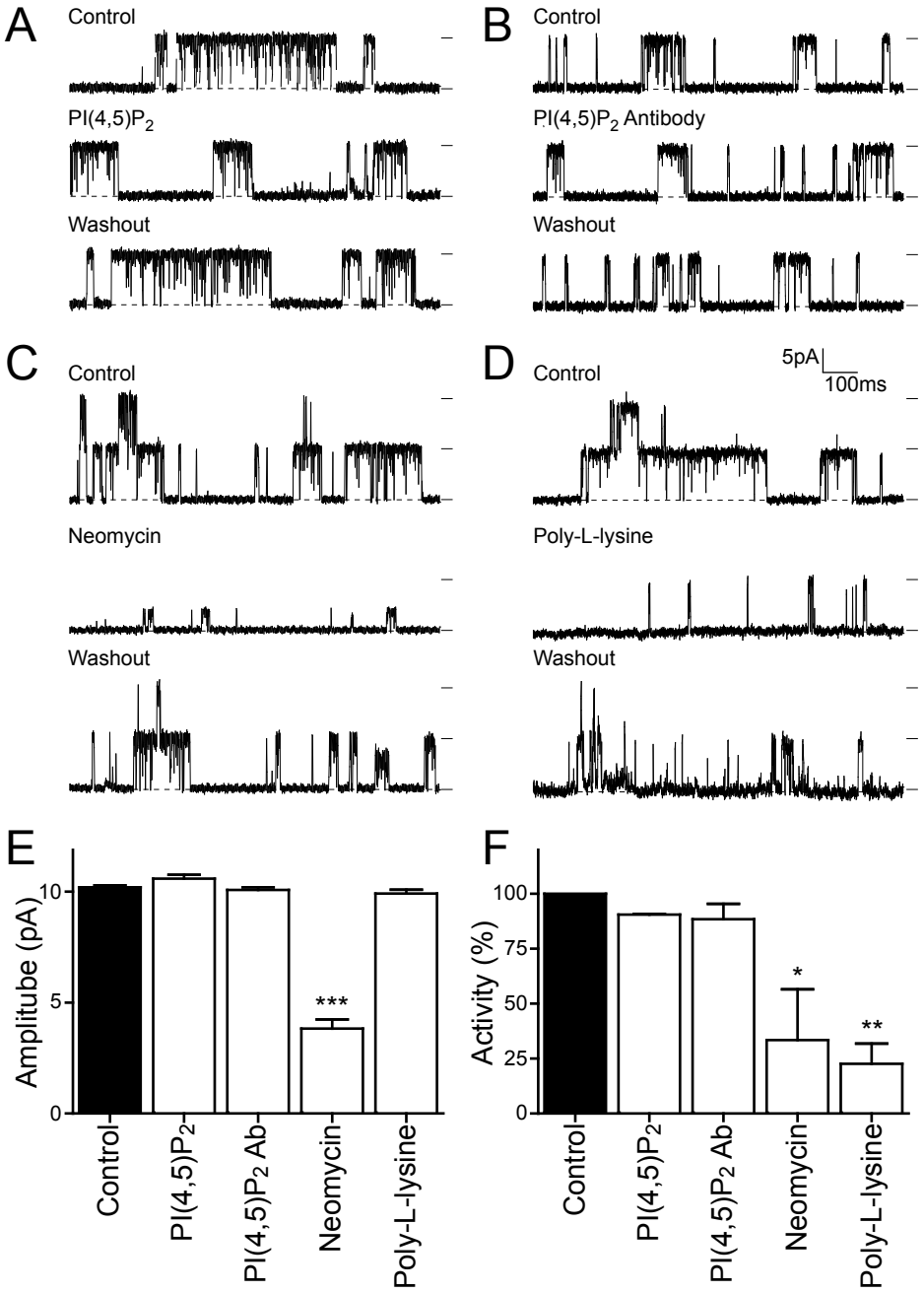

Figure 4.13. Phosphoinositides do not modulate the BK channel. STREX channel activity from an excised inside-out patches in equimolar (140 mM) K^+ gradients and 0.1 µM Ca^{2+}. (A) Bath application of 10 µM $PI(4,5)P_2$ sonicated for 30 minutes prior to application. (B) Bath application of $PI(4,5)P_2$ monoclonal antibody (10 µg/µl). (C) Wash in of Neomycin (5 mM). (D) Wash in of Poly-L-lysine (5 µg/µl). Control recordings after 10 minutes stabilization and the time course shown after drug application is 2 minutes post-drug, with washout recordings shown after 5 minutes. (E) Bar graph illustrates absolute single channel amplitude at +40 mV. (F) Bar graph illustrates channel activity (I/i) expressed as a percentage of control. All data are Means ± S.E.M (n > 3) * p<0.05, ** p<0.01, *** p<0.001, compared to STREX (ANOVA with tukey post hoc test).

rundown period during which they propose that $PI(4,5)P_2$ would become depleted and lead to BK channel rundown (Vaithianathan *et al.*, 2008). The time course for application of anti-$PI(4,5)P_2$ to shift activation in HCN channels has been reported as $t_{1/2}$ ~3.6 minutes in oocytes (Pian *et al.*, 2006) and an almost instant effect of anti-$PI(4,5)P_2$ has been described, over a period of several seconds, in deactivating the $PI(4,5)P_2$ modulated Kir2.1 channel in oocytes (Xie *et al.*, 2008). However, cytosolic application of the $PI(4,5)P_2$ -antibody (10 µg/µl) in the same recording conditions described previously, had no observable effect on channel activity or single channel conductance in HEK293 cells (Figure 4.13B,E & F), even after 10 minutes of bath application (n=3).

The third approach taken was to use neomycin, an aminoglycoside polycation that is reported to bind specifically to $PI(4,5)P_2$ sequestering it and therefore an indicator of a channel's affinity for $PI(4,5)P_2$ (Schulze *et al.*, 2003). Neomycin is a positively charged compound that blocks $PI(4,5)P_2$ based on an electrostatic mechanism. In STREX channels it had differing effects on channel activity and single channel amplitude (Figure 4.13C). Upon application of neomycin (5 mM) via wash in, single channel amplitude decreased from 10 to 4.8 pA within 1 minute of application and channel activity also significantly decreased (Figure 4.13E & F). Channel activity either remained low or was completely eliminated after ~3 minutes incubation with neomycin, however this effect could be washed out after 5 minutes. These effects seen with neomycin look more like a classic pore block than a reduction in $PI(4,5)P_2$ modulation of the channel. Indeed neomycin has been shown in other channels to block slowly inactivating Ca^{2+} channels (Suarez-Kurtz & Reuben, 1987) and inward Ca^{2+} current (Gustin & Hennessey, 1988). Previous studies on native BK channels also identified neomycin specifically as a potent "fast" blocker from the cytoplasmic side of the channel that may compete for the K^+ ion binding inside the pore (Nomura *et al.*, 1990). Therefore neomycin is not a good indicator of $PI(4,5)P_2$ modulation of the BK channel as it has additional effects in channel pore block. Care should be taken when using this compound to identify $PI(4,5)P_2$ modulation of ion channels.

Finally, poly-L-lysine is another polycation agent used in multiple studies to sequester $PI(4,5)P_2$. Therefore, to examine the role of $PI(4,5)P_2$ using another agent, poly-L-lysine (5 µg/µl) was applied to inside-out patches in equimolar potassium gradients (140 mM) and 0.33 µM Ca^{2+} at +40 mV, as before.

Interestingly, initial application of poly-L-lysine had a different effect to that described of neomycin. Poly-L-lysine decreased channel activity to ~20% without a change in single channel amplitude for several minutes after application (Figure 4.13D,E & F). However, after 3-4 minutes single channel conductance also decreased (from 9.9 ± 0.2 to 3.4 ± 0.5 pA at +40 mV – data not shown). Unlike neomycin, the effects of poly-L-lysine could not be reversed as quickly taking more than 10 minutes wash out and in 2 out of 4 experiments could not be washed back to control levels at all. Therefore unlike the "fast" blocking properties of neomycin, poly-L-lysine appears initially to have characteristics of a "slow" channel block such as that seen with the classic BK channel blocker TEA, which reduces single channel open probability without affecting single channel amplitude (Wangemann & Takeuchi, 1993). Poly-L-lysine may operate by decreasing the surface potential around the entrance to the internal vestibule of the channel pore. The BK channel, unlike other K^+ conducting channels has two negative rings at the entrance to the channel pore (See Figure 1.6)(Brelidze *et al.*, 2003). The strong positive charge of poly-L-lysine may decrease the negative surface potential that lines the inner vestibule of the cytoplasmic side of the BK channel pore which is thought to increase the pool of available K^+ ions and contribute to the unique large conductance properties of the BK channel. However, ultimately poly-L-lysine decreases channel conductance possibly through a similar mechanism of binding within the channel vestibule. Indeed previous studies have demonstrated that poly-L-lysine does decrease both channel activity and conductance of BK channels in tracheal myocytes (Oshiro *et al.*, 2000) however in these recording conditions, channel activity decreases initially with a latent decrease in single channel amplitude after several minutes.

These polycations that are used non-specifically to sequester $PI(4,5)P_2$ may have additional actions in channel block. Whilst such observations have not been recorded in voltage-gated K^+ channels this may be due to the different structure of the pore region in comparison to the much larger BK channel pore (see chapter 1, section 1.4.2). It certainly highlights the importance of understanding the potential additional actions drugs may have and certainly in the case of the BK channel these polycations appear to occlude the ion-conducting pathway at a site within the pore possibly close to where the narrow K^+ selective region begins.

4.3 Discussion

Alternative splicing of the STREX insert at the C2 splice site located in the linker between the two RCK domains, introduces a series of basic charged residues, just upstream of the key palmitoylation site, which is functional in controlling association of the STREX C-terminus at the plasma membrane, via palmitoylation.

4.3.1 The polybasic domain is a functional membrane targeting domain

By identifying, using basic-hydrophobic analysis, that the polybasic domain just upstream of the key palmitoylation site in STREX could potentially form a membrane targeting domain, a site directed mutagenesis strategy was taken to disrupt the influence of the overall basic charge.

A series of eleven basic residues that comprise the polybasic domain largely show strong evolutionary conservation across vertebrates suggesting a positive selection pressure may have retained this region as an important component of the STREX channel. Site directed mutation of the basic charge, separately in two regions within the polybasic domain - one inside STREX and one outside of STREX, demonstrated that membrane association of fluorescently tagged STREX C-terminal constructs could be influenced by the polybasic domain. By taking this approach to examine the two regions within the polybasic domain the data suggests that it is probable that the entire polybasic domain is necessary to maintain a strong basic environment for association with the negatively charged plasma membrane.

4.3.2 Disruption of the polybasic domain shifts STREX channel properties towards the ZERO channel phenotype

Polybasic mutant channels were initially examined by a membrane potential assay to discriminate differences in channel properties driven by calcium influx. It was apparent that mutagenesis of basic residues with negative charges to disrupt the basic region had the maximal effect in significantly shifting the polybasic mutant

channel's response to calcium influx. In the same manor imaging studies also highlighted a decreased localisation of the polybasic mutant C-terminal constructs at the plasma membrane. It is possible that this decreased membrane targeting may underlie the shift in channel activity that was described by the membrane potential assay. In electrophysiological studies to assess voltage- and calcium- sensing properties of the polybasic mutant channels, mutation with negative residues in the region outside of STREX (K627E:R631E) shifted the voltage for half maximal activation by ~ +31 mV and also slowed the time constant for channel deactivation. This rightward shift in channel activity of the STREX (K627E:R631E) channel to more positive potentials, appears to reflect a shift towards the insertless ZERO channel phenotype which is shifted by a similar proportion (ZERO shift was ~ +34 mV see Figure 3.6). Despite the K627E:R631E mutation almost appearing to resemble the ZERO channel phenotype, substitution of negative residues in the region within STREX (R640E:R642E) only shifted the voltage for half maximal activation by ~ +16 mV. This was not statistically significant, but did however follow the general trend of shifting towards the ZERO channel phenotype. Together it appears that the region just upstream of the STREX insert may be more important in influencing channel activity. However, this does not rule out that there may be additional sites that may also determine gating/Ca^{2+} sensitivity in STREX channels not related to the polybasic domain.

As would be predicted the K627A:R631A mutant channel activity was only marginally rightward shifted when compared to the larger shift induced by mutation with negative charges. Substitution with alanine residues would be expected to decrease the effect of basic charge with a neutral charge and would not necessarily disrupt the overall basic charge of the polybasic domain. To test if this assumption would be correct, an experiment could be designed to mutate all of the basic residues in the polybasic domain to alanine residues which might be expected to mimic the negative residue substitutions that disrupt the polybasic domain, as it would no longer be present in the channel. Interestingly, opposed to the other polybasic mutations made in the channel, the R640A:R402A mutant channel showed a dramatic leftward shift in STREX channel activity by ~ -35 mV, with the channel activating at more negative potentials of -60 mV and with a significantly faster time constant for the channel's activating kinetics. It is unknown what may mediate this effect but it will be discussed in the next section. The single channel

amplitude and voltage dependence of all these mutant channels was unchanged suggesting that the calcium- sensitive component of the channel must be modified in STREX channels with a non-functional polybasic domain. From this data it is apparent that the functional polybasic domain is important in conferring additional calcium- sensitivity to the STREX channel over the ZERO channel. The polybasic domain has been shown to influence membrane association of the C-terminus and so it is possible that the polybasic domain may be important in controlling membrane targeting of the RCK1-RCK2 linker by controlling palmitoylation of the STREX C645:C646 site.

4.3.3 The polybasic domain controls palmitoylation of the STREX C645:C646 site

Palmitoylated cysteines are often located in the vicinity of additional lipid anchors or regions rich in basic residues (Bijlmakers & Marsh, 2003; Dietrich & Ungermann, 2004). The presence of a polybasic domain would presumably significantly enhance the overall membrane binding energy of a palmitoylated domain through electrostatic interactions (Resh, 1994). In addition, palmitoylation of proteins by DHHC's require that the palmitoylated domain is located close to either the plasma or intercellular membranes where the DHHC enzymes are located (Fukata *et al.*, 2006). Therefore the local environment surrounding a palmitoylation site is potentially important for stability at the membrane. In theory, if the polybasic domain is important for palmitoylation then disruption of the polybasic domain could destabilize the palmitoylation status of the nearby C645:C646 site leading to decreased membrane association of the STREX C-terminus, as seen in the imaging assays (Figure 4.3). By examining the effect of disrupting the polybasic domain using the palmitoylation prediction algorithm, the predictive scores for the palmitoylation site in STREX were found to be decreased. Although the palmitoylation prediction scores only decreased by a small amount, this may indicate that disruption of the polybasic sequence could potentially affect the palmitoylation status of the nearby site. Therefore to directly assess how the polybasic domain might influence palmitoylation, radiolabelled ^{3}H-palmitate incorporation into the STREX C-terminal constructs with neutral and negative

substitutions in the polybasic domain was tested using a biochemical assay. Substitution of basic residues by negatively charged residues almost totally abolished palmitoylation suggesting that the polybasic domain must be important for palmitoylation of the STREX domain. In the case of the alanine substitution within the STREX basic region (R640A:R642A), as predicted by the palmitoylation prediction algorithm, there was a dramatic increase in palmitoylation.

The mechanism underlying how the R640A:R642A mutant might increase the palmitoylation status of the STREX C-terminal constructs is unknown, however this may explain the mechanism behind the dramatic leftward shift in channel activity previously described. Alanine mutation at this site may change the structural conformation of the region allowing greater accessibility to the target cysteine residues for palmitoylation in all four subunits of the functional channel. Alternatively, mutation in this region may even be important for palmitoylation of the adjacent cysteine residue, C649, which in the wild-type STREX channel is predicted to be palmitoylated, although in HEK293 cells under normal conditions, was found not to be the case. What is clear from this data is that the surrounding environment around a target palmitoylation site is important and can regulate the palmitoylation status of the protein.

In a recently published follow-up study from our lab, we showed that overexpression of DHHCs that endogenously control STREX palmitoylation, can also palmitoylate the cysteine residue (C649) immediately downstream of the C645:C646 site. This demonstrates that palmitoylation is able to target this residue under different conditions and that potentially this residue could be targeted as a result of structural adaptations that allow greater accessibility (see appendix #3; (Tian *et al.*, 2010)).

4.3.4 The polybasic domain's non specific interaction with the plasma membrane

The electrostatic partner of the polybasic domain in STREX is unknown. However, the evidence suggests that $PI(4,5)P_2$ is not the target for the polybasic domain as there was no apparent change in channel properties, as seen in the mutated polybasic domains in mutant channels, with the addition of $PI(4,5)P_2$ or the addition

of the PI(4,5)P_2 monoclonal antibody that would block the actions of PI(4,5)P_2 in the channel recordings. Polybasic domains have been identified to associate with the plasma membrane through general electrostatic interactions with the cytosolic-membrane interface which has an appreciable negative charge in contrast to other intracellular membranes that have less charge (McLaughlin *et al.*, 2002; Mulgrew-Nesbitt *et al.*, 2006). Therefore it is more likely that the polybasic domain in the RCK1-RCK2 linker located just upstream from the key palmitoylation site in STREX probably interacts with the negatively charged plasma membrane via a non-specific interaction. A potential partner for the polybasic domain would be the negatively charged monovalent acidic phosphatidylserine (PS) that constitutes ~25% of the inner leaflet of the plasma membrane (McLaughlin *et al.*, 2002; Mulgrew-Nesbitt *et al.*, 2006).

4.3.5 Control of membrane targeting by phosphorylation – an electrostatic switch

In chapter 3, phosphorylation at the PKA phosphorylation site within STREX, S636, was shown to disrupt the STREX C-terminal construct's association at the plasma membrane. Phosphorylation of a serine residue introduces a phosphoryl group that adds two negative charges to a modified protein (Kim *et al.*, 1994a; Stryer, 1997). It was hypothesized that insertion of a negative charge into a largely basic region would be of functional significance if the basic domain was functionally important, as has been shown in this chapter. In the STREX membrane targeting sequence shown below, the PKA phosphorylated serine (shown in bold) is located close to the midpoint of the polybasic domain (all basic residues in the polybasic domain are defined by (**+**) charges).

STREX membrane targeting sequence:

(**++** I **++** CGC **++** P **+** M**S**IY **++** M **++**)

The introduction of 2 negative charges would, in the same way as shown by the mutagenesis studies, disrupt the series of basic charge weakening the electrostatic interaction and decreasing membrane association, but through a physiological mechanism. Therefore the question is, does phosphorylation act as a physiological mechanism to disrupt C-terminal targeting at the plasma membrane?

The polybasic domain in STREX contains 6 arginine residues and 5 lysine residues and no acidic residues and therefore has a charge of about +13 at a neutral pH (pH ~7) (Kim *et al.*, 1994a; Kim *et al.*, 1994b). Phosphorylation at the STREX S636 PKA phosphorylation site would be expected to switch the overall net charge of the region to +11, but crucially, it would theoretically break the large polybasic domain into two smaller basic regions with a net charge of between +5 & +6 and +2 & +3. These smaller basic regions on their own are perhaps not strong enough to secure membrane binding or to stabilise the environment for efficient palmitoylation of the STREX domain. In Figure 4.12 it was demonstrated that mutation of the S636 phosphorylation site did abolish ^{3}H-palmitate incorporation into STREX C-terminal constructs. This suggests that phosphorylation disrupts the stability of the polybasic region surrounding the palmitoylation site thereby decreasing efficient palmitoylation of STREX. Therefore, this physiological mechanism of regulation proposes that reversible membrane binding could be achieved by phosphorylation at the S636 site in STREX. This implies that phosphorylation could act as an 'electrostatic switch' regulating the stability of membrane association of the STREX membrane targeting domain, in native cells.

The dynamic interaction between phosphorylation and palmitoylation was expanded in published work from our lab where it was found that phosphorylation of the STREX domain by PKA which leads to channel inhibition is conditional on the STREX domain being palmitoylated leading to subsequent dissociation from the plasma membrane (see appendix #1; (Tian *et al.*, 2008a)).

Together this data suggests that membrane targeting of the STREX domain is important for mediating the properties of the STREX channel and that phosphorylation can mediate dissociation of the STREX membrane targeting domain by destabilising the functional polybasic domain and disrupting the stability of palmitoylation at the nearby site.

4.3.6 The structure of the polybasic domain and STREX insert

The RCK1-RCK2 linker has been described as an unstructured region (Lee *et al.*, 2009a; Wang & Sigworth, 2009; Wu *et al.*, 2010; Yuan *et al.*, 2010) so what

Figure 4.14
The STREX channel membrane targeting domain

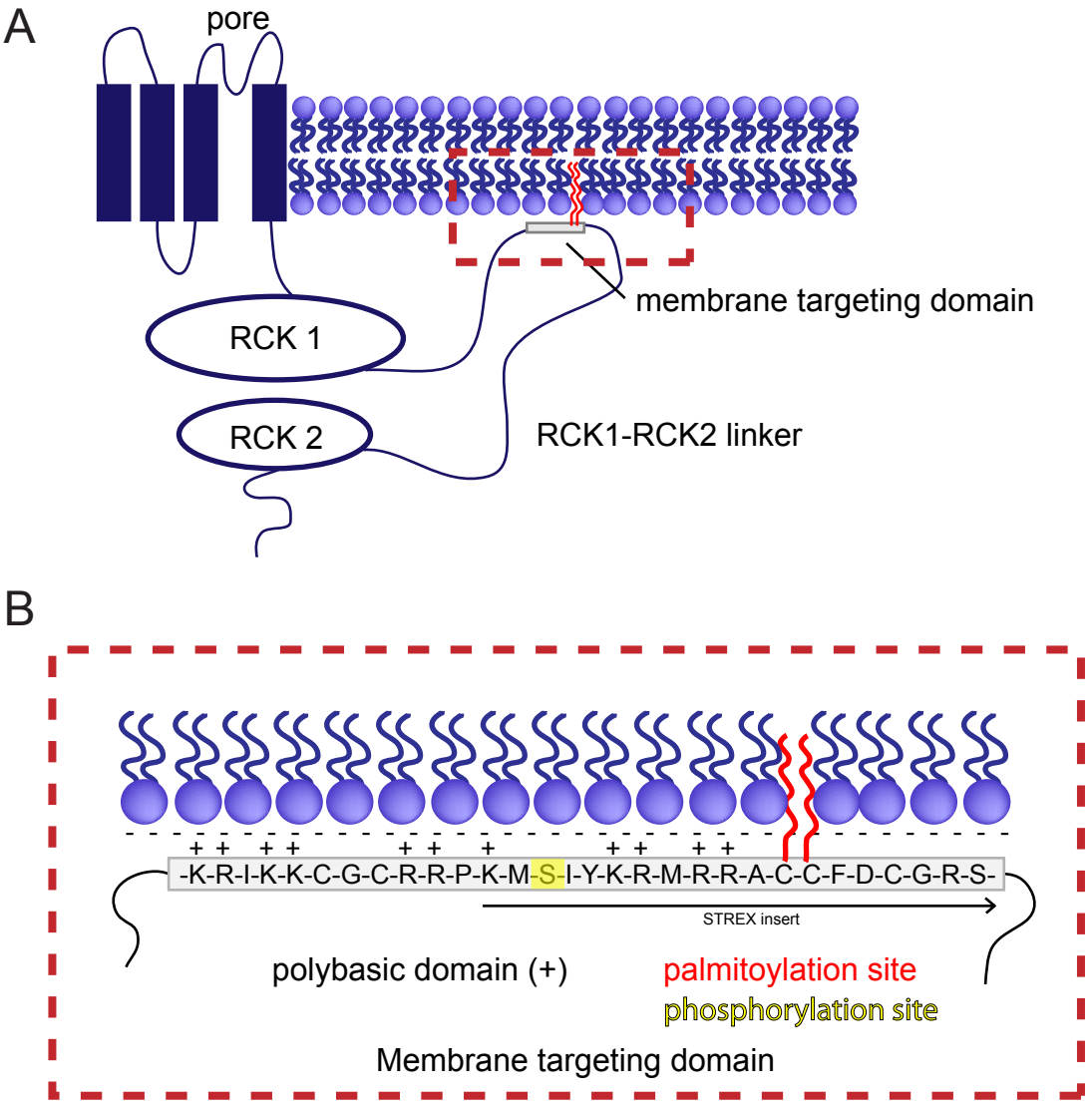

Figure 4.14. The STREX channel membrane targeting domain. (A) Model illustrating the membrane targeting domain in the RCK1-RCK2 intracellular linker of the STREX channel comprising of the polybasic domain and palmitoylation site. (B) Magnified region of the membrane targeting domain as shown by broken red box in A. Palmitate residues are illustrated in red and basic charged residues are illustrated by (+). The STREX insert is highlighted by a solid black underline but only the first 19 residues are shown for diagramatic purposes. The membrane targeting domain forms a flat interaction domain that tethers the RCK1-RCK2 linker to the plasma membrane. The PKA phosphorylation site that can destabilize membrane association is indicated by a yellow box.

implications are there for the structure of this linker upon alternative splicing of the STREX insert. The palmitoylation site in STREX would presumably penetrate the lipid membrane tethering the region to the membrane. The structure of polybasic domains that are implicated in electrostatic association with the plasma membrane are generally described as being flat, a property that can distinguish polybasic membrane targeting domains from those that target the nucleus and bind DNA which tend to have significant curvature (Honig & Nicholls, 1995; Mulgrew-Nesbitt *et al.*, 2006). Therefore it is possible that the membrane targeting domain is a linear structure composed of a polybasic domain electrostatically attracted to the negatively charge lipid membrane and with an anchoring palmitoylation site that penetrates the lipid bilayer at the C-terminal end (Figure 4.14). This would impose structure on the RCK1-RCK2 linker by incorporating both elements into a membrane targeting domain. As discussed before (see section 3.3.5) the linker potentially would be long enough to reach the plasma membrane and stabilise association of the membrane targeting domain which appears to require both elements of palmitoylation and the polybasic domain (Figure 4.14).

It is clear that these structural differences imposed on the RCK1-RCK2 linker with insertion of the alternatively spliced STREX insert, contribute to the increased calcium sensitivity inherent to the STREX channel when compare to insertless ZERO channel and this may be reflected in a conformational change in the RCK interface and calcium binding site as discussed previously (see section 3.3.5).

4.3.7 A polybasic domain as a nuclear localisation signal?

In the imaging assays that examined the fluorescently tagged C-terminal constructs with and without the STREX insert along with the various mutations both in this chapter and in chapter 3, the STREX C-terminal constructs localised at the plasma membrane (~60-70 %), however in ~91% of all cells there was strong nuclear localisation. Disruption of the polybasic domain, as with mutation of the key palmitoylation residues in the previous chapter (see Figure 3.2), diminished membrane association of the STREX C-terminal constructs which appeared to be then targeted directly to the nucleus. The insertless ZERO C-terminal constructs also appeared in the nucleus as well as having a diffuse presence in the cytosol.

This would not be expected for a cytosolic domain and may be indicative of a nuclear localisation signal present in the C-terminus.

Classical nuclear localisation signals are characterised by short stretches of basic amino acids (Pouton *et al.*, 2007). The simian virus 40 large T-antigen has a single cluster of basic residues (P**KKKRK**V) (Kalderon *et al.*, 1984), whereas nucleoplasmin requires two clusters of essentially basic regions (**KR**PAATKKAGQA**KKKK)** (Robbins *et al.*, 1991) and the oncoprotein c-Myc has a fairly unique sequence of only three basic residues (PAA**KR**V**K**LD) (Dang & Lee, 1988). In the STREX channel, the polybasic sequence is as follows, (**KR**I**KK**CGC**RR**P**K**MSIY**KR**M**RR**) and could therefore potentially function as a nuclear localisation signal perhaps similar to the bipartite nature of the nuclear localisation signal inherent to the nucleoplasmin protein. However, what was most interesting and perhaps increasingly supportive of this theory was that double alanine mutations of basic residues in the STREX segment of the polybasic domain (R640A:R642A) completely abolished all nuclear localisation of the STREX C-terminal constructs (see Figure 4.3B). This implies that a nuclear localisation signal may have been disrupted. Whilst this does not fully explain why the insertless ZERO constructs that would only have 6 of the 11 basic amino acids in the polybasic domain is also able to localise at the nucleus, although ZERO C-terminal constructs also show a diffuse cytoplasmic presence not apparent in with STREX C-terminal constructs, it may reflect the importance of the sequence composition of a nuclear localisation signal which may still be functional in the ZERO C-terminus. The importance of the composition of neutral, basic and acidic amino acids within the sequence of a nuclear localisation signal has been demonstrated by mutagenesis studies in c-Myc (Makkerh *et al.*, 1996). Indeed it has been shown that polybasic clusters functioning as nuclear localisation signals can be prevented by hydrophobic amino acids (Heo *et al.*, 2006) and presumably this would also be true to some extent for lipid additions such as palmitoylation just immediately downstream of the polybasic domain in STREX.

Therefore whether the polybasic domain in STREX would be capable of functioning as a nuclear localisation signal with the presence of a palmitoylation site just downstream is unknown and even if palmitoylation was blocked in STREX, could then the C-terminus even locate at the nucleus? The ZERO channel, that does not

contain the STREX insert, has six basic residues without a nearby hydrophobic palmitoylation site and therefore could potentially function as a nuclear localisation signal if the C-terminus was able to operate as an independent domain. In fact recent evidence has suggested that the C-terminus of the Slo3 channel can be expressed in a variety of tissues, including brain, as a fragment that may regulate both the Slo3 and Slo1 channel (Wrighton & Lippiat, 2010). Therefore it is plausible that the C-terminus of the BK channel could be independently functional and could specifically target the nucleus, but to what effect? In another study that examined the role of a C-terminal proteolytic fragment that is part of the $Ca_V1.2$ channel, it showed that it could act as a transcription factor that autoregulates $Ca_V1.2$ transcription in cardiac myocytes (Schroder *et al.*, 2009). Therefore, whether the C-terminus of the BK channel, in native cells, can be expressed as an independent domain either as a whole fragment or a partial fragment is unknown. Indeed, whether it would able target the nucleus to be of functional relevance would require further investigation.

It remains to be seen whether these observations of the C-terminal domain of the BK channel are functionally significant or just an artefact of overexpression.

4.3.8 Challenges for the future

Challenges for the future will be to examine (i) the degree of regulation by phosphorylation of the palmitoylated membrane targeting domain in native cells (ii) by what mechanism is palmitoylation of STREX increased by mutation of residues in the local vicinity (iii) is the polybasic domain a nuclear localisation signal and if so could the C-terminus have a functional role within the nucleus (iv) to define the structure of the RCK1-RCK2 linker with and without STREX (v) what effect STREX may have on the RCK gating domain, assembly interface and accessibility of Ca^{2+} binding.

4.3.9 In Summary

Together this data demonstrates that the polybasic domain in the STREX channel is an important component of a functional membrane targeting domain. The polybasic domain comprises an important basic region surrounding the target palmitoylation site in STREX that controls the stability of palmitoylation and therefore membrane association. Tethering of the RCK1-RCK2 linker, upon alternative splicing of the STREX insert, to the plasma membrane configures the STREX channel to have a greater calcium sensitivity presumably by mediating structural adaptations in the gating domain or calcium binding site and regulates PKA mediated channel inhibition which is conditional on STREX palmitoylation.

CHAPTER FIVE

PALMITOYLATION controls CELL SURFACE EXPRESSION of BK

5.1 Chapter 5 introduction

5.1.1 Additional palmitoylation sites in the BK channel

Previously, the alternatively spliced STREX insert within the C-terminus of the BK channel was identified to contain a single di-cysteine palmitoylation site (see chapter 3). C-terminal constructs that lack the STREX insert (ZERO) were not palmitoylated suggesting that there are no additional palmitoylation sites within the C-terminus of the BK channel. Palmitoylation of the STREX C645:C646 site was shown to control membrane targeting of the STREX domain which regulates the channel's increased calcium sensitivity over the ZERO channel phenotype and mediates channel inhibition by PKA phosphorylation. However, additional studies on full length channels lacking the STREX insert indicated that the channel could still be palmitoylated at a site that must exist outside of the C-terminus.

Palmitoylation has been shown to occur at two independent sites within the same protein and can also mediate two completely unrelated mechanisms in the target protein. AMPA receptor subunits GluR1-GluR4 are palmitoylated at two distinct sites, one is located at the N-terminal transmembrane domain 2 and the second is located in the C-terminal domain. Increased palmitoylation at the transmembrane domain site increases accumulation of the receptor in the Golgi, however when palmitoylation is increased at the C-terminal site, it inhibits interaction with the 4.1N protein which stabilizes cell surface expression (Hayashi *et al.*, 2005), suggesting a dynamic role for palmitoylation in the regulation of trafficking and recycling of AMPA receptor subunits in neurons.

Palmitoylation has been shown to have multiple roles in controlling protein function in different ion channels including: the modulation of voltage-gated Kv1.1 channels (Gubitosi-Klug *et al.*, 2005) and the L-, N-, and P/Q-type Ca^{2+} channels (Chien *et al.*, 1996). Palmitoylation also plays an important role in regulating phosphorylation in BK channels (Tian *et al.*, 2008a) and in the glutamate receptor (GluR6) ligand-gated ion channel (Pickering *et al.*, 1995); as well as regulating cell surface stability of $GABA_A$ receptor ligand-gated channels (Rathenberg *et al.*, 2004), targeting to lipid microdomains of the P2X7 receptor ATP-gated cationic channel (Gonnord *et al.*,

2009) and channel internalisation of voltage-gated Kv1.5 ion channels (Jindal *et al.*, 2008). Additionally, palmitoylation can control structural assembly of sodium channels (Schmidt & Catterall, 1987) and the structural formation of aquaporin-4 channels (Suzuki *et al.*, 2008).

Therefore the role of palmitoylation in ion channels and other proteins can be multifaceted in the control of distinct protein functions. Multiple palmitoylation sites within a protein may indeed have distinct roles in channel function or may regulate a single mechanism through palmitoylation and de-palmitoylation at distinct sites.

In a proteomic screen for palmitoylated proteins in the adult rat brain (Kang *et al.*, 2008) the BK channel was identified to be a palmitoylated protein. In the brain, generally the ZERO channel variant would be expressed as STREX channels have been shown to be expressed in low levels (MacDonald *et al.*, 2006). Therefore it is possible that a palmitoylation site exists outside of the STREX insert. Moreover, using a protein prediction algorithm (CSS-palm) an additional potential palmitoylation site was identified in the intracellular linker that links the S0 and S1 transmembrane domains (S0-S1 linker) (Figure 5.1).

5.1.2 Working hypothesis

In this chapter, the hypothesis is that there are additional palmitoylation sites in the BK channel that may be functionally distinct from the previously identified STREX palmitoylation site.

5.1.3 Aims to be addressed in this chapter

5.1.3.1 Are there additional palmitoylation sites in the BK channel and do they target the plasma membrane?

In order to identify additional palmitoylation sites in the BK channel, potential cysteine residues predicted using the CSS-Palm algorithm were investigated using a

Figure 5.1
Sequence alignment of conserved cysteine residues in the S0-S1 linker of the BK channel

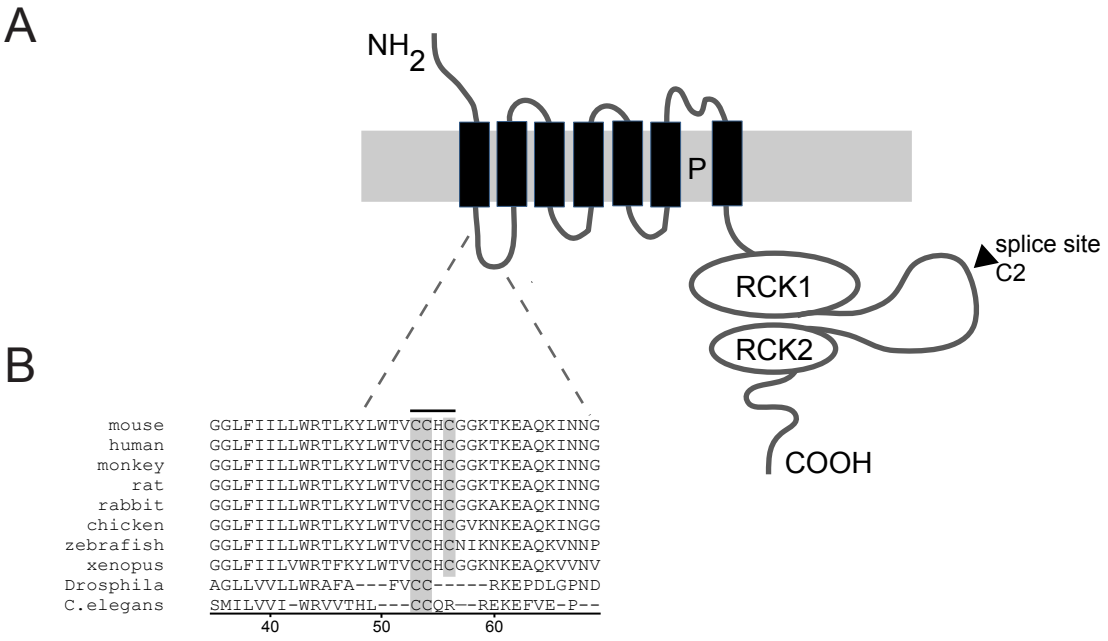

Figure 5.1. Sequence alignment of conserved cysteine residues in the S0-S1 linker of the BK channel. (A) Schematic illustrating the topology of the BK channel pore forming α-subunit. Highlighted is the S0-S1 linker (dash lines) and the C2 splice site (black triangle). (B) Sequence alignment indicates evolutionary conserved cysteine residues in the intracellular linker between transmembrane domain S0 and S1 (indicated in grey), across vertebrates and *Drosophila* and *C.Elegans*. Channel sequence of the mouse is numbered from MDALI start site (accession number AF156674) and illustrated beginning at glycine residue 35 (the S0-S1 linker includes residue 44-114).

site directed mutagenesis study and examining ^{3}H-palmitate incorporation into full length channel constructs. To determine whether a palmitoylation site is functional in membrane targeting, short protein fragments containing the palmitoylation site were created fused with fluorescent tags. These fusion proteins were transfected into HEK293 cells to determine membrane expression and used to examine the effect of mutagenesis of the palmitoylation site on cellular location which was then clarified with pharmacological treatment to abolish palmitoylation the mechanism involved.

5.1.3.2 What is the function of an additional palmitoylation site in BK channels?

To examine the functional effect of the palmitoylation site within the S0-S1 linker, ZERO channels were screened using a membrane potential assay that can discriminate different channel phenotypes based on altered calcium- and voltage-sensitivity or changes in cell surface expression. Channel variants with mutations in the identified palmitoylation site that showed different responses in the membrane potential assay were then examined by electrophysiological patch clamp techniques to determine any changes in calcium- and voltage- sensitivity. Mutant channels that demonstrated no difference in channel properties were then N-terminally tagged and immunofluorescently labelled extracellularly to ascertain any changes in cell membrane expression relative to total protein expression by confocal microscopy and biochemical analysis.

5.1.3.3 Are palmitoylation sites functionally linked within a protein?

It is important to identify whether palmitoylation can occur at two separate palmitoylation domains within the same channel protein and whether they can be independently regulated. Therefore to determine whether the two palmitoylation sites that are present in the STREX splice variant of the BK channel, can function independently, STREX channels containing the intact C645:C646 palmitoylation site were examined with mutation of the secondary palmitoylation site. This identified whether the STREX palmitoylation site could influence palmitoylation at the second N-terminal S0-S1 linker site.

5.2 Results

5.2.1 A palmitoylation site in the S0-S1 linker of the BK channel

To investigate whether there might be additional palmitoylation sites in the BK channel, the ZERO channel sequence was examined using the Clustering and Scoring Strategy Palmitoylation algorithm (CSS-palm). The murine BK channel sequence, accession number: AF156674 (incorporating start site MDALI to the end of the intracellular carboxyl tail ending at cysteine residue 1226, VEDEC) was input into the algorithm. Deletion of the STREX insert diminished all palmitoylation in C-terminal constructs (see Figure 3.8) suggesting that only cysteine residues that scored highly outside of the C-terminus could be potential palmitoylation sites. The CSS-palm algorithm predicted a region with high probability that could act as a palmitoylation domain, located in the S0-S1 intracellular linker. In the S0-S1 linker three cysteine residues C53, C54 and C56 (numbered starting from MDALI) were identified that scored highly with values of 1.54, 1.48, 0.92 respectively (Table 5.1). Therefore, this region in the S0-S1 linker could represent a palmitoylation site that would be present in all BK channel variants (Figure 5.1A).

Sequence alignment of the three cysteine residues in the S0-S1 linker (C53, C54 & C56) indicate strong evolutionary conservation across vertebrates with conservation of a double cysteine motif (C53 & C54) extending across *Drosophila* and *C. Elegans*. Therefore, it would appear that these cysteine residues may be functionally important to the BK channel (Figure 5.1B).

5.2.2 BK channels are palmitoylated at the S0-S1 linker

To investigate if the C53, C54, C56 cysteine residues are palmitoylated in vivo within the S0-S1 linker of the full length ZERO channel, ^{3}H-palmitate incorporation was examined in HEK293 cells. Mutation of the identified cysteine residues in the S0-S1 linker would indicate which residues are important for palmitoylation of the ZERO channel. The representative fluorograph (Figure 5.2 upper) illustrating radiolabelled ^{3}H-palmitate incorporation into full length ZERO channels show that

Table 5.1
Predicted palmitoylation scores for cysteine residues in the ZERO channel

Position	Peptide	CSS-palm v2.0 score	Location
14	EVPCDSR	1.34	extracellular N-terminus
53	WTVCCHC	1.54	intracellular S0-S1 loop
54	TVCCHCG	1.48	intracellular S0-S1 loop
56	CCHCGGK	0.92	intracellular S0-S1 loop
141	IESCQNF	1.10	extracellular S1-S2 loop
557	CELCFVK	0.87	intracellular C-terminus
800	CDMCVIL	0.82	intracellular C-terminus
1166	EDEC***	1.74	intracellular C-terminus *

Table 5.1. Predicted palmitoylation scores for cysteine residues in the ZERO channel. Scores indicate CSS-palm prediction; a higher score represents higher probability. CSS-palm scores were determined with the published CSS-palm v2.0 at http://bioinformatics.lcd-ustc.org/css_palm by inputing the protein sequence of the entire ZERO BK channel (starting at MDALI and spanning the whole C-terminus to cysteine residue C1226; accession number: AF156674) Predicted palmitoylated cysteine residues in intracellular domains excluding the C terminus are highlighted in grey. * cysteine score at end of peptide is not reliable.

Figure 5.2
BK channels are palmitoylated in the intracellular S0-S1 linker

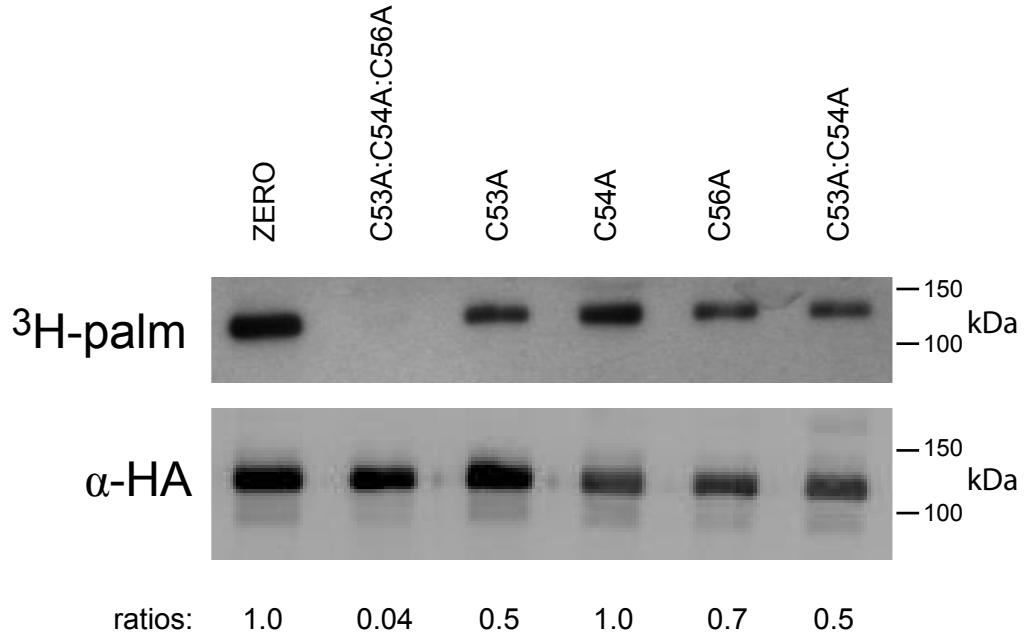

Figure 5.2. BK channels are palmitoylated in the intracellular S0-S1 linker. (A) Representative fluorographs (upper) and western blots (lower) of full-length ZERO-HA channels and ZERO channels with mutation of key cysteine residues in the S0-S1 linker, expressed in HEK293 cells. Constructs were labelled with ^{3}H-palmitate for 4 hours and immunoprecipitated (IP) by using α-HA magnetic microbeads and detected by fluorography. Ratios (normalised to the wild-type ZERO channel) of ^{3}H-palmitate detection in comparison to total protein expression are included.

triple mutation of the identified cysteine residues to alanine (C53A:C54A:C56A) within the S0-S1 linker can completely abolish palmitoylation in the ZERO channel. Individual point mutation of the cysteine residues that make up the palmitoylation motif decreased the level of ^{3}H-palmitate incorporation by ~ 30-50% in the C53A, C53A:C54A and C56A mutant channels but did not affect palmitoylation in the C54A mutant channel. This suggests that the triple cysteine residues are a key constituent of the S0-S1 linker palmitoylation motif. Western blot analysis confirmed that total protein expression between the single double and triple mutants was largely unchanged in the assays (Figure 5.2 lower); hence the palmitoylation fluorographs reflect the degree of ^{3}H-palmitate incorporation into the full length channel constructs (Figure 5.2).

This data suggests that channels with mutated residues at the C53A:C54A:C56A site in the S0-S1 linker, are not palmitoylated and therefore can be described as de-palmitoylated channels.

5.2.3 The S0-S1 targets the plasma membrane which is diminished by mutation of the C53:54:56A site

To examine whether this newly identified palmitoylation motif in the S0-S1 linker may be able to interact with the plasma membrane in same manner as the palmitoylated STREX domain (see chapter 3, Figure 3.2), fusion proteins containing only the S0-S1 linker were created. The S0-S1 linker constructs incorporated the intracellular linker between the two transmembrane domains, S0 and S1, beginning at residue R44 and ending at residue R114 expressed in a fluorescently labelled pEYFP-N1 vector (see section 2.1.1 & Figure 2.1) (Figure 5.3A). The aim was to identify whether this motif could interact with the plasma membrane and what the functional contribution of each cysteine residue was within the palmitoylation motif.

Transient expression of the S0-S1 linker fusion protein in HEK293 cells, resulted in robust expression at the plasma membrane, with 68% of cell transfected (n=850) showing strong fluorescence at the plasma membrane. Most constructs had strong intracellular expression with diffuse or punctuate fluorescence in the cytoplasm of 97% of cells (n=850) (Figure 5.3B). A site directed mutagenesis approach was used to disrupt the cysteine residues predicted to be palmitoylated in the S0-S1 motif to

Figure 5.3
Palmitoylation targets the S0-S1 linker to the plasma membrane

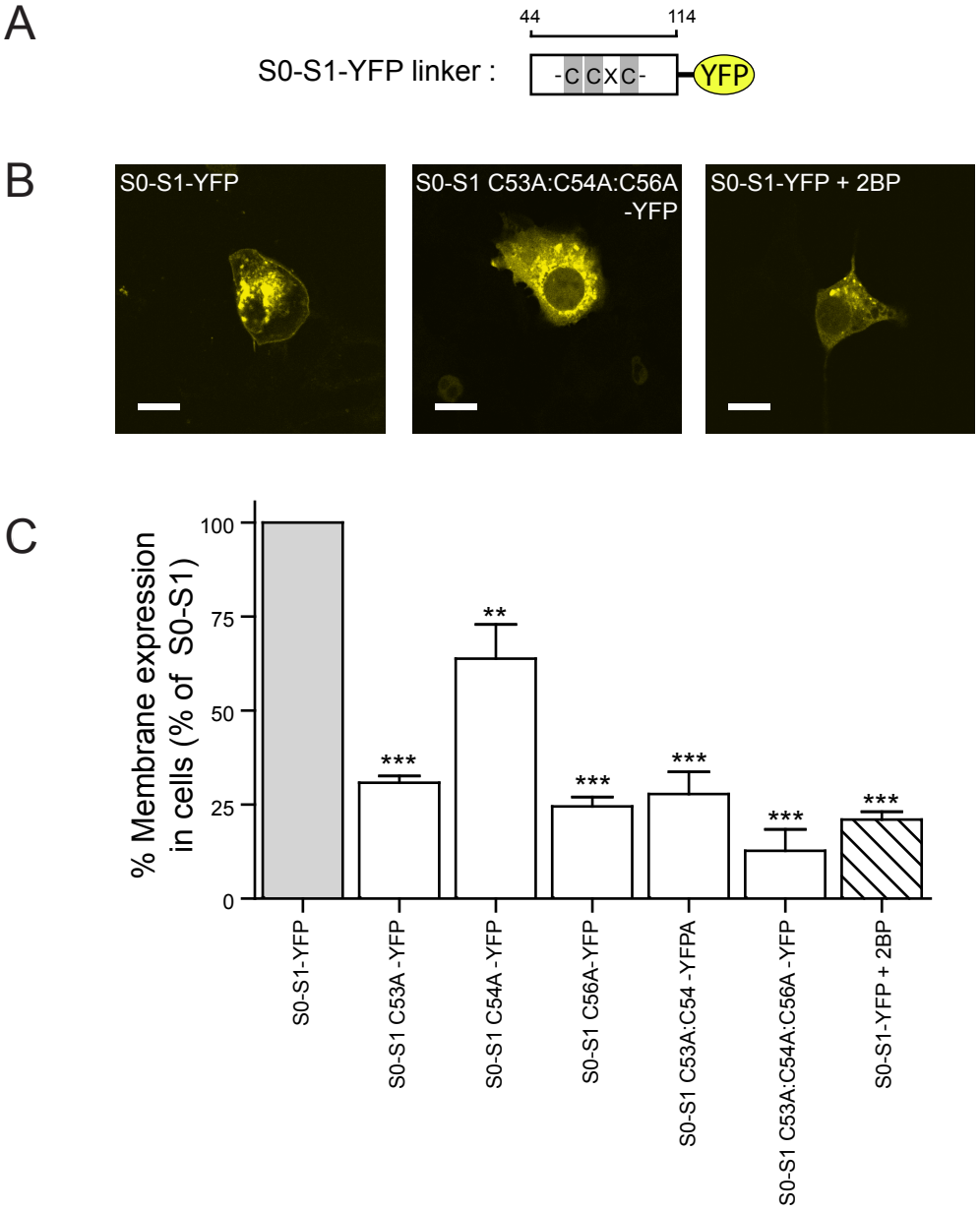

Figure 5.3. Palmitoylation targets the S0-S1 linker to the plasma membrane. (A) Schematic of the S0-S1 linker-YFP fusion construct. (B) Representative single cell confocal images of the S0-S1 linker, S0-S1 C53A:C54A:C56A, and the S0-S1 linker incubated with an inhibitor of palmitoylation 2BP (100 μM) for 24 hours, expressed in HEK293 cells. (Scale bars: 10 μm). (C) Summary bar graph of the respective mutations of three cysteine residues in relation to localization at the plasma membrane expressed as a percentage of S0-S1 (where S0-S1 is normalised to 100%). (For all S0-S1 linker constructs, N>3, n>330 cells analysed) ** $p<0.01$ *** $p<0.001$ compared to S0-S1 (ANOVA with Tukey post hoc test).

identify the functional contribution of each cysteine residue in membrane association. Mutation of individual cysteine residues by point mutation to a neutral alanine (A) residue resulted in decreased expression at the plasma membrane. All mutant channels are expressed in relation to the wild-type S0-S1 linker construct at the plasma membrane which was normalised to 100%. Mutation of C53A resulted in a significant decrease to 30.8 ± 1.8% of wild-type S0-S1, associating at plasma membrane, C54A showed a smaller decrease with 63.9 ± 9.1% of wild-type S0-S1, at the plasma membrane and C56A showed the greatest decrease of the single point mutations with 24.6 ± 2.4% of wild-type S0-S1, at the plasma membrane. This suggested that each residue is important for the association of the S0-S1 linker at the plasma membrane. Mutagenesis of the double cysteine residues that are placed side by side (C53A:C54A), the same configuration as the palmitoylation motif in STREX (C645A:C646A), was also examined to identify if this may be a consensus sequence typical of a palmitoylation site in the BK channel. The C53A:C54A mutation in the S0-S1 linker resulted in a decrease of 27.9 ± 5.8% of wild-type S0-S1 at the plasma membrane, suggesting that the mutation could still not fully abolish association with the plasma membrane. The next step was to mutate all three cysteine residues in a triple mutation, C53A:C54A:C56A which resulted in the lowest expression at the plasma membrane with 12.7 ± 5.8 % of wild-type S0-S1 appearing to associate at the plasma membrane (for all S0-S1 linker constructs, n > 330 cells counted) (Figure 5.3B&C).

The S0-S1 fusion proteins showed very little nuclear localisation but in constructs that were not present at the plasma membrane they showed strong fluorescence in what appeared to be intracellular organelles encapsulating the nucleus, reminiscent of ER or Golgi localisation. However because the S0-S1 linker studied was only a protein fragment and would probably not reflect the full length channel, this was not examined any further.

To investigate the effect of inhibition of palmitoylation on the short S0-S1 linker constructs, cells were incubated with the palmitoylation inhibitor 2-bromopalmitate (2-BP) which decreased the association of the S0-S1 linker at the plasma membrane similar to the double and triple cysteine mutant to 21 ± 2.1% of wild-type control S0-S1, at the plasma membrane (Figure 5.3B&C). This suggests that the S0-S1 linker motif does associate with the plasma membrane through palmitoylation.

Together this data suggests that the triple cysteine motif identified in the S0-S1 linker is a novel palmitoylation motif found within all BK channels.

5.2.4 Palmitoylation of the S0-S1 linker is functionally important to the BK channel

To investigate the functional effect of the S0-S1 linker palmitoylation motif in the ZERO channel, mutated full length channels were transiently transfected into HEK293 cells and examined as previously described by a membrane potential assay (Saleem *et al.*, 2009)(see section 2.3.3). As before, mutated channels were transiently transfected into HEK293 cells and seeded into 96 well assay plates. The FLIPR-blue dye (Molecular Devices) was administered to the cells to allow the dye to load into the cell membrane. The assay was then run in the Flexstation ® II during which cells were stimulated by 1 µM Ionomycin, a calcium ionophore, to activate the BK channel by calcium influx. Changes in fluorescence were then measured over a time course of 180 seconds.

The ZERO channel was measured as the control hyperpolarising response to channel activation by calcium influx (ionomycin 1 µM). The peak value in these assays was taken at t=70s and these values could then be expressed as the isolated channel current by subtracting the control HEK response from the transiently transfected channel response within the assay plate and then normalised to 100%. Therefore channels with mutations in the S0-S1 linker could be expressed according to the ZERO channel response (Figure 5.4). A representative trace illustrating the raw data of the ZERO channel, the S0-S1 mutant channels and un-transfected HEK293 response to ionomycin is shown in (Figure 5.4A).

Mutation of the triple (C53A:C54A:C56A) cysteine residues within the identified palmitoylation motif in the S0-S1 linker significantly attenuated the hyperpolarising response of the channels to 39.0 ± 5.5 % of wild-type ZERO (n= >15) (Figure 5.4A&B). The functional effect of point mutations in the individual and double cysteine residues in the S0-S1 linker was not statistically significantly shifted with respect to the ZERO channel response (Figure 5.4B). Mutation of individual cysteine residues shifted the apparent response to, C53A 96.2 ± 10.7%, C54A 86.0 ± 14.8% and C56A 79.6 ± 18.9% and in the double to C53A:C54A 54.8 ± 6.2% (n= >11). This

Figure 5.4
Activation of BK channels by calcium influx is attenuated in S0-S1 mutant channels

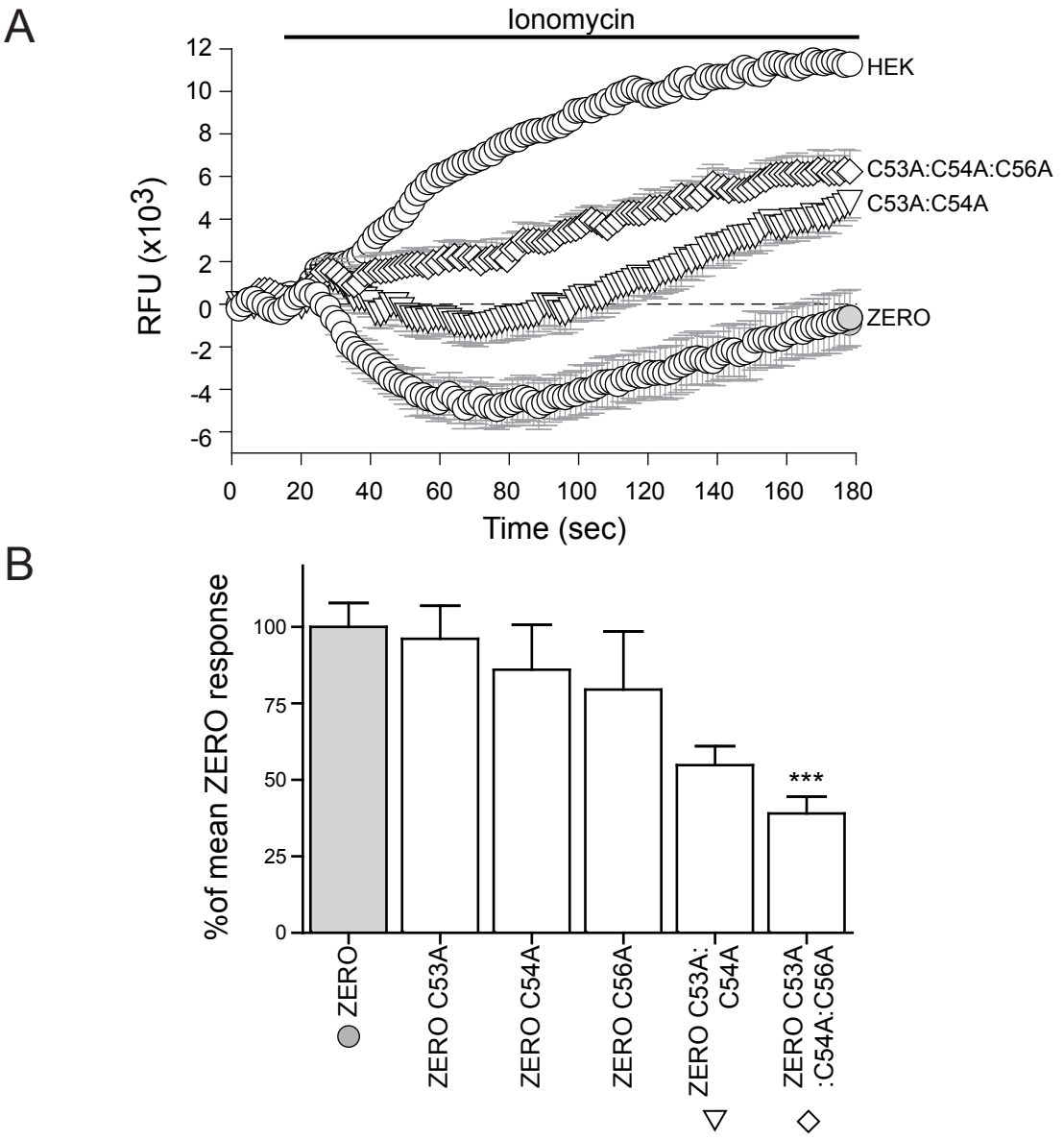

Figure 5.4. Activation of BK channels by calcium influx is attenuated in S0-S1 mutant channels. (A) Representative time course plots of mean change in relative fluorescence units (RFU) of the FLIPR-blue membrane potential dye in HEK293 cells expressing ZERO (grey circles, ●), ZERO C53A:C54A (inverted triangles,▽), ZERO C53A:C54A:C56A (diamonds,◇), and mock-transfected HEK293 (open circles, ○), in response to calcium influx induced by 1 μM Ionomycin. (B) Summary bar chart of the membrane potential change for each construct expressed as a percentage of the maximal hyperpolarisation with HEK293 subtraction elicited in HEK293 cells expressing in the ZERO (grey) variant (where ZERO is 100%). Data was determined at the maximum hyperpolarising response in the wild-type ZERO channel (t=70s) in the time course plots in (A). All data are Means ± S.E.M (N=3, n>24), *** p<0.001, compared to ZERO (ANOVA with Tukey post hoc test).

data suggests that there was a significant decrease in the response to ionomycin of the ZERO C53A:C54A:C56A mutant channels relative to the wild-type ZERO channels; therefore the triple cysteine motif must be functionally important to the BK channel.

5.2.5 Single channel amplitude is not affected in de-palmitoylated BK channels

The membrane potential assay cannot discriminate between: shifts in the calcium/voltage sensitivity of the channel; altered channel conductance; or changes in expression of functional channels at the plasma membrane. As the C53A:C54A:C56A mutant channel showed the greatest change in membrane potential, palmitoylation incorporation and in the imaging assays, the functional impact of the ZERO C53A:C54A:C56A mutant channel was compared to that of the wild type ZERO variant channel hereafter.

To investigate the properties of the C53A:C54A:C56A mutant channels that may mediate the attenuated response to ionomycin in the membrane potential assay, isolated channels were examined electrophysiologically. To determine whether the reduction in the sensitivity to ionomycin might be mediated by a reduced single channel amplitude, the triple cysteine mutant (C53A:C54A:C56A) channel was examined relative to the wild type ZERO channel over a range of membrane potentials (Figure 5.5). Measurements were made at a range of voltage potentials (-80 mV to +80 mV) in equimolar (140 mM) potassium gradients and at 1 µM [Ca^{2+}] in excised inside-out patches (Figure 5.5). Single channel slope conductance in excised inside-out patches was unchanged between ZERO and ZERO C53A:C54A:C56A channels (ZERO, 231 ± 3.9 pS and ZERO C53A:C54A:C56A, 227 ± 5.4 pS) (Figure 5.5A). Representative recordings at +40 mV and -40 mV illustrate the mean single channel amplitude (Figure 5.5B), these were as follows; ZERO 10.7 ± 0.1 & -10.4 ± 0.1 pA and, ZERO C53A:C54A:C56A 10.7 ± 0.3 & -10.7 ± 0.2 pA (n=3).

Figure 5.5
Single channel amplitude is not changed in de-palmitoylated BK channels

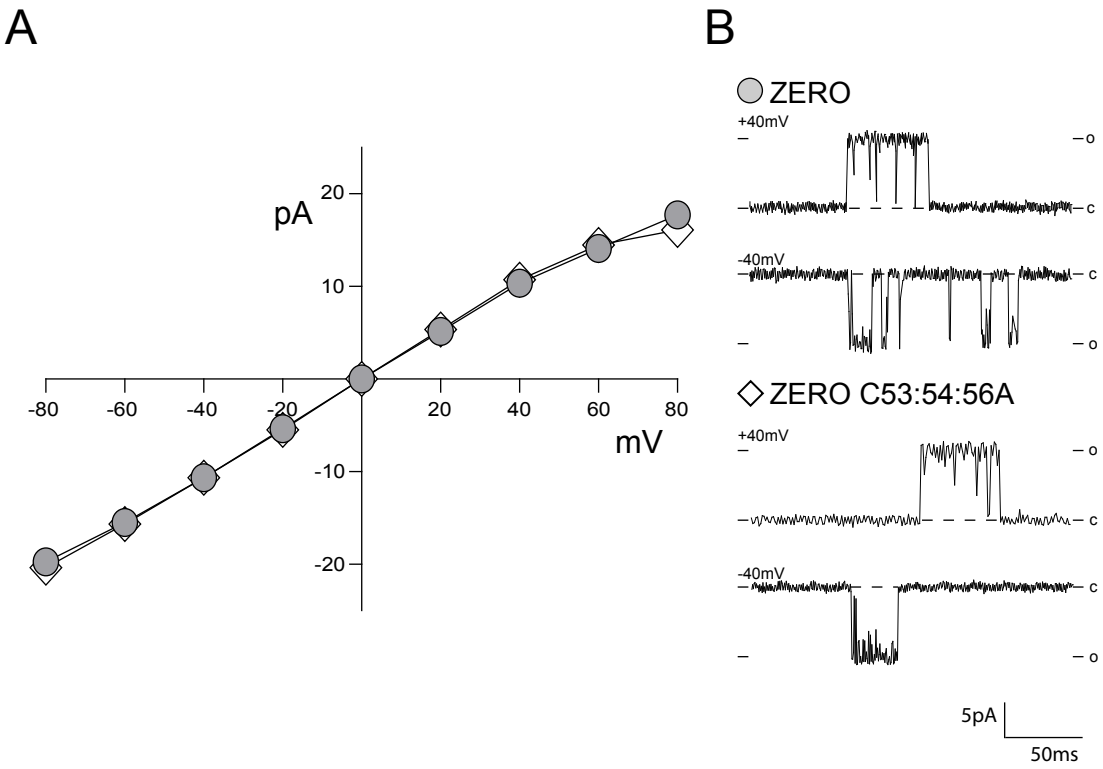

Figure 5.5. Single channel amplitude is not changed in de-palmitoylated BK channels. (A) Current voltage plot for ZERO channels (grey circles, ◯) and triple cysteine mutant C53A:C54A:C56A channels (diamonds, ◇), illustrating that single channel conductance in 1 μM free Ca^{2+} and equimolar (140 mM) potassium gradients (N=3). Single channel conductance derived from the slope of the line. The conductance of the ZERO channel is 231.2 ± 3.9 pS and the triple cysteine C53A:C54A:C56A mutant channel is 227.1 ± 5.4 pS. (B) Representative single channel recordings of excised inside-out patches at +40 and -40 mV.

Therefore the attenuated response to ionomycin in the membrane potential assay of the C53A:C54A:C56A mutant channels cannot be mediated by a reduction in single channel amplitude relative to the wild-type ZERO channel.

5.2.6 S0-S1 palmitoylation has no effect on intrinsic channel activity

Macropatch recordings were carried out over a physiological range of intracellular calcium (0.33 to 10 µM $[Ca^{2+}]_i$) to determine the calcium- and voltage- sensitivity of the mutant channels. Recordings were made as described previously in equimolar (140 mM) potassium gradients by inside-out patch clamp analysis (Figure 5.6). Representative currents illustrate the typical outward component of the ZERO variant of the BK channel and mutant channel currents in response to a depolarising voltage step protocol (-120 to +120 mV) from a holding potential of -80 mV (Figure 5.6A). Activation (G/G_{MAX}) curves were obtained by plotting normalised tail current amplitudes versus the respective test potential. These curves were fitted to a Boltzmann equation whereby the voltage for half activation ($V_{0.5MAX}$) could be determined. In 1 µM free calcium, the mid-point of the physiological calcium range for activation of the ZERO channel, the voltage for half activation of ZERO was 11.1 ± 9.2 mV. The triple cysteine mutant C53A:C54A:C56A channel showed no significant difference in the half maximal voltage for activation of the channel (12.5 ± 5.7 mV) when compared to the wild-type ZERO channel (Figure 5.6B). The $V_{0.5MAX}$ across the calcium range of 0.33 – 10 µM free calcium for ZERO and the C53A:C54A:C56A mutant channel was not significantly different suggesting that the calcium sensitivity of the channel is unchanged with mutation of the S0-S1 palmitoylation site (Figure 5.6C).

To examine the voltage sensitivity of the C53A:C54A:C56A mutant channel relative to the wild-type ZERO channel, a logarithmic transformation to linearize the activating component of the normalised (G/G_{MAX}) curves in Figure 5.6B were plotted against the depolarised potentials of 0 mV to +120 mV (Figure 5.7). This data showed that the voltage dependence of the ZERO C53A:C54A:C56A channel was not significantly changed from wild-type ZERO channels. These data suggest that neither changes in single channel conductance nor channel calcium- and voltage-sensitivity underlie the reduced activity of the

Figure 5.6
Calcium sensitivity is un-affected in de-palmitoylated channels

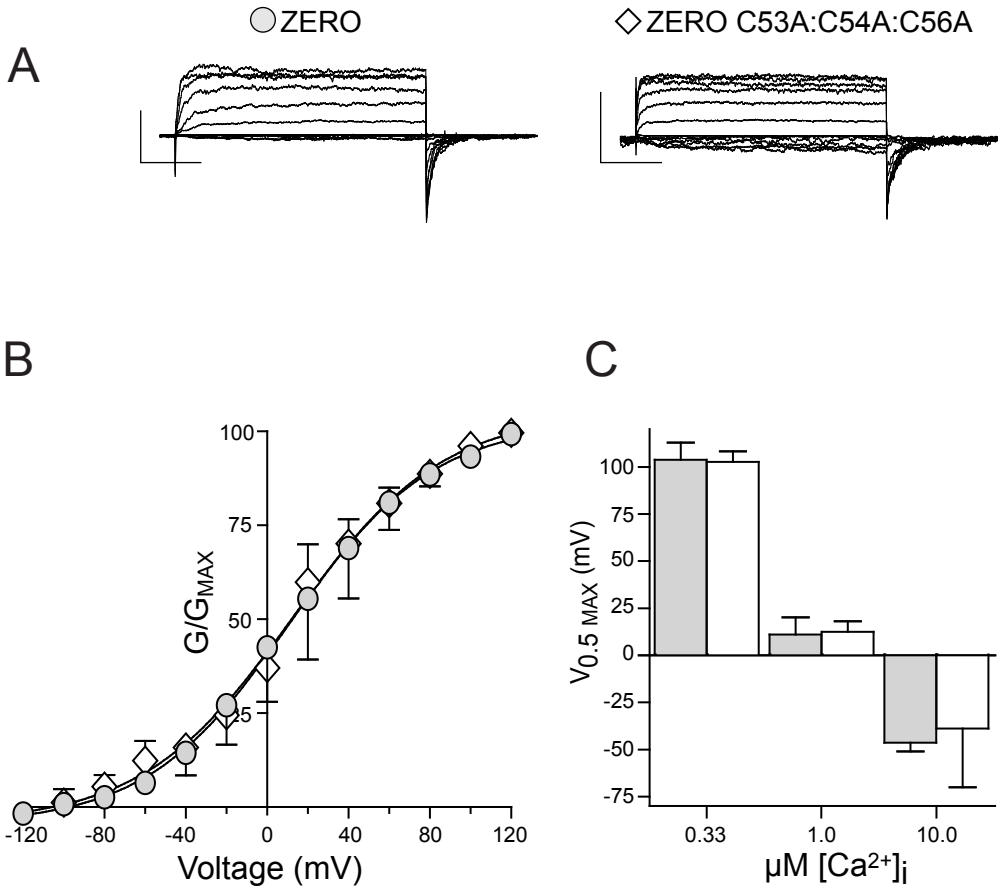

Figure 5.6. Calcium sensitivity is un-affected in de-palmitoylated channels. (A) Representative macropatch recordings traces showing BK currents in response to a depolarising voltage step protocol (-120mV to +120mV) from a holding potential of -80mV from excised inside-out patch recordings in equimolar potassium gradients and 1 μM free Ca^{2+} (Scale bars: 1 nA / 25 ms) (B) G/G_{MAX} conductance curves show no change in channel activation at 1 μM free Ca^{2+} between ZERO (grey circles,●) and ZERO C53A:C54A:C56A (diamonds,◇). (C) Summary bar graph illustrates no significant changes in $V_{0.5MAX}$ across the physiological calcium range 0.33 μM – 10 μM free Ca^{2+}. All data are Means ± S.E.M (n >3).

Figure 5.7
The voltage dependence of the ZERO C53A:C54A:C56A channel is unchanged

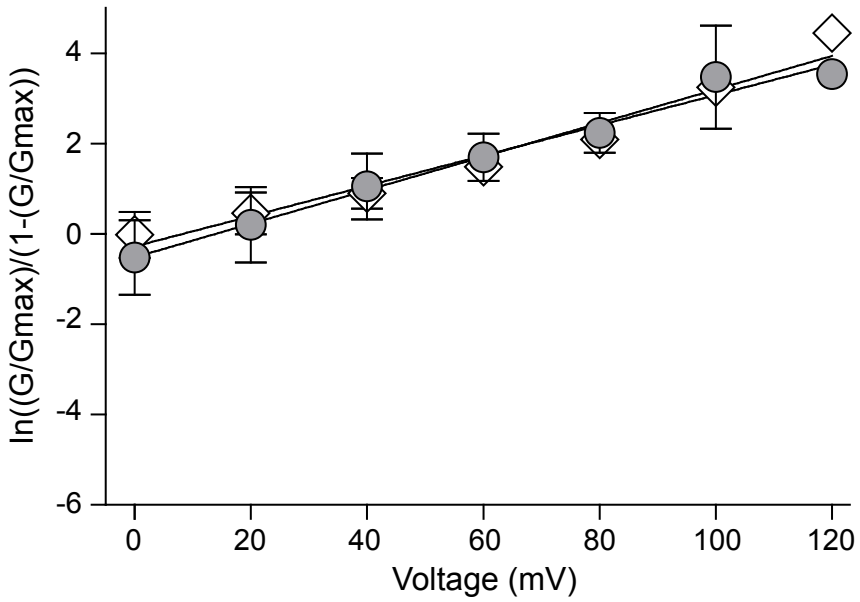

Figure 5.7. The voltage dependence of the ZERO C53A:C54A:C56A channel is unchanged. A logarithmic transformation of the G/G_{MAX} activation curves over depolarised potentials 0 - 120 mV as described in Figure 5.6B. ZERO (grey circles,●), and C53A:C54A:C56A (diamonds, ◇). The voltage dependence was derived from the slope of the line.

Figure 5.8
Number of functional ZERO C53A:C54A:C56A channels appears reduced in membrane patches when compared to wild-type ZERO channels

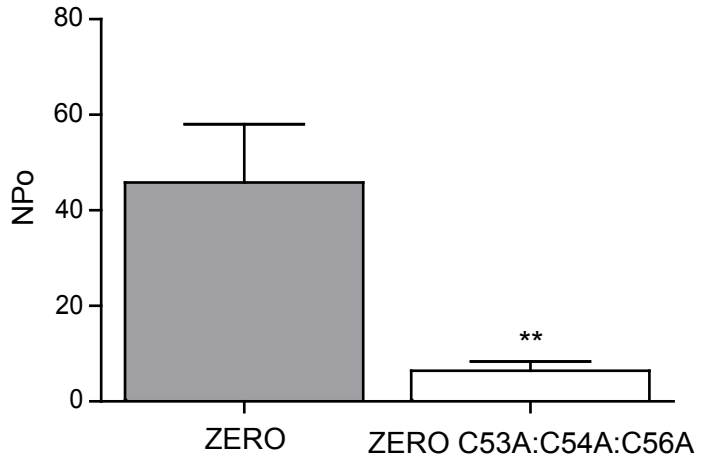

Figure 5.8. Number of functional ZERO C53A:C54A:C56A channels appears reduced in membrane patches when compared to wild-type ZERO channels. Bar graph illustrating the average number of functional channels in membrane patches assessed by determining total conductance (I) divided by single channel amplitude (i) to inidcated NPo in macropatch recordings and indicated as number of channels in single channel recordings. ZERO C53:C54A:C56A N=26, ZERO N=12. Data represents Means ± S.E.M (N=3, n>24), ** $p<0.01$, compared to ZERO (t-test).

C53A:C54A:C56A mutant channels observed in the membrane potential assays. However, during patch clamp analysis there appeared to be fewer of the ZERO C53A:C54A:C56A mutant channels at the plasma membrane (ZERO C53A:C54A:C56A channels were reduced by ~70%, n=26) when compared to wild-type ZERO channels (n=12) (Figure 5.8).

Therefore, we examined cell surface expression of the ZERO channel and the mutant (ZERO C53A:C54A:C56A) channel by using quantitative immunofluorescence.

5.2.7 Palmitoylation is an important determinant of BK channel cell surface expression.

To determine whether the triple cysteine C53A:C54A:C56A mutant channel might disrupt the normal expression of channels at the plasma membrane, channel constructs were created with extracellular N- terminal FLAG- tag epitopes that enabled detection on the extracellular surface of HEK293 cells. Constructs also had C- terminal -HA tag epitopes to determine total protein expression. In non-permeabilised cells, the extracellular N-terminal Flag- tagged channels were labelled with a primary antibody (Anti-flag M2 mouse monoclonal antibody) and then fluorescently labelled with a secondary antibody (Alexa fluor 594 conjugated anti-mouse IgG antibody) to measure Flag- tagged channels that would represent channels that were only present on the cell surface. After permeabilisation the –HA tag was labelled with a primary antibody (anti-HA rabbit polyclonal antibody) and subsequently fluorescently labelled with a secondary antibody (Alexa 488 conjugated anti-Rabbit IgG) to detect cells that efficiently expressed all transfected –HA tag channel protein. In a field of view, cells were counted by confocal microscopy initially at wavelength GFP-Green-488 nm to detect cells that were efficiently transfected with –HA tagged channel protein and labelled by the respective secondary antibody. In the same field of view cells were then counted at the TexasRed-594 nm wavelength to detect the number of channels that showed efficient expression of the FLAG- tagged antibody that indicates channels expressed at the cell surface prior to permeabilisation (Figure 5.9).

Figure 5.9
Palmitoylation of the S0-S1 linker regulates cell surface expression of BK channels

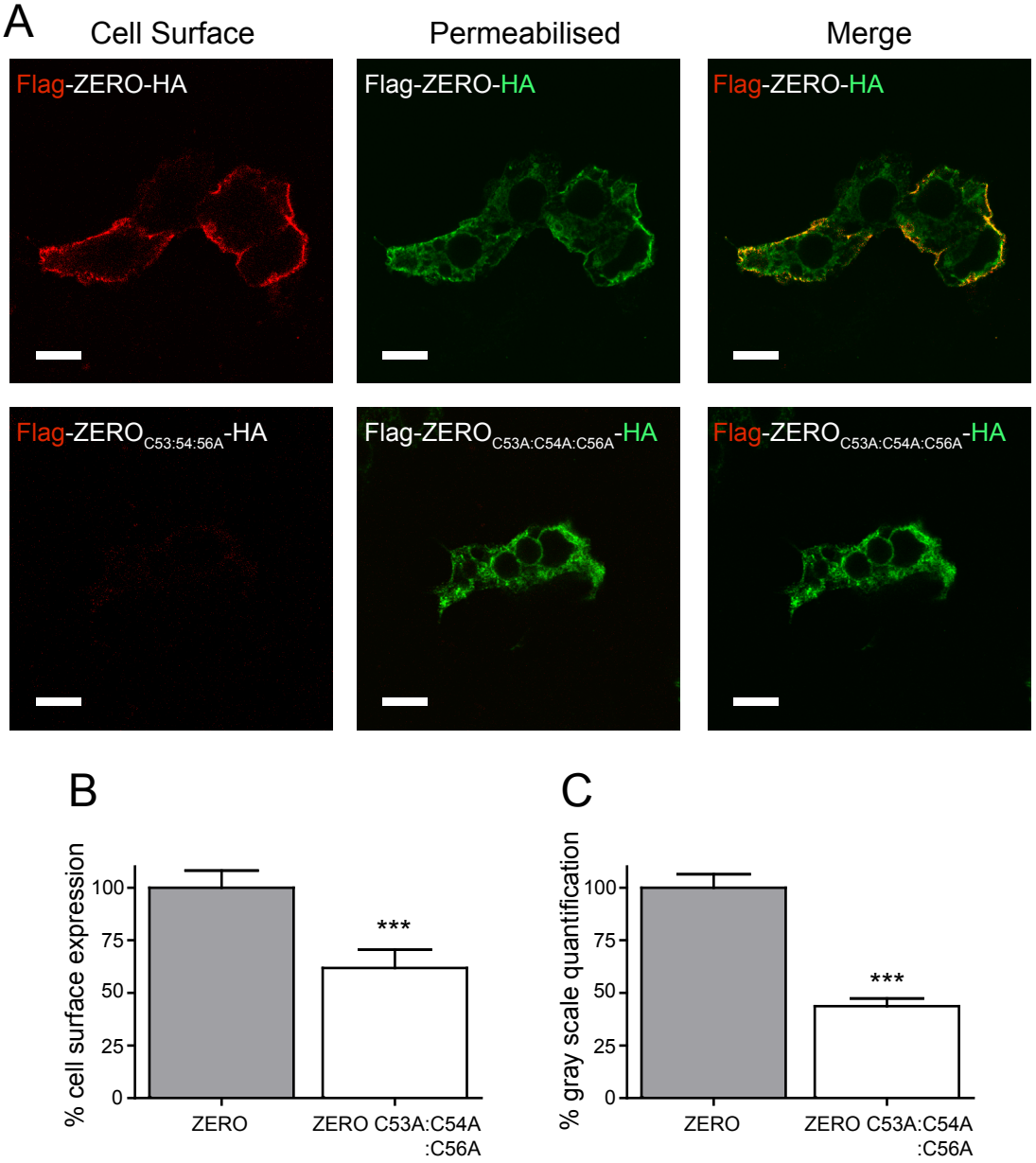

Figure 5.9. Palmitoylation of the S0-S1 linker regulates cell surface expression of BK channels. (A) Representative confocal images of HEK293 cells expressing Flag-ZERO-HA (top panels), and Flag-ZERO C53A:C54A:C56A-HA (bottom panels). The extracellular Flag- epitope was labelled (red) under non-permeabilised conditions (cell surface) with the C terminal –HA epitope tag (green) labelled following cell permeabilisation. Flag- and –HA labelling from the same cell are then overlaid (merge). Scale bars are 10 μM. (B) Percentage of cells expressing channel constructs at the plasma membrane as a percentage of ZERO normailsed to 100%. (C) Quantification of greyscale fluorescence for channels at the plasma membrane as a percentage of ZERO normalised to 100%. Data are Means ± S.E.M (n >3). *** $p < 0.01$, ANOVA with post hoc Tukey test compared to ZERO.

Representative confocal images show the wild type ZERO channel (top panels) of cell surface expression of Flag- tagged channel protein in RED (cell surface), the permeabilised cells subsequently labelled for -HA in GREEN (permeabilised) and Flag- and –HA labelling from the same cell are then shown in overlaid images (merge) (Figure 5.9A). The S0-S1 linker palmitoylation deficient channel, ZERO C53A:C54A:C56A, (bottom panel) shows significantly reduced cell surface expression of Flag- tagged channel protein in RED in this field of view (cell surface), but permeabilised cells subsequently labelled for -HA in GREEN illustrate normal expression of channel protein (permeabilised). An overlain image shows no evidence of surface expression (merge) (Figure 5.9A).

Flag-ZERO-HA channels showed robust Flag- tag expression at the cell surface in 60% of permeabilised transfected cells. With the ZERO channel expression at the plasma membrane normalised to 100%, the ZERO C53A:C54A:C56A mutant channel showed a reduced Flag- tag expression to ~68% of total transfected cells at the cell surface, identified by cell counting at a set level of microscope intensity (see methods 2.4.6) (Figure 5.9B). By using quantitative immunofluorescent analysis, using Image-J software (see methods 2.4.6), to examine N-terminal Flag- tagged ZERO C53A:C54A:C56A mutant channels, a more significant decrease in cell surface expression of ~55% in relation to the ZERO channel was observed (Figure 5.9C). Therefore, this data suggests that mutation of the S0-S1 palmitoylation site in ZERO channels decreases cell surface expression.

The N-terminal S0-S1 linker palmitoylation site (C53:C54:C56) is an independent motif upstream of the previously identified palmitoylation site in the STREX insert located in the intracellular C-terminus (C645:C646) (see chapter 3, Figure 3.1). It would not be expected that these two distal palmitoylation sites in the STREX splice variant of the BK channel would be structurally linked and therefore it would be predicted that the C53:C54:C56 S0-S1 palmitoylation site would still be palmitoylated in the STREX channel independent of the C645:C646 STREX palmitoylation site and therefore would still regulate cell surface expression of the STREX channel.

Figure 5.10
Disruption of the S0-S1 palmitoylation motif in the STREX channel reduces palmitoylation

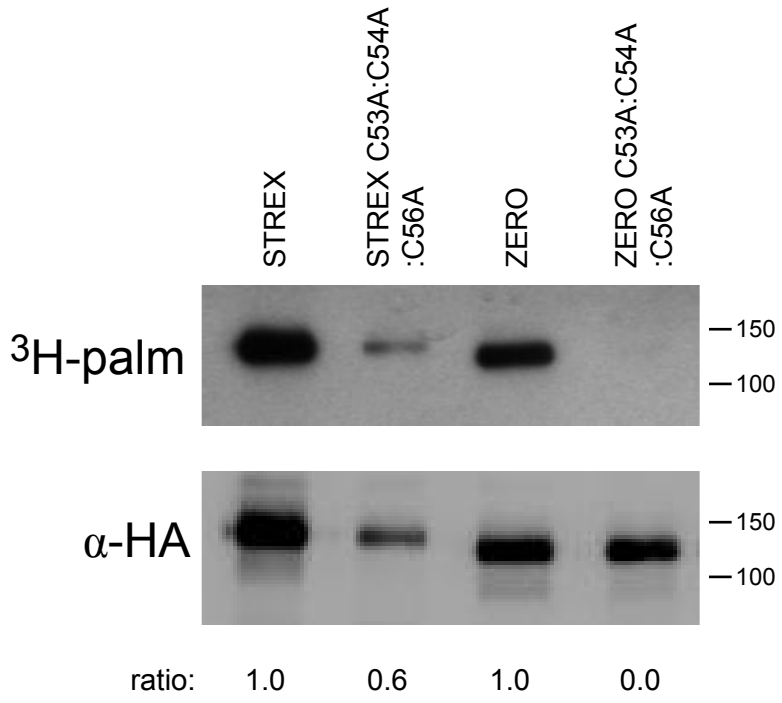

Figure 5.10. Disruption of the S0-S1 palmitoylation motif in the STREX channel reduces palmitoylation. (A) Representative fluorographs (upper) and western blots (lower) of full-length STREX-HA channels, STREX C53A:C54A:C56A-HA, ZERO-HA and ZERO C53A:C54A:C56A-HA channels expressed in HEK293 cells. Constructs were labelled with ^{3}H-palmitate for 4 hours and immunoprecipitated (IP) by using α-HA magnetic microbeads and detected by fluorography. Ratios are shown demonstrating ^{3}H-palmitate incorporation versus total protein expression.

5.2.8 STREX channels are still palmitoylated when the S0-S1 linker palmitoylation motif is mutated

To examine the palmitoylation status of the STREX channel in channels that have mutations in the S0-S1 linker palmitoylation site (STREX C53A:C54A:C56A), ^{3}H-palmitate incorporation into full length STREX and mutant BK channel proteins was examined in HEK293 cells (Figure 5.10). The representative fluorograph (upper panel, lane 1&2) illustrates that triple mutation of the identified S0-S1 palmitoylation motif can reduce ^{3}H-palmitate incorporation into the STREX C53A:C54A:C56A channels by ~40% (Figure 5.10). The same mutation in the ZERO channel (upper panel, lane 3&4) completely abolished palmitoylation suggesting that in STREX the C645:C646 site can still be palmitoylated. The western blot analysis (lower panel) in this particular experiment shows that protein expression between the STREX channel variants was not equivalent however the C53A:C54A:C56A mutations do not compromise STREX expression in other assays (Figure 5.10)

Therefore mutation of the S0-S1 linker palmitoylation motif reduces the total palmitoylation status of the STREX channel but does not abolish it suggesting that palmitoylation must still occur at the STREX palmitoylation site.

5.2.9 S0-S1 palmitoylation is functionally important in STREX channels that are also palmitoylated within STREX

To investigate the functional effect of the S0-S1 palmitoylation motif in STREX channels, mutated channels STREX C53A:C54A:C56A were examined using the membrane potential assay as previously described (Saleem *et al.*, 2009)(see section 2.3.3).

The STREX channel was measured as the control hyperpolarising response to channel activation by calcium influx (ionomycin 1 µM). The peak value in these assays was taken at t=70s and these values could then be expressed as the isolated channel current by subtracting the control HEK response from the transiently transfected channel response within the assay plate and then normalised to 100%. Therefore STREX channels with mutations in the S0-S1 linker could be expressed according to the wild-type STREX channel response (Figure 5.11). A

Figure 5.11
Disruption of the S0-S1 linker palmitoylation site in STREX splice variant channels also attenuates the ionomycin driven channel activation

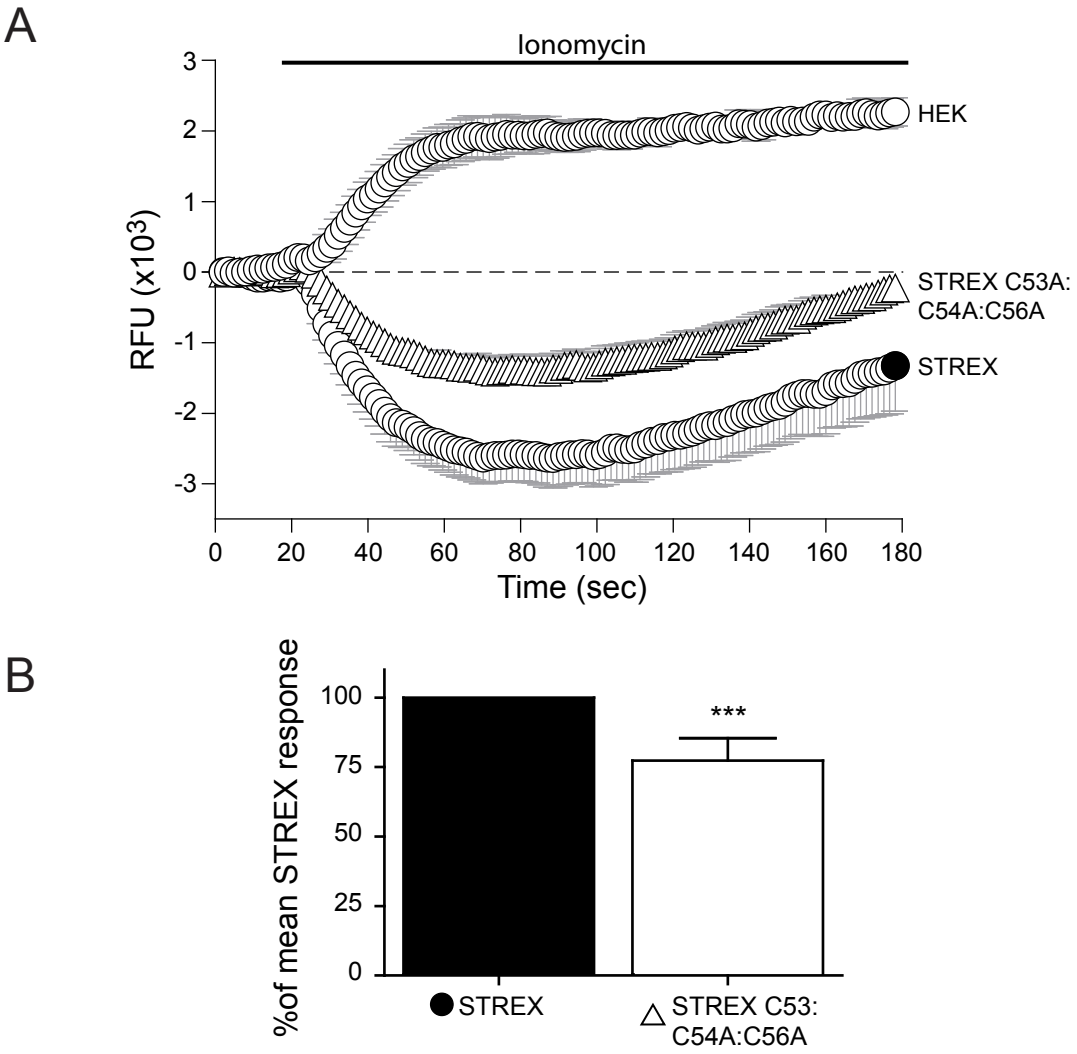

Figure 5.11. Disruption of the S0-S1 linker palmitoylation site in STREX splice variant channels also attenuates the ionomycin driven channel activation. (A) Representative time course plots of mean change in relative fluorescence units (RFU) of the FLIPR-blue membrane potential dye in HEK293 cells expressing STREX (black circles, ●), STREX C53A:C54A:C56A (upright triangles,△), and mock-transfected HEK293 (open circles, ○), in response to calcium influx induced by 1 μM Ionomycin. (B) Summary bar chart of the membrane potential change for each construct expressed as a percentage of the maximal hyperpolarisation with HEK293 subtraction elicited in HEK293 cells expressing in the STREX (black) variant (where STREX is 100%). Data was determined at the maximum hyperpolarising response in the wild-type STRE channel (t=70s) in the time course plots in (A). All data are Means ± S.E.M (N=3, n>24), *** p<0.001, compared to STREX (ANOVA with Tukey post hoc test).

representative trace illustrating the raw data of the STREX channel, the S0-S1 mutant channel (STREX C53A:C54A:C56A) and un-transfected HEK293 response to ionomycin is shown in (Figure 5.11A).

The mutated STREX C53A:C54A:C56A channel hyperpolarising response to ionomycin was significantly attenuated to 73.0 ± 4.6 % of wild-type STREX (n= >21) (Figure 5.11B). Therefore mutation of the S0-S1 linker palmitoylation motif in STREX is functionally significant and has a similar effect as observed in the ZERO channel in reducing the apparent channel response to increased intracellular calcium.

5.2.10 Palmitoylation of the S0-S1 linker controls cell surface expression of STREX channels

Therefore to determine whether the S0-S1 linker palmitoylation site also controls cell surface expression of the STREX splice variant of the BK channel, N-terminal Flag-tag and C-terminal –HA tag constructs were created for both wild type STREX and the S0-S1 linker palmitoylation deficient STREX C53A:C54A:C56A channel, to examine plasma membrane expression in HEK293 cells (Figure 5.12) as previously described.

Representative confocal images show the wild type STREX channel (top panels) of cell surface expression of Flag- tagged channel protein in RED (cell surface), the permeabilised cells subsequently labelled for -HA in GREEN (permeabilised) and Flag- and –HA labelling from the same cell are then shown in overlaid images (merge) (Figure 5.12A). The S0-S1 linker palmitoylation deficient channel, STREX C53A:C54A:C56A, (bottom panel) shows significantly reduced cell surface expression of Flag- tagged channel protein in RED in this field of view (cell surface), but permeabilised cells subsequently labelled for -HA in GREEN illustrate normal expression of channel protein (permeabilised). An overlain image shows no evidence of surface expression (merge) (Figure 5.12A).

Flag-STREX-HA channels showed robust Flag- tag expression at the cell surface in 80% of permeabilised transfected cells. With the STREX channel expression at the

Figure 5.12
The S0-S1 palmitoylation motif also controls cell surface expression of STREX channels

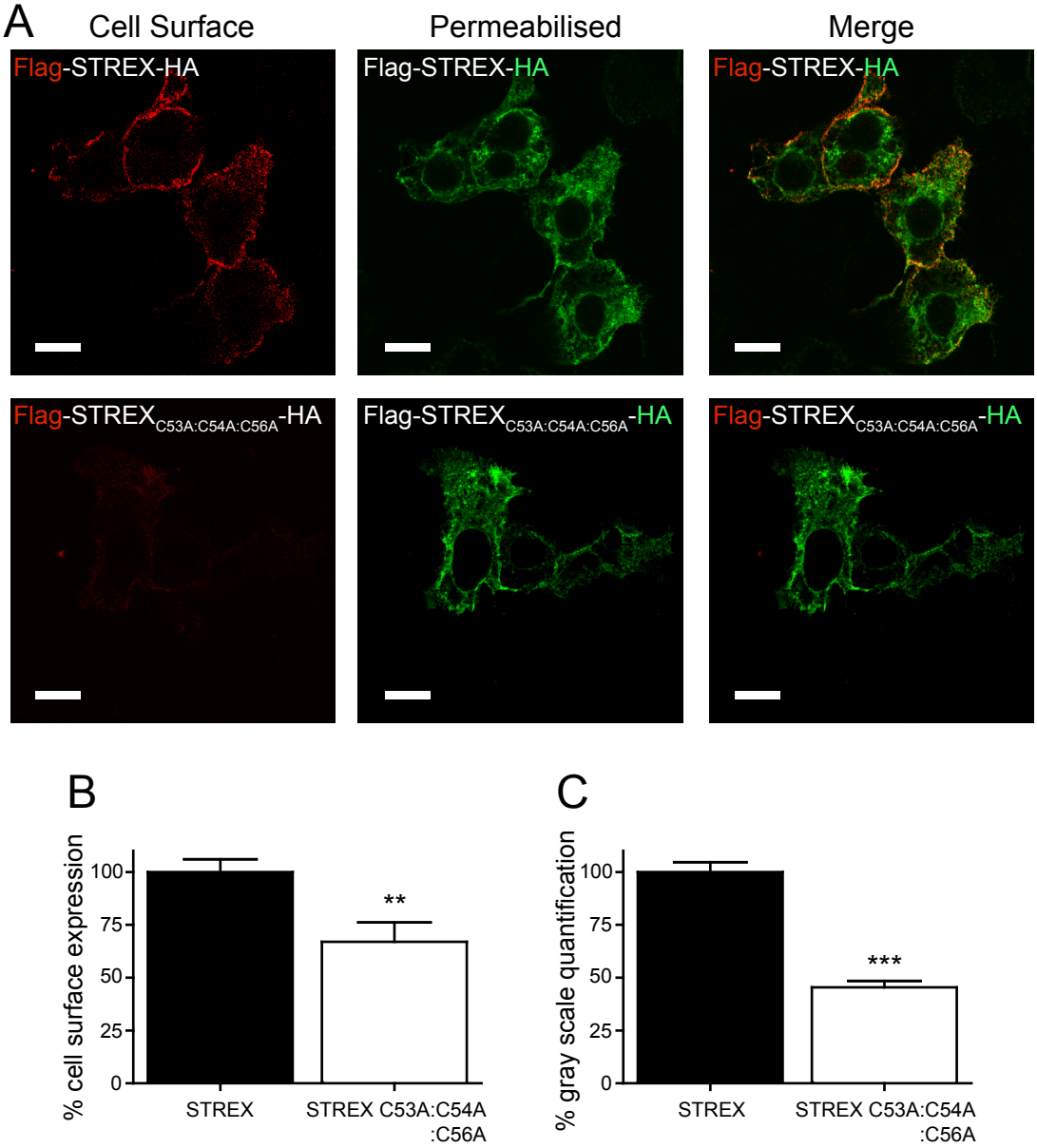

Figure 5.12. The S0-S1 palmitoylation motif also controls cell surface expression of STREX channels. (A) Representative confocal images of HEK293 cells expressing Flag-STREX-HA (top panels), and Flag- STREX C53A:C54A:C56A -HA (bottom panels). The extracellular Flag-epitope was labelled (red) under non-permeabilised conditions (cell surface) with the C-terminal –HA epitope tag (green) labelled following cell permeabilisation. Flag- and –HA labelling from the same cell are then overlaid (merge). Scale bars are 10 µm. (B) Percentage of cells expressing channel constructs at the plasma membrane as a percentage of STREX normailsed to 100%. (C) Quantification of greyscale fluorescence for channels at the plasma membrane as a percentage of STREX normalised to 100%. Data are Means ± S.E.M (n >3). *** $p < 0.01$, ANOVA with post hoc Tukey test compared to STREX.

plasma membrane normalised to 100%, the S0-S1 linker palmitoylation deficient STREX C53A:C54A:C56A channel showed a reduced Flag- tag expression to ~67% of total transfected cells at the cell surface, identified by cell counting at a set level of microscope intensity (see methods 2.4.6) (Figure 5.12B). By using quantitative immunofluorescent analysis of N-terminal Flag- tagged STREX C53A:C54A:C56A mutant channels showed a greater decrease in cell surface expression to ~45% was seen in relation to the wild-type STREX channel (see methods 2.4.6) (Figure 5.12C). Therefore, mutation of the S0-S1 palmitoylation site in STREX channels that contain an intact palmitoylation site in the C-terminus also decreases cell surface expression. This data suggests that the S0-S1 linker palmitoylation site acts independently of the C645:C646 palmitoylation site in STREX to control cell surface expression of the STREX splice variant of the BK channel.

Together this data presents a novel mechanism whereby a palmitoylation motif located in the S0-S1 linker can regulate cell surface expression of all BK channels.

5.3 Discussion

Here, a palmitoylation site has been identified that is present in all functionally expressed BK channels, located in the N-terminal intracellular S0-S1 linker. Palmitoylation at this site plays a critical role in the control of cell surface expression of BK channels. Aspects of this work have been published in the Journal of Biological Chemistry (see appendix #4; (Jeffries *et al.*, 2010a)).

5.3.1 BK channels are palmitoylated in the S0-S1 linker

Using a palmitoylation prediction algorithm to examine the entire BK channel sequence, a series of cysteine residues in the S0-S1 linker were identified as a potential palmitoylation site. The identified three cysteine residues (C53:C54:C56) were found to be conserved across vertebrates and largely conserved in *Drosophila* and *C.Elegans*, suggesting evolutionary retention of a functionally important region. Mutation of the three cysteine residues (C53A:C54A:C56A) completely abolished radiolabelled ^{3}H-palmitate incorporation into full length channels, therefore identifying this site as a single palmitoylation site in the ZERO variant of the BK channel. Palmitoylation of the S0-S1 linker was found to target the linker region to the plasma membrane, with mutation of all three cysteine residues decreasing membrane targeting to ~13% of the control S0-S1 linker. Incubation with a palmitoylation inhibitor 2BP also decreased membrane targeting to a similar degree to ~21% of the control S0-S1 linker. These short constructs were largely located in the cytoplasm when not tethered to the plasma membrane as would be predicted for an intracellular linker. This demonstrates that the S0-S1 linker is palmitoylated and can target to the plasma membrane.

5.3.2 Palmitoylation at the S0-S1 linker controls cells surface expression but not channel activity

To examine the functional significance of de-palmitoylated BK channels, channels with mutations in the S0-S1 linker palmitoylation site were examined by a membrane potential assay that can discriminate differences in channel properties or a change

in the expression of functional channels at the cell surface. Mutation of the triple (C53A:C54A:C56A) cysteine residues within the identified palmitoylation site significantly attenuated channel activation driven by ionomycin in mutant channels by ~60% when compared to the wild-type ZERO channel. Mutations in single or double residues did not have any significant effect. This apparent reduction in activation by ionomycin was not mediated by changes in single channel conductance, voltage dependence of the channel nor was it due to changes in calcium sensitivity. However, during electrophysiological patch clamp analysis decreased numbers of the palmitoylation deficient channels were noted in the membrane patches examined. As the membrane potential assay cannot discriminate between shifts in the calcium/voltage sensitivity of the channel; altered channel conductance, nor changes in expression of functional channels at the plasma membrane, the cell surface expression of the mutant channels were examined.

Mutation of the S0-S1 linker palmitoylation site significantly reduced cell surface expression to ~45% of wild-type ZERO channels using quantitative immunofluorescence despite total protein expression being unaffected. To investigate whether palmitoylation of the S0-S1 linker controls cell surface expression of channels that are also palmitoylated at the distinct C-terminal alternatively spliced STREX insert, STREX channels were examined with mutations in the S0-S1 linker. A similar decrease in cell surface expression of STREX channels with mutations in the S0-S1 linker palmitoylation site to ~45% of wild-type STREX channels when expressed as 100% using quantitative immunoflourescence. Therefore palmitoylation of the S0-S1 linker appears to be distinct and can function independently as a modulator of cell surface expression even if additional palmitoylation sites are expressed in splice variants of the BK channel.

5.3.3 The importance of palmitoylation at the S0-S1 linker

As protein palmitoylation is a highly dynamic and reversible process palmitoylation would have the ability to regulate surface expression and therefore cellular excitability on a fast timescale. In proteomic screens, BK channels have been identified as being palmitoylated in the adult rat brain (Kang *et al.*, 2008), a tissue in

which the major channel variant is the ZERO channel with STREX channels expressed at relatively low levels (MacDonald *et al.*, 2006). Therefore palmitoylation of the S0-S1 linker in the ZERO channel variant may be an important determinant of cell surface expression in neurons as a mechanism to regulate cellular excitability. Regulation of cell surface expression of BK channels has been shown to be modified in ageing coronary arteries (Marijic *et al.*, 2001), in smooth muscle cells of the uterus during pregnancy (Song *et al.*, 1999), colonic epithelia in response to aldosterone (Sorensen *et al.*, 2008) and during malignant glioma tumor cell proliferation (Weaver *et al.*, 2004). While multiple mechanisms may control steady state surface expression, palmitoylation may be an important additional mechanism for regulation of BK channel expression at the plasma membrane, in the control of a wide range of physiological functions.

5.3.4 How might palmitoylation of the S0-S1 linker control cell surface expression?

How palmitoylation may interplay with other trafficking signals, including those that we have recently identified in the RCK1-RCK2 linker of the BK channel (see appendix #2; (Chen *et al.*, 2010)) is currently unknown, however palmitoylation of the S0-S1 linker could modulate cell surface expression of the BK channel by dynamic regulation of any of the multiple processes involved in the trafficking pathway to the plasma membrane. Palmitoylation may play a role in (i) facilitating export from the ER (ii) stabilisation at the plasma membrane (iii) decreased retrieval from the plasma membrane effectively increasing membrane expression or (iv) may control recycling of channels.

The S0-S1 linker region has been shown previously to be important for controlling cell surface expression. A human splice variant of the BK channel which inserts a 44 amino acid sequence in the S0-S1 intracellular linker just downstream of the C53:C54:C56 palmitoylation site (mk44), introduces a motif for endoproteolytic digestion and a site for N-myristoylation site that results in trapping of the channel in the ER (Korovkina *et al.*, 2001). Endoproteolytic cleavage of this site allows the S0 transmembrane domain to traffic independently of the rest of the channel. Whilst another splice variant in the human BK channel within the S0-S1 linker called SV1,

has also been implicated in ER retention. The SV1 splice variant introduces 33 amino acids to the end of the S0-S1 linker that includes an ER retention-retrieval motif, CVLF (Zarei *et al.*, 2004).

Indeed the S0 region is also important for regulation by β-subunits (Wallner *et al.*, 1996; Meera *et al.*, 1997; Lippiat *et al.*, 2003; Liu *et al.*, 2008; Wu *et al.*, 2009; Liu *et al.*, 2010). Recent structural studies examining intra-α subunit di-sulfide cross-linking has demonstrated that the S0 transmembrane domain is located outside of the voltage sensing S1-S4 domains (Liu *et al.*, 2010) and can form a major contact with the transmembrane domain 2 (TM2) of regulatory β1 (Liu *et al.*, 2010) and β4 (Wu *et al.*, 2009) subunits. Co-expression studies suggest a role for β-subunits in controlling BK channel cell surface expression and β1- and β2- subunits have been shown to regulate cell surface expression (Toro *et al.*, 2006; Zarei *et al.*, 2007). Therefore, increasing evidence supports an important role for the S0-S1 region in the control of BK channel cell surface expression.

5.3.5 The local environment is important for palmitoylation

As previously mentioned there is no consensus sequence for a potential palmitoylated cysteine motif, however, what is becoming more and more apparent is that the local environment surrounding a palmitoylated cysteine residue is important. Palmitoylated residues have been described to be located close to (i) regions of basic charge, as described for the STREX palmitoylation site (see chapter 4) and evident in some Ras proteins and G-proteins (Heo *et al.*, 2006; Crouthamel *et al.*, 2008) (ii) additional lipid modifications such as myristic acid or prenyl groups as seen in Src family kinases and Gα subunits (Bijlmakers & Marsh, 2003; Dietrich & Ungermann, 2004) and (iii) located near to transmembrane domains where they are able to interact with the plasma membrane (Bijlmakers & Marsh, 2003; Dietrich & Ungermann, 2004) as is the case with the S0-S1 linker palmitoylation site.

Indeed the S0-S1 palm site does not appear to have additional lipid modifications nearby although it does require palmitoylation of 3 cysteine residues to create a functional motif. Whilst the S0-S1 linker also does not have any nearby polybasic regions it is situated within 10 amino acids of the S0 transmembrane domain and therefore close to a membrane targeting sequence fulfilling the theory that the

palmitoylated site must be able to interact with the plasma membrane through additional signals or sequences nearby. Whether the local environment is crucial for (i) the ability of target cysteines to be palmitoylated, (ii) in locating the region to the plasma membrane which is rich in palmitoylating enzymes or (iii) to mediate stability of palmitoylated cysteines once associated with the membrane, is unknown.

In the STREX domain, PKA phosphorylation of a serine close to the site of palmitoylation was shown to regulate membrane interaction of the C-terminus (see sections 3.2.1.1 & 4.2.1.1). However, PKA phosphorylation of a downstream tandem serine motif in the S0-S1 linker, shown to be phosphorylated in vivo (Yan *et al.*, 2008), by using phosphomimetic or phosphonull mutations had no effect on S0-S1 linker interaction with the plasma membrane suggesting that not all palmitoylated regions can be controlled in the same way.

5.3.6 The role of distinct palmitoylation sites in proteins

Together the data illustrates that the BK channel may express two functionally distinct palmitoylation-dependant membrane interaction domains: the C-terminal alternatively spliced STREX insert and the constitutively expressed site in the S0-S1 linker. Palmitoylation at two independent sites has been described in other proteins that can mediate two completely unrelated mechanistic controls in the target protein. AMPA ligand-gated cation channels are palmitoylated at two distinct sites, one controlled by a Golgi specific PAT (Keller *et al.*, 2004) which promotes accumulation in the Golgi and decreased cell surface expression (Hayashi *et al.*, 2005) and a second that appears to be involved in activity dependant internalisation from the plasma membrane (Hayashi *et al.*, 2005). The distinct functional effects of palmitoylation at the STREX site in influencing channel properties and in the S0-S1 linker in controlling cell surface expression, suggest that palmitoylation at these sites may be independently regulated.

5.3.7 Challenges for the future

Challenges for the future will be to examine (i) Are there extrinsic factors that regulate palmitoylation (ii) over what timescale does palmitate turnover occur (iii) the role of palmitoylation in trafficking to or from the plasma membrane (iv) regulation of palmitoylation within the cell.

5.3.7.1 Are there extrinsic factors that regulate palmitoylation?

One of the major questions to be addressed in the future is how is palmitoylation regulated? It has been suggested that extrinsic factors can regulate palmitoylation. Glutamate treatment has been shown to regulate de-palmitoylation of the AMPA receptor in neurons (Hayashi *et al.*, 2009) and palmitate cycling in the PSD-95 protein is increased by calcium influx through NMDA receptors (El-Husseini Ael *et al.*, 2002). Therefore, whether there may be other physiological mechanisms that can regulate the palmitoylation status, particularly in the BK channel in control of cell surface expression which would be crucial for regulation of cellular excitability, remains unknown.

5.3.7.2 On what timescale does palmitate turnover occur?

The timescale during which a protein can remain palmitoylated at the plasma membrane is variable. In the BK channel the length of time the channel could be palmitoylated could influence long term expression at the plasma membrane (as discussed in this chapter) or functional regulation by calcium and/or phosphorylation (see chapter 3) as previously described. Studies in other proteins to determine the half-life of palmitate in Ras proteins report 20 minutes for N-Ras (Magee *et al.*, 1987) and 2 hours for H-Ras (Lu & Hofmann, 1995; Baker *et al.*, 2003) suggesting a fast turnover rate that may regulate cycles of palmitoylation therefore maintaining subcellular distribution of the protein for further specific trafficking to plasma membrane. This reversible nature of palmitoylation allows proteins to shuttle between the plasma membrane and intracellular compartments or relocalise when required in the cell. However, there is also evidence of many proteins such as SNAP25 that do appear to be stably palmitoylated (Kang *et al.*, 2004). Whether the

palmitoylation status of the BK channel at the two independent sites is cyclic or stable is again unknown.

5.3.7.3 The palmitoylation membrane trafficking pathway - from Golgi to membrane and back?

It remains to be elucidated at which step in the trafficking pathway the S0-S1 linker within the BK channel is palmitoylated. The role of the enzymes (DHHC's) that control palmitoylation of ion channels is not well known. They can be promiscuous in their ability to palmitoylate target proteins. For example, DHHC-3 is localised in Golgi (Keller *et al.*, 2004), DHHC-17 has been identified in several vesicular structures including sorting/recycling and endosomal structures (Huang *et al.*, 2004) and DHHC-5 -20 and -21 are found at the plasma membrane (Ohno *et al.*, 2006), although generally their localisation is poorly understood (see appendix # 3; (Tian *et al.*, 2010)). The four potential S0-S1 palmitoylation sites that would be present in the tetrameric channel could be palmitoylated or de-palmitoylated at any stage promoting trafficking, stabilisation or recycling at the plasma membrane. Indeed palmitoylation could be responsible for specific targeting or localisation to microdomains, such as lipid rafts, within the plasma membrane and therefore mediating the functional characteristics of specific domains within the cell. In trafficking between intracellular compartments, palmitoylation has been shown to be important for regulating ER export of yeast chitin synthase (Chs3) (Lam *et al.*, 2006) whilst inhibition of protein palmitoylation has been shown to prevent efficient transport of the opioid receptor to the plasma membrane (Petaja-Repo *et al.*, 2006).

Therefore, it is plausible to envisage a highly regulated process of palmitoylation and de-palmitoylation through a series of docking sites from Golgi or ER, via transport proteins or secretory vesicles, to the membrane. The role of palmitoylation in membrane targeting is well described and therefore, events of palmitoylation could target the proteins to the membrane of transport structures, with de-palmitoylation releasing it to traffick onwards to the next transport structure towards the plasma membrane. Hence de-palmitoylated channels may become stunted in the intracellular machinery leading to decreased cell surface expression as seen with the S0-S1 mutant palmitoylation deficient BK channel (Figure 5.13). In the small

Figure 5.13
The BK channel palmitoylation membrane trafficking pathway - from Golgi to membrane and back?

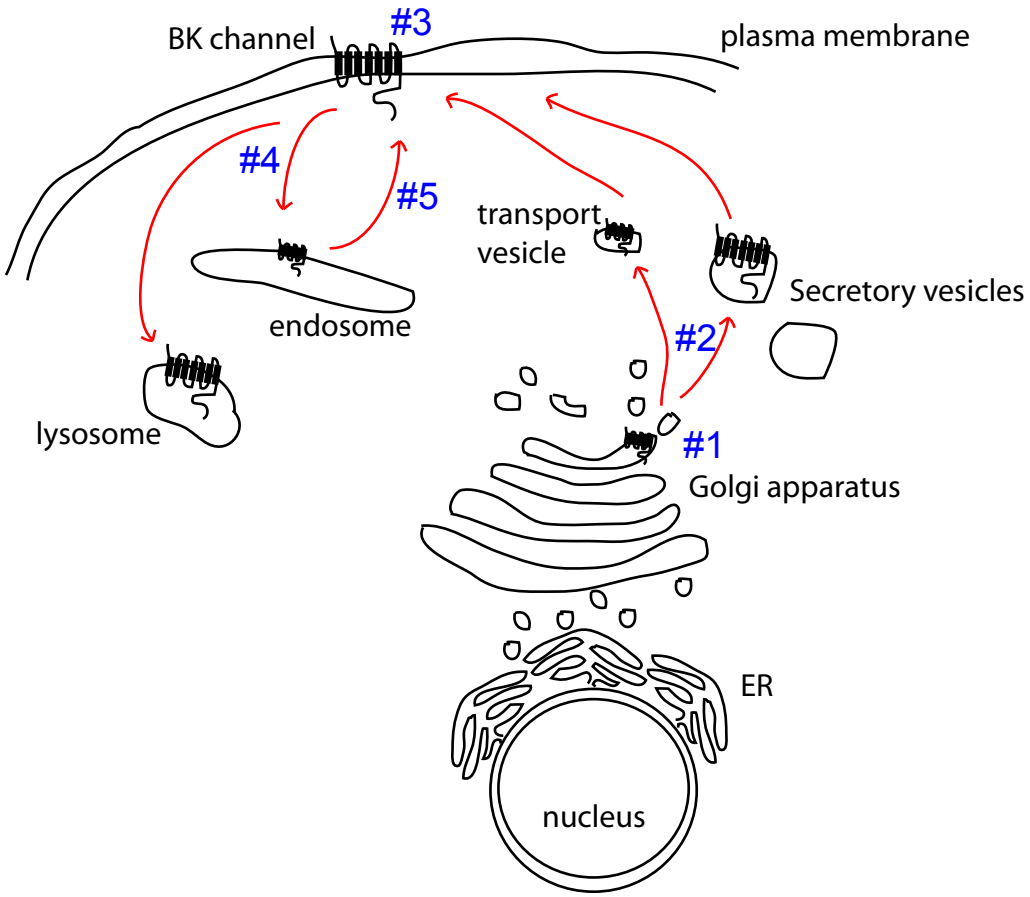

Figure 5.13. The palmitoylation membrane trafficking pathway - from Golgi to membrane and back? Model of a cell showing the functional machinery responsible for building of the protein channel, trafficking to the plasma membrane and recycling of channels off the channel membrane. Several proposed sites where palmitoylation could occur are marked with numbers and indicate sites as follows: #1 Palmitoylation at Golgi could target BK to plasma membrane, #2 or de-palmitoylation may release BK from Golgi membrane were it is re-palmitoylated in transport vesicle, #3 Palmitoylation could stabilise BK at plasma membrane, #4 De-palmitoylation could allow internalised recycling of BK off the membrane, #5 Palmitoylation targets BK back to membrane from endosome completing cycle.

S0-S1 linker-YFP protein fragments, inhibition of palmitoylation by 2-BP or site directed mutagenesis confined the S0-S1 linker to structures reminiscent of Golgi or ER (Figure 5.3B), suggesting that maybe these small proteins never left the Golgi apparatus. However, the location of the small S0-S1 linker proteins would probably not reflect trafficking of the full length channel. Additionally, palmitoylation could also play a role in stability of the channel at the plasma membrane with de-palmitoylation releasing the channel to be internalised to a storage structure such as an endosome ready for speedy trafficking to the plasma membrane when required or even targeting for degradation to a lysosome. De-palmitoylated BK channels could therefore be internalised faster, decreasing the number of channels on the cell surface. These questions remain to be addressed in future studies.

5.3.8 In summary

This data reveals that the S0-S1 linker contains a constitutively expressed palmitoylation site that regulates cell surface expression of BK channels independently of additional sites that may be expressed within the channel.

CHAPTER SIX

GENERAL DISCUSSION

6.1 General discussion

6.1.1 Aims of the thesis

In this thesis the primary aims were to identify (i) whether the cysteine rich STREX insert functions as a membrane targeting domain through palmitoylation of key cysteine residues (ii) whether a series of basic residues introduced upon splicing of the STREX insert can control the ability of palmitoylation to anchor STREX at the plasma membrane and (iii) whether there are additional palmitoylation sites in the BK channel that may be functionally distinct from the STREX palmitoylation site.

6.1.2 STREX is a membrane targeting domain controlled by palmitoylation

The STREX domain functions as a membrane targeting domain controlled by palmitoylation. Disruption of a key palmitoylation site in the STREX domain shifts the increased calcium-sensitivity of the STREX channel back towards the less calcium-sensitive ZERO (insertless) channel phenotype. Palmitoylation of STREX is regulated by a polybasic domain which in turn is controlled by PKA-mediated phosphorylation, acting as an electrostatic switch.

These findings that membrane targeting of STREX could mediate increased calcium-sensitivity in BK channels suggest that the channel phenotype could be regulated dynamically by control of the polybasic domain through phosphorylation which would influence the palmitoylation status and thereby the membrane targeting properties of the STREX domain. This has implications on cellular excitability. The STREX channel can respond more quickly than the ZERO channel to elevations in local levels of calcium. This increased sensitivity could then be switched off in order that the channel adopts a less sensitive phenotype when required, by disrupting the stability of the membrane association via palmitoylation of the STREX domain. Whether there may be other mechanisms to regulate the palmitoylation status of STREX and therefore mediating the properties of the channel is unknown.

6.1.2.1 Is palmitoylation the key to mediating the increased calcium sensitivity of STREX channels?

Palmitoylation of the STREX splice variant of the BK channel was abolished by mutation of a dual cysteine site in the STREX domain. Mutation of this palmitoylation site shifted channel activity to more depolarised potentials towards the activation range for the insertless ZERO channel variant. Whilst imaging assays revealed that membrane association was diminished in the de-palmitoylated STREX C-terminal constructs. Together this data argues that membrane targeting of the STREX domain to the plasma membrane confers increased calcium sensitivity to the STREX channel.

How does membrane targeting of STREX mediate these properties? Membrane targeting of the RCK1-RCK2 linker via the STREX insert may induce a conformational or structural rearrangement which increases the calcium sensitivity of the gating apparatus in the BK channel. An increased channel activity could be mediated by (a) increased tension on the channel pore facilitating channel opening or (b) by increasing accessibility of calcium at the calcium binding sites within the C-terminal domain. It is possible that a conformational change may involve altering the dynamics at the assembly interface between the two RCK domains, particularly considering recent crystal structural analysis that has shown the calcium bowl to be located at the assembly interface (Wang & Sigworth, 2009; Wu *et al.*, 2010; Yuan *et al.*, 2010). A structural rearrangement of the assembly interface induced by membrane targeting of STREX could facilitate increased calcium accessibility to the calcium bowl therefore increasing the apparent calcium sensitivity of the channel. Indeed studies that have looked at the length of the RCK1-RCK2 linker have suggested that this region may indeed be important for mediating the dynamics of the RCK interface (Lee *et al.*, 2009a). By dissociating the STREX membrane targeting domain from the plasma membrane, the structural conformation presumably would be lost, whether it be tension on the pore or accessibility of calcium to modulate the gating domain, and the channel would resume a ZERO-like conformation (see Figure 6.1).

Structural analysis would be required to examine this hypothesis. Future studies could examine the crystal structure of the C-terminus of the ZERO and STREX channel in the presence of calcium, to identify whether the structural conformation of

Figure 6.1. Working model of palmitoylation of BK channels

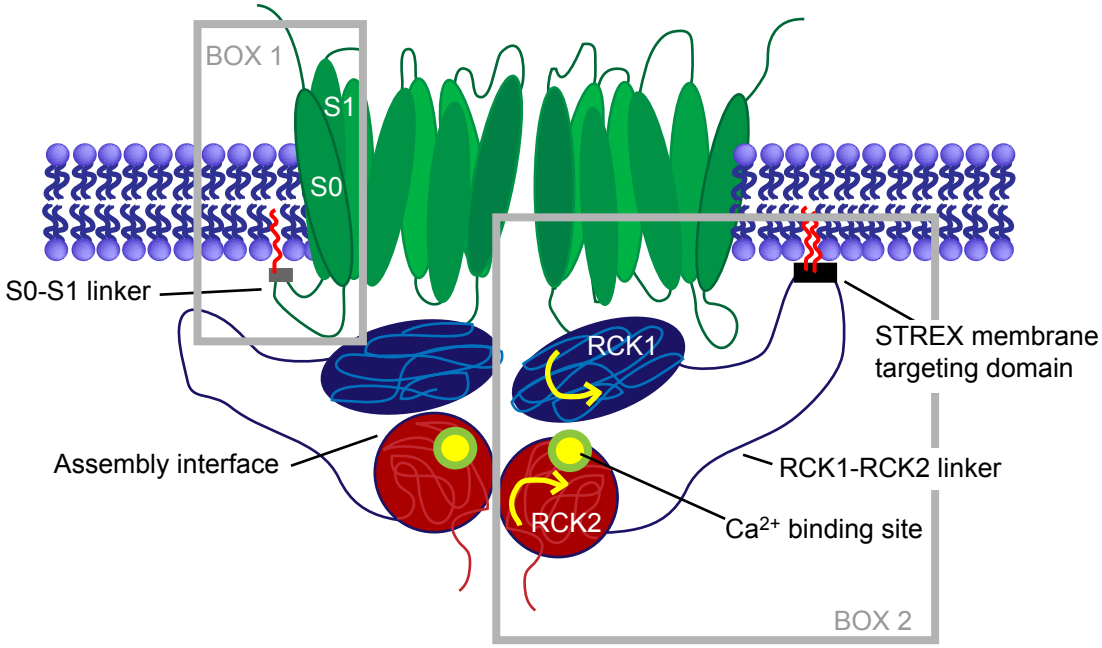

Figure 6.1. Working model of palmitoylation of BK channels. Globular model (2 subunit domains shown) based on the crystal structural studies from Yuan et al., 2010 and Wu et al., 2010. (BOX 1) The constitutively expressed S0-S1 linker palmitoylation site can interact with the plasma membrane controlling cell surface expression of BK channels. (BOX 2) Palmitoylation of the STREX membrane targeting domain may induce a structural change in the RCK1-RCK2 interface making the high affinity calcium binding site more accessible increasing the channel sensitivity to calcium. Destabilisation of the STREX membrane targeting domain releases the RCK gating domain to return to its normal conformation (see left side of diagram) resulting in decreased channel sensitivity to calcium, hence the STREX channel reverts back to the ZERO channel phenotype. (Palmitoylation is shown as a red zigzag line).

the RCK gating domains and the assembly interface or even the position of the calcium binding sites has been altered in the STREX splice variant. Perhaps a more accessible study might be to label the calcium bowl and/or RCK interface with a probe and by using high powered fluorescence-resonance energy transfer (FRET) microscopy (Duncan *et al.*, 2004), quantitatively study conformational changes in the RCK1-RCK2 interface of the STREX C-terminus of the BK channel. Although such studies would have limitations governed by the size of the probes currently available, with developing technology it is not inconceivable that in the future, probes may be made available that will be small enough so they don't affect the structure of the protein being studied.

6.1.2.2 Does phosphorylation within the polybasic domain act as an electrostatic switch controlling membrane targeting of the STREX domain?

Whilst palmitoylation of a cysteine residue cannot be precisely predicted, many palmitoylation sites require either (i) additional lipophilic modifications (ii) a polybasic domain (iii) or to be close to transmembrane domains (Bijlmakers & Marsh, 2003; Dietrich & Ungermann, 2004). The polybasic domain just upstream from the palmitoylation site in STREX was shown to control palmitoylation of STREX influencing membrane association of the C-terminus. Mutations in the polybasic domain suggest that this region may be important to stabilise palmitoylation at this site rather than to specifically target the region to the membrane. Mutation of the basic residues inside STREX to alanine (R640A:R642A), increased palmitoylation. By contrast all negative substitutions decreased palmitoylation, suggesting that perhaps the structure within this region or accessibility of the cysteine motif may be reliant upon a favourable local environment.

PKA-mediated phosphorylation of STREX has been previously shown to inhibit channel activity (Tian *et al.*, 2001; Tian *et al.*, 2004). Interestingly, phosphorylation in STREX was shown to disassociate the STREX C-terminal constructs from the plasma membrane through abolishing palmitoylation of the STREX domain. Phosphorylation of STREX presumably destabilises the association of the STREX C-terminal constructs at the plasma membrane by breaking up the polybasic

domain. Phosphorylation of STREX therefore is a physiological mechanism that functions as an electrostatic switch to control membrane association of STREX by palmitoylation. The PKA-mediated inhibition of STREX channels (Tian *et al.*, 2001; Tian *et al.*, 2004) could therefore represent a shift from a more calcium sensitive phenotype that is inherent in STREX channels, to a less calcium sensitive phenotype, i.e. a ZERO-like phenotype, that is identified as channel inhibition.

Electrophysiological studies examining PKA-regulation of STREX channels in zero calcium would eliminate the calcium sensitive component of the channel and could therefore determine whether PKA-mediated inhibition still occurs in STREX channels not activated by calcium, although low channel activity in zero calcium may make this a difficult experiment to carry out. However, such an experiment would be able to describe whether PKA-mediated inhibition in STREX channels results in a shift from a high to low calcium sensitive phenotype.

Modulation of the STREX membrane targeting domain could therefore be a mechanism for regulating cellular excitability on a fast and dynamic timescale. Alternative splicing of STREX is under hormonal control and will produce a channel with increased sensitivity to calcium; this effectively increases repolarisation and therefore allows faster excitation of cells, if required. However, splicing would take time due to the synthesis and trafficking of new channels to the plasma membrane. A more dynamic control of STREX channel properties would be if palmitoylation of the STREX insert could be hormonally regulated. For example if de-palmitoylation was controlled by extrinsic factors, then the membrane association of the STREX channel could be destabilised leading to a less calcium sensitive ZERO-like channel. Alternatively, and perhaps even more dynamic, intracellular regulation by phosphorylation of the STREX domain could destabilise STREX at plasma membrane which will inhibit or shift channel activity to the less calcium sensitive phenotype, therefore changing cellular excitability on a timescale of seconds-minutes.

Crucially it will be important to determine in the full length STREX channel whether the RCK1-RCK2 linker does interact with the plasma membrane through palmitoylation of the STREX domain under physiological conditions. The structure of the RCK1-RCK2 linker cannot presently be defined due to its predicted unstructured composition; therefore whether STREX, which may generate structure in this region,

would allow crystallisation of this region would be interesting to study. Another important avenue to explore would be the palmitoyl acyl transferases (DHHC's) involved in regulating palmitoylation of STREX and also the palmitoyl protein thioesterases (PPT) involved in de-palmitoylating STREX and where these processes occur in the cell and over what timescale. Additionally, the interaction between phosphorylation and palmitoylation could represent a general phenomenon present in other ion channels or proteins as a mechanism to regulate the effects of protein lipidation. Many of the techniques used in this study could be applied to potential palmitoylation sites in other ion channels that have yet to be explored.

6.1.3 Palmitoylation in the S0-S1 linker of the BK channel regulates cell surface expression

Through screening and mutagenesis studies an additional palmitoylation site was identified, located in the S0-S1 linker. Palmitoylation at the S0-S1 linker was shown to regulate cell surface expression, without affecting the calcium- or voltage- sensing properties of the channel.

6.1.3.1 How does palmitoylation of the S0-S1 linker regulate cell surface expression?

The S0-S1 palmitoylation site differs from the STREX palmitoylation site in that it does not have an adjacent polybasic domain nor does disruption of a nearby phosphorylation site disrupt palmitoylation at this site. The S0-S1 site is in the vicinity of a transmembrane domain and therefore located close to the plasma membrane, whereby palmitoylation can occur (see Figure 6.1).

How palmitoylation may interplay with other trafficking motifs located within the BK channel is unknown. The processes, both intrinsic and extrinsic, that regulate palmitoylation will need to studied to understand how palmitoylation and de-palmitoylation may regulate cell surface expression of BK channels. It would be interesting to study the mechanism of how surface expression is modulated by palmitoylation. Live cell imaging of fluorescently labelled channels at the cell surface

under conditions were they would be expected to be palmitoylated compared to subsequent application of a palmitoylation inhibitor, may reveal where in the trafficking pathway is palmitoylation of BK channels most important. Does palmitoylation regulate forward trafficking meaning that de-palmitoylated channels find it difficult to reach the plasma membrane or does it regulate surface stability whereby de-palmitoylation prompts faster internalisation? Little is known about the mechanisms involved in BK channel delivery and retrieval from the plasma membrane and the role of palmitoylation may play in these processes remains to be discovered.

The regulation of BK channels on the cell membrane is crucial to defining the excitability of a cell. Palmitoylation may be an important mechanism whereby a cell can dynamically control cell surface expression of BK channels and therefore regulate cellular processes.

6.1.3.2 Two distinct palmitoylation sites with different functional properties

One of the key findings of this work is that two palmitoylation sites in one protein can be independently regulated to control two distinct functions within the channel protein (Figure 6.1). These findings will be interesting for the study of other proteins that may also be palmitoylated at multiple sites. Further studies examining specifically the palmitoylating enzymes responsible for cycles of palmitoylation and de-palmitoylation will also be important to identify location of these palmitoylation sites in the cell and how they may control the various channel functions and cellular physiology.

6.1.4 Final overview

This is the first evidence for palmitoylation of the BK channel. Palmitoylation of the BK channel has been shown to occur at two distinct sites, one in STREX and one in the constitutively expressed S0-S1 linker, which are functionally diverse but operate in both cases via anchoring of intracellular domains to the plasma membrane.

REFERENCES

References

Adelman JP, Shen KZ, Kavanaugh MP, Warren RA, Wu YN, Lagrutta A, Bond CT & North RA. (1992). Calcium-activated potassium channels expressed from cloned complementary DNAs. *Neuron* **9,** 209-216.

Ahluwalia J, Tinker A, Clapp LH, Duchen MR, Abramov AY, Pope S, Nobles M & Segal AW. (2004). The large-conductance Ca^{2+}-activated K^+ channel is essential for innate immunity. *Nature* **427,** 853-858.

Ainavarapu SR, Brujic J, Huang HH, Wiita AP, Lu H, Li L, Walther KA, Carrion-Vazquez M, Li H & Fernandez JM. (2007). Contour length and refolding rate of a small protein controlled by engineered disulfide bonds. *Biophys J* **92,** 225-233.

Armstrong CM & Bezanilla F. (1974). Charge movement associated with the opening and closing of the activation gates of the Na channels. *J Gen Physiol* **63,** 533-552.

Atkinson NS, Robertson GA & Ganetzky B. (1991). A component of calcium-activated potassium channels encoded by the Drosophila slo locus. *Science* **253,** 551-555.

Baker TL, Zheng H, Walker J, Coloff JL & Buss JE. (2003). Distinct rates of palmitate turnover on membrane-bound cellular and oncogenic H-ras. *J Biol Chem* **278,** 19292-19300.

Bao L, Kaldany C, Holmstrand EC & Cox DH. (2004). Mapping the BK_{Ca} channel's "Ca^{2+} bowl": side-chains essential for Ca^{2+} sensing. *J Gen Physiol* **123,** 475-489.

Bao L, Rapin AM, Holmstrand EC & Cox DH. (2002). Elimination of the BK(Ca) channel's high-affinity Ca(2+) sensitivity. *J Gen Physiol* **120,** 173-189.

Bartels DJ, Mitchell DA, Dong X & Deschenes RJ. (1999). Erf2, a novel gene product that affects the localization and palmitoylation of Ras2 in Saccharomyces cerevisiae. *Mol Cell Biol* **19,** 6775-6787.

Beisel KW, Rocha-Sanchez SM, Ziegenbein SJ, Morris KA, Kai C, Kawai J, Carninci P, Hayashizaki Y & Davis RL. (2007). Diversity of Ca^{2+}-activated K^+ channel transcripts in inner ear hair cells. *Gene* **386,** 11-23.

Ben-Tal N, Honig B, Peitzsch RM, Denisov G & McLaughlin S. (1996). Binding of small basic peptides to membranes containing acidic lipids: theoretical models and experimental results. *Biophys J* **71,** 561-575.

Bentrop D, Beyermann M, Wissmann R & Fakler B. (2001). NMR structure of the "ball-and-chain" domain of KCNMB2, the beta 2-subunit of large

conductance Ca^{2+}- and voltage-activated potassium channels. *J Biol Chem* **276,** 42116-42121.

Benzer S. (1967). Behavioral mutants of *Drosophila* isolated by countercurrent distribution. *Proc Natl Acad Sci U S A* **58,** 1112-1119.

Benzer S. (1971). From the gene to behavior. *Jama* **218,** 1015-1022.

Bezanilla F. (2008a). How membrane proteins sense voltage. *Nat Rev Mol Cell Biol* **9,** 323-332.

Bezanilla F. (2008b). Ion channels: from conductance to structure. *Neuron* **60,** 456-468.

Bhattacharjee A, Gan L & Kaczmarek LK. (2002). Localization of the Slack potassium channel in the rat central nervous system. *J Comp Neurol* **454,** 241-254.

Bian S, Favre I & Moczydlowski E. (2001). Ca^{2+}-binding activity of a COOH-terminal fragment of the Drosophila BK channel involved in Ca2+-dependent activation. *Proc Natl Acad Sci U S A* **98,** 4776-4781.

Bielefeldt K, Rotter JL & Jackson MB. (1992). Three potassium channels in rat posterior pituitary nerve terminals. *J Physiol* **458,** 41-67.

Biggin PC, Roosild T & Choe S. (2000). Potassium channel structure: domain by domain. *Curr Opin Struct Biol* **10,** 456-461.

Bijlmakers MJ & Marsh M. (2003). The on-off story of protein palmitoylation. *Trends Cell Biol* **13,** 32-42.

Bivona TG, Quatela SE, Bodemann BO, Ahearn IM, Soskis MJ, Mor A, Miura J, Wiener HH, Wright L, Saba SG, Yim D, Fein A, Perez de Castro I, Li C, Thompson CB, Cox AD & Philips MR. (2006). PKC regulates a farnesyl-electrostatic switch on K-Ras that promotes its association with Bcl-XL on mitochondria and induces apoptosis. *Mol Cell* **21,** 481-493.

Black DL. (2000). Protein diversity from alternative splicing: a challenge for bioinformatics and post-genome biology. *Cell* **103,** 367-370.

Blatz AL & Magleby KL. (1986). Single apamin-blocked Ca-activated K^+ channels of small conductance in cultured rat skeletal muscle. *Nature* **323,** 718-720.

Bloch M, Ousingsawat J, Simon R, Schraml P, Gasser TC, Mihatsch MJ, Kunzelmann K & Bubendorf L. (2007). KCNMA1 gene amplification promotes tumor cell proliferation in human prostate cancer. *Oncogene* **26,** 2525-2534.

Brelidze TI & Magleby KL. (2005). Probing the geometry of the inner vestibule of BK channels with sugars. *J Gen Physiol* **126,** 105-121.

Brelidze TI, Niu X & Magleby KL. (2003). A ring of eight conserved negatively charged amino acids doubles the conductance of BK channels and prevents inward rectification. *Proc Natl Acad Sci U S A* **100,** 9017-9022.

Brenner R, Chen QH, Vilaythong A, Toney GM, Noebels JL & Aldrich RW. (2005). BK channel beta4 subunit reduces dentate gyrus excitability and protects against temporal lobe seizures. *Nat Neurosci* **8,** 1752-1759.

Brenner R, Jegla TJ, Wickenden A, Liu Y & Aldrich RW. (2000a). Cloning and functional characterization of novel large conductance calcium-activated potassium channel beta subunits, hKCNMB3 and hKCNMB4. *J Biol Chem* **275,** 6453-6461.

Brenner R, Perez GJ, Bonev AD, Eckman DM, Kosek JC, Wiler SW, Patterson AJ, Nelson MT & Aldrich RW. (2000b). Vasoregulation by the beta1 subunit of the calcium-activated potassium channel. *Nature* **407,** 870-876.

Brzeska H, Guag J, Remmert K, Chacko S & Korn ED. (2010). An experimentally based computer search identifies unstructured membrane-binding sites in proteins: application to class I myosins, PAKS, and CARMIL. *J Biol Chem* **285,** 5738-5747.

Butler A, Tsunoda S, McCobb DP, Wei A & Salkoff L. (1993). mSlo, a complex mouse gene encoding "maxi" calcium-activated potassium channels. *Science* **261,** 221-224.

Candia S, Garcia ML & Latorre R. (1992). Mode of action of iberiotoxin, a potent blocker of the large conductance Ca(2+)-activated K^+ channel. *Biophys J* **63,** 583-590.

Carrion-Vazquez M, Marszalek PE, Oberhauser AF & Fernandez JM. (1999). Atomic force microscopy captures length phenotypes in single proteins. *Proc Natl Acad Sci U S A* **96,** 11288-11292.

Chanda B, Asamoah OK, Blunck R, Roux B & Bezanilla F. (2005). Gating charge displacement in voltage-gated ion channels involves limited transmembrane movement. *Nature* **436,** 852-856.

Chatterjee O, Taylor LA, Ahmed S, Nagaraj S, Hall JJ, Finckbeiner SM, Chan PS, Suda N, King JT, Zeeman ML & McCobb DP. (2009). Social stress alters expression of large conductance calcium-activated potassium channel subunits in mouse adrenal medulla and pituitary glands. *J Neuroendocrinol* **21,** 167-176.

Chen L, Jeffries O, Rowe IC, Liang Z, Knaus HG, Ruth P & Shipston MJ. (2010). Membrane trafficking of large conductance calcium-activated potassium channels is regulated by alternative splicing of a transplantable, acidic trafficking motif in the RCK1-RCK2 linker. *J Biol Chem* **285,** 23265-23275.

Chen L, Tian L, MacDonald SH, McClafferty H, Hammond MS, Huibant JM, Ruth P, Knaus HG & Shipston MJ. (2005). Functionally diverse complement of large

conductance calcium- and voltage-activated potassium channel (BK) alpha-subunits generated from a single site of splicing. *J Biol Chem* **280,** 33599-33609.

Chi S & Qi Z. (2006). Regulatory effect of sulphatides on BK_{Ca} channels. *Br J Pharmacol* **149,** 1031-1038.

Chien AJ, Carr KM, Shirokov RE, Rios E & Hosey MM. (1996). Identification of palmitoylation sites within the L-type calcium channel beta2a subunit and effects on channel function. *J Biol Chem* **271,** 26465-26468.

Chiu YH, Alvarez-Baron C, Kim EY & Dryer SE. (2010). Dominant-negative regulation of cell surface expression by a pentapeptide motif at the extreme COOH terminus of an Slo1 calcium-activated potassium channel splice variant. *Mol Pharmacol* **77,** 497-507.

Christ GJ, Day N, Santizo C, Sato Y, Zhao W, Sclafani T, Bakal R, Salman M, Davies K & Melman A. (2004). Intracorporal injection of hSlo cDNA restores erectile capacity in STZ-diabetic F-344 rats in vivo. *Am J Physiol Heart Circ Physiol* **287,** H1544-1553.

Chung SK, Reinhart PH, Martin BL, Brautigan D & Levitan IB. (1991). Protein kinase activity closely associated with a reconstituted calcium-activated potassium channel. *Science* **253,** 560-562.

Claverie JM. (2001). Gene number. What if there are only 30,000 human genes? *Science* **291,** 1255-1257.

Clayton GM, Altieri S, Heginbotham L, Unger VM & Morais-Cabral JH. (2008). Structure of the transmembrane regions of a bacterial cyclic nucleotide-regulated channel. *Proc Natl Acad Sci U S A* **105,** 1511-1515.

Copley RR. (2004). Evolutionary convergence of alternative splicing in ion channels. *Trends Genet* **20,** 171-176.

Crouthamel M, Thiyagarajan MM, Evanko DS & Wedegaertner PB. (2008). N-terminal polybasic motifs are required for plasma membrane localization of Galpha(s) and Galpha(q). *Cell Signal* **20,** 1900-1910.

Dang CV & Lee WM. (1988). Identification of the human c-myc protein nuclear translocation signal. *Mol Cell Biol* **8,** 4048-4054.

Di Paolo G & De Camilli P. (2006). Phosphoinositides in cell regulation and membrane dynamics. *Nature* **443,** 651-657.

Diaz L, Meera P, Amigo J, Stefani E, Alvarez O, Toro L & Latorre R. (1998). Role of the S4 segment in a voltage-dependent calcium-sensitive potassium (hSlo) channel. *J Biol Chem* **273,** 32430-32436.

Dietrich LE & Ungermann C. (2004). On the mechanism of protein palmitoylation. *EMBO Rep* **5,** 1053-1057.

Dong J, Shi N, Berke I, Chen L & Jiang Y. (2005). Structures of the MthK RCK domain and the effect of Ca^{2+} on gating ring stability. *J Biol Chem* **280,** 41716-41724.

Doyle DA, Morais Cabral J, Pfuetzner RA, Kuo A, Gulbis JM, Cohen SL, Chait BT & MacKinnon R. (1998). The structure of the potassium channel: molecular basis of K^+ conduction and selectivity. *Science* **280,** 69-77.

Du W, Bautista JF, Yang H, Diez-Sampedro A, You SA, Wang L, Kotagal P, Luders HO, Shi J, Cui J, Richerson GB & Wang QK. (2005). Calcium-sensitive potassium channelopathy in human epilepsy and paroxysmal movement disorder. *Nat Genet* **37,** 733-738.

Duncan RR, Bergmann A, Cousin MA, Apps DK & Shipston MJ. (2004). Multi-dimensional time-correlated single photon counting (TCSPC) fluorescence lifetime imaging microscopy (FLIM) to detect FRET in cells. *J Microsc* **215,** 1-12.

Dworetzky SI, Trojnacki JT & Gribkoff VK. (1994). Cloning and expression of a human large-conductance calcium-activated potassium channel. *Brain Res Mol Brain Res* **27,** 189-193.

El-Husseini AE, Craven SE, Chetkovich DM, Firestein BL, Schnell E, Aoki C & Bredt DS. (2000). Dual palmitoylation of PSD-95 mediates its vesiculotubular sorting, postsynaptic targeting, and ion channel clustering. *J Cell Biol* **148,** 159-172.

El-Husseini Ael D, Schnell E, Dakoji S, Sweeney N, Zhou Q, Prange O, Gauthier-Campbell C, Aguilera-Moreno A, Nicoll RA & Bredt DS. (2002). Synaptic strength regulated by palmitate cycling on PSD-95. *Cell* **108,** 849-863.

Elkins T, Ganetzky B & Wu CF. (1986). A Drosophila mutation that eliminates a calcium-dependent potassium current. *Proc Natl Acad Sci U S A* **83,** 8415-8419.

Erxleben C, Everhart A, Florance H, Shipston M, Rossie S & Armstrong DL. (2002a). Full length KCNMA1 channels cannot make heads and tails with STREX. *Biophys J* **82,** 997.

Erxleben C, Everhart AL, Romeo C, Florance H, Bauer MB, Alcorta DA, Rossie S, Shipston MJ & Armstrong DL. (2002b). Interacting effects of N-terminal variation and strex exon splicing on slo potassium channel regulation by calcium, phosphorylation, and oxidation. *J Biol Chem* **277,** 27045-27052.

Evans AM, Hardie DG, Peers C, Wyatt CN, Viollet B, Kumar P, Dallas ML, Ross F, Ikematsu N, Jordan HL, Barr BL, Rafferty JN & Ogunbayo O. (2009). Ion channel regulation by AMPK: the route of hypoxia-response coupling in thecarotid body and pulmonary artery. *Ann N Y Acad Sci* **1177,** 89-100.

Faber ES & Sah P. (2003). Calcium-activated potassium channels: multiple contributions to neuronal function. *Neuroscientist* **9,** 181-194.

Farley J & Rudy B. (1988). Multiple types of voltage-dependent Ca^{2+}-activated K^+ channels of large conductance in rat brain synaptosomal membranes. *Biophys J* **53,** 919-934.

Fernandez-Fernandez JM, Tomas M, Vazquez E, Orio P, Latorre R, Senti M, Marrugat J & Valverde MA. (2004). Gain-of-function mutation in the KCNMB1 potassium channel subunit is associated with low prevalence of diastolic hypertension. *J Clin Invest* **113,** 1032-1039.

Ferrer J, Wasson J, Salkoff L & Permutt MA. (1996). Cloning of human pancreatic islet large conductance Ca(2+)-activated K^+ channel (hSlo) cDNAs: evidence for high levels of expression in pancreatic islets and identification of a flanking genetic marker. *Diabetologia* **39,** 891-898.

Fodor AA & Aldrich RW. (2009). Convergent evolution of alternative splices at domain boundaries of the BK channel. *Annu Rev Physiol* **71,** 19-36.

Folch J & Lees M. (1951). Proteolipides, a new type of tissue lipoproteins; their isolation from brain. *J Biol Chem* **191,** 807-817.

Franciolini F & Petris A. (1989). Evolution of ionic channels of biological membranes. *Mol Biol Evol* **6,** 503-513.

Frank J. (2006). Three-Dimensional Electron Microscopy of Macromolecular Assemblies. *Oxford University Press;* .

Fukata M, Fukata Y, Adesnik H, Nicoll RA & Bredt DS. (2004). Identification of PSD-95 palmitoylating enzymes. *Neuron* **44,** 987-996.

Fukata Y & Fukata M. (2010). Protein palmitoylation in neuronal development and synaptic plasticity. *Nat Rev Neurosci* **11,** 161-175.

Fukata Y, Iwanaga T & Fukata M. (2006). Systematic screening for palmitoyl transferase activity of the DHHC protein family in mammalian cells. *Methods* **40,** 177-182.

Galvani L. (1794). *Dell'uso e dell'attività dell'arco conduttore*. S.Tommaso d'Aquino.

Garcia-Calvo M, Knaus HG, McManus OB, Giangiacomo KM, Kaczorowski GJ & Garcia ML. (1994). Purification and reconstitution of the high-conductance, calcium-activated potassium channel from tracheal smooth muscle. *J Biol Chem* **269,** 676-682.

Gardos G. (1958). The function of calcium in the potassium permeability of human erythrocytes. *Biochim Biophys Acta* **30,** 653-654.

Ghatta S, Nimmagadda D, Xu X & O'Rourke ST. (2006). Large-conductance, calcium-activated potassium channels: structural and functional implications. *Pharmacol Ther* **110,** 103-116.

Giangiacomo KM, Garcia ML & McManus OB. (1992). Mechanism of iberiotoxin block of the large-conductance calcium-activated potassium channel from bovine aortic smooth muscle. *Biochemistry* **31,** 6719-6727.

Goldstein JL. (2001). Laskers for 2001: knockout mice and test-tube babies. *Nat Med* **7,** 1079-1080.

Gonnord P, Delarasse C, Auger R, Benihoud K, Prigent M, Cuif MH, Lamaze C & Kanellopoulos JM. (2009). Palmitoylation of the P2X7 receptor, an ATP-gated channel, controls its expression and association with lipid rafts. *Faseb J* **23,** 795-805.

Graham FL, Smiley J, Russell WC & Nairn R. (1977). Characteristics of a human cell line transformed by DNA from human adenovirus type 5. *J Gen Virol* **36,** 59-74.

Gribkoff VK, Starrett JE, Jr. & Dworetzky SI. (2001a). Maxi-K potassium channels: form, function, and modulation of a class of endogenous regulators of intracellular calcium. *Neuroscientist* **7,** 166-177.

Gribkoff VK, Starrett JE, Jr., Dworetzky SI, Hewawasam P, Boissard CG, Cook DA, Frantz SW, Heman K, Hibbard JR, Huston K, Johnson G, Krishnan BS, Kinney GG, Lombardo LA, Meanwell NA, Molinoff PB, Myers RA, Moon SL, Ortiz A, Pajor L, Pieschl RL, Post-Munson DJ, Signor LJ, Srinivas N, Taber MT, Thalody G, Trojnacki JT, Wiener H, Yeleswaram K & Yeola SW. (2001b). Targeting acute ischemic stroke with a calcium-sensitive opener of maxi-K potassium channels. *Nat Med* **7,** 471-477.

Gubitosi-Klug RA, Mancuso DJ & Gross RW. (2005). The human Kv1.1 channel is palmitoylated, modulating voltage sensing: Identification of a palmitoylation consensus sequence. *Proc Natl Acad Sci U S A* **102,** 5964-5968.

Gustin M & Hennessey TM. (1988). Neomycin inhibits the calcium current of Paramecium. *Biochim Biophys Acta* **940,** 99-104.

Gutman GA, Chandy KG, Grissmer S, Lazdunski M, McKinnon D, Pardo LA, Robertson GA, Rudy B, Sanguinetti MC, Stuhmer W & Wang X. (2005). International Union of Pharmacology. LIII. Nomenclature and molecular relationships of voltage-gated potassium channels. *Pharmacol Rev* **57,** 473-508.

Ha TS, Jeong SY, Cho SW, Jeon H, Roh GS, Choi WS & Park CS. (2000). Functional characteristics of two BKCa channel variants differentially expressed in rat brain tissues. *Eur J Biochem* **267,** 910-918.

Hagen BM, Bayguinov O & Sanders KM. (2003). Beta 1-subunits are required for regulation of coupling between Ca^{2+} transients and Ca^{2+}-activated K^+ (BK) channels by protein kinase C. *Am J Physiol Cell Physiol* **285,** C1270-1280.

Hall SK & Armstrong DL. (2000). Conditional and unconditional inhibition of calcium-activated potassium channels by reversible protein phosphorylation. *J Biol Chem* **275,** 3749-3754.

Hancock JF, Cadwallader K, Paterson H & Marshall CJ. (1991). A CAAX or a CAAL motif and a second signal are sufficient for plasma membrane targeting of ras proteins. *Embo J* **10,** 4033-4039.

Hancock JF, Magee AI, Childs JE & Marshall CJ. (1989). All ras proteins are polyisoprenylated but only some are palmitoylated. *Cell* **57,** 1167-1177.

Hancock JF, Paterson H & Marshall CJ. (1990). A polybasic domain or palmitoylation is required in addition to the CAAX motif to localize p21ras to the plasma membrane. *Cell* **63,** 133-139.

Haug T, Sigg D, Ciani S, Toro L, Stefani E & Olcese R. (2004). Regulation of K^+ flow by a ring of negative charges in the outer pore of BK_{Ca} channels. Part I: Aspartate 292 modulates K+ conduction by external surface charge effect. *J Gen Physiol* **124,** 173-184.

Hayashi T, Rumbaugh G & Huganir RL. (2005). Differential regulation of AMPA receptor subunit trafficking by palmitoylation of two distinct sites. *Neuron* **47,** 709-723.

Hayashi T, Thomas GM & Huganir RL. (2009). Dual palmitoylation of NR2 subunits regulates NMDA receptor trafficking. *Neuron* **64,** 213-226.

Heginbotham L, Lu Z, Abramson T & MacKinnon R. (1994). Mutations in the K^+ channel signature sequence. *Biophys J* **66,** 1061-1067.

Heginbotham L & MacKinnon R. (1992). The aromatic binding site for tetraethylammonium ion on potassium channels. *Neuron* **8,** 483-491.

Heo WD, Inoue T, Park WS, Kim ML, Park BO, Wandless TJ & Meyer T. (2006). PI(3,4,5)P3 and PI(4,5)P2 lipids target proteins with polybasic clusters to the plasma membrane. *Science* **314,** 1458-1461.

Hille B. (1989). The Sharpey-Schafer Lecture. Ionic channels: evolutionary origins and modern roles. *Q J Exp Physiol* **74,** 785-804.

Honig B & Nicholls A. (1995). Classical electrostatics in biology and chemistry. *Science* **268,** 1144-1149.

Horrigan FT & Aldrich RW. (1999). Allosteric voltage gating of potassium channels II. Mslo channel gating charge movement in the absence of Ca(2+). *J Gen Physiol* **114,** 305-336.

Horrigan FT & Aldrich RW. (2002). Coupling between voltage sensor activation, Ca^{2+} binding and channel opening in large conductance (BK) potassium channels. *J Gen Physiol* **120,** 267-305.

Horrigan FT, Cui J & Aldrich RW. (1999). Allosteric voltage gating of potassium channels I. Mslo ionic currents in the absence of Ca(2+). *J Gen Physiol* **114,** 277-304.

Horrigan FT, Heinemann SH & Hoshi T. (2005). Heme regulates allosteric activation of the Slo1 BK channel. *J Gen Physiol* **126,** 7-21.

Huang K, Yanai A, Kang R, Arstikaitis P, Singaraja RR, Metzler M, Mullard A, Haigh B, Gauthier-Campbell C, Gutekunst CA, Hayden MR & El-Husseini A. (2004). Huntingtin-interacting protein HIP14 is a palmitoyl transferase involved in palmitoylation and trafficking of multiple neuronal proteins. *Neuron* **44,** 977-986.

Hurley JH, Cahill AL, Currie KP & Fox AP. (2000). The role of dynamic palmitoylation in Ca^{2+} channel inactivation. *Proc Natl Acad Sci U S A* **97,** 9293-9298.

Imlach WL, Finch SC, Miller JH, Meredith AL & Dalziel JE. (2010). A role for BK channels in heart rate regulation in rodents. *PLoS One* **5,** e8698.

Islas LD & Sigworth FJ. (1999). Voltage sensitivity and gating charge in Shaker and Shab family potassium channels. *J Gen Physiol* **114,** 723-742.

Jan LY & Jan YN. (1992). Structural elements involved in specific K^+ channel functions. *Annu Rev Physiol* **54,** 537-555.

Jeffries O, Geiger N, Rowe IC, Tian L, McClafferty H, Chen L, Bi D, Knaus HG, Ruth P & Shipston MJ. (2010a). Palmitoylation of the S0-S1 linker regulates cell surface expression of voltage- and calcium- activated potassium (BK) channels. *J Biol Chem*. (e-pub Aug-6)

Jeffries O, McGahon MK, Bankhead P, Lozano MM, Scholfield CN, Curtis TM & McGeown JG. (2010b). cAMP/PKA-dependent increases in Ca^{2+} Sparks, oscillations and SR Ca stores in retinal arteriolar myocytes after exposure to vasopressin. *Invest Ophthalmol Vis Sci* **51,** 1591-1598.

Jiang Y, Lee A, Chen J, Cadene M, Chait BT & MacKinnon R. (2002a). Crystal structure and mechanism of a calcium-gated potassium channel. *Nature* **417,** 515-522.

Jiang Y, Lee A, Chen J, Cadene M, Chait BT & MacKinnon R. (2002b). The open pore conformation of potassium channels. *Nature* **417,** 523-526.

Jiang Y, Lee A, Chen J, Ruta V, Cadene M, Chait BT & MacKinnon R. (2003a). X-ray structure of a voltage-dependent K^+ channel. *Nature* **423,** 33-41.

Jiang Y, Pico A, Cadene M, Chait BT & MacKinnon R. (2001). Structure of the RCK domain from the E. coli K^+ channel and demonstration of its presence in the human BK channel. *Neuron* **29,** 593-601.

Jiang Y, Ruta V, Chen J, Lee A & MacKinnon R. (2003b). The principle of gating charge movement in a voltage-dependent K^+ channel. *Nature* **423,** 42-48.

Jiang Z, Wallner M, Meera P & Toro L. (1999). Human and rodent MaxiK channel beta-subunit genes: cloning and characterization. *Genomics* **55,** 57-67.

Jindal HK, Folco EJ, Liu GX & Koren G. (2008). Posttranslational modification of voltage-dependent potassium channel Kv1.5: COOH-terminal palmitoylation modulates its biological properties. *Am J Physiol Heart Circ Physiol* **294,** H2012-2021.

Kalderon D, Richardson WD, Markham AF & Smith AE. (1984). Sequence requirements for nuclear location of simian virus 40 large-T antigen. *Nature* **311,** 33-38.

Kamb A, Iverson LE & Tanouye MA. (1987). Molecular characterization of Shaker, a Drosophila gene that encodes a potassium channel. *Cell* **50,** 405-413.

Kang R, Swayze R, Lise MF, Gerrow K, Mullard A, Honer WG & El-Husseini A. (2004). Presynaptic trafficking of synaptotagmin I is regulated by protein palmitoylation. *J Biol Chem* **279,** 50524-50536.

Kang R, Wan J, Arstikaitis P, Takahashi H, Huang K, Bailey AO, Thompson JX, Roth AF, Drisdel RC, Mastro R, Green WN, Yates JR, 3rd, Davis NG & El-Husseini A. (2008). Neural palmitoyl-proteomics reveals dynamic synaptic palmitoylation. *Nature* **456,** 904-909.

Kaplan WD & Trout WE, 3rd. (1969). The behavior of four neurological mutants of Drosophila. *Genetics* **61,** 399-409.

Keller CA, Yuan X, Panzanelli P, Martin ML, Alldred M, Sassoe-Pognetto M & Luscher B. (2004). The gamma2 subunit of GABA(A) receptors is a substrate for palmitoylation by GODZ. *J Neurosci* **24,** 5881-5891.

Kim EY, Ridgway LD, Zou S, Chiu YH & Dryer SE. (2007a). Alternatively spliced C-terminal domains regulate the surface expression of large conductance calcium-activated potassium channels. *Neuroscience* **146,** 1652-1661.

Kim EY, Zou S, Ridgway LD & Dryer SE. (2007b). Beta1-subunits increase surface expression of a large-conductance Ca^{2+}-activated K^+ channel isoform. *J Neurophysiol* **97,** 3508-3516.

Kim HJ, Lim HH, Rho SH, Eom SH & Park CS. (2006). Hydrophobic interface between two regulators of K+ conductance domains critical for calcium-dependent activation of large conductance Ca^{2+}-activated K^+ channels. *J Biol Chem* **281,** 38573-38581.

Kim J, Blackshear PJ, Johnson JD & McLaughlin S. (1994a). Phosphorylation reverses the membrane association of peptides that correspond to the basic domains of MARCKS and neuromodulin. *Biophys J* **67,** 227-237.

Kim J, Shishido T, Jiang X, Aderem A & McLaughlin S. (1994b). Phosphorylation, high ionic strength, and calmodulin reverse the binding of MARCKS to phospholipid vesicles. *J Biol Chem* **269,** 28214-28219.

Knaus HG, Eberhart A, Glossmann H, Munujos P, Kaczorowski GJ & Garcia ML. (1994a). Pharmacology and structure of high conductance calcium-activated potassium channels. *Cell Signal* **6,** 861-870.

Knaus HG, Eberhart A, Kaczorowski GJ & Garcia ML. (1994b). Covalent attachment of charybdotoxin to the beta-subunit of the high conductance Ca(2+)-activated K^+ channel. Identification of the site of incorporation and implications for channel topology. *J Biol Chem* **269,** 23336-23341.

Knaus HG, Folander K, Garcia-Calvo M, Garcia ML, Kaczorowski GJ, Smith M & Swanson R. (1994c). Primary sequence and immunological characterization of beta-subunit of high conductance Ca(2+)-activated K^+ channel from smooth muscle. *J Biol Chem* **269,** 17274-17278.

Knaus HG, Garcia-Calvo M, Kaczorowski GJ & Garcia ML. (1994d). Subunit composition of the high conductance calcium-activated potassium channel from smooth muscle, a representative of the mSlo and slowpoke family of potassium channels. *J Biol Chem* **269,** 3921-3924.

Knaus HG, McManus OB, Lee SH, Schmalhofer WA, Garcia-Calvo M, Helms LM, Sanchez M, Giangiacomo K, Reuben JP, Smith AB, 3rd & et al. (1994e). Tremorgenic indole alkaloids potently inhibit smooth muscle high-conductance calcium-activated potassium channels. *Biochemistry* **33,** 5819-5828.

Ko JH, Ibrahim MA, Park WS, Ko EA, Kim N, Warda M, Lim I, Bang H & Han J. (2009). Cloning of large-conductance Ca(2+)-activated K(+) channel alpha-subunits in mouse cardiomyocytes. *Biochem Biophys Res Commun* **389,** 74-79.

Korovkina VP, Fergus DJ, Holdiman AJ & England SK. (2001). Characterization of a novel 132-bp exon of the human maxi-K channel. *Am J Physiol Cell Physiol* **281,** C361-367.

Kosloff M, Elia N & Selinger Z. (2002). Structural homology discloses a bifunctional structural motif at the N-termini of G alpha proteins. *Biochemistry* **41,** 14518-14523.

Koval OM, Fan Y & Rothberg BS. (2007). A role for the S0 transmembrane segment in voltage-dependent gating of BK channels. *J Gen Physiol* **129,** 209-220.

Kuo A, Gulbis JM, Antcliff JF, Rahman T, Lowe ED, Zimmer J, Cuthbertson J, Ashcroft FM, Ezaki T & Doyle DA. (2003). Crystal structure of the potassium channel KirBac1.1 in the closed state. *Science* **300,** 1922-1926.

Kwon SH & Guggino WB. (2004). Multiple sequences in the C terminus of MaxiK channels are involved in expression, movement to the cell surface, and apical localization. *Proc Natl Acad Sci U S A* **101,** 15237-15242.

Kyte J & Doolittle RF. (1982). A simple method for displaying the hydropathic character of a protein. *J Mol Biol* **157,** 105-132.

Lagrutta A, Shen KZ, North RA & Adelman JP. (1994). Functional differences among alternatively spliced variants of Slowpoke, a Drosophila calcium-activated potassium channel. *J Biol Chem* **269,** 20347-20351.

Lai GJ & McCobb DP. (2002). Opposing actions of adrenal androgens and glucocorticoids on alternative splicing of Slo potassium channels in bovine chromaffin cells. *Proc Natl Acad Sci U S A* **99,** 7722-7727.

Lam KK, Davey M, Sun B, Roth AF, Davis NG & Conibear E. (2006). Palmitoylation by the DHHC protein Pfa4 regulates the ER exit of Chs3. *J Cell Biol* **174,** 19-25.

Latorre R, Vergara C & Hidalgo C. (1982). Reconstitution in planar lipid bilayers of a Ca^{2+}-dependent K^+ channel from transverse tubule membranes isolated from rabbit skeletal muscle. *Proc Natl Acad Sci U S A* **79,** 805-809.

Latorre R, Vergara C & Moczydlowski E. (1983). Properties of a Ca^{2+}-activated K^+ channel in a reconstituted system. *Cell Calcium* **4,** 343-357.

Laude AJ & Prior IA. (2008). Palmitoylation and localisation of RAS isoforms are modulated by the hypervariable linker domain. *J Cell Sci* **121,** 421-427.

Lee JH, Kim HJ, Kim HD, Lee BC, Chun JS & Park CS. (2009a). Modulation of the conductance-voltage relationship of the BK(Ca) channel by shortening the cytosolic loop connecting two RCK domains. *Biophys J* **97,** 730-737.

Lee SY, Banerjee A & MacKinnon R. (2009b). Two separate interfaces between the voltage sensor and pore are required for the function of voltage-dependent K(+) channels. *PLoS Biol* **7,** e47.

Lemmon MA. (2003). Phosphoinositide recognition domains. *Traffic* **4,** 201-213.

Levitan IB. (1994). Modulation of ion channels by protein phosphorylation and dephosphorylation. *Annu Rev Physiol* **56,** 193-212.

Li W & Aldrich RW. (2004). Unique inner pore properties of BK channels revealed by quaternary ammonium block. *J Gen Physiol* **124,** 43-57.

Liman ER, Tytgat J & Hess P. (1992). Subunit stoichiometry of a mammalian K^+ channel determined by construction of multimeric cDNAs. *Neuron* **9,** 861-871.

Linder ME & Deschenes RJ. (2007). Palmitoylation: policing protein stability and traffic. *Nat Rev Mol Cell Biol* **8,** 74-84.

Lippiat JD, Standen NB & Davies NW. (2000). A residue in the intracellular vestibule of the pore is critical for gating and permeation in Ca^{2+}-activated K^+ (BKCa) channels. *J Physiol* **529 Pt 1,** 131-138.

Lippiat JD, Standen NB, Harrow ID, Phillips SC & Davies NW. (2003). Properties of BK(Ca) channels formed by bicistronic expression of hSloalpha and beta1-4 subunits in HEK293 cells. *J Membr Biol* **192,** 141-148.

Liu G, Niu X, Wu RS, Chudasama N, Yao Y, Jin X, Weinberg R, Zakharov SI, Motoike H, Marx SO & Karlin A. (2010). Location of modulatory beta subunits in BK potassium channels. *J Gen Physiol* **135,** 449-459.

Liu G, Zakharov SI, Yang L, Deng SX, Landry DW, Karlin A & Marx SO. (2008). Position and role of the BK channel alpha subunit S0 helix inferred from disulfide crosslinking. *J Gen Physiol* **131,** 537-548.

Liu Y, Hudetz AG, Knaus HG & Rusch NJ. (1998). Increased expression of Ca2+-sensitive K^+ channels in the cerebral microcirculation of genetically hypertensive rats: evidence for their protection against cerebral vasospasm. *Circ Res* **82,** 729-737.

Loane DJ, Hicks GA, Perrino BA & Marrion NV. (2006). Inhibition of BK channel activity by association with calcineurin in rat brain. *Eur J Neurosci* **24,** 433-441.

Long SB, Campbell EB & Mackinnon R. (2005). Voltage sensor of Kv1.2: structural basis of electromechanical coupling. *Science* **309,** 903-908.

Long SB, Tao X, Campbell EB & MacKinnon R. (2007). Atomic structure of a voltage-dependent K^+ channel in a lipid membrane-like environment. *Nature* **450,** 376-382.

Lopez AJ. (1998). Alternative splicing of pre-mRNA: developmental consequences and mechanisms of regulation. *Annu Rev Genet* **32,** 279-305.

Lovell PV & McCobb DP. (2001). Pituitary control of BK potassium channel function and intrinsic firing properties of adrenal chromaffin cells. *J Neurosci* **21,** 3429-3442.

Lu JY & Hofmann SL. (1995). Depalmitoylation of CAAX motif proteins. Protein structural determinants of palmitate turnover rate. *J Biol Chem* **270,** 7251-7256.

Lu R, Alioua A, Kumar Y, Eghbali M, Stefani E & Toro L. (2006). MaxiK channel partners: physiological impact. *J Physiol* **570,** 65-72.

Ma Z, Lou XJ & Horrigan FT. (2006). Role of charged residues in the S1-S4 voltage sensor of BK channels. *J Gen Physiol* **127,** 309-328.

MacDonald SH, Ruth P, Knaus HG & Shipston MJ. (2006). Increased large conductance calcium-activated potassium (BK) channel expression accompanied by STREX variant downregulation in the developing mouse CNS. *BMC Dev Biol* **6,** 37.

MacKinnon R. (2004a). Nobel Lecture. Potassium channels and the atomic basis of selective ion conduction. *Biosci Rep* **24,** 75-100.

Mackinnon R. (2004b). Structural biology. Voltage sensor meets lipid membrane. *Science* **306,** 1304-1305.

MacKinnon R, Cohen SL, Kuo A, Lee A & Chait BT. (1998). Structural conservation in prokaryotic and eukaryotic potassium channels. *Science* **280,** 106-109.

Magee AI, Gutierrez L, McKay IA, Marshall CJ & Hall A. (1987). Dynamic fatty acylation of p21N-ras. *Embo J* **6,** 3353-3357.

Maher AD & Kuchel PW. (2003). The Gardos channel: a review of the Ca^{2+}-activated K^+ channel in human erythrocytes. *Int J Biochem Cell Biol* **35,** 1182-1197.

Makkerh JP, Dingwall C & Laskey RA. (1996). Comparative mutagenesis of nuclear localization signals reveals the importance of neutral and acidic amino acids. *Curr Biol* **6,** 1025-1027.

Marijic J, Li Q, Song M, Nishimaru K, Stefani E & Toro L. (2001). Decreased expression of voltage- and Ca(2+)-activated K(+) channels in coronary smooth muscle during aging. *Circ Res* **88,** 210-216.

Marrion NV & Tavalin SJ. (1998). Selective activation of Ca^{2+}-activated K^+ channels by co-localized Ca^{2+} channels in hippocampal neurons. *Nature* **395,** 900-905.

Marty A. (1981). Ca-dependent K^+ channels with large unitary conductance in chromaffin cell membranes. *Nature* **291,** 497-500.

McCartney CE, McClafferty H, Huibant JM, Rowan EG, Shipston MJ & Rowe IC. (2005). A cysteine-rich motif confers hypoxia sensitivity to mammalian large conductance voltage- and Ca-activated K (BK) channel alpha-subunits. *Proc Natl Acad Sci U S A* **102,** 17870-17876.

McCobb DP, Hara Y, Lai GJ, Mahmoud SF & Flugge G. (2003). Subordination stress alters alternative splicing of the Slo gene in tree shrew adrenals. *Horm Behav* **43,** 180-186.

McLaughlin S & Murray D. (2005). Plasma membrane phosphoinositide organization by protein electrostatics. *Nature* **438,** 605-611.

McLaughlin S, Wang J, Gambhir A & Murray D. (2002). PIP(2) and proteins: interactions, organization, and information flow. *Annu Rev Biophys Biomol Struct* **31,** 151-175.

McManus OB, Helms LM, Pallanck L, Ganetzky B, Swanson R & Leonard RJ. (1995). Functional role of the beta subunit of high conductance calcium-activated potassium channels. *Neuron* **14,** 645-650.

Meech & Strumwasser. (1970). Intracellular calcium injection activates potassium conductance in aplysia nerve cells. *fed proc* **29,** 834a

Meera P, Wallner M, Song M & Toro L. (1997). Large conductance voltage- and calcium-dependent K+ channel, a distinct member of voltage-dependent ion channels with seven N-terminal transmembrane segments (S0-S6), an extracellular N terminus, and an intracellular (S9-S10) C terminus. *Proc Natl Acad Sci U S A* **94,** 14066-14071.

Meredith AL, Thorneloe KS, Werner ME, Nelson MT & Aldrich RW. (2004). Overactive bladder and incontinence in the absence of the BK large conductance Ca^{2+}-activated K^+ channel. *J Biol Chem* **279,** 36746-36752.

Mitchell DA, Vasudevan A, Linder ME & Deschenes RJ. (2006). Protein palmitoylation by a family of DHHC protein S-acyltransferases. *J Lipid Res* **47,** 1118-1127.

Moczydlowski E. (1986). *Single-Channel enzymology.* Plenum, New York.

Morrow JP, Zakharov SI, Liu G, Yang L, Sok AJ & Marx SO. (2006). Defining the BK channel domains required for beta1-subunit modulation. *Proc Natl Acad Sci U S A* **103,** 5096-5101.

Mulgrew-Nesbitt A, Diraviyam K, Wang J, Singh S, Murray P, Li Z, Rogers L, Mirkovic N & Murray D. (2006). The role of electrostatics in protein-membrane interactions. *Biochim Biophys Acta* **1761,** 812-826.

Naruse K, Tang QY & Sokabe M. (2009). Stress-Axis Regulated Exon (STREX) in the C terminus of BK(Ca) channels is responsible for the stretch sensitivity. *Biochem Biophys Res Commun* **385,** 634-639.

Nelson MT, Cheng H, Rubart M, Santana LF, Bonev AD, Knot HJ & Lederer WJ. (1995). Relaxation of arterial smooth muscle by calcium sparks. *Science* **270,** 633-637.

Nomura K, Naruse K, Watanabe K & Sokabe M. (1990). Aminoglycoside blockade of Ca2(+)-activated K^+ channel from rat brain synaptosomal membranes incorporated into planar bilayers. *J Membr Biol* **115,** 241-251.

Ohno Y, Kihara A, Sano T & Igarashi Y. (2006). Intracellular localization and tissue-specific distribution of human and yeast DHHC cysteine-rich domain-containing proteins. *Biochim Biophys Acta* **1761,** 474-483.

Olesen SP, Munch E, Moldt P & Drejer J. (1994). Selective activation of Ca(2+)-dependent K^+ channels by novel benzimidazolone. *Eur J Pharmacol* **251,** 53-59.

Orio P, Rojas P, Ferreira G & Latorre R. (2002). New disguises for an old channel: MaxiK channel beta-subunits. *News Physiol Sci* **17,** 156-161.

Oshiro T, Sasaki T, Nara M, Tamada T, Shimura S, Maruyama Y & Shirato K. (2000). Suppression of maxi-K channel and membrane depolarization by synthetic polycations in single tracheal myocytes. *Am J Respir Cell Mol Biol* **22,** 528-534.

Pallotta BS. (1985). Calcium-activated potassium channels in rat muscle inactivate from a short-duration open state. *J Physiol* **363,** 501-516.

Pantazis A, Gudzenko V, Savalli N, Sigg D & Olcese R. (2010). Operation of the voltage sensor of a human voltage- and Ca^{2+}-activated K^+ channel. *Proc Natl Acad Sci U S A* **107,** 4459-4464.

Papazian DM. (1999). Potassium channels: some assembly required. *Neuron* **23,** 7-10.

Papazian DM, Schwarz TL, Tempel BL, Jan YN & Jan LY. (1987). Cloning of genomic and complementary DNA from Shaker, a putative potassium channel gene from Drosophila. *Science* **237,** 749-753.

Papazian DM, Shao XM, Seoh SA, Mock AF, Huang Y & Wainstock DH. (1995). Electrostatic interactions of S4 voltage sensor in Shaker K+ channel. *Neuron* **14,** 1293-1301.

Pedone KH & Hepler JR. (2007). The importance of N-terminal polycysteine and polybasic sequences for G14alpha and G16alpha palmitoylation, plasma membrane localization, and signaling function. *J Biol Chem* **282,** 25199-25212.

Peers C, Wyatt CN & Evans AM. (2010). Mechanisms for acute oxygen sensing in the carotid body. *Respir Physiol Neurobiol*.

Peers C. (1990) Hypoxic suppression of K+ currents in type I carotid body cells: selective effect on the Ca2+- activated K+ current. *Neurosci Lett* **119**, 253-2 56.

Petaja-Repo UE, Hogue M, Leskela TT, Markkanen PM, Tuusa JT & Bouvier M. (2006). Distinct subcellular localization for constitutive and agonist-modulated palmitoylation of the human delta opioid receptor. *J Biol Chem* **281,** 15780-15789.

Petkov GV, Bonev AD, Heppner TJ, Brenner R, Aldrich RW & Nelson MT. (2001). Beta1-subunit of the Ca^{2+}-activated K^+ channel regulates contractile activity of mouse urinary bladder smooth muscle. *J Physiol* **537,** 443-452.

Pian P, Bucchi A, Robinson RB & Siegelbaum SA. (2006). Regulation of gating and rundown of HCN hyperpolarization-activated channels by exogenous and endogenous PIP2. *J Gen Physiol* **128,** 593-604.

Pickering DS, Taverna FA, Salter MW & Hampson DR. (1995). Palmitoylation of the GluR6 kainate receptor. *Proc Natl Acad Sci U S A* **92,** 12090-12094.

Piskorowski R & Aldrich RW. (2002). Calcium activation of BK(Ca) potassium channels lacking the calcium bowl and RCK domains. *Nature* **420,** 499-502.

Pongs O, Kecskemethy N, Muller R, Krah-Jentgens I, Baumann A, Kiltz HH, Canal I, Llamazares S & Ferrus A. (1988). Shaker encodes a family of putative potassium channel proteins in the nervous system of Drosophila. *Embo J* **7,** 1087-1096.

Posson DJ, Ge P, Miller C, Bezanilla F & Selvin PR. (2005). Small vertical movement of a K^+ channel voltage sensor measured with luminescence energy transfer. *Nature* **436,** 848-851.

Pouton CW, Wagstaff KM, Roth DM, Moseley GW & Jans DA. (2007). Targeted delivery to the nucleus. *Adv Drug Deliv Rev* **59,** 698-717.

Quirk JC & Reinhart PH. (2001). Identification of a novel tetramerization domain in large conductance K(ca) channels. *Neuron* **32,** 13-23.

Raffaelli G, Saviane C, Mohajerani MH, Pedarzani P & Cherubini E. (2004). BK potassium channels control transmitter release at CA3-CA3 synapses in the rat hippocampus. *J Physiol* **557,** 147-157.

Ranganathan R. (1994). Evolutionary origins of ion channels. *Proc Natl Acad Sci U S A* **91,** 3484-3486.

Rathenberg J, Kittler JT & Moss SJ. (2004). Palmitoylation regulates the clustering and cell surface stability of GABAA receptors. *Mol Cell Neurosci* **26,** 251-257.

Reinhart PH & Levitan IB. (1995). Kinase and phosphatase activities intimately associated with a reconstituted calcium-dependent potassium channel. *J Neurosci* **15,** 4572-4579.

Ren J, Wen L, Gao X, Jin C, Xue Y & Yao X. (2008). CSS-Palm 2.0: an updated software for palmitoylation sites prediction. *Protein Eng Des Sel* **21,** 639-644.

Resh MD. (1994). Myristylation and palmitylation of Src family members: the fats of the matter. *Cell* **76,** 411-413.

Resh MD. (1999). Fatty acylation of proteins: new insights into membrane targeting of myristoylated and palmitoylated proteins. *Biochim Biophys Acta* **1451,** 1-16.

Resh MD. (2006a). Palmitoylation of ligands, receptors, and intracellular signaling molecules. *Sci STKE* **2006,** re14.

Resh MD. (2006b). Trafficking and signaling by fatty-acylated and prenylated proteins. *Nat Chem Biol* **2,** 584-590.

Resh MD. (2006c). Use of analogs and inhibitors to study the functional significance of protein palmitoylation. *Methods* **40,** 191-197.

Robbins J, Dilworth SM, Laskey RA & Dingwall C. (1991). Two interdependent basic domains in nucleoplasmin nuclear targeting sequence: identification of a class of bipartite nuclear targeting sequence. *Cell* **64,** 615-623.

Rosenblatt KP, Sun ZP, Heller S & Hudspeth AJ. (1997). Distribution of Ca^{2+}-activated K^+ channel isoforms along the tonotopic gradient of the chicken's cochlea. *Neuron* **19,** 1061-1075.

Ruttiger L, Sausbier M, Zimmermann U, Winter H, Braig C, Engel J, Knirsch M, Arntz C, Langer P, Hirt B, Muller M, Kopschall I, Pfister M, Munkner S, Rohbock K, Pfaff I, Rusch A, Ruth P & Knipper M. (2004). Deletion of the Ca^{2+}-activated potassium (BK) alpha-subunit but not the BKbeta1-subunit leads to progressive hearing loss. *Proc Natl Acad Sci U S A* **101,** 12922-12927.

Saito M, Nelson C, Salkoff L & Lingle CJ. (1997). A cysteine-rich domain defined by a novel exon in a slo variant in rat adrenal chromaffin cells and PC12 cells. *J Biol Chem* **272,** 11710-11717.

Saleem F, Rowe IC & Shipston MJ. (2009). Characterization of BK channel splice variants using membrane potential dyes. *Br J Pharmacol* **156,** 143-152.

Salkoff L, Baker K, Butler A, Covarrubias M, Pak MD & Wei A. (1992). An essential 'set' of K^+ channels conserved in flies, mice and humans. *Trends Neurosci* **15,** 161-166.

Salkoff L, Butler A, Ferreira G, Santi C & Wei A. (2006). High-conductance potassium channels of the SLO family. *Nat Rev Neurosci* **7,** 921-931.

Salkoff L & Jegla T. (1995). Surfing the DNA databases for K^+ channels nets yet more diversity. *Neuron* **15,** 489-492.

Sausbier M, Arntz C, Bucurenciu I, Zhao H, Zhou XB, Sausbier U, Feil S, Kamm S, Essin K, Sailer CA, Abdullah U, Krippeit-Drews P, Feil R, Hofmann F, Knaus HG, Kenyon C, Shipston MJ, Storm JF, Neuhuber W, Korth M, Schubert R, Gollasch M & Ruth P. (2005). Elevated blood pressure linked to primary hyperaldosteronism and impaired vasodilation in BK channel-deficient mice. *Circulation* **112,** 60-68.

Sausbier M, Hu H, Arntz C, Feil S, Kamm S, Adelsberger H, Sausbier U, Sailer CA, Feil R, Hofmann F, Korth M, Shipston MJ, Knaus HG, Wolfer DP, Pedroarena CM, Storm JF & Ruth P. (2004). Cerebellar ataxia and Purkinje cell dysfunction caused by Ca^{2+}- activated K^+ channel deficiency. *Proc Natl Acad Sci U S A* **101,** 9474-9478.

Schmalhofer WA, Sanchez M, Dai G, Dewan A, Secades L, Hanner M, Knaus HG, McManus OB, Kohler M, Kaczorowski GJ & Garcia ML. (2005). Role of the C-terminus of the high-conductance calcium-activated potassium channel in channel structure and function. *Biochemistry* **44,** 10135-10144.

Schmidt JW & Catterall WA. (1987). Palmitylation, sulfation, and glycosylation of the alpha subunit of the sodium channel. Role of post-translational modifications in channel assembly. *J Biol Chem* **262,** 13713-13723.

Schmidt MF, Bracha M & Schlesinger MJ. (1979). Evidence for covalent attachment of fatty acids to Sindbis virus glycoproteins. *Proc Natl Acad Sci U S A* **76,** 1687-1691.

Schmidt MF & Schlesinger MJ. (1979). Fatty acid binding to vesicular stomatitis virus glycoprotein: a new type of post-translational modification of the viral glycoprotein. *Cell* **17,** 813-819.

Schreiber M & Salkoff L. (1997). A novel calcium-sensing domain in the BK channel. *Biophys J* **73,** 1355-1363.

Schreiber M, Wei A, Yuan A, Gaut J, Saito M, Salkoff L, Dourado M, Butler A, Walton N & Jegla T. (1998). Slo3, a novel pH-sensitive K^+ channel from mammalian spermatocytes SLO-2, a K^+ channel with an unusual Cl- dependence. Eight potassium channel families revealed by the C. elegans genome project. *J Biol Chem* **273,** 3509-3516.

Schreiber M, Yuan A & Salkoff L. (1999). Transplantable sites confer calcium sensitivity to BK channels. *Nat Neurosci* **2,** 416-421.

Schroder E, Byse M & Satin J. (2009). L-type calcium channel C terminus autoregulates transcription. *Circ Res* **104,** 1373-1381.

Schubert R & Nelson MT. (2001). Protein kinases: tuners of the BKCa channel in smooth muscle. *Trends Pharmacol Sci* **22,** 505-512.

Schulze D, Krauter T, Fritzenschaft H, Soom M & Baukrowitz T. (2003). Phosphatidylinositol 4,5-bisphosphate (PIP2) modulation of ATP and pH sensitivity in Kir channels. A tale of an active and a silent PIP2 site in the N terminus. *J Biol Chem* **278,** 10500-10505.

Shen KZ, Lagrutta A, Davies NW, Standen NB, Adelman JP & North RA. (1994). Tetraethylammonium block of Slowpoke calcium-activated potassium channels expressed in Xenopus oocytes: evidence for tetrameric channel formation. *Pflugers Arch* **426,** 440-445.

Shipston MJ & Armstrong DL. (1996). Activation of protein kinase C inhibits calcium-activated potassium channels in rat pituitary tumour cells. *J Physiol-London* **493,** 665-672.

Shipston MJ, Duncan RR, Clark AG, Antoni FA & Tian L. (1999). Molecular components of large conductance calcium-activated potassium (BK) channels in mouse pituitary corticotropes. *Mol Endocrinol* **13,** 1728-1737.

Smith CW & Valcarcel J. (2000). Alternative pre-mRNA splicing: the logic of combinatorial control. *Trends Biochem Sci* **25,** 381-388.

Sobey CG. (2001). Potassium channel function in vascular disease. *Arterioscler Thromb Vasc Biol* **21,** 28-38.

Song M, Zhu N, Olcese R, Barila B, Toro L & Stefani E. (1999). Hormonal control of protein expression and mRNA levels of the MaxiK channel alpha subunit in myometrium. *FEBS Lett* **460,** 427-432.

Sorensen MV, Matos JE, Sausbier M, Sausbier U, Ruth P, Praetorius HA & Leipziger J. (2008). Aldosterone increases KCa1.1 (BK) channel-mediated colonic K+ secretion. *J Physiol* **586,** 4251-4264.

Sprossmann F, Pankert P, Sausbier U, Wirth A, Zhou XB, Madlung J, Zhao H, Bucurenciu I, Jakob A, Lamkemeyer T, Neuhuber W, Offermanns S, Shipston MJ, Korth M, Nordheim A, Ruth P & Sausbier M. (2009). Inducible knockout mutagenesis reveals compensatory mechanisms elicited by constitutive BK channel deficiency in overactive murine bladder. *Febs J* **276,** 1680-1697.

Strong M, Chandy KG & Gutman GA. (1993). Molecular evolution of voltage-sensitive ion channel genes: on the origins of electrical excitability. *Mol Biol Evol* **10,** 221-242.

Stryer L. (1997). *Biochemistry*. W.H.Freeman and Company, New York.

Suarez-Kurtz G & Reuben JP. (1987). Effects of neomycin on calcium channel currents in clonal GH3 pituitary cells. *Pflugers Arch* **410,** 517-523.

Suzuki H, Nishikawa K, Hiroaki Y & Fujiyoshi Y. (2008). Formation of aquaporin-4 arrays is inhibited by palmitoylation of N-terminal cysteine residues. *Biochim Biophys Acta* **1778,** 1181-1189.

Tanaka Y, Koike K & Toro L. (2004). MaxiK channel roles in blood vessel relaxations induced by endothelium-derived relaxing factors and their molecular mechanisms. *J Smooth Muscle Res* **40,** 125-153.

Tang XD, Xu R, Reynolds MF, Garcia ML, Heinemann SH & Hoshi T. (2003). Haem can bind to and inhibit mammalian calcium-dependent Slo1 BK channels. *Nature* **425,** 531-535.

Tao X, Lee A, Limapichat W, Dougherty DA & MacKinnon R. (2010). A gating charge transfer center in voltage sensors. *Science* **328,** 67-73.

Thomas P & Smart TG. (2005). HEK293 cell line: a vehicle for the expression of recombinant proteins. *J Pharmacol Toxicol Methods* **51,** 187-200.

Tian L, Coghill LS, McClafferty H, MacDonald SH, Antoni FA, Ruth P, Knaus HG & Shipston MJ. (2004). Distinct stoichiometry of BKCa channel tetramer phosphorylation specifies channel activation and inhibition by cAMP-dependent protein kinase. *Proc Natl Acad Sci U S A* **101,** 11897-11902.

Tian L, Duncan RR, Hammond MS, Coghill LS, Wen H, Rusinova R, Clark AG, Levitan IB & Shipston MJ. (2001). Alternative splicing switches potassium channel sensitivity to protein phosphorylation. *J Biol Chem* **276,** 7717-7720.

Tian L, Jeffries O, McClafferty H, Molyvdas A, Rowe IC, Saleem F, Chen L, Greaves J, Chamberlain LH, Knaus HG, Ruth P & Shipston MJ. (2008a). Palmitoylation gates phosphorylation-dependent regulation of BK potassium channels. *Proc Natl Acad Sci U S A* **105,** 21006-21011.

Tian L, McClafferty H, Chen L & Shipston MJ. (2008b). Reversible tyrosine protein phosphorylation regulates large conductance voltage- and calcium-activated potassium channels via cortactin. *J Biol Chem* **283,** 3067-3076.

Tian L, McClafferty H, Jeffries O & Shipston MJ. (2010). Multiple palmitoyltransferases are required for palmitoylation-dependent regulation of large conductance potassium (BK) channels. *J Biol Chem*.

Tian LJ, Coghill LS, MacDonald SHF, Armstrong DL & Shipston MJ. (2003). Leucine zipper domain targets cAMP-dependent protein kinase to mammalian BK channels. *J Biol Chem* **278,** 8669-8677.

Tian LJ, Knaus HG & Shipston MJ. (1998). Glucocorticoid regulation of calcium-activated potassium channels mediated by serine/threonine protein phosphatase. *J Biol Chem* **273,** 13531-13536.

Tian LJ & Shipston MJ. (1998). Steroid regulation of BK channels in neuroendocrine cells. *Naunyn-Schmiedebergs Arch Pharmacol* **358,** W57.

Toro B, Cox N, Wilson RJ, Garrido-Sanabria E, Stefani E, Toro L & Zarei MM. (2006). KCNMB1 regulates surface expression of a voltage and Ca2+-activated K^+ channel via endocytic trafficking signals. *Neuroscience* **142,** 661-669.

Toro L, Wallner M, Meera P & Tanaka Y. (1998). Maxi-K(Ca), a Unique Member of the Voltage-Gated K Channel Superfamily. *News Physiol Sci* **13,** 112-117.

Tseng-Crank J, Foster CD, Krause JD, Mertz R, Godinot N, DiChiara TJ & Reinhart PH. (1994). Cloning, expression, and distribution of functionally distinct Ca(2+)-activated K^+ channel isoforms from human brain. *Neuron* **13,** 1315-1330.

Vaithianathan T, Bukiya A, Liu J, Liu P, Asuncion-Chin M, Fan Z & Dopico A. (2008). Direct regulation of BK channels by phosphatidylinositol 4,5-bisphosphate as a novel signaling pathway. *J Gen Physiol* **132,** 13-28.

Venter JC, Adams MD, Myers EW, Li PW, Mural RJ, Sutton GG, Smith HO, Yandell M, Evans CA, Holt RA, Gocayne JD, Amanatides P, Ballew RM, Huson DH, Wortman JR, Zhang Q, Kodira CD, Zheng XH, Chen L, Skupski M, Subramanian G, Thomas PD, Zhang J, Gabor Miklos GL, Nelson C, Broder S, Clark AG, Nadeau J, McKusick VA, Zinder N, Levine AJ, Roberts RJ, Simon M, Slayman C, Hunkapiller M, Bolanos R, Delcher A, Dew I, Fasulo D, Flanigan M, Florea L, Halpern A, Hannenhalli S, Kravitz S, Levy S, Mobarry C, Reinert K, Remington K, Abu-Threideh J, Beasley E, Biddick K, Bonazzi V, Brandon R, Cargill M, Chandramouliswaran I, Charlab R, Chaturvedi K, Deng Z, Di Francesco V, Dunn P, Eilbeck K, Evangelista C, Gabrielian AE, Gan W, Ge W, Gong F, Gu Z, Guan P, Heiman TJ, Higgins ME, Ji RR, Ke Z, Ketchum KA, Lai Z, Lei Y, Li Z, Li J, Liang Y, Lin X, Lu F, Merkulov GV, Milshina N, Moore HM, Naik AK, Narayan VA, Neelam B, Nusskern D, Rusch DB, Salzberg S, Shao W, Shue B, Sun J, Wang Z, Wang A, Wang X, Wang J, Wei M, Wides R, Xiao C, Yan C, Yao A, Ye J, Zhan M, Zhang W, Zhang H, Zhao Q, Zheng L, Zhong F, Zhong W, Zhu S, Zhao S, Gilbert D, Baumhueter S, Spier G, Carter C, Cravchik A, Woodage T, Ali F, An H, Awe A, Baldwin D, Baden H, Barnstead M, Barrow I, Beeson K, Busam D, Carver A, Center A, Cheng ML, Curry L, Danaher S, Davenport L, Desilets R, Dietz S, Dodson K, Doup L, Ferriera S, Garg N, Gluecksmann A, Hart B, Haynes J, Haynes C, Heiner C, Hladun S, Hostin D, Houck J, Howland T, Ibegwam C, Johnson J, Kalush F, Kline L, Koduru S, Love A, Mann F, May D, McCawley S, McIntosh T, McMullen I, Moy M, Moy L, Murphy B, Nelson K, Pfannkoch C, Pratts E, Puri V, Qureshi H, Reardon M, Rodriguez R, Rogers YH, Romblad D, Ruhfel B, Scott R, Sitter C, Smallwood M, Stewart E, Strong R, Suh E, Thomas R, Tint NN, Tse S, Vech C, Wang G, Wetter J, Williams S, Williams M, Windsor S, Winn-Deen E, Wolfe K, Zaveri J, Zaveri K, Abril JF, Guigo R, Campbell MJ, Sjolander KV, Karlak B, Kejariwal A, Mi H, Lazareva B, Hatton T, Narechania A, Diemer K, Muruganujan A, Guo N, Sato S, Bafna V, Istrail S, Lippert R, Schwartz R, Walenz B, Yooseph S, Allen D, Basu A, Baxendale J, Blick L, Caminha M, Carnes-Stine J, Caulk P, Chiang YH, Coyne M, Dahlke C, Mays A, Dombroski M, Donnelly M, Ely D, Esparham S, Fosler C, Gire H, Glanowski S, Glasser K, Glodek A, Gorokhov M, Graham K, Gropman B, Harris M, Heil J, Henderson S, Hoover J, Jennings D, Jordan C, Jordan J, Kasha J, Kagan L, Kraft C, Levitsky A, Lewis M, Liu X, Lopez J, Ma D, Majoros W, McDaniel J, Murphy S, Newman M, Nguyen T, Nguyen N, Nodell M, Pan S, Peck J, Peterson M, Rowe W, Sanders R, Scott J, Simpson M, Smith T, Sprague A, Stockwell T, Turner R, Venter E, Wang M, Wen M, Wu D, Wu M, Xia A, Zandieh A & Zhu X. (2001). The sequence of the human genome. *Science* **291,** 1304-1351.

Verkhratsky A, Krishtal OA & Petersen OH. (2006). From Galvani to patch clamp: the development of electrophysiology. *Pflugers Arch* **453,** 233-247.

Wallner M, Meera P & Toro L. (1996). Determinant for beta-subunit regulation in high-conductance voltage-activated and Ca(2+)-sensitive K^+ channels: an additional transmembrane region at the N terminus. *Proc Natl Acad Sci U S A* **93,** 14922-14927.

Wang L & Sigworth FJ. (2009). Structure of the BK potassium channel in a lipid membrane from electron cryomicroscopy. *Nature* **461,** 292-295.

Wangemann P & Takeuchi S. (1993). Maxi-K^+ channel in single isolated cochlear efferent nerve terminals. *Hear Res* **66,** 123-129.

Weaver AK, Liu X & Sontheimer H. (2004). Role for calcium-activated potassium channels (BK) in growth control of human malignant glioma cells. *J Neurosci Res* **78,** 224-234.

Webb Y, Hermida-Matsumoto L & Resh MD. (2000). Inhibition of protein palmitoylation, raft localization, and T cell signaling by 2-bromopalmitate and polyunsaturated fatty acids. *J Biol Chem* **275,** 261-270.

Wei A, Covarrubias M, Butler A, Baker K, Pak M & Salkoff L. (1990). K^+ current diversity is produced by an extended gene family conserved in Drosophila and mouse. *Science* **248,** 599-603.

Wei A, Solaro C, Lingle C & Salkoff L. (1994). Calcium sensitivity of BK-type KCa channels determined by a separable domain. *Neuron* **13,** 671-681.

Werner ME, Zvara P, Meredith AL, Aldrich RW & Nelson MT. (2005). Erectile dysfunction in mice lacking the large-conductance calcium-activated potassium (BK) channel. *J Physiol* **567,** 545-556.

White RE, Kryman JP, El-Mowafy AM, Han G & Carrier GO. (2000). cAMP-dependent vasodilators cross-activate the cGMP-dependent protein kinase to stimulate BK(Ca) channel activity in coronary artery smooth muscle cells. *Circ Res* **86,** 897-905.

White RE, Schonbrunn A & Armstrong DL. (1991). Somatostatin stimulates Ca(2+)-activated K^+ channels through protein dephosphorylation. *Nature* **351,** 570-573.

Widmer HA, Rowe IC & Shipston MJ. (2003). Conditional protein phosphorylation regulates BK channel activity in rat cerebellar Purkinje neurons. *J Physiol* **552,** 379-391.

Williams SE, Wootton P, Mason HS, Bould J, Iles DE, Riccardi D, Peers C & Kemp PJ. (2004). Hemoxygenase-2 is an oxygen sensor for a calcium-sensitive potassium channel. *Science* **306,** 2093-2097.

Wimley WC & White SH. (1996). Experimentally determined hydrophobicity scale for proteins at membrane interfaces. *Nat Struct Biol* **3,** 842-848.

Womack MD & Khodakhah K. (2004). Dendritic control of spontaneous bursting in cerebellar Purkinje cells. *J Neurosci* **24,** 3511-3521.

Wrighton D & Lippiat J. (2010). An expressed cytoplasmic Slo3 fragment regulates both Slo3 and Slo1 K channels. T*he Physiological Society meeting, abstract*. Manchester.

Wu RS, Chudasama N, Zakharov SI, Doshi D, Motoike H, Liu G, Yao Y, Niu X, Deng SX, Landry DW, Karlin A & Marx SO. (2009). Location of the beta 4 transmembrane helices in the BK potassium channel. *J Neurosci* **29,** 8321-8328.

Wu Y, Yang Y, Ye S & Jiang Y. (2010). Structure of the gating ring from the human large-conductance Ca(2+)-gated K(+) channel. *Nature* **466,** 393-397.

Xia XM, Ding JP, Zeng XH, Duan KL & Lingle CJ. (2000). Rectification and rapid activation at low Ca^{2+} of Ca^{2+}-activated, voltage-dependent BK currents: consequences of rapid inactivation by a novel beta subunit. *J Neurosci* **20,** 4890-4903.

Xia XM, Zeng X & Lingle CJ. (2002). Multiple regulatory sites in large-conductance calcium-activated potassium channels. *Nature* **418,** 880-884.

Xie J & McCobb DP. (1998). Control of alternative splicing of potassium channels by stress hormones. *Science* **280,** 443-446.

Xie LH, John SA, Ribalet B & Weiss JN. (2008). Phosphatidylinositol-4,5-bisphosphate (PIP2) regulation of strong inward rectifier Kir2.1 channels: multilevel positive cooperativity. *J Physiol* **586,** 1833-1848.

Yan J, Olsen JV, Park KS, Li W, Bildl W, Schulte U, Aldrich RW, Fakler B & Trimmer JS. (2008). Profiling the phospho-status of the BKCa channel alpha subunit in rat brain reveals unexpected patterns and complexity. *Mol Cell Proteomics* **7,** 2188-2198.

Yuan A, Dourado M, Butler A, Walton N, Wei A & Salkoff L. (2000). SLO-2, a K^+ channel with an unusual Cl- dependence. *Nat Neurosci* **3,** 771-779.

Yuan A, Santi CM, Wei A, Wang ZW, Pollak K, Nonet M, Kaczmarek L, Crowder CM & Salkoff L. (2003). The sodium-activated potassium channel is encoded by a member of the Slo gene family. *Neuron* **37,** 765-773.

Yuan P, Leonetti MD, Pico AR, Hsiung Y & Mackinnon R. (2010). Structure of the Human BK Channel Ca^{2+}-Activation Apparatus at 3.0 A Resolution. *Science*.

Yusifov T, Savalli N, Gandhi CS, Ottolia M & Olcese R. (2008). The RCK2 domain of the human BKCa channel is a calcium sensor. *Proc Natl Acad Sci U S A* **105,** 376-381.

Zarei MM, Eghbali M, Alioua A, Song M, Knaus HG, Stefani E & Toro L. (2004). An endoplasmic reticulum trafficking signal prevents surface expression of a

voltage- and Ca^{2+}-activated K^+ channel splice variant. *Proc Natl Acad Sci U S A* **101,** 10072-10077.

Zarei MM, Song M, Wilson RJ, Cox N, Colom LV, Knaus HG, Stefani E & Toro L. (2007). Endocytic trafficking signals in KCNMB2 regulate surface expression of a large conductance voltage and Ca(2+)-activated K^+ channel. *Neuroscience* **147,** 80-89.

Zarei MM, Zhu N, Alioua A, Eghbali M, Stefani E & Toro L. (2001). A novel MaxiK splice variant exhibits dominant-negative properties for surface expression. *J Biol Chem* **276,** 16232-16239.

Zeng XH, Xia XM & Lingle CJ. (2005). Divalent cation sensitivity of BK channel activation supports the existence of three distinct binding sites. *J Gen Physiol* **125,** 273-286.

Zhang JH, Chung TD & Oldenburg KR. (1999). A Simple Statistical Parameter for Use in Evaluation and Validation of High Throughput Screening Assays. *J Biomol Screen* **4,** 67-73.

Zhou F, Xue Y, Yao X & Xu Y. (2006). CSS-Palm: palmitoylation site prediction with a clustering and scoring strategy (CSS). *Bioinformatics* **22,** 894-896.

Zhou XB, Arntz C, Kamm S, Motejlek K, Sausbier U, Wang GX, Ruth P & Korth M. (2001). A molecular switch for specific stimulation of the BKCa channel by cGMP and cAMP kinase. *J Biol Chem* **276,** 43239-43245.

Zhou XB, Wang GX, Ruth P, Huneke B & Korth M. (2000). BK(Ca) channel activation by membrane-associated cGMP kinase may contribute to uterine quiescence in pregnancy. *Am J Physiol Cell Physiol* **279,** C1751-1759.

Zhou XB, Wulfsen I, Utku E, Sausbier U, Sausbier M, Wieland T, Ruth P & Korth M. (2010). Dual role of protein kinase C on BK channel regulation. *Proc Natl Acad Sci U S A* **107,** 8005-8010.

Zhu N, Eghbali M, Helguera G, Song M, Stefani E & Toro L. (2005). Alternative splicing of Slo channel gene programmed by estrogen, progesterone and pregnancy. *FEBS Lett* **579,** 4856-4860.

APPENDICES

Appendices

#1 Tian L, Jeffries O, McClafferty H, Molyvdas A, Rowe IC, Saleem F, Chen L, Greaves J, Chamberlain LH, Knaus HG, Ruth P, Shipston MJ. (2008) Palmitoylation gates phosphorylation-dependent regulation of BK potassium channels. Proc Natl Acad Sci U S A. Dec 30;105(52):21006-11.

#2 Chen L, Jeffries O, Rowe IC, Liang Z, Knaus HG, Ruth P, Shipston MJ. (2010) Membrane trafficking of large conductance calcium-activated potassium channels is regulated by alternative splicing of a transplantable, acidic trafficking motif in the RCK1-RCK2 linker. J Biol Chem. Jul 23;285(30):23265-75.

#3 Tian L, McClafferty H, Jeffries O, Shipston MJ. (2010) Multiple palmitoyl-transferases are required for palmitoylation-dependent regulation of large conductance calcium- and voltage-activated potassium channels. J Biol Chem. Jul 30;285(31):23954-62.

#4 Jeffries O, Geiger N, Rowe IC, Tian L, McClafferty H, Chen L, Bi D, Knaus HG, Ruth P, Shipston MJ. (2010) Palmitoylation of the S0-S1 linker regulates cell surface expression of voltage- and calcium- activated potassium (BK) channels. J Biol Chem. Aug 6, e-pub. In press.

Palmitoylation gates phosphorylation-dependent regulation of BK potassium channels

Lijun Tian[a,1], Owen Jeffries[a,1], Heather McClafferty[a,1], Adam Molyvdas[a], Iain C. M. Rowe[a], Fozia Saleem[a], Lie Chen[a], Jennifer Greaves[a], Luke H. Chamberlain[a], Hans-Guenther Knaus[b], Peter Ruth[c], and Michael J. Shipston[a,2]

[a]Centre for Integrative Physiology, College of Medicine and Veterinary Medicine, University of Edinburgh, Edinburgh EH89XD, Untied Kingdom; [b]Division for Molecular and Cellular Pharmacology, Medical University Innsbruck, 6020 Innsbruck, Austria; and [c]Department of Pharmacology and Toxicology, University of Tuebingen, 72076 Tuebingen, Germany

Edited by Ramón Latorre, Universidad de Valparaíso, Valparaíso, Chile, and approved November 10, 2008 (received for review July 10, 2008)

Large conductance calcium- and voltage-gated potassium (BK) channels are important regulators of physiological homeostasis and their function is potently modulated by protein kinase A (PKA) phosphorylation. PKA regulates the channel through phosphorylation of residues within the intracellular C terminus of the pore-forming α-subunits. However, the molecular mechanism(s) by which phosphorylation of the α-subunit effects changes in channel activity are unknown. Inhibition of BK channels by PKA depends on phosphorylation of only a single α-subunit in the channel tetramer containing an alternatively spliced insert (STREX) suggesting that phosphorylation results in major conformational rearrangements of the C terminus. Here, we define the mechanism of PKA inhibition of BK channels and demonstrate that this regulation is conditional on the palmitoylation status of the channel. We show that the cytosolic C terminus of the STREX BK channel uniquely interacts with the plasma membrane via palmitoylation of evolutionarily conserved cysteine residues in the STREX insert. PKA phosphorylation of the serine residue immediately upstream of the conserved palmitoylated cysteine residues within STREX dissociates the C terminus from the plasma membrane, inhibiting STREX channel activity. Abolition of STREX palmitoylation by site-directed mutagenesis or pharmacological inhibition of palmitoyl transferases prevents PKA-mediated inhibition of BK channels. Thus, palmitoylation gates BK channel regulation by PKA phosphorylation. Palmitoylation and phosphorylation are both dynamically regulated; thus, cross-talk between these 2 major posttranslational signaling cascades provides a mechanism for conditional regulation of BK channels. Interplay of these distinct signaling cascades has important implications for the dynamic regulation of BK channels and physiological homeostasis.

KCNMA1 | acylation | protein kinase A | maxi-K

Large conductance calcium- and voltage-gated potassium (BK) channels are potently regulated by protein phosphorylation (1) and are important determinants of neuronal, cardiovascular, endocrine, and epithelial function where channel dysfunction may lead to major disorders such as hypertension (2, 3), ataxia (4), epilepsy (5, 6), and incontinence (7). BK channels are potently regulated by phosphorylation, and several putative phosphorylation motifs on the pore-forming α-subunit have been identified (8–12). However, as for other potassium channels, the molecular basis through which phosphorylation of the α-subunit effects changes in BK channel activity is essentially unknown.

BK channel pore-forming α-subunits are encoded by a single gene, *KCNMA1* (13), and native BK channels show functional heterogeneity in their response to protein kinase A (PKA)-mediated phosphorylation. This diversity results, in large part, from the extensive alternative pre-mRNA splicing of the pore-forming α-subunits (10, 12). Previous studies have demonstrated that PKA phosphorylation of a conserved C-terminal phosphorylation motif. $RQPS_{899}$ results in BK channel activation (9, 10, 14). Inclusion of the stress regulated exon (STREX) (15) in the intracellular C terminus generates an additional PKA consensus motif (serine residue 3 of the STREX insert, S3) that results in channel inhibition by PKA (10, 14). PKA inhibition of STREX follows a single-subunit rule, whereby only 1 α-subunit within the BK channel tetramer is required to be phosphorylated by PKA on S3 for inhibition to be conferred (14). Thus, phosphorylation of a single STREX α-subunit probably induces major conformational rearrangements in the BK channel C terminus to mediate channel inhibition.

The STREX insert is cysteine-rich (6 of 58 aa) that, when included into the BK channel α-subunit C terminus, generates a cysteine-rich domain (CRD) in the intracellular linker between the 2 regulator of conductance (RCK) domains (Fig. 1*A*). In many proteins, including other voltage- and ligand-gated ion channels (16–21), cysteine residues are common targets for protein palmitoylation, the covalent attachment of a palmitate lipid to a cysteine residue via a thioester bond. Palmitoylation can exert diverse effects on protein function including allowing cytosolic protein domains to anchor to the plasma membrane (22–24).

We thus hypothesized that palmitoylation of the STREX insert might target the C-terminal domain of the BK channel to the plasma membrane independently of the N-terminal transmembrane domains. Furthermore, this suggested a mechanism by which phosphorylation of a single STREX subunit could result in channel inhibition—through regulation of STREX domain interaction with the plasma membrane. To test these hypotheses, we exploited an integrated imaging, electrophysiological, and biochemical approach. We demonstrate that PKA-inhibition of BK channels results from dissociation of the STREX domain from the plasma membrane. Importantly, palmitoylation of STREX provides a conditional gate for regulation of BK channel activity by PKA phosphorylation.

Results and Discussion

STREX Insert Is a Membrane-Anchoring Domain of the Cytosolic C Terminus of the BK Channel. To address whether the cysteine-rich STREX domain is a membrane-anchoring module we developed an imaging assay to screen the ability of the STREX insert, and its cognate cysteine residues, to anchor the STREX C terminus to the plasma membrane in the absence of the N-terminal transmembrane domains of the α-subunit. We generated fluorescent −GFP fusion constructs of the entire BK channel C terminus (Fig. 1*B*) as well as constructs that encompass the CRD as fluorescent fusions with

Author contributions: L.T., H.-G.K., P.R., and M.J.S. designed research; L.T., O.J., H.M., A.M., I.C.M.R., F.S., and M.J.S. performed research; H.M., L.C., J.G., and L.H.C. contributed new reagents/analytic tools; L.T., O.J., H.M., A.M., I.C.M.R., F.S., and M.J.S. analyzed data; and M.J.S. wrote the paper.

The authors declare no conflict of interest.

This article is a PNAS Direct Submission.

Freely available online through the PNAS open access option.

[1]L.T., O.J., and H.M. contributed equally to this work.

[2]To whom correspondence should be addressed. E-mail: mike.shipston@ed.ac.uk.

This article contains supporting information online at www.pnas.org/cgi/content/full/0806700106/DCSupplemental.

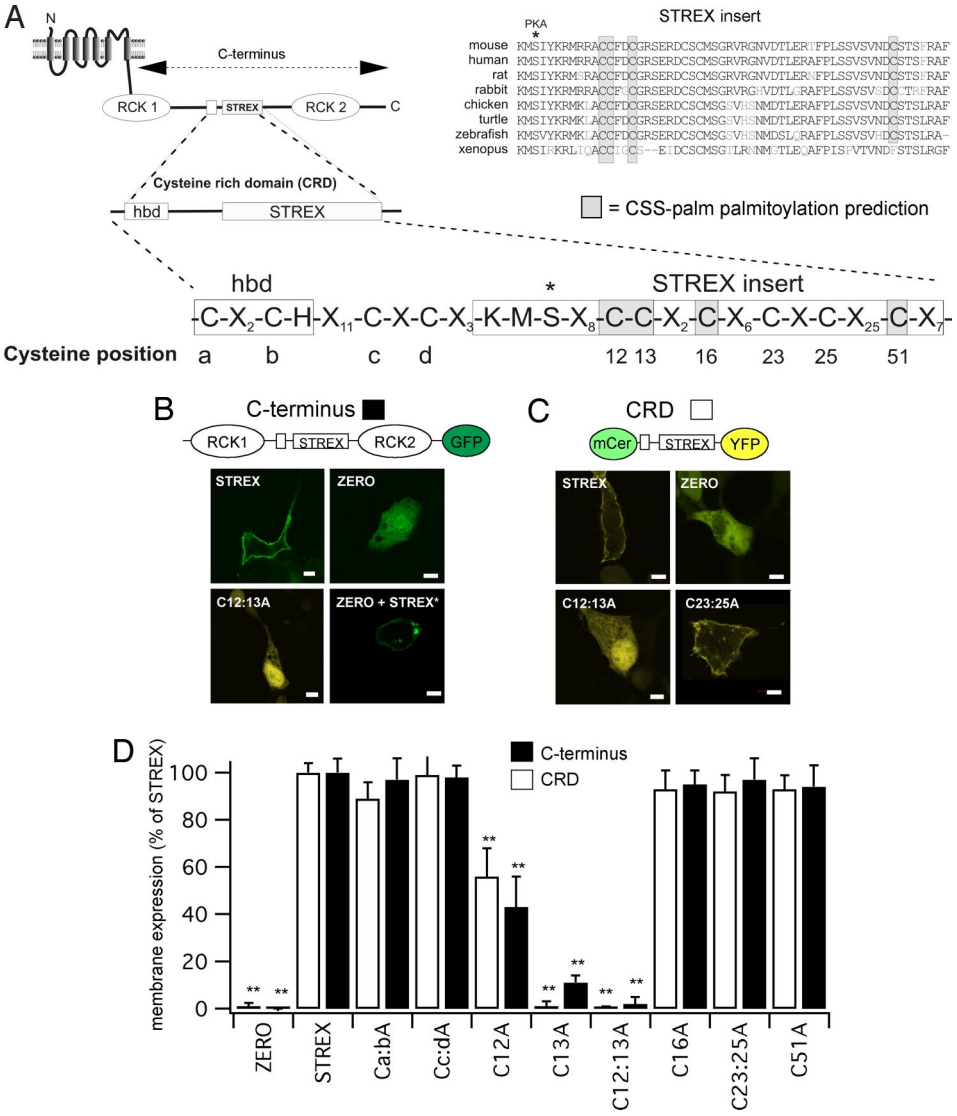

Fig. 1. STREX targets BK channel C terminus to the plasma membrane. (*A*) Schematic illustrating the topology of the BK channel pore forming α-subunit. The STREX insert is located in the linker between the 2 predicted regulator of K^+ conductance (RCK) domains in the intracellular C terminus. Inclusion of STREX generates a CRD encompassing the heme-binding domain (hbd) and STREX. Sequence alignment indicates evolutionarily conserved cysteine residues in the STREX insert predicted to be palmitoylated by the CSS-palm algorithm (shaded) and the PKA phosphorylation site serine S3 (indicated by the asterisk). Cysteine residues are numbered in the CRD as follows: STREX residues numbered from the first STREX residue (K) and upstream cysteines labeled by letters. (*B* and *C*) Schematic of C-terminal GFP fusion (*B*) and CRD domain (*C*) fused between CFP and YFP constructs and representative single confocal section images of STREX, STREX cysteine mutants C12:13A and C23:25A, and the ZERO variant (STREX insert excluded) expression in HEK293 cells. In B *Lower Right*, the C-terminal ZERO–GFP fusion construct was cotransfected with a modified C-terminal STREX construct (STREX*) in which the −GFP tag of STREX was replaced with an −HA epitope. (Scale bars: 5 μm.) (*D*) Summary bar chart of the respective C-terminal (■) or CRD (□) construct localization at the plasma membrane expressed as a percentage of the respective STREX expression. Data are means ± SEM, $N > 12$, $n > 350$ for each construct. **, $P < 0.01$ compared with respective STREX construct (ANOVA with Student–Neuman–Keuls post hoc test).

flanking mCer- and/or −YFP fusion proteins to mimic the STREX linker region between the RCK domains (Fig. 1*C*).

Expression of STREX C-terminal (Fig. 1*B*) or CRD constructs (Fig. 1*C*) resulted in robust plasma membrane expression of the fusion proteins in HEK293 cells in the absence of full-length BK channels or transmembrane segments. Identical results were also obtained in cells that endogenously express STREX variant channels including murine anterior pituitary corticotrope (AtT20) cells, rat pheochromocytoma PC12 cells, and human insulinoma INS-1 cells (data not shown). In contrast, in all these systems, expression of C-terminal, or CRD, fusion proteins that lack the STREX insert (ZERO constructs), but that are otherwise identical to the STREX constructs, did not localize to the membrane (Fig. 1 *B–D*). Coexpression of an −HA-tagged STREX C terminus (STREX*) rescued the ZERO C-terminal −GFP fusion protein localization to the plasma membrane (Fig. 1*B Lower Right*). Thus, a STREX subunit within a heteromeric assembly is sufficient to localize the BK channel C terminus at the plasma membrane. These data demonstrate that STREX acts as a membrane-targeting/anchoring domain and that the key plasma membrane localization motifs must reside within the CRD domain.

To determine whether the cysteine residues within the CRD control membrane localization of the STREX C terminus, we mutated cysteine residues to alanine in both the C-terminal and CRD STREX constructs. Mutation of residue C13 to alanine alone almost abolished membrane targeting in both fusion proteins (Fig. 1*D*), and mutation of its upstream vicinal cysteine residue (C12) significantly reduced membrane localization. The double-mutant C12:13A abolished membrane targeting of both fusion proteins (Fig. 1 *B–D*). In contrast, mutation of any of the other cysteine residues within the CRD had no significant effect on membrane localization (Fig. 1 *B–D*).

Palmitoylation of STREX Is Required for Membrane Targeting of the C Terminus. Using the CSS-palm palmitoylation algorithm (25), we predicted that 4 of the 6 cysteine residues within the STREX insert might be palmitoylated (Fig. 1*A* and Table S1), with cysteine residues 12 and 13 in STREX having the highest CSS-palm scores. Because mutation of C12 and C13 abolished membrane targeting of the STREX C terminus, this data suggests that palmitoylation of these residues controls STREX C terminus association with the plasma membrane. These STREX cysteine residues are highly evolutionarily conserved in vertebrates (Fig. 1*A*).

To directly address whether BK channels are in fact palmitoylated in vivo, we assayed ^{3}H-palmitate incorporation into full-length channels, and the CRD construct, expressed in HEK293 cells. Both full-length ZERO and STREX channels were robustly palmitoylated in HEK293 cells by endogenous palmitoyl transferases (Fig.

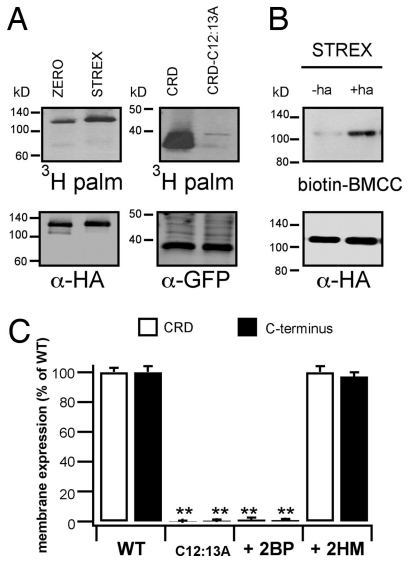

Fig. 2. Palmitoylation of STREX required for membrane localization. (*A*) Representative fluorographs (*Upper*) and Western blots (*Lower*) of full-length STREX-HA and ZERO-HA channels (*Left*) and the wild-type STREX and mutant C12:13A CRD-YFP constructs (*Right*) expressed in HEK293 cells. Constructs were labeled with ^{3}H-palmitate for 4 h and the respective constructs immunoprecipitated (IP) by using α-HA or α-GFP magnetic microbeads respectively and detected by fluorography. (*B*) Representative blots from a cysteine-accessibility assay after IP and treatment of STREX channels with 1 M neutral hydroxylamine to cleave endogenous palmitate thioester bonds to cysteine residues. Accessible cysteines were probed by using biotin-BMCC (*Upper*) with total protein probed by α-HA (*Lower*). (*C*) Summary imaging data of STREX and C12:13A C terminus (■) or CRD (□) as in Fig. 1 *B–D* and the effect of 24-h pretreatment of cells with the palmitoyltransferase inhibitor 2-bromopalmitate (2-BP, 100 μM) or the myristoylation inhibitor 2-hydroxymyristate (2-HM, 0.1–1 mM). Data are means ± SEM, $N > 14$, $n > 950$ for each construct/treatment. **, $P < 0.01$ compared with respective STREX construct (ANOVA with Student–Neuman–Keuls post hoc test).

2*A*). Importantly, the STREX CRD construct is robustly palmitoylated, and ^{3}H-palmitate incorporation was essentially abolished in the C12:13A mutant, suggesting that these residues are the major sites of palmitoylation within the CRD (Fig. 2*A*). As an alternative biochemical approach to confirm endogenous palmitoylation of STREX channels on cysteine residues, we also exploited a cysteine-accessibility assay (26) after treatment of STREX channels with 1 M neutral hydroxylamine (ha). Ha cleaves the thioester bond between endogenous palmitate and cysteine residues, allowing previously palmitoylated cysteine residues to become accessible to the sulfydryl-specific reagent biotin-BMCC (Fig. 2*B*). Functionally, pretreatment of HEK293 cells with the palmitoyl transferase inhibitor 2-bromopalmitate [2-BP (27)] also abolished membrane targeting of the STREX C terminus and CRD fusion proteins in the imaging assays (Fig. 2*C*) as for the palmitoylation-deficient C12:13A mutant. As a control for general effects on posttranslational lipid modification, the myristoylation inhibitor 2-hydroxymyristate had no significant effect on C-terminal or CRD targeting in these assays (Fig. 2*C*), and the vehicle (0.1% DMSO) was also without effect (data not shown). Thus, although the ^{3}H-palmitate-incorporation assays and CSS-palm predictions reveal that cysteine residues common to both the full-length ZERO and STREX channels may be palmitoylated, only the C12 and C13 residues are functionally important for membrane localization of the STREX C terminus at the plasma membrane. Taken together, these data support the hypothesis that the key determinant of STREX domain association with the plasma membrane results from palmitoylation of the STREX insert.

PKA Phosphorylation Dissociates the STREX C Terminus from the Plasma Membrane. PKA inhibition of STREX channels results from phosphorylation of serine residue 3 within the STREX insert (10, 14) that is just upstream of the site of palmitoylation (C12:13). We reasoned that phosphorylation of S3, which would introduce a negative charge into an otherwise basic region immediately upstream of C12:13, might result in destabilization of the STREX domain with the plasma membrane leading to significant structural rearrangements and thus channel inhibition. We took 3 approaches to test this idea. First, we generated the STREX PKA phosphomimetic S3E by mutating STREX S3 to glutamic acid. The S3E mutation abolished STREX C-terminal or CRD construct localization at the plasma membrane (Fig. 3 *A* and *C*). The serine-to-aspartate mutation (S3D, data not shown) also significantly reduced membrane expression, suggesting that both the S3E and S3D mutants largely mimic PKA phosphorylation of S3. In contrast, phosphomimetic mutation of S899 in the downstream C terminus, which is the major site for PKA activation (9, 10, 14), had no significant effect on STREX C terminus association with the plasma membrane (Fig. 3 *A* and *C*). However, the phosphomimetic mutations do not allow us to distinguish between a plasma membrane trafficking defect and a reduced association of the C-terminal domains once at the plasma membrane. Thus, in the second series of experiments, we acutely treated HEK293 cells, expressing the wild-type STREX C-terminal or CRD constructs at the plasma membrane, with the membrane-permeable cAMP analogue 8-CPT-cAMP to establish whether constructs resident at the plasma membrane could be dissociated by PKA phosphorylation. Pretreatment of cells with 0.1 mM 8CPT-cAMP, in the presence or absence of 10 nM okadaic acid, significantly reduced membrane association of the STREX constructs (Fig. 3*B*). Importantly, cAMP-induced dissociation was abolished by pretreatment with the cell-permeable PKA inhibitor H89. In contrast, activation of protein kinase G (PKG) or C (PKC) had no effect on STREX localization at the plasma membrane (Fig. 3*D*). In addition, neither acute (<3% O_2), hypoxia (Fig. 3*D*), which also regulates BK channels through the STREX insert (28), nor ionomycin-induced calcium elevation or KCl-induced depolarization (Fig. S1) had any significant effect on the plasma membrane localization of STREX. These data support a model in which PKA phosphorylation of STREX results in dissociation of the STREX domain from the plasma membrane.

Palmitoylation Gates BK Channel Regulation by PKA. If this model were correct, we would predict that PKA inhibition of STREX BK channels would be lost in channels that are not palmitoylated. To test this hypothesis, we examined the regulation of wild-type STREX channels and the STREX palmitoylation-deficient mutant C12:13A in electrophysiological assays. STREX channels are robustly inhibited by endogenous PKA closely associated with the channel upon exposure of the intracellular face of the patch to cAMP (Fig. 3 *E* and *G*). The effect of cAMP is abolished by the PKA inhibitor PKI_{5-24}, but not by inhibitors of PKG, PKC, or CaMKII (Fig. S2) and is mimicked by application of exogenous catalytic subunit of PKA (PKAc) (Fig. 3*G*). Although full-length C12:13A channels are robustly expressed at the plasma membrane (Fig. 3 *F* and *H*), suggesting the full-length C12:13A mutant is not itself trafficking deficient, cAMP or PKAc fail to inhibit this mutant. Furthermore, the inhibitory effect of cAMP on wild-type STREX channels was abolished in cells pretreated overnight with the inhibitor of palmitoylation, 2-BP (Fig. 3*G*). The C12:13A mutation, and inhibition of STREX channel palmitoylation by 2-BP, which both dissociate the C terminus from the plasma membrane (Fig. 2*C*), resulted in a right shift in the half-maximal voltage for activation (Fig. S3*a*). Reduced basal activity per se is not responsible for the loss of cAMP-mediated inhibition because cAMP potently inhibited STREX channels recorded under conditions to match the shift in $V_{0.5}$ resulting from the C12:13A

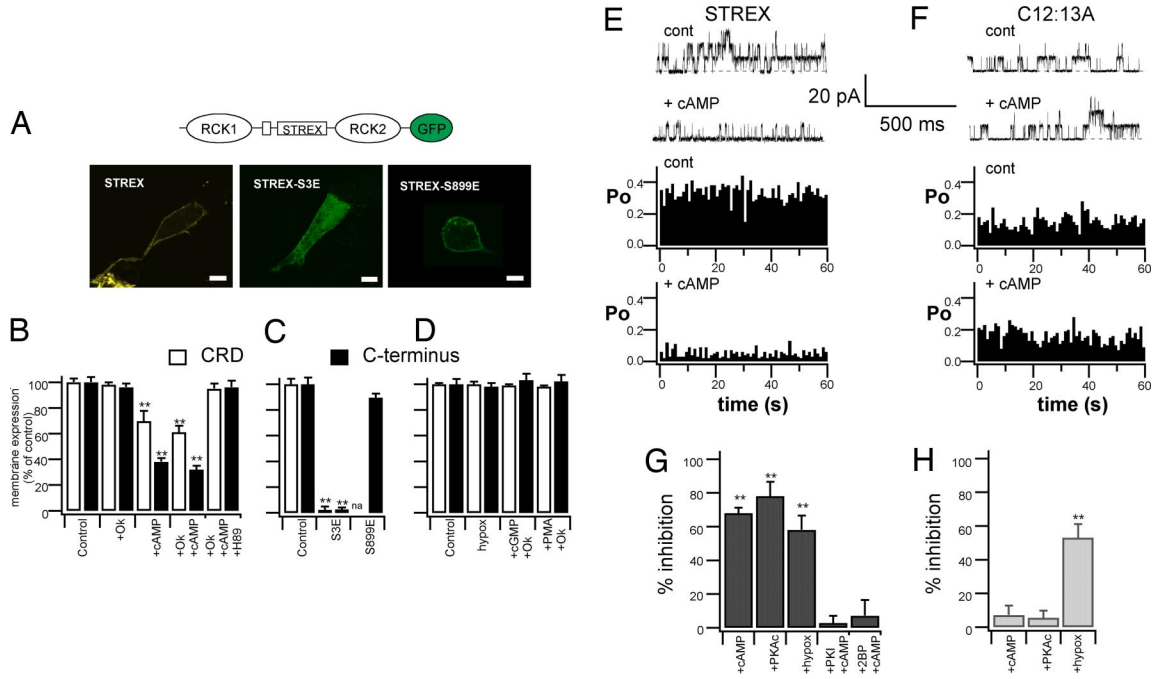

Fig. 3. PKA phosphorylation of STREX dissociates STREX from plasma membrane. (*A*) Representative single confocal sections from HEK293 cells expressing wild-type STREX C-terminal constructs and the corresponding STREX and C-terminal PKA phosphorylation site phosphomimetic constructs S3E and S899E. (Scale bars: 5 μm.) (*B*) Effect of cell-permeable cAMP analogue 8-CPT-cAMP (0.1 mM, 10–30 min) on STREX C terminus (■) or CRD (□) membrane localization in the presence or absence of 10 nM okadaic acid or the PKA inhibitor H89 (1 μM). (*C*) Summary of S3E and S899E construct expression at the plasma membrane (na, S899 site not present in CRD construct). (*D*) Effect of acute hypoxia (<3% O_2), PKG activation with the cell-permeable cGMP analogue 8-CPT-cGMP (0.1 mM in the presence of 10 nM okadaic acid) or PKC activation with the phorbol ester PMA (100 nM in the presence of 10 nM okadaic acid) on construct localization at the plasma membrane. Data are means ± SEM, $N > 4$, $n > 350$. (*E* and *F*) Representative single-channel traces and diary plots of single-channel mean open probability (Po) from isolated inside-out patches of HEK293 cells expressing full-length STREX (*E*) or C12:13A (*F*) channels before and 10 min after exposure to cAMP. Single channels were assayed in physiological K^+ gradients exposed to 0.2 μM free calcium and 2 mM Mg-ATP. (*G* and *H*) Inhibition of STREX (*G*) or C12:13A (*H*) channel Po by cAMP (0.1–1.0 mM) in the presence or absence of the PKA inhibitor PKI_{5-24} (0.45 μM) or 24-h cell pretreatment with 100 μM 2-BP; application of catalytic subunit of PKAc (300 nM) or exposure to acute hypoxia (<3%O_2). Data are means ± SEM, n = 5–14 for each treatment. **, $P < 0.01$ compared with respective control (ANOVA with Student–Neuman–Keuls post hoc test).

mutation (e.g., at −20 mV in 0.1 μM free calcium, inhibition was 67 ± 7% of control, n = 12).

Palmitoylation appears to specifically gate PKA-mediated inhibition of STREX channels because the palmitoylation status of STREX does not alter its intrinsic hypoxia sensitivity (28) (Fig. 3 *G* and *H*) or the regulation by PKG-dependent phosphorylation (Fig. S3*b*). Moreover, inhibition of palmitoylation by 2-BP does not modulate PKA-dependent activation of the ZERO splice variant (Fig. S3*c*) that depends on phosphorylation of a PKA consensus motif (S899) outwith the STREX insert.

Furthermore, the model proposed for palmitoylation-dependent gating of PKA inhibition of STREX would be expected to adhere to a "same-subunit" rule based on the previous demonstration that only a single subunit of STREX needs to be phosphorylated at S3 for channel inhibition (14). The same-subunit model would predict that PKA inhibition, as a result of phosphorylation of STREX at S3, would occur only if the same subunit is also palmitoylated at C12:13. By using a TEA-pore mutation strategy (Y334V) to determine channel subunit stoichiometry (14), cotransfection of subunits that could be palmitoylated but not phosphorylated (constructs with S3A mutation) together with subunits that could be phosphorylated but not palmitoylated (constructs with C12:13A mutation) revealed that cAMP was unable to inhibit channel activity (mean change in activity was 4 ± 10%, n = 12). In contrast, introduction of even a single subunit that could be both phosphorylated and palmitoylated (i.e., a wild-type STREX subunit) with subunits that could be palmitoylated but not phosphorylated (S3A constructs) resulted in robust channel inhibition by cAMP (inhibition was 71 ± 6%, n = 8). These data demonstrate that palmitoylation of the same subunit in which the channel is phosphorylated is required for PKA-mediated inhibition.

To examine whether palmitoylation gates native STREX channel regulation, we examined the regulation of BK channels in mouse anterior pituitary corticotrope (AtT20) cells. STREX variant channels are robustly expressed in this system and are potently inhibited by cAMP-dependent protein phosphorylation (29). cAMP potently inhibited the outward paxilline-sensitive (BK) current in these cells (Fig. 4). Pretreatment of AtT20 cells with 2-BP abolished cAMP-mediated inhibition of the BK current in the whole-cell configuration (Fig. 4). Similar data were obtained in perforated-patch recordings: 8-CPT-cAMP-mediated inhibition of the paxilline-sensitive current in 2-BP-treated cells was only 7 ± 8% (n = 4) of that observed by 8-CPT-cAMP in vehicle-treated controls.

BK channels are remarkable in the range of physiological processes they control, their functional heterogeneity as a result of alternative splicing of the single gene encoding the pore-forming α-subunits, and their extensive regulation by reversible protein phosphorylation. Our data reveal the molecular basis for PKA-mediated inhibition of BK channels through the regulation of STREX domain interaction with the plasma membrane. Palmitoylation of the STREX domain uniquely allows the large intracellular C terminus of the STREX splice variant to associate with the plasma membrane and, importantly, gates the regulation of STREX channels by PKA. Critically, this regulation depends on the site of palmitoylation being adjacent to the site of phosphorylation in the same subunit polypeptide. Importantly, STREX channel activation by PKG-mediated phosphorylation was not affected by palmitoylation status. Furthermore, PKA-activation of ZERO

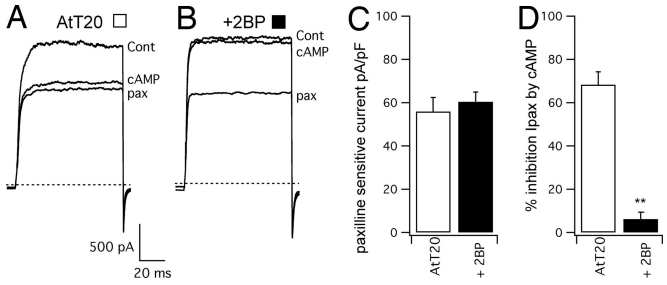

Fig. 4. Palmitoylation gates PKA inhibition of BK channels in native cells. (*A* and *B*) Representative whole-cell outward current traces from mouse anterior pituitary corticotrope (AtT20) cells pretreated with vehicle (0.01% DMSO) (*A*) or 2-BP (24 h, 100 μM) (*B*) before (control) or 10 min after intracellular dialysis with 0.1 mM cAMP or extracellular application of a 1 μM concentration of the BK channel inhibitor paxilline. Cells were voltage clamped at −50 mV in physiological potassium gradients and traces shown recorded during voltage steps to +40 mV for 100 ms. (*C*) Mean current density (pA/pF) of paxilline-sensitive current from vehicle- and 2-BP-treated AtT20 cells determined 90 ms into the pulse at +40 mV. (*D*) Percentage inhibition of paxilline-sensitive current (Ipax) by cAMP in vehicle- and 2-BP-treated cells. Data are means ± SEM, $n = 9$ for each treatment. **, $P < 0.01$ compared with cAMP inhibition in vehicle control (ANOVA with Student–Neuman–Keuls post hoc test).

channels was not affected by inhibitors of protein palmitoylation. PKA and PKG activation of BK channels is independent of the STREX insert and is thought to be mediated by consensus phosphorylation sites in the more distal C terminus (8–10, 12, 14). Importantly, these sites are not juxtaposed to predicted sites of palmitoylation, further supporting our model in which the cross-talk between PKA inhibition and palmitoylation status of STREX depends on both PKA phosphorylation and palmitoylation being in close proximity on the same subunit in the tetramer, thus obeying the single-subunit rule of PKA inhibition (14).

To what extent may such cross-talk between these major, dynamically regulated, lipid and phosphorylation signaling pathways occur in other ion channels? Protein phosphorylation is a fundamental mechanism to control ion channel function, and increasing evidence suggests that multiple ion channels are also regulated by palmitoylation (16–21). We would predict that phosphorylation–palmitoylation cross-talk is likely to occur when sites of palmitoylation are flanked by sites of serine/threonine phosphorylation. In support of this, our pilot sequence analysis reveals (M.J.S. and I.C.M.R., unpublished work) that in several ion channels reported or predicted to be palmitoylated, the sites of palmitoylation are frequently flanked by putative sites for serine/threonine phosphorylation (M.J.S. and I.C.M.R., unpublished work). For example, in ligand-gated GluR6 receptors, the identified sites of palmitoylation are flanked by potential PKC phosphorylation sites, and it has been reported that palmitoylation modifies PKC-mediated phosphorylation of GluR6 receptors (20). Thus, cross-talk between these major posttranslational regulatory pathways, at the level of a single ion channel polypeptide as reported here for BK channels, is likely to be of much broader significance to conditionally regulate a variety of other ion channels.

Although our data reveal that native BK channels are regulated by this palmitoylation–PKA phosphorylation cross-talk, significant challenges for the future will be to examine: (*i*) physiologically relevant signaling pathways that dynamically regulate BK channel palmitoylation and (*ii*) the functional relevance of this cross-talk on cellular and systems physiology. For example, PKA inhibition of BK channels is important for the control of stress hormone secretion in AtT20 pituitary corticotrope cells, and inhibitors of secretion can prevent PKA-mediated regulation of BK channels in this system (29). However, because palmitoylation also controls multiple levels of hormone secretion, including components of the secretory apparatus per se, a major goal for the future will be to develop tools to dissect the relative importance of palmitoylation cross-talk at the level of BK channels compared with other palmitoylation-dependent pathways in native systems.

Palmitoylation, like protein phosphorylation, is a dynamically regulated mechanism (22, 23, 30). Thus, elucidation of signaling pathways that control ion channel palmitoylation, together with examination of cross-talk with phosphorylation signaling pathways as reported here, will provide important insights into the role of these distinct signaling pathways in the control of BK, and other ion channel function and their role in physiological homeostasis.

Materials and Methods

Channel Constructs. The generation of full-length murine ZERO and STREX channel epitope-tagged as well as TEA-pore mutant (Y334V) constructs have been described (14, 31). C-terminal −GFP constructs, the respective CRD constructs, and site-directed mutants were generated and sequence-verified as described in *SI Methods*.

Cell Lines, Transfection, and Treatments. ***HEK293 cells and mouse anterior pituitary corticotrope AtT20 D16:16.*** HEK293 cells and mouse anterior pituitary corticotrope AtT20 D16:16 (passage 18–32) were subcultured essentially as described (10, 14, 29). Cells were transiently transfected by using Lipofectamine 2000 (Invitrogen) or Fugene-HD.

Cell treatments: The palmitoylation inhibitor 2-bromopalmitate (2-BP; Sigma) was made as a fresh 100 mM stock in DMSO and applied at a final concentration of 100 μM overnight. For the myristoylation inhibitor 2-hydroxmyristate (2-HM; Sigma) fresh stock solutions were made either complexed to BSA, or dissolved in DMSO as for 2-BP, and applied at 0.1–1 mM final concentration in each well. For acute imaging assays, cells were incubated for 1 h in DMEM containing 15 mM Hepes and 0.25% BSA (pH 7.4) at 37 °C before incubation for 10–30 min with fresh medium containing the respective drug treatment before rapid fixing. For acute hypoxia, medium was continuously bubbled with nitrogen gas (O_2 level are <3%, equivalent to <25 mmHg) and during fixation.

Imaging Assays. Cells were fixed with 4% paraformaldehyde, mounted in Mowiol, and analyzed under epifluorescence by using an inverted Nikon Eclipse 2000 microscope with a 100× oil objective lens. Confocal images were acquired on a Zeiss LSM510 laser scanning microscope with a 63× oil Plan Apochromat (N.A. = 1.4) objective lens, in multitracking mode to minimize channel cross-talk. Membrane expression was quantified by using the LSM browser or Volocity software as described in *SI Methods*. Data are shown as mean ± SEM for *N* independent experiments where *n* = minimum total number of cells analyzed across experiments for each construct.

Palmitoylation Prediction and Palmitoylation Assays. ***CSS-palm prediction.*** We exploited the published CSS-palm palmitoylation algorithm (25) to predict cysteine residues within the entire coding sequence of the murine STREX BK channel α-subunit as well as the STREX insert alone (see Table S1). Sequences were analyzed with both the published CSS-palm v1.0 algorithm as well as the recently refined CSS-palm v2.0 web interface. In both cases palmitoylation prediction was initially set to the highest cutoff in both algorithms.

^{3}H palmitic acid incorporation. HEK293 cells were transiently transfected in 6-well cluster dishes (≈3 × 10^6 cells per well) with full-length STREX-HA, ZERO-HA channels or the STREX CRD-YFP and CRD-C12:13A-YFP constructs, respectively. Forty-eight hours after transfection, cells were washed, and 1 mL of fresh DMEM containing 10 mg/ml fatty acid-free BSA was added for 30 min at 37 °C. Cells were incubated in DMEM/BSA containing 0.8 mCi/ml ^{3}H-palmitic acid for 4 h at 37 °C, and then the medium containing the free label was removed. Cells were lysed in 150 mM NaCl, 50 mM Tris-Cl, 1% Triton X-100 (pH 8.0), and channel fusion proteins were captured by using magnetic microbeads coupled to HA/GFP antibody (μMACS epitope tag isolation kits, Miltenyi Biotec). After washing columns with 150 mM NaCl, 1% Nonidet P-40, 0.5% deoxycholate, 0.1% SDS, 50 mM Tris-Cl (pH 8.0), followed by washes with 50 mM Tris-Cl (pH 7.5) captured proteins were eluted in SDS/PAGE sample buffer [50 mM Tris-Cl (pH 6.8), 5 mM DTT, 1% SDS, 1 mM EDTA, 0.005% bromophenol blue, 10% glycerol] prewarmed to 95 °C. The recovered samples were separated by SDS/PAGE, transferred to nitrocellulose membranes, and probed with either a monoclonal GFP antibody (1:3,000; Clontech) or polyclonal HA antibody (1:1,000; Zymed). A duplicate membrane was dried, sprayed with En^{3}hance fluorographic spray (PerkinElmer–Cetus) and exposed to light-sensitive film at −80 °C by using a Kodak Biomax transcreen LE (Amersham).

Cysteine-accessibility assays. Cysteine-accessibility assays were performed essentially as described by Drisdel (26). Cells were lysed at 4 °C in buffer containing 150

mM NaCl, 50 mM Hepes (pH 7.5), 1.5 mM $MgCl_2$, 1 mM EDTA, and 1% Triton-X-100 containing 25–50 mM *N*-ethylmaleimide (NEM) to block reactive cysteines. Cell lysates were spun, supernatants precleared with protein-G beads (Sigma), and incubated overnight at 4 °C with mouse monoclonal α-HA antibody. Immunopurified channels were rapidly washed 3 times in lysis buffer without NEM and treated with 1 M ha (+ha) (pH 7.4) for 1 h or 1 M Tris·HCl (pH 7.4) as a control (−ha). After washing, beads were exposed to the sulfydryl-specific biotinylating reagent biotin-BMCC (10 μM; Pierce) for 2 h at room temperature. Labeled proteins were run on SDS/PAGE, transferred to PVDF membrane, and probed with streptavidin-conjugated horseradish peroxidase (HRP) and detected by ECL.

Electrophysiological Assays. ***HEK293 cells.*** Single-channel current recordings were performed in the inside-out configuration of the patch-clamp technique, at room temperature (20–24 °C). The pipette solution (extracellular) contained 140 mM NaCl, 5 mM KCl, 1 mM $CaCl_2$, 2 mM $MgCl_2$, 20 mM glucose, 10 mM Hepes (pH 7.4). The bath solution (intracellular) contained 140 mM KCl, 5 mM NaCl, 2 mM $MgCl_2$, 1 mM BAPTA, 30 mM glucose, 10 mM Hepes, 1 mM ATP (pH 7.3) with free calcium $[Ca^{2+}]_i$ buffered to 0.2 μM, unless indicated otherwise. Channel activity was determined during 60-s depolarizations to +40 mV. Data acquisition and voltage protocols were controlled by an Axopatch 200 B amplifier and pCLAMP9 software (Axon Instruments). All recordings were sampled at 10 kHz and filtered at 2 kHz. Channel activity was allowed to stabilize for at least 10 min after patch excision before addition of drugs. Catalytic subunit of PKAc was from Promega. The 8-CPT-cGMP, 8-CPT-cAMP, KT5823, chelerythrine chloride, KN-62, and PKI_{5-24} were from Calbiochem.

Single-channel open probability (P_o) was derived either from single-channel analysis using pSTAT (Axon Instruments) or WINEDR (Version 2.3.9, J. Dempster, University of Strathclyde, U.K.). To determine the mean percentage change in channel activity after a treatment, mean Po or N*Po was measured immediately before and 10 min after the respective drug application. The effect of cAMP and/or PKAc on channel activity was typically maximal by ≈5 min and remained stable over the next 10–30 min after application to inside-out patches. The effect of PKA-mediated phosphorylation was abolished in the absence of Mg-ATP and could be reversed upon application of the catalytic subunit of protein phosphatase 2A (data not shown).

Mouse anterior pituitary corticotrope (AtT20) cells. Whole-cell currents were recording in the conventional whole-cell recording mode of the patch-clamp technique. The bath solution (extracellular) contained 140 mM NaCl, 5 mM KCl, 2 mM $MgCl_2$, 1 mM $CaCl_2$, 10 mM Hepes, and 20 mM glucose (pH 7.4) with or without 0.002 tetrodotoxin. The patch pipette (intracellular) contained 140 mM KCl, 2 mM $MgCl_2$, 10 mM Hepes, 30 mM glucose, 1 mM BAPTA, and 1 mM ATP (pH 7.4) with intracellular free calcium ($[Ca^{2+}]_i$) buffered to 200 nM. Perforated-patch recordings were conducted by using amphotericin in the patch pipette. Cells were voltage clamped at −50 mV and depolarized to the respective potentials for 100 ms with leak subtraction applied by using a P/4 protocol and series resistance compensation of >50%. Steady-state outward current was determined 90 ms into the pulse and was stable for ≈30 min under these conditions.

Statistical Analysis. All data are presented as means ± SEM with N = number of independent experiments and n = number of individual cells analyzed in imaging assays. Data were analyzed by ANOVA with post hoc Student–Neuman–Keuls test with significance set at $P < 0.01$.

ACKNOWLEDGMENTS. We thank Dr. Trudi Gillespie of the IMPACT imaging facility in the Centre for Integrative Physiology for assistance in confocal imaging and David L Armstrong for critical reading of earlier versions of the manuscript. James Maurice, Emily Ripley, and Jean-Marc Huibant contributed to pilot analysis of fusion protein localization. O.J. and A.M. were supported by Biotechnology and Biological Sciences Research Council PhD studentships and F.S. by a Medical Research Council PhD studentship. This work was supported by The Wellcome Trust.

1. Levitan IB (1999) in *Adv Second Messenger Phosphoprotein Res* 33:3–22.
2. Brenner R, *et al.* (2000) Vasoregulation by the beta 1 subunit of the calcium-activated potassium channel. *Nature* 407:870–876.
3. Sausbier M, *et al.* (2005) Elevated blood pressure linked to primary hyperaldosteronism and impaired vasodilation in BK channel-deficient mice. *Circulation* 112:60–68.
4. Sausbier M, *et al.* (2004) Cerebellar ataxia and Purkinje cell dysfunction caused by Ca^{2+}-activated K^+ channel deficiency. *Proc Natl Acad Sci USA* 101:9474–9478.
5. Brenner R, *et al.* (2005) BK channel beta 4 subunit reduces dentate gyrus excitability and protects against temporal lobe seizures. *Nat Neurosci* 8:1752–1759.
6. Du W, *et al.* (2005) Calcium-sensitive potassium channelopathy in human epilepsy and paroxysmal movement disorder. *Nat Genet* 37:733–738.
7. Meredith AL, Thorneloe KS, Werner ME, Nelson MT, Aldrich RW (2004) Overactive bladder and incontinence in the absence of the BK large conductance Ca^{2+}-activated K^+ channel. *J Biol Chem* 279:36746–36752.
8. Alioua A, *et al.* (1998) The large conductance, voltage-dependent, and calcium sensitive K^+ channel, Hslo, is a target of cGMP-dependent protein kinase phosphorylation in vivo. *J Biol Chem* 273:32950–32956.
9. Nara M, Dhulipala PD, Wang YX, Kotlikoff MI (1998) Reconstitution of beta-adrenergic modulation of large conductance, calcium-activated potassium (maxi-K) channels in *Xenopus* oocytes. Identification of the cAMP-dependent protein kinase phosphorylation site. *J Biol Chem* 273:14920–14924.
10. Tian L, *et al.* (2001) Alternative splicing switches potassium channel sensitivity to protein phosphorylation. *J Biol Chem* 276:7717–7720.
11. Yan J, *et al.* (2008) Profiling the phospho-status of the BKCa channel α-subunit in rat brain reveals unexpected patterns and complexity. *Mol Cell Proteomics* M800063-MCP200).
12. Zhou XB, *et al.* (2001) A molecular switch for specific stimulation of the BKCa channel by cGMP and cAMP kinase. *J Biol Chem* 276:43239–43245.
13. Butler A, Tsunoda S, McCobb DP, Wei A, Salkoff L (1993) mSlo, a complex mouse gene encoding ''maxi'' calcium-activated potassium channels. *Science* 261:221–224.
14. Tian L, *et al.* (2004) Distinct stoichiometry of BKCa channel tetramer phosphorylation specifies channel activation and inhibition by cAMP-dependent protein kinase. *Proc Natl Acad Sci USA* 101:11897–11902.
15. Xie J, McCobb DP (1998) Control of alternative splicing of potassium channels by stress hormones. *Science* 280:443–446.
16. Gubtosi-Klug RA, Mancuso DJ, Gross RW (2005) The human Kv1.1 channel is palmitoylated, modulating voltage sensing: Identification of a palmitoylation consensus sequence. *Proc Natl Acad Sci USA* 102:5964–5968.
17. Hayashi T, Rumbaugh G, Huganir RL (2005) Differential regulation of AMPA receptor subunit trafficking by palmitoylation at two distinct sites. *Neuron* 47:709–723.
18. Hurley JH, Cahill AL, Currie KPM, Fox AP (2000) The role of dynamic palmitoylation in Ca^{2+} channel inactivation. *Proc Natl Acad Sci USA* 97:9293–9298.
19. Jindal HK, Folco EJ, Liu GX, Koren G (2008) Posttranslational modification of voltage-dependent potassium channel Kv1.5: COOH-terminal palmitoylation modulates its biological properties. *Am J Physiol* 294:H2012–H2021.
20. Pickering DS, Taverna FA, Salter MW, Hampson DR (1995) Palmitoylation of the GluR6 kainate receptor. *Proc Natl Acad Sci USA* 92:12090–12094.
21. Schmidt JW, Catterall WA (1987) Palmitoylation, sulfation, and glycosylation of the alpha subunit of the sodium channel. Role of posttranslational modifications in channel assembly *J Biol Chem* 262:13713–13723.
22. Bijlmakers M-J, Marsh M (2003) The on–off story of protein palmitoylation. *Trends Cell Biol* 13:32–42.
23. Linder ME, Deschenes RJ (2007) Palmitoylation: Policing protein stability and traffic. *Nat Rev Mol Cell Biol* 8:74–84.
24. Resh MD (2006) Trafficking and signalling by fatty acylated and prenylated proteins. *Nat Chem Biol* 2:584–590.
25. Zhou F, Xue Y, Yao X, Xu Y (2006) CSS-Palm: Palmitoylation site prediction with a clustering and scoring strategy (CSS). *Bioinformatics* 22:894–896.
26. Drisdel R, Green W (2004) Labelling and quantifying sites of protein palmitoylation. *BioTechniques* 36:276–285.
27. Resh MD (2006) Use of analogs and inhibitors to study the functional significance of protein palmitoylation. *Methods* 40:191–197.
28. McCartney CE, *et al.* (2005) A cysteine-rich motif confers hypoxia sensitivity to mammalian large conductance voltage- and Ca-activated K (BK) channel alpha-subunits. *Proc Natl Acad Sci USA* 102:17870–17875.
29. Shipston MJ, Kelly JS, Antoni FA (1996) Glucocorticoids block protein kinase A inhibition of calcium-activated potassium channels. *J Biol Chem* 271:9197–9200.
30. Smotrys JE, Linder ME (2004) Palmitoylation of intracellular signalling proteins: Regulation and function. *Annu Rev Biochem* 73:559–587.
31. Chen L, *et al.* (2005) Functionally diverse complement of large conductance calcium- and voltage-activated potassium channel (BK) alpha-subunits generated from a single site of splicing. *J Biol Chem* 280:33599–33609.

⌘ *Author's Choice*

THE JOURNAL OF BIOLOGICAL CHEMISTRY VOL. 285, NO. 30, pp. 23265–23275, July 23, 2010

Membrane Trafficking of Large Conductance Calcium-activated Potassium Channels Is Regulated by Alternative Splicing of a Transplantable, Acidic Trafficking Motif in the RCK1-RCK2 Linker*

Received for publication, May 1, 2010 Published, JBC Papers in Press, May 17, 2010, DOI 10.1074/jbc.M110.139758

Lie Chen[‡], Owen Jeffries[‡], Iain C. M. Rowe[‡], Zhi Liang[‡], Hans-Guenther Knaus[§], Peter Ruth[¶], and Michael J. Shipston[‡1]

From the [‡]Centre for Integrative Physiology, College of Medicine & Veterinary Medicine, University of Edinburgh, Edinburgh EH8 9XD, Scotland, United Kingdom, the [§]Division for Molecular and Cellular Pharmacology, Department of Medical Genetics, Molecular and Clinical Pharmacology, Medical University Innsbruck, Peter-Mayr Strasse 1, 6020 Innsbruck, Austria, and [¶]Pharmacology and Toxicology, Institute of Pharmacy, University Tuebingen, 72076 Tuebingen, Germany

Trafficking of the pore-forming α-subunits of large conductance calcium- and voltage-activated potassium (BK) channels to the cell surface represents an important regulatory step in controlling BK channel function. Here, we identify multiple trafficking signals within the intracellular RCK1-RCK2 linker of the cytosolic C terminus of the channel that are required for efficient cell surface expression of the channel. In particular, an acidic cluster-like motif was essential for channel exit from the endoplasmic reticulum and subsequent cell surface expression. This motif could be transplanted onto a heterologous nonchannel protein to enhance cell surface expression by accelerating endoplasmic reticulum export. Importantly, we identified a human alternatively spliced BK channel variant, *hSloΔ*$_{579-664}$, in which these trafficking signals are excluded because of in-frame exon skipping. The *hSloΔ*$_{579-664}$ variant is expressed in multiple human tissues and cannot form functional channels at the cell surface even though it retains the putative RCK domains and downstream trafficking signals. Functionally, the *hSloΔ*$_{579-664}$ variant acts as a dominant negative subunit to suppress cell surface expression of BK channels. Thus alternative splicing of the intracellular RCK1-RCK2 linker plays a critical role in determining cell surface expression of BK channels by controlling the inclusion/exclusion of multiple trafficking motifs.

Large conductance calcium- and voltage-activated potassium (BK)[2] channels are widely expressed in mammalian cells where they play an important role in a diverse range of physiological processes ranging from the control of blood flow (1, 2) to the control of neuronal excitability and neurotransmitter release (3, 4). Indeed, a number of disorders, including hypertension (1, 2), epilepsy (5), incontinence (6), and sexual dysfunction (7) may result from perturbations of BK channel function. Correct cellular targeting of BK channels is an important regulatory mechanism, and changes in cell surface expression of these channels have been associated with different physiological demands, for example during pregnancy (8), with aging in coronary arteries (9), and with aldosterone-induced potassium secretion from the gut (10).

BK channels assemble as tetramers of pore-forming α-subunits, encoded by a single gene that undergoes extensive pre-mRNA splicing and can form complexes with a family of regulatory β-subunits (11). Increasing evidence suggests that alternative splicing at the N or C termini of BK channel α-subunits is a major determinant of BK channel cell surface expression. For example, inclusion of the alternatively spliced SV1 insert at the intracellular N terminus results in expression of an endoplasmic reticulum (ER) retention motif, CVLF, that prevents efficient export of the channel from the ER (12). In addition, the N-terminal mk44 variant (13) is endoproteolytically cleaved, resulting in plasma membrane localization of the N terminus of the mk44 variant and intracellular retention of the remaining cleaved pore-forming C terminus. Alternative splicing of the very C terminus of α-subunits is also a major determinant of cell surface expression, although the regulatory mechanisms are poorly understood (14). Alternative splicing that results in premature truncation of the BK channel α-subunit C terminus also results in intracellular retention of the channel as exemplified by the murine Δe23 (15) and rabbit rbSlo2 (16) as a result of a loss of putative C-terminal ER export signals as well as the RCK2 domain (15, 16).

Recent data also suggest that the intracellular C-terminal linker between the two predicted regulator of potassium conductance domains (see Fig. 1*a*, RCK1 and RCK2) is also an important determinant of BK channel surface expression. First, a rat splice variant SVcyt that has an ~80-amino acid in-frame deletion of the linker region is poorly expressed at the cell surface (17). Second, deletion of >30 amino acids in the linker regions produces nonfunctional channels that lack significant cell surface expression (18). However, the mechanism(s) re-

* This work was supported by the Wellcome Trust.
⌘ *Author's Choice*—Final version full access.
[1] To whom correspondence should be addressed: Centre for Integrative Physiology, Hugh Robson Bldg., University of Edinburgh, Edinburgh EH8 9XD, UK. Tel.: 44-131-6503253; Fax: 44-131-6506521; E-mail: mike.shipston@ed.ac.uk.
[2] The abbreviations used are: BK channel, large conductance calcium- and voltage-activated potassium channel; ER, endoplasmic reticulum; HEK, human embryonic kidney; IP, immunoprecipitation; NORS, no regular secondary structure; RCK, regulator of potassium conductance; HA, hemagglutinin; eYFP, enhanced yellow fluorescent protein; ANOVA, analysis of variance.

sponsible for the trafficking defect in these linker deletion mutants are not known.

In this report, we identify multiple trafficking motifs within the intracellular RCK1-RCK2 linker that control cell surface expression of BK channel α-subunits expressed in mammalian cells. Importantly, we reveal an acidic cluster-like motif (DD*XXD*XXXI) that is critical for cell surface expression of the channel that can be transplanted to a heterologous nonchannel protein to enhance membrane expression. Furthermore, we have isolated a widely expressed human BK channel splice variant (hSloΔ$_{579-664}$), in which the exons encoding these trafficking motifs are excluded. Exclusion of these exons results in an in-frame 86-amino acid deletion that encodes a channel that is a dominant negative of cell surface expression. Taken together, our data reveal that alternative splicing of the RCK1-RCK2 linker region, resulting in inclusion/exclusion of multiple trafficking motifs, is an important determinant of BK channel cell surface expression.

EXPERIMENTAL PROCEDURES

Cloning of the hSloΔ$_{579-664}$ Variant, Channel Mutagenesis, and GABA$_B$R1a Constructs—A human tissue rapid scan cDNA pool (Origene) was screened for splice variants by PCR-amplifying a region between exons 15 and 25 (see Fig. 1*a*) of the human BK channel α-subunit with the forward and reverse primer pairs: 5′-TTgCCAACCTCTTCTCC-3′ and 5′-gTgCTTgAgCTCATGggTAAT-3′, respectively. PCR amplicons were cloned into the pCR®II-TOPO vector (Invitrogen). To generate full-length BK channel α-subunit cDNAs, the novel variant *hSloΔ$_{579-664}$* amplicon from pCR®II-TOPO was subcloned into the murine BK channel α-subunit with an N-terminal FLAG tag and/or a C-terminal HA or eYFP tag described previously (15, 19–21). Site-directed mutations were generated using the QuikChange® site-directed mutagenesis kit (Stratagene) using standard procedures. All of the amino acid numbering is based on the human BK channel α-subunit (*hSlo*) with start methionine at MDALI (accession number AAD31173).

GABA$_B$R1a receptor plasmids with N-terminal extracellular HA-GABA$_B$R1a and HA-GABA$_B$R1a-ASRR plasmids were kind gifts from Prof. Lily Jan (University of California at San Francisco) (22). To engineer the DD*XXD*XXXI sequence at the C terminus of both constructs, we PCR-amplified the C terminus with forward (5′-TTTgCCAAggAggAACCAAAg-3′) and reverse (5′-CTCTAgATCAAATTCTTTTgggATCTgTgACgTCATCCTTgTAAAgCA-3′) primers. The reverse primer encodes a DD*XXD*XXXI sequence, and the resultant PCR amplicons were ligated into the GABA$_B$R1a plasmids using ClaI and XbaI restriction sites. All of the sequences were confirmed by automated sequencing on both strands (MWG-Biotech).

Quantitative Real Time-PCR TaqMan™ Assay—Quantitative analysis of the human BK channel variant transcripts was performed using a TaqMan™ assay (15). The probes and primer sets of total *hSlo* and *hSloΔ$_{579-664}$* were designed with Primer Express v1.2. TaqMan™ probes, labeled at the 5′ end with 6-carboxyfluorescein and at the 3′ end with 6-carboxytetramethylrhodamine were synthesized by ABI (Applied Biosystems). The following TaqMan™ assays were used to screen cDNAs from human tissues: for total *hSlo*: forward, 5′-gTCTCAAATgAAATgTACACAgAATATCTCT-3′; reverse, 5′-gCAgACTTgTACTCAATggCTATCA-3′; and probe, 5′-CCTTCgTgggTCTgTCCTTCCCTACTgTT-3′; and for hSloΔ$_{579-664}$: forward, 5′-gCTCCTAATgATAgCCATTgAgTACA-3′; reverse, 5′-TgATCATTgCCAggAATTAACAAg-3′; and probe, 5′-CCAACCgAgAgAgCCggCATgA-3′. The efficiency, correlation coefficient (R^2), and limit of detection for each TaqMan™ assay were: for total *hSlo*: 2.03, 0.97, and <0.3 fg of cDNA; and for *hSloΔ$_{579-664}$*: 2.02, 0.99, and <0.3 fg of cDNA. All of the data were analyzed using ABI Prism 7000 SDS software version 1.0 (Applied Biosystems). Transcript expression was determined from standard curves generated using dilutions of the respective splice variant plasmid DNA, and variant expression is given as a percentage of total BK channel transcripts in each tissue.

HEK293 Cell Culture and Immunofluorescence—HEK293 cells were maintained and transfected as described (15, 21). Cell surface labeling of the N-terminal FLAG epitope of BK channels in nonpermeabilized HEK293 cells was performed (15) using mouse monoclonal anti-FLAG M2 antibody (50 μg/ml Sigma) and Alexa-594-conjugated anti-mouse rabbit IgG (Molecular Probes). The cells were subsequently fixed in 4% paraformaldehyde for 30 min, permeabilized with 0.3% Triton X-100 for 10 min, and blocked with phosphate-buffered saline containing 3% bovine serum albumin plus 0.05% Triton X-100 for 30 min. The intracellular C-terminal HA epitope tag was detected using 0.5 μg/ml anti-HA polyclonal rabbit antibody (Zymed Laboratories Inc.) and Alexa-488-conjugated anti-rabbit chicken IgG (Molecular Probes), and the cells were mounted using Mowiol.

Confocal images were acquired on a Zeiss LSM510 laser scanning microscope using a 63× oil Plan Apochromat (NA = 1.4) objective lens in multi-tracking mode to minimize channel cross-talk and analyzed as described (19). FLAG surface expression was quantified in two ways: (i) using a threshold method to detect the total number of all transfected cells that displayed FLAG surface expression in each group and (ii) using absolute measures based on ratios of surface FLAG (extracellular) fluorescence to intracellular signal (eYFP or HA as appropriate) in a random subset of all cells analyzed using Image J. The data were then normalized to the corresponding control group (100%) as indicated in the respective figure legend. In these experimental paradigms the data obtained for relative surface expression using the threshold method were quantitatively the same as using the absolute ratio measure, therefore these data were pooled. In Fig. 2*b* >90% of all of the transfected cells display surface expression of the respective e22 and zero variants; however, we could not detect surface expression of the hSloΔ$_{579-664}$ variant in any cell examined. The same approach was used for the HA-tagged GABA$_B$R1a receptor constructs except that distinct fluorescent second antibodies directed against the N-terminal HA tag were used in nonpermeabilized and permeabilized conditions.

To assay co-localization of the channels with the ER, HEK293 cells were co-transfected with the HA-tagged channels and the pdsRed-ER (Clontech) vector. The HA tag was detected as above, and confocal images taken at Nyquist sampling rates were collected and analyzed as described previously (23). The

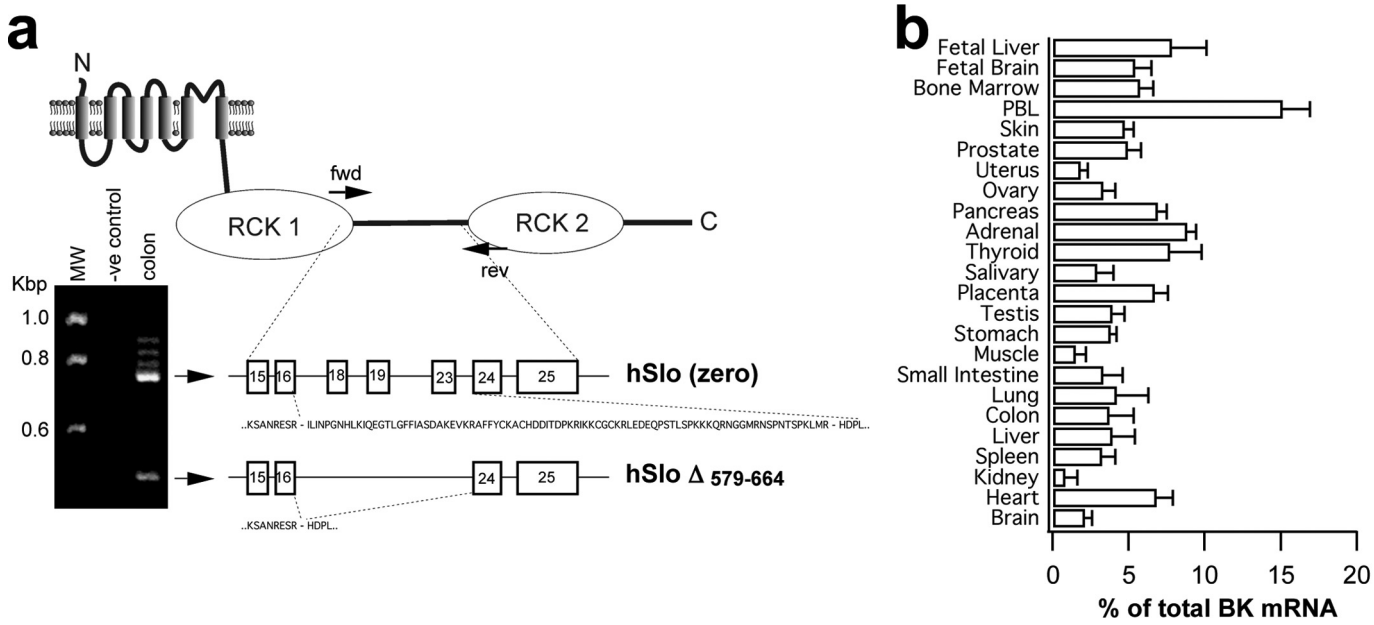

FIGURE 1. **Cloning and tissue mRNA expression of a human BK channel splice variant, hSlo$\Delta_{579-664}$, with an in-frame 86-amino acid deletion in the RCK1-RCK2 linker region.** *a*, schematic illustrating the topology of a BK channel α-subunit with an extracellular N terminus and a large intracellular C terminus. Exon (*numbered open boxes*) structure for the hSlo zero variant (with no alternatively spliced inserts in this region) and the hSlo$\Delta_{579-664}$ variant are shown. The representative agarose gel illustrates multiple amplicons generated by the forward (*fwd*) and reverse (*rev*) primers in human colon cDNA. The *upper* and *lower arrows* indicate the human hSlo zero and hSlo$\Delta_{579-664}$ variants, respectively, with the corresponding amino acid sequence. hSlo$\Delta_{579-664}$ results from an 86-amino acid in-frame deletion; thus the rest of the intracellular C terminus including RCK2, the calcium bowl, and other essential trafficking motifs for cell surface expression are retained. *b*, hSlo$\Delta_{579-664}$ variant mRNA levels expressed as percentages of total BK channel mRNA transcripts in selected human tissues determined using TaqMan™ analysis. All of the data are the means ± S.E., $n = 3$/tissue region. *MW*, molecular mass.

images were deconvolved using Huygens software (Scientific Volume Imaging) and analyzed using ImageJ (National Institutes of Health) to obtain the Pearson's correlation coefficient. Coefficients range from 1 to −1. A value of 1 indicates a complete positive correlation between the two channels, whereas −1 stands for a negative correlation.

Immunoprecipitation and Western Blotting—Immunoprecipitation (IP) and Western blotting were performed as previously described (15). HEK293 cells were solubilized at 4 °C in lysis buffer (NLB) containing 150 mM NaCl, 50 mM HEPES, pH 7.5, 1.5 mM $MgCl_2$, 10 mM sodium pyrophosphate, 20 mM NaF, 1 mM EDTA, 5 mM EGTA, 10% (v/v) glycerol, 1% Triton X-100, and complete protease inhibitor mixture (Roche Applied Science). After preclearing, the channels were immunoprecipitated with anti-HA (rabbit polyclonal; Zymed Laboratories Inc.) or anti-FLAG M2 monoclonal mouse antibody (Sigma). Negative control IPs included: (i) IP of mock transfected cells; (ii) IP from cells transfected with channels without the cognate epitope tag; (iii) beads alone; or (iv) irrelevant IP antibody. Bound complexes were separated through a 10% SDS-PAGE gel and electroblotted to polyvinylidene difluoride membrane and probed for the HA or FLAG tag using rabbit polyclonal anti-HA (Zymed Laboratories Inc.), 0.5 μg/ml, or mouse monoclonal anti-FLAG M2 (Sigma), 20 μg/ml. The blots were incubated with horseradish peroxidase-conjugated anti-rabbit IgG/or anti-mouse IgG secondary antibody (1/5000 dilution; Sigma) for 1 h at room temperature. The signals were detected using ECL.

Cell Surface Biotinylation Assay—Plasmids expressing HA- or eYFP-tagged BK channels were transiently transfected into HEK293 cells with Exgen 500 (Fermentas). 48 h post-transfection, the cells were washed three times with Hanks' buffered salt solution and then incubated on ice for 2 h in the presence of 5 μg/ml of Sulfo-NHS-LC-biotin (Pierce). After three washes in ice-cold 100 mM glycine in Hanks' buffered salt solution, the cells were lysed in NLB lysis buffer with protease inhibitor mixture (Roche Applied Science). Biotinylated cell lysates were incubated with streptavidin-immobilized beads (Pierce) overnight at 4 °C, washed three times with cold Hanks' buffered salt solution, and washed once with water. The biotinylated membrane BK channel proteins were removed from the beads by incubating at 45 °C for 15 min in 2× Laemmli protein sample buffer, separated by SDS-PAGE, and detected with anti-HA or green fluorescent protein antibody using Western blot. Parallel control biotinylation assays were conducted with: (i) mock transfected cells, (ii) cells immunoprecipitated with streptavidin beads in the absence of biotin incubation, and (iii) immunoprecipitation with an irrelevant antibody.

Fluorescent Membrane Potential Assay—The membrane potential assays were performed in transfected HEK293 cells using FLIPR® membrane potential blue dye (Molecular Devices, Sunnyvale, CA) essentially as described (24). Briefly, the cells were plated in black-walled, clear-bottomed 96-well plates and loaded with dye for 30 min at 37 °C. The assays were performed at 22 °C using a FlexStation® II system (Molecular Devices), and the channels were activated by applying 1 μM of the calcium ionophore, ionomycin, 16 s after the experiment began. The fluorescence changes were read at high sensitivity at 180 s at intervals of 1.52 s with excitation/emission wavelengths of 530/565 nm, respectively. A decrease in relative fluorescent units, with respect

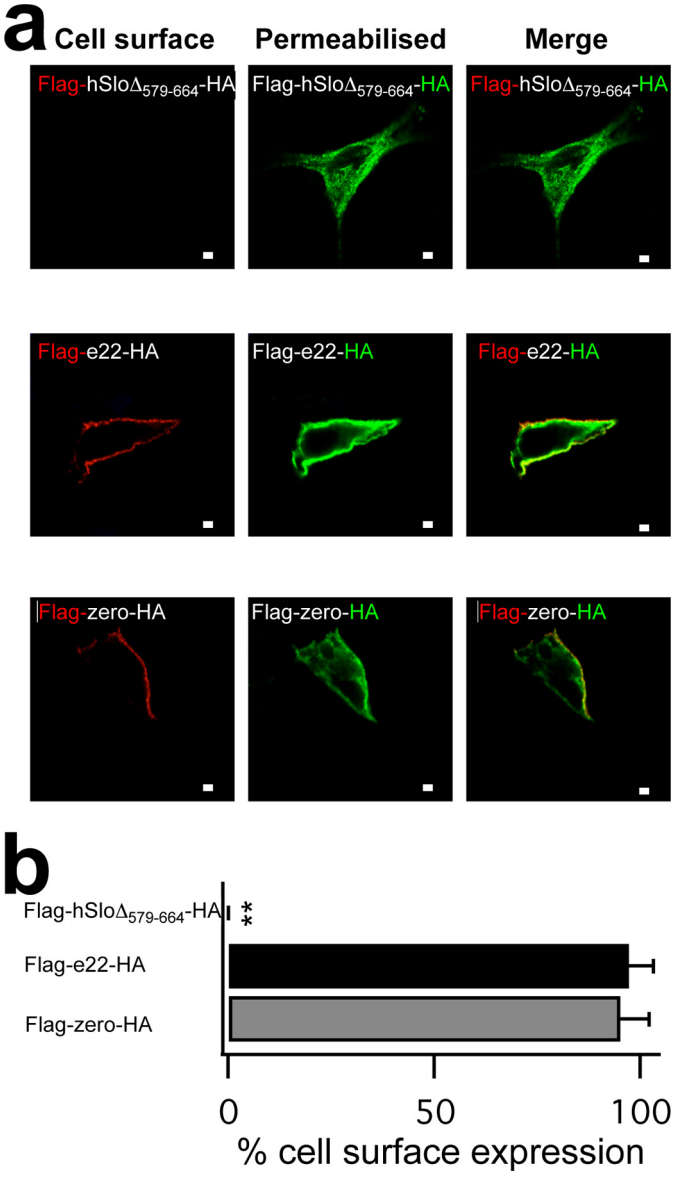

FIGURE 2. **Lack of cell surface expression of the hSloΔ$_{579-664}$ variant.** *a*, representative confocal images of HEK293 cells expressing FLAG-hSloΔ$_{579-664}$-HA (*top panels*), FLAG-e22-HA (*middle panels*), or FLAG-zero-HA (*bottom panels*). The extracellular FLAG epitope was labeled (*red*) under nonpermeabilized conditions (cell surface) with the C-terminal HA epitope tag (*green*) labeled following cell permeabilization. FLAG and HA labeling from the same cell are then overlaid (*Merge*). The FLAG-e22-HA construct is a splice variant with an alternatively spliced exon (exon 22) included between exons 19 and 23. The *scale bars* are 2 μm. *b*, quantification of surface expression expressed as a percentage of the total number of transfected cells with detectable cell surface (FLAG) expression for experiments as performed in *a*. The data are the means ± S.E. from a minimum of three independent experiments with >600 cells analyzed/group. **, $p < 0.01$, ANOVA with post hoc Dunnett's test compared with FLAG-zero-HA construct.

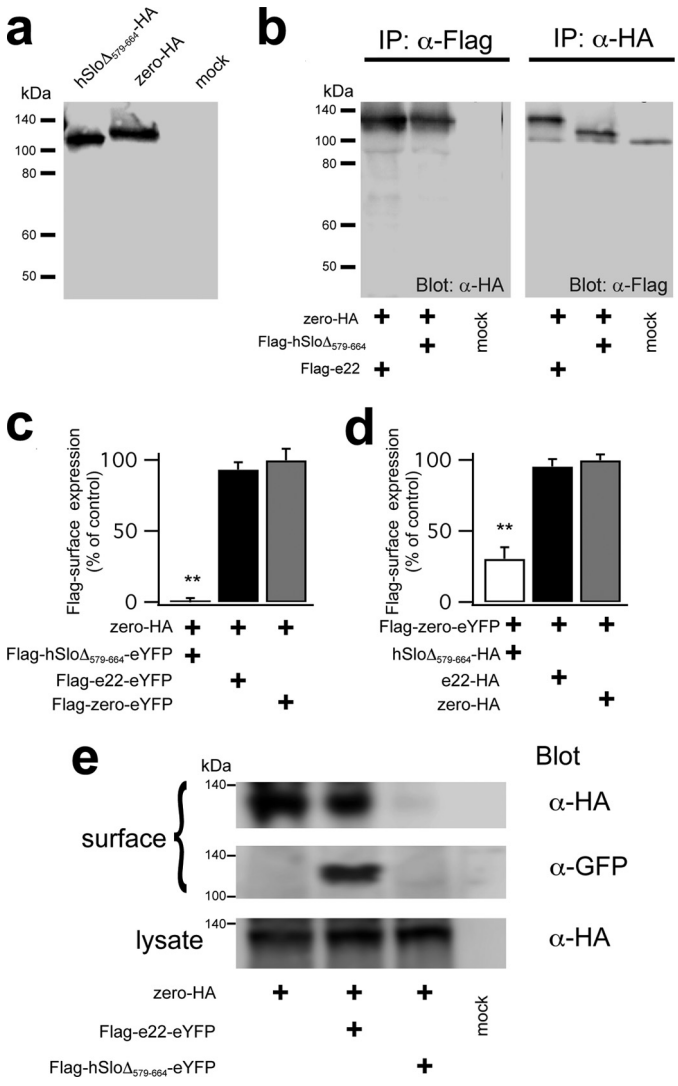

FIGURE 3. **The hSloΔ$_{579-664}$ variant is a dominant negative of cell surface expression.** *a*, Western blot of total cell lysates from the FLAG-hSloΔ$_{579-664}$-HA and FLAG-zero-HA variants expressed in HEK293 cells. *b*, representative blots from co-immunoprecipitation (*IP*) experiments from HEK293 cells co-expressing the zero-HA variant with either the FLAG-hSloΔ$_{579-664}$ or FLAG-e22 variants. *Left panel*, channels were immunoprecipitated with mouse anti-FLAG M2 antibody, and blots were probed with rabbit anti-HA antibody. *Right panel*, channels were immunoprecipitated with rabbit anti-HA antibody and probed with mouse anti-FLAG M2 antibody. *c*, zero-HA subunits were co-expressed with either FLAG-hSloΔ$_{579-664}$-eYFP, FLAG-e22-eYFP, or FLAG-zero-eYFP channels in HEK293 cells, and cell surface (FLAG) expression was quantified. *d*, FLAG-zero-eYFP subunits were co-expressed with either hSloΔ$_{579-664}$-HA, e22-HA or zero-HA channels in HEK293 cells. In *c* and *d*, the data are the cell surface FLAG staining values expressed as percentages of control (surface FLAG-zero-eYFP levels when co-expressed with the zero-HA construct) under nonpermeabilized conditions. *e*, representative Western blots of HA or green fluorescent protein immunoreactivity from cell surface biotinylation assays of HEK293 cells expressing the indicated constructs and corresponding whole cell lysates. All data are the means ± S.E. from a minimum of six independent experiments with >700 cells analyzed/group in *c* and *d* and three independent experiments in *a*, *b*, and *e*. **, $p < 0.01$, ANOVA with post hoc Dunnett's test compared with other groups.

to mock transfected HEK293 cells, reflects membrane hyperpolarization (BK channel activation).

BK channel activation was fully blocked by 1–10 μM paxilline (not shown; see Ref. 23). The data were analyzed with SoftMax Pro and exported to Igor Pro, Microsoft Excel, and/or Prism for further analysis. To compare between mutants, the relative fluorescent units were determined 70 s into the assay. The response of each channel mutant was then normalized to the hyperpolarization response of the zero channel (100%).

Statistics—Statistical analysis was performed using Igor Pro v6.0 using a one-way ANOVA with a Dunnett's post hoc test for significance between groups at $p < 0.05$.

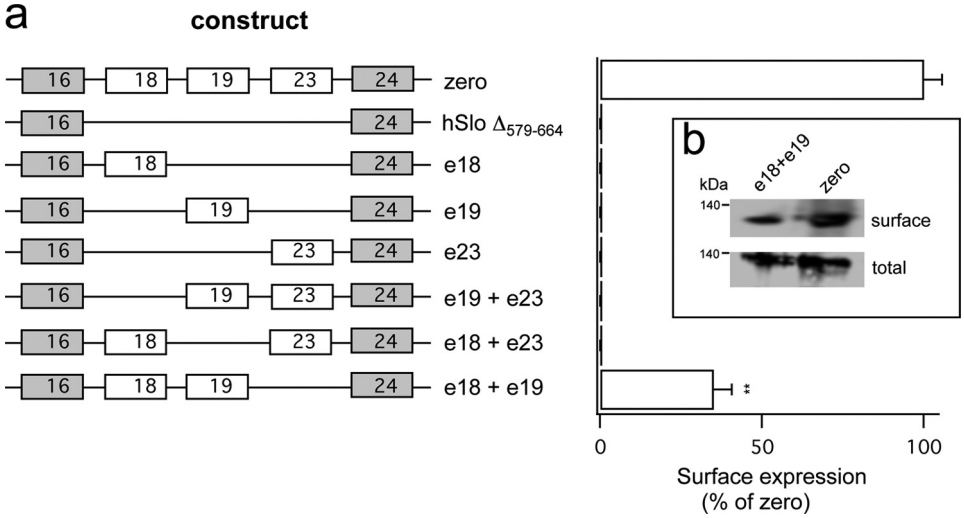

FIGURE 4. **Exon 18 and exon 19, but not exon 23, are essential for BK channel cell surface expression.** *a*, in-frame deletion mutants of exons 18, 19, and 23 that are excluded in the hSlo$\Delta_{579-664}$ trafficking-deficient variant were expressed in HEK293 cells. Constructs contained an N-terminal extracellular FLAG tag and a C-terminal HA tag. Cell surface expression was assayed in imaging experiments under nonpermeabilized conditions by probing for the FLAG tag as in Fig. 3. The data are expressed as percentages of control FLAG-zero-HA cell surface expression. *b*, *inset*, representative Western blots of HA immunoreactivity from cell surface biotinylation assays of HEK293 cells expressing the zero or e18 + e19 constructs and corresponding whole cell lysates. All of the data are the means ± S.E. from a minimum of three independent experiments with >650 cells analyzed/group. **, $p < 0.01$, ANOVA with post hoc Dunnett's test compared with all other groups.

RESULTS

Cloning of a Human BK Channel Splice Variant with an 86-Amino Acid Deletion in the RCK1-RCK2 Linker, hSlo$\Delta_{579-664}$—We isolated a human BK channel splice variant, hSlo$\Delta_{579-664}$, from human colon tissue cDNAs using reverse transcription-PCR primers to amplify the region spanning exons 15–25 (Fig. 1*a*) that encompasses the C-terminal region of the predicted RCK1 domain and the unstructured (NORS) RCK1-RCK2 linker (18). Using these primers, multiple sized amplicons were generated that encoded for previously identified splice variants at sites of splicing C1 and C2, including the human zero variant that lacks inserts at these sites (Fig. 1*a*). From the amplicons we identified a significantly smaller sized product than the insertless zero variant that results from skipping three exons, producing a deletion of 86 amino acids between isoleucine 579 and arginine 664. The exclusion of exons 18, 19, and 23 results in splicing from exons 16 to 24, leading to an in-frame deletion with the splice variant retaining the more C-terminal RCK2 domain (25), the "calcium bowl" required for calcium sensitivity of the channels, as well as C-terminal ER export signals (16). We have named this splice variant hSlo$\Delta_{579-664}$ (based on amino acid numbering system for hSlo variant starting at MDALI, accession number AAD31173). This variant represents the human ortholog of the previously described rat splice variant SVcyt (17). To quantify the expression of mRNAs encoding the hSlo$\Delta_{579-664}$ splice variant in different human tissues, we designed and carried out TaqMan™ real time quantitative PCR assays. Total BK channel transcripts (normalized to β-actin) were highest in prostate, brain, muscle, and uterus and lowest in heart, thyroid, plasma blood cell, and bone marrow (data not shown). In most tissues, the proportion of total BK transcripts that expressed the new variant, hSlo$\Delta_{579-664}$, was less than 10% (Fig. 1*b*). The proportional expression of the new variant hSlo$\Delta_{579-664}$, was highest in those tissues, such as heart, thyroid, plasma blood cell, and fetal liver, which express the lowest total BK channel transcript levels.

hSlo$\Delta_{579-664}$ Is a Dominant Negative of Cell Surface Expression—Fusion of green fluorescent protein to the C terminus of the rat SVcyt homolog resulted in trapping of the SVcyt variant into the cytoplasm of mammalian cells with no detectable current (17). In addition, recent data suggest that deletion of >30 amino acids in the RCK1-RCK2 linker results in nonfunctional channels (18). To address whether the hSlo$\Delta_{579-664}$ splice variant could be expressed at the cell surface and form functional channels, we took two approaches.

First, we asked whether single channel/macropatch BK currents were detectable in HEK293 cells expressing the hSlo$\Delta_{579-664}$ variant using both untagged constructs as well as channels with an N-terminal FLAG epitope and a C-terminal HA epitope. No identifiable BK channel currents were observed in either 39 cell attached patches or 29 excised inside out patches exposed over the potential range ±100 mV and with >100 μM free calcium. In contrast, using the zero variant under identical conditions, we observed multiple channels in >55% of patches in cell-attached or excised patch configurations (data not shown). A similar lack of functional expression was also observed in fluorescent membrane potential assays (*e.g.* see Fig. 8).

Second, to determine whether the hSlo$\Delta_{579-664}$ was expressed at the cell surface, we transfected the FLAG-hSlo$\Delta_{579-664}$-HA construct in HEK293 cells (Fig. 2). In nonpermeabilized cells, the extracellular N-terminal FLAG tag could not be detected in immunofluorescence assays in any cell ($n > 1500$ cells analyzed), suggesting that the channel could not insert into the plasma membrane (Fig. 2). In contrast, in the same experiments two distinct splice variants (FLAG-e22-HA and FLAG-zero-HA variants (15)) showed robust FLAG tag expression at the cell surface in >90% of nonpermeabilized, transfected cells (Fig. 2). To confirm that the lack of FLAG epitope detection with the FLAG-hSlo$\Delta_{579-664}$-HA variant was not due to a lack of protein expression, we analyzed expression of the HA epitope tag in the same cells under permeabilized conditions (Fig. 2*a*). The hSlo$\Delta_{579-664}$ variant displayed robust expression in both immunocytochemical (Fig. 2*a*) and Western blot (Fig. 3*a*) assays. Indeed, total cellular protein levels of the hSlo$\Delta_{579-664}$ construct were not significantly different from that observed with zero constructs, suggesting that the lack of cell surface expression does not result from decreased synthesis and/or increased degradation of the hSlo$\Delta_{579-664}$

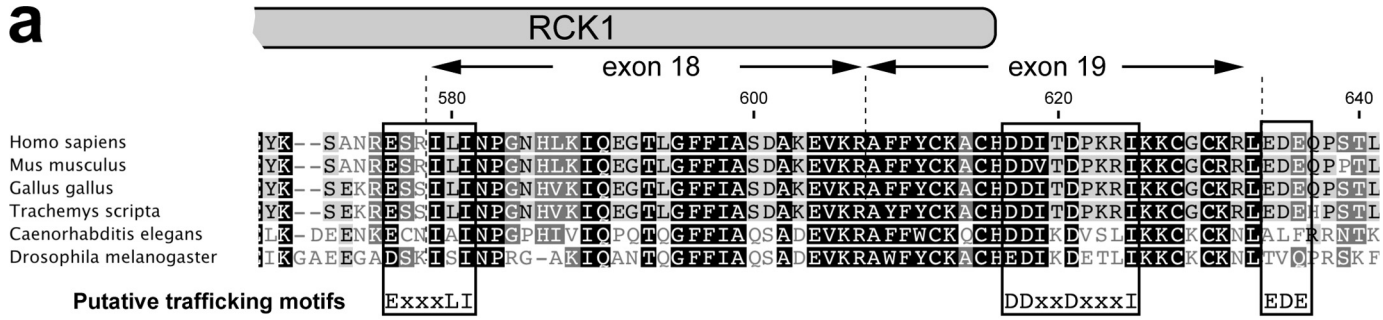

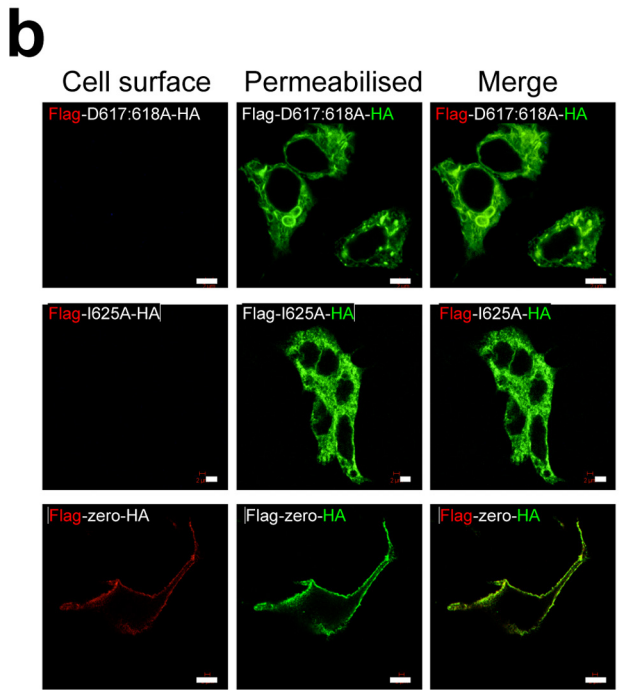

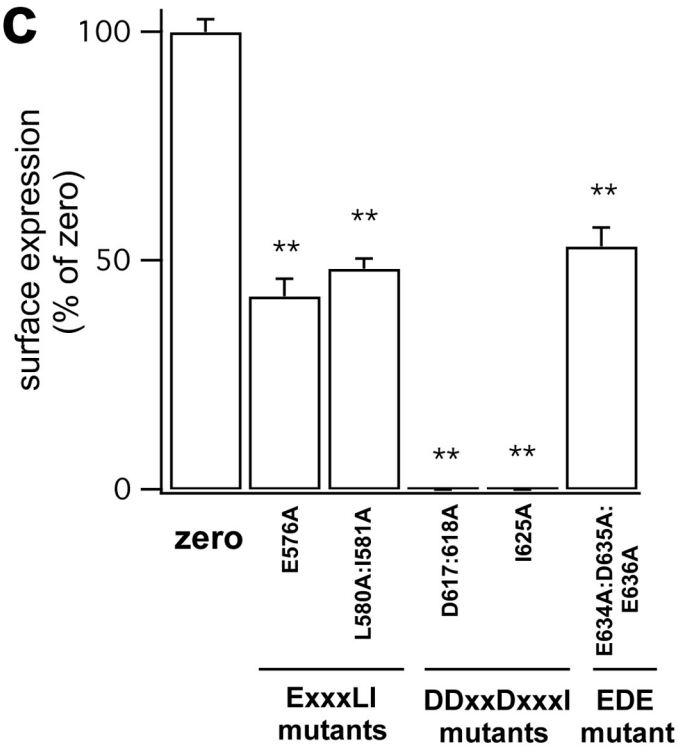

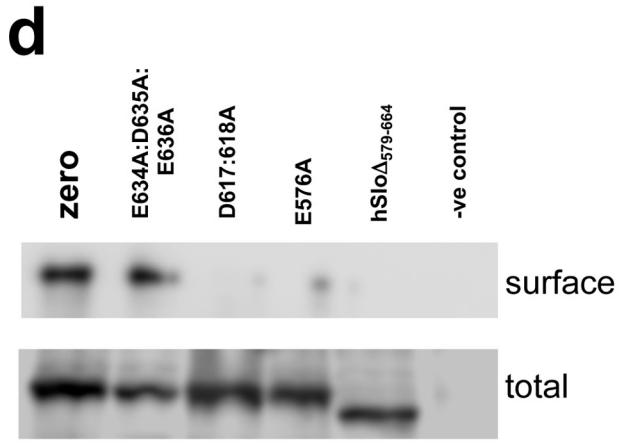

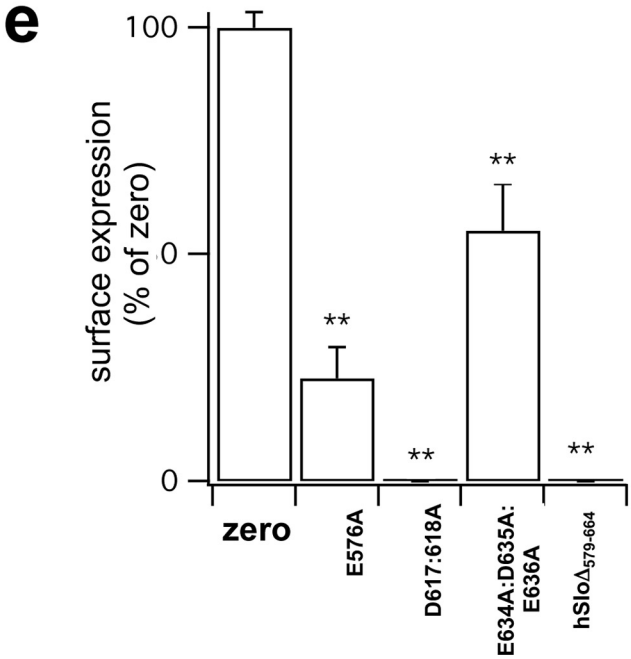

variant (Fig. 3*a*). As expected from the 86-amino acid deletion, the hSlo$\Delta_{579-664}$ variant was detectable as an ~110-kDa immunoreactive band in Western blots (Fig. 3*a*). Probing for the hSlo$\Delta_{579-664}$ variant in intact HEK293 cells revealed that the hSlo$\Delta_{579-664}$ variant was retained in intracellular structures within the cytoplasm. Although a functional role for intracellular BK channels has been reported, for example in mitochondria (26), the hSlo$\Delta_{579-664}$ variant did not co-localize with mitochondrial markers (data not shown) in HEK293 cells but was extensively trapped in the ER (Figs. 5 and 6). Taken together, these data suggest that a homomeric hSlo$\Delta_{579-664}$ variant is trafficking-deficient, is trapped intracellularly, and is thus unable to form functional channels at the plasma membrane.

Because BK channels exist as tetramers, the hSlo$\Delta_{579-664}$ variant may be able to assemble with other BK channel splice variant α-subunits. To test this idea, we first performed reciprocal co-immunoprecipitation assays by expressing a FLAG-tagged hSlo$\Delta_{579-664}$ variant with HA-tagged zero subunits (Fig. 3*b*). Co-expression of the FLAG-hSlo$\Delta_{579-664}$ variant with the zero-HA variant resulted in robust, reciprocal co-immunoprecipitation of both variants (Fig. 3*b*). Similar co-immunoprecipitation was observed using the e22 splice variant (Fig. 3*b*), which also shows robust cell surface expression (Fig. 2), or between hSlo$\Delta_{579-664}$-HA and FLAG-zero (not shown). Thus hSlo$\Delta_{579-664}$ can heteromultimerize with other BK channel α-subunits, suggesting that channel assembly *per se* is not compromised.

We next asked whether cell surface expression of the hSlo$\Delta_{579-664}$ variant may be rescued upon co-expression with cell surface trafficking competent α-subunits. We thus expressed a FLAG-hSlo$\Delta_{579-664}$-eYFP variant with the zero-HA construct to allow simultaneous monitoring of expression of both constructs in the same cell while assaying for the external FLAG epitope tag (Fig. 3*c*) in nonpermeabilized cell surface assays. However, no significant rescue of the hSlo$\Delta_{579-664}$ variant was observed. As controls, the co-expression of zero-HA had no effect on either FLAG-e22-eYFP or FLAG-zero-eYFP surface expression (Fig. 3*c*). This was confirmed in cell surface biotinylation assays (Fig. 3*e*).

Because other BK channel α-subunit splice variants may act as dominant negative regulators of cell surface expression (15, 27), we thus asked whether the hSlo$\Delta_{579-664}$ variant could control cell surface expression of other variants. Using a FLAG-tagged zero-eYFP construct (FLAG-zero-eYFP) co-expressed with the hSlo$\Delta_{579-664}$-HA, zero-HA, or e22-HA variants allowed us to assay cells in which both constructs were co-expressed while independently assaying for cell surface expression using the FLAG epitope. Co-expression of FLAG-zero-eYFP and hSlo$\Delta_{579-664}$-HA constructs resulted in a significant reduction (>60%) of cell surface expression of FLAG-zero-eYFP (Fig. 3*d*). The effect of hSlo$\Delta_{579-664}$-HA was not due to an overexpression artifact because co-expression of FLAG-zero-eYFP with e22-HA was without effect on FLAG-zero-eYFP surface expression.

Identical data were obtained in cells co-expressing FLAG-zero channels lacking the eYFP tag with hSlo$\Delta_{579-664}$-HA; surface FLAG expression in the presence of hSlo$\Delta_{579-664}$-HA was 37.6 ± 4.2% of FLAG-zero, whereas co-expression with e22-HA resulted in FLAG surface expression that was 95.0 ± 5.6% of FLAG-zero channels. The residual cell surface expression of FLAG-zero channels in these immunofluorescence assays when co-expressed with hSlo$\Delta_{579-664}$ most likely results from formation of homomultimers of FLAG-zero at the cell surface because in both imaging and cell surface biotinylation assays (Fig. 3*e*), we could not detect hSlo$\Delta_{579-664}$ at the cell surface. As hSlo$\Delta_{579-664}$ and zero channels express at similar levels in HEK293 cells (Fig. 3*a*); this may indicate that the efficiency of heteromultimerization is compromised when channel subunits incorporate the hSlo$\Delta_{579-664}$ variant.

The dominant negative effects of hSlo$\Delta_{579-664}$ data were recapitulated with biochemical assays of cell surface biotinylation (Fig. 3*e*). No significant surface expression could be detected of either zero-HA or FLAG-hSlo$\Delta_{579-664}$-eYFP in cells expressing both constructs supporting the dominant negative role of hSlo$\Delta_{579-664}$. In contrast, robust surface expression of both FLAG-e22-eYFP and zero-HA could be detected in cells co-expressing these constructs (Fig. 3*e*). These data suggest that the hSlo$\Delta_{579-664}$ variant acts as a dominant negative of cell surface expression.

Exons 18 and 19, but Not Exon 23, Are Essential for Cell Surface Expression—Because the hSlo$\Delta_{579-664}$ variant could heteromultimerize with other BK channel α-subunits and act as a dominant negative of cell surface expression, we hypothesized that the mechanism underlying the trafficking defect was not a result of incorrect channel assembly, because of the 86-amino acid deletion, but rather arose from the deletion of essential, discrete trafficking signals within the RCK-RCK2 linker upon exclusion of exons 18, 19, and 23 in the hSlo$\Delta_{579-664}$ variant.

As a first step to test this idea, we assayed the contribution of the individual exons 18, 19, and 23, which are excluded in the hSlo$\Delta_{579-664}$ variant, to cell surface expression by determining

FIGURE 5. **An acidic cluster-like motif in exon 19 is essential for cell surface expression.** *a*, ClustalW sequence alignment of exons 18 and exon 19 from human (*Homo sapiens*, accession number AAD31173), mouse (*Mus musculus*, accession number AAL69971), chicken (*Gallus gallus*, accession number NP_989555), turtle (*Trachemys scripta*, accession number AAC41281), worm (*Caenorhabditis elegans*, accession number NP_001024259), and fly (*Drosophila melanogaster*, accession number NP_524486). The exons form the extreme C terminus of the computationally predicted RCK1 domain and the start of the unstructured RCK1-RCK2 linker. Three putative trafficking/sorting motifs predicted in this region are shown with only the acidic DD*XXD*X*XX*I motif fully conserved across phyla. Amino acid numbering is based on the amino acid sequence of the human sequence AAD31173 that starts with MDALI. *b*, representative confocal sections from HEK293 cells transfected with the DD*XXD*X*XX*I mutants (D617A/D618A and I625A) and zero channels with the N-terminal epitope labeled under nonpermeabilized conditions and the intracellular C-terminal HA tag under permeabilized conditions. The *scale bars* are 2 μm. *c*, summary bar chart of cell surface FLAG expression of trafficking/sorting motif mutants in which amino acids within the proposed motifs are mutated to alanine. Cell surface expression is expressed as a percentage of the FLAG-zero-HA construct using FLAG surface expression in nonpermeabilized assays as in Fig. 2. *d*, representative Western blots of HA immunoreactivity from cell surface biotinylation assays of HEK293 cells expressing the corresponding constructs and whole cell lysates. *e*, summary bar chart of cell surface biotinylation data as in *d*. All of the data are the means ± S.E. from a minimum of three independent experiments with >720 cells analyzed/group in *c*. **, $p < 0.01$, ANOVA with post hoc Dunnett's test compared with the zero channel.

whether cell surface expression of the hSlo$\Delta_{579-664}$ variant could be rescued by the reinsertion of single or double exons in combination (Fig. 4). We thus generated a number of chimaeras in which one or two exons were ligated in-frame between exons 16 and 24 in the hSlo$\Delta_{579-664}$ variant. Inclusion of exons 18, 19, or 23 alone (constructs e18, e19, or e23) did not rescue any cell surface expression of the hSlo$\Delta_{579-664}$ variant. Similarly, inclusion of exon 19 with exon 23 (e19 + e23) or exon 18 with exon 23 (e18 + e23) did not rescue cell surface expression of the hSlo$\Delta_{579-664}$ variant. In contrast, inclusion of both exons 18 and 19 (e18 + e19) partially rescued cell surface expression in both quantitative immunofluorescence assays (Fig. 4*a*) as well cell surface biotinylation assays (Fig. 4*b*). These data suggest that: (i) exon 23 is not essential *per se* for cell surface expression; (ii) the length of the amino acid insertion *per se* is not important for cell surface expression; and (iii) exons 18 and 19 are required for cell surface expression, and thus their exclusion is likely to result in loss of putative trafficking signals.

An Acidic Cluster Motif in the RCK1-RCK2 Linker Is Required for Cell Surface Expression—To further refine our analysis, we aligned exons 18 and 19 from the zero variants of BK channel orthologs from man to flies (Fig. 5*a*). This revealed the high conservation of this region that spans the very C terminus of the computationally predicted RCK1 domain and the start of the unstructured (NORS) RCK1-RCK2 linker region (18).

Examination of the amino acid sequence encoded by exons 18, 19, and 23 (Fig. 5*a*) revealed three regions that may act as putative trafficking motifs: (i) The junction of exon 16 and exon 18 encodes a putative TGN-endosome trafficking signal in vertebrate BK channels (E*XXX*LI) similar to the consensus (D/E)*XXX*L(L/I). However, (D/E)*XXX*L(L/I) motifs show considerable degeneracy (28) with an R*XXX*LL signal exploited in the Glut4 transporter (29) and an E*XXX*LI motif in AQP4 (30). (ii) Exon 19 encodes a putative acidic cluster signal DD*XX*D that is important for trafficking of a number of potassium channels (22, 31–34). In addition, the acidic cluster may also form part of a D*XX*LL-like motif (D*XXX*I) that is predicted (using the PredictProtein server; data not shown) to form a short α-helical structure. Intriguingly, such a short α-helical region is commonly observed in other ER exit signals with little primary sequence homology (16, 35) and is predicted to play an important role in the more C-terminal ER exit signal in BK channels (16). Furthermore, this short α-helical region represents the only computationally predicted structured region in the otherwise unstructured NORS (no regular secondary structure) RCK1-RCK2 linker (18) conserved from man to flies. (iii) The very 5′ start of exon 23 encodes another putative acidic motif (EDE) that is conserved in vertebrates.

We took a site-directed mutagenesis approach using the zero variant to examine the contribution of these putative trafficking signals in BK channel cell surface expression (Fig. 5, *b* and *c*). Mutation of Glu^{576} or of Leu^{580} and Ile^{581} to alanine to disrupt the E*XXX*LI motif at the exon 16-exon 18 junction, as well as alanine mutation of the EDE motif in exon 23, significantly reduced cell surface labeling of the zero variant in imaging assays but did not abolish it (Fig. 5*c*). Furthermore, a combination of mutations at both sites did not abolish cell surface labeling, because expression was still 20.1 ± 4.2% of the zero variant.

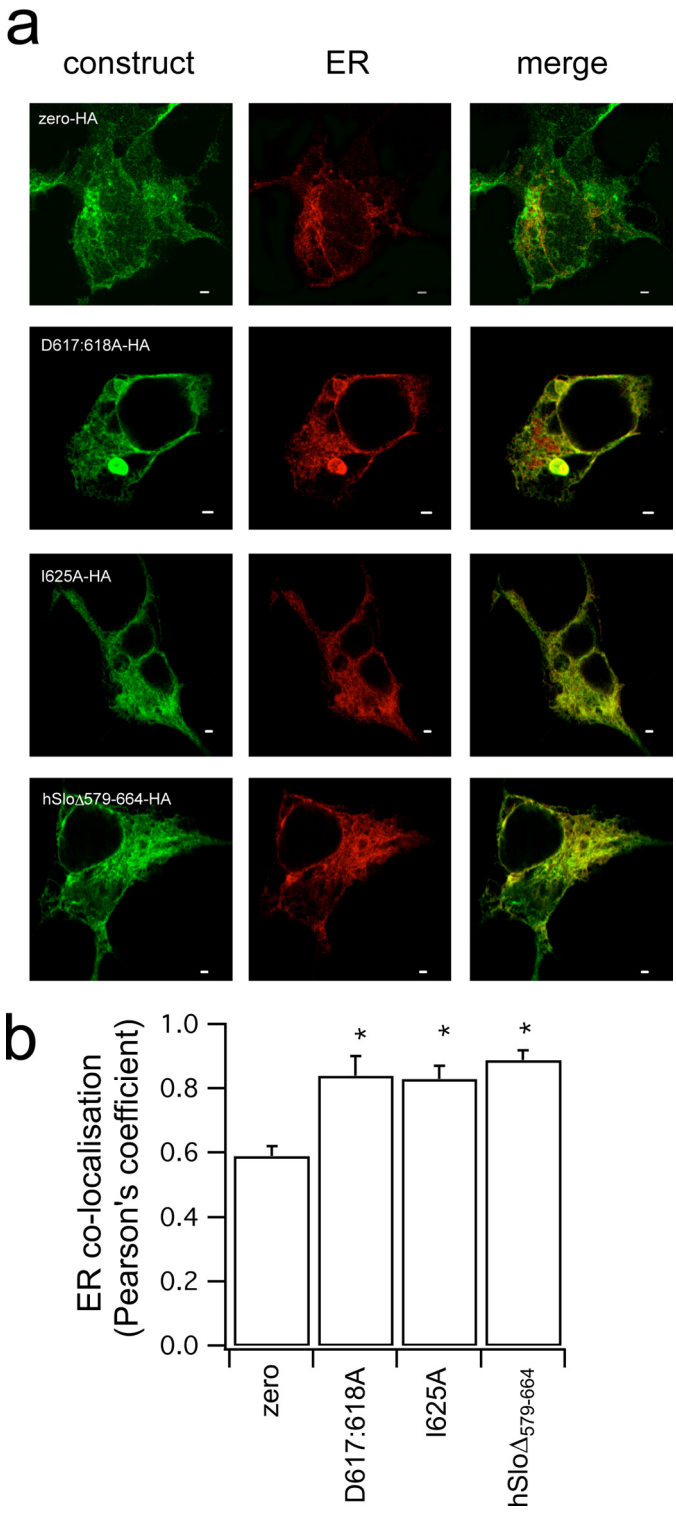

FIGURE 6. **Trafficking-deficient BK channel mutants are trapped in the ER.** *a*, representative single confocal sections from permeabilized cells co-transfected with the corresponding HA-tagged BK channel site-directed mutant (construct, *green*) and the endoplasmic reticulum marker expression plasmid pdsRed-ER (*ER*, *red*). The merged images are shown in the *right-hand panels*. *b*, summary bar graph of Pearson's correlation coefficient for quantitative co-localization of the respective HA-tagged channels with the pdsRed-ER marker (a value of 1.0 would indicate complete co-localization). *, $p < 0.05$, ANOVA with post hoc Dunnett's test compared with the zero channel.

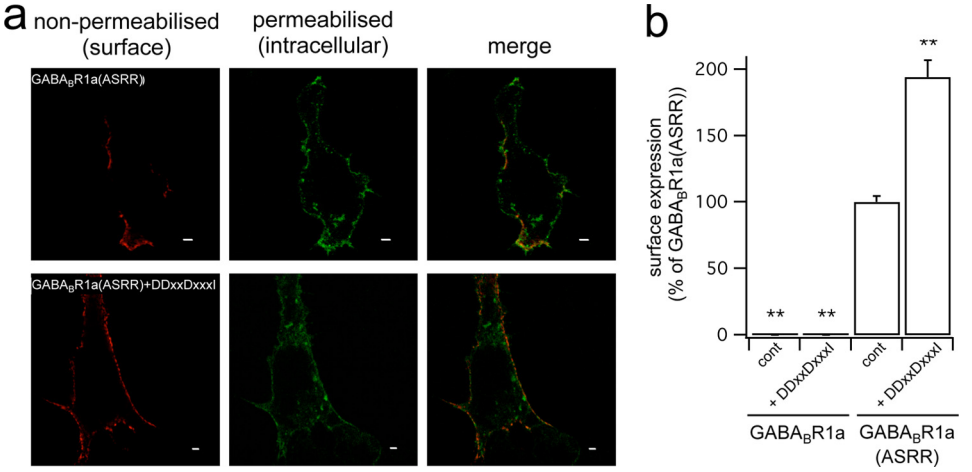

FIGURE 7. **Acidic cluster sequence (DD*XX*D*XXX*I) is a transplantable ER export motif.** *a*, representative single confocal sections from HEK293 cells expressing the GABA$_B$R1a receptor with (*GABA$_B$R1a(ASRR)+DDXXDXXXI*) and without (*GABA$_B$R1a(ASRR)*) the DD*XX*D*XXX*I motif engineered onto the C terminus. The N-terminal (extracellular) HA epitope tag was labeled under nonpermeabilized (*left panels*, *red*) and permeabilized (*middle panels*, *green*) conditions in the same cell with the merged images shown in the *right-hand panels*. The GABA$_B$R1a receptor contained an arginine to alanine mutation (ASRR) compared with the wild type GABA$_B$R1a receptor. The *scale bars* are 2 μm. *b*, summary bar graph of quantitative surface/intracellular HA expression normalized to the ratio for the GABA$_B$R1a(ASRR) expressing cells (100%). **, $p < 0.01$, ANOVA with post hoc Dunnett's test compared with the zero channel (n = 16–19/group).

In contrast, mutation of the DD*XX*D*XXX*I motif (D617A/D618A or I625A constructs) completely abolished cell surface labeling in imaging assays as with the hSlo$\Delta_{579-664}$ variant (Fig. 5, *b* and *c*). To confirm the lack of cell surface expression in these mutants, we also performed cell surface biotinylation assays (Fig. 5, *d* and *e*). Mutation of the DD*XX*D*XXX*I motif (D617A/D618A mutant) again abolished cell surface expression as for the hSlo$\Delta_{579-664}$ splice variant. In contrast, mutation of the E*XXX*LI or EDE motifs (E576A or E634A/D635A/E636A, respectively) significantly reduced but did not abolish cell surface expression of the channel (Fig. 5, *d* and *e*). However, because mutation of the EDE motif alone significantly reduced surface expression, this would suggest that the inability to fully rescue surface expression with the e18 + e19 construct in Fig. 4 is a result of the loss of the EDE sequence within exon 23 in the e18 + e19 construct. Mutation of the DD*XX*D*XXX*I motif also completely abolished cell surface labeling in the e18 + e19 construct, further confirming the essential requirement for this sequence (not shown).

The mutant channels were now predominantly ER-localized as determined by co-localization assays (Fig. 6, *a* and *b*). We determined the Pearson's correlation coefficient in quantitative immunofluorescence imaging assays with the channel constructs upon co-expression with the ER marker pdsRed-ER (Clontech). For the zero variant the coefficient was 0.59 ± 0.05, which was significantly (ANOVA, post hoc Dunnett's test $p <$ 0.01) increased with the hSlo$\Delta_{579-664}$ variant as well as the D617A/D618A and I625A mutants (Fig. 6*b*), demonstrating trapping of these mutants in the ER.

Because the DD*XX*D*XXX*I acidic-like motif plays a dominant role in determining cell surface expression, we thus asked whether this motif could function as a transplantable trafficking signal. We exploited the GABA$_B$R1a receptor (a nonchannel subunit of the G-protein-coupled receptor for the γ-aminobutyric acid neurotransmitter), which is normally retained in the ER by a R*XX*RR-dependent ER retrieval and retention mechanism to examine whether the DD*XX*D*XXX*I motif could enhance cell surface expression of the receptor as for acidic trafficking motifs identified in other potassium channels (22). We engineered the DD*XX*D*XXX*I motif onto the intracellular C terminus of the GABA$_B$R1a receptor and monitored cell surface to intracellular expression by probing for the extracellular N-terminal HA tag under nonpermeablized and permeabilized conditions using quantitative immunofluorescence (Fig. 7). In agreement with previous studies (22), the DD*XX*D*XXX*I motif could not rescue surface expression of the wild type GABA$_B$R1a receptor (Fig. 7*b*). However, in GABA$_B$R1a receptors with an arginine to alanine point mutation in its ER retention/retrieval R*XX*RR motif (ASRR mutant), surface expression of the GABA$_B$R1a receptor was now detectable. Importantly, surface expression was significantly enhanced (almost 2-fold) by transplanting the DD*XX*D*XXX*I motif from the BK channel. Thus the DD*XX*D*XXX*I sequence cannot override the ER retention/retrieval signal but can accelerate ER export in the absence of the R*XX*RR motif as demonstrated for other acidic ER export signals from inwardly rectifying potassium channels (22). To verify that the D617A/D618A and I625A mutations resulted in a significant reduction of functional BK channel expression at the plasma membrane, we exploited a membrane potential assay (24) to interrogate BK channel activation in response to ionomycin-induced (1 μM) calcium influx in HEK293 cells using the voltage-sensitive dye FLIPR blue (Molecular Devices). In response to ionomycin HEK293 cells, expressing the functional zero channel variant elicited a robust hyperpolarization compared with mock transfected HEK293 cells (Fig. 8*a*). No significant hyperpolarization in membrane potential was observed in cells expressing hSlo$\Delta_{579-664}$ (Fig. 8). Membrane hyperpolarization was significantly attenuated (to less than 40% of zero) in cells expressing either the D617A/D618A or the I625A mutant in line with the reduced membrane expression in imaging assays. The residual hyperpolarization with both mutants suggests that low numbers of D617A/D618A and I625A channels may reach the cell surface and that this level is below the limit of detection in our cell surface labeling assays. Taken together, these data reveal that the acidic cluster-like motif in exon 19 represents a transplantable trafficking motif that plays a critical role in controlling cell surface expression of BK channels.

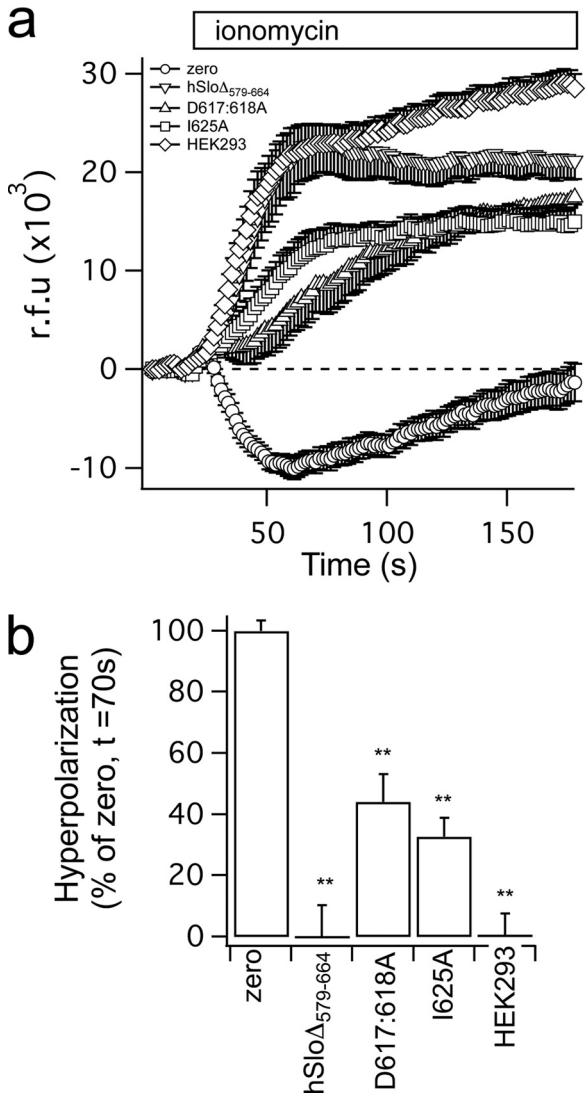

FIGURE 8. **Acidic cluster sequence (DD*XX*D*XXX*I) is required for efficient functional channel expression.** *a*, time course plots of change in relative fluorescence units (*r.f.u*) of the FLIPR blue membrane potential dye in HEK293 cells expressing zero (○), hSlo$\Delta_{579-664}$ (▽), D617A/D618A (△), I625A (■), or mock transfected HEK293 cells (◇) in response to calcium influx induced by 1 μM ionomycin. A decrease in fluorescence relative to the HEK293 cell response indicates a net hyperpolarization of the membrane potential resulting from activation of BK channels. *b*, summary bar chart of the membrane potential change for each construct in *a* expressed as a percentage of the maximal hyperpolarization elicited in HEK293 cells expressing the zero variant (100%). The data were determined at $t = 70$ s in the time course plots in *a*. All of the data are the means ± S.E. ($n = 9–12$). **, $p < 0.01$, ANOVA with post hoc Dunnett's test compared with the zero channel response.

DISCUSSION

We have identified three distinct motifs within the intracellular RCK1-RCK2 linker of BK channels that control their cell surface expression. In particular, an acidic cluster-like motif, DD*XX*D*XXX*I, is critical for cell surface expression and is highly conserved from flies to man. This acidic motif can be transplanted to nonchannel proteins to accelerate ER export but cannot override pre-existing ER retention signals, as described for other acidic motifs (22). Importantly, alternative splicing of a human BK channel splice variant hSlo$\Delta_{579-664}$ that excludes the exons encoding this motif results in a trafficking-deficient BK channel that acts as a dominant negative for cell surface expression.

The DD*XX*D*XXX*I motif may comprise both an acidic cluster motif as well as a degenerate D*XX*LL motif. Indeed in worms and flies, a D*XX*LI motif is retained, whereas the third position is an arginine in vertebrates. Thus, although the motif does not share sequence conservation with other trafficking motifs, it is intriguing that the D*XXX*I motif is predicted to form a short α-helix at the very beginning of the predicted linker region that otherwise lacks a regular secondary structure (18). A short α-helical structure is a feature commonly associated with ER export signals that do not show sequence homology (16, 35) as suggested for the more C-terminal ER export sequence in BK channels (16). Acidic cluster motifs are also commonly used as ER export signals, including in other potassium channels (22, 31, 33, 34). These features also appear crucial for cell surface expression of BK channels. In contrast, the EDE acidic cluster in exon 23 is not essential for surface expression, but mutagenesis does significantly reduce it. Similar acidic clusters have been reported in other transmembrane proteins including inwardly rectifying and TASK3 potassium channels (22, 31, 33, 34). The E*XXX*LI motif is most likely a member of the (D/E)*XXX*L(L/I) sorting motif that shows considerable degeneracy; in fact, in AQP4 channels an E*XXX*LI motif is essential for correct trafficking (30).

The demonstration here of *exclusion* of the ER export DD*XX*D*XXX*I acidic motif by alternative splicing in the intracellular C-terminal linker of BK channels nicely contrasts with the *inclusion* of an hydrophobic (CVLF) ER retention signal through alternative splicing of the N-terminal intracellular S0-S1 loop of BK channels (12). Taken together, these data strongly support the hypothesis that alternative splicing plays a major role in controlling cell surface expression of ion channels and that this can be achieved in the same channel by diametrically opposite mechanisms: through either exclusion or inclusion of cognate trafficking motifs.

Why do BK channels have multiple trafficking motifs whose inclusion can be controlled by alternative splicing? Because BK channels have pleitropic functions in virtually all tissues of the body, it is likely that multiple trafficking and sorting signals are required to allow the correct surface expression and subcellular localization of BK channels relevant to the target tissue of interest. Furthermore, increasing evidence suggests that cell surface expression of BK channels is dynamically regulated, both through signals that may regulate splicing and through post-translational modifications and assembly with distinct regulatory β-subunits. Thus these multiple mechanisms are likely coordinated to expose or mask the correct complement of trafficking and sorting signals to allow appropriate distribution of BK channels within distinct cell types. Indeed, alternative splicing of the rat SVcyt ortholog of hSlo$\Delta_{579-664}$ is dynamically regulated in corporeal tissue in models of diabetes (17). Whether the dominant negative function of hSlo$\Delta_{579-664}$ is physiologically relevant in this or other model systems remains to be explored. Clearly the inclusion (13, 27) or exclusion (as observed with the hSlo$\Delta_{579-664}$ variant here) of trafficking motifs through alternative splicing most likely represents a fundamental mechanism for controlling BK channel cell sur-

face expression under a variety of physiological and pathophysiological conditions.

Acknowledgments—We thank Heather McClafferty and Lijun Tian and other members of the respective laboratories for critical discussions during this work and Trudi Gillespie and the IMPACT imaging facility for assistance in confocal imaging assays. The $GABA_{BR}1a$ receptor wild type and ASRR constructs were generous gifts from Lily Jan (University of California at San Francisco).

REFERENCES

1. Sausbier, M., Arntz, C., Bucurenciu, I., Zhao, H., Zhou, X. B., Sausbier, U., Feil, S., Kamm, S., Essin, K., Sailer, C. A., Abdullah, U., Krippeit-Drews, P., Feil, R., Hofmann, F., Knaus, H. G., Kenyon, C., Shipston, M. J., Storm, J. F., Neuhuber, W., Korth, M., Schubert, R., Gollasch, M., and Ruth, P. (2005) *Circulation* **112,** 60–68
2. Brenner, R., Peréz, G. J., Bonev, A. D., Eckman, D. M., Kosek, J. C., Wiler, S. W., Patterson, A. J., Nelson, M. T., and Aldrich, R. W. (2000) *Nature* **407,** 870–876
3. Raffaelli, G., Saviane, C., Mohajerani, M. H., Pedarzani, P., and Cherubini, E. (2004) *J. Physiol.* **557,** 147–157
4. Sausbier, M., Hu, H., Arntz, C., Feil, S., Kamm, S., Adelsberger, H., Sausbier, U., Sailer, C. A., Feil, R., Hofmann, F., Korth, M., Shipston, M. J., Knaus, H. G., Wolfer, D. P., Pedroarena, C. M., Storm, J. F., and Ruth, P. (2004) *Proc. Natl. Acad. Sci. U.S.A.* **101,** 9474–9478
5. Du, W., Bautista, J. F., Yang, H., Diez-Sampedro, A., You, S. A., Wang, L., Kotagal, P., Lüders, H. O., Shi, J., Cui, J., Richerson, G. B., and Wang, Q. K. (2005) *Nat. Genet.* **37,** 733–738
6. Meredith, A. L., Thorneloe, K. S., Werner, M. E., Nelson, M. T., and Aldrich, R. W. (2004) *J. Biol. Chem.* **279,** 36746–36752
7. Werner, M. E., Zvara, P., Meredith, A. L., Aldrich, R. W., and Nelson, M. T. (2005) *J. Physiol.* **567,** 545–556
8. Song, M., Zhu, N., Olcese, R., Barila, B., Toro, L., and Stefani, E. (1999) *FEBS Lett.* **460,** 427–432
9. Marijic, J., Li, Q., Song, M., Nishimaru, K., Stefani, E., and Toro, L. (2001) *Circ. Res.* **88,** 210–216
10. Sørensen, M. V., Matos, J. E., Sausbier, M., Sausbier, U., Ruth, P., Praetorius, H. A., and Leipziger, J. (2008) *J. Physiol.* **586,** 4251–4264
11. Butler, A., Tsunoda, S., McCobb, D. P., Wei, A., and Salkoff, L. (1993) *Science* **261,** 221–224
12. Zarei, M. M., Eghbali, M., Alioua, A., Song, M., Knaus, H. G., Stefani, E., and Toro, L. (2004) *Proc. Natl. Acad. Sci. U.S.A.* **101,** 10072–10077
13. Korovkina, V. P., Brainard, A. M., and England, S. K. (2006) *J. Physiol.* **573,** 329–341
14. Ma, D., Nakata, T., Zhang, G., Hoshi, T., Li, M., and Shikano, S. (2007) *FEBS Lett.* **581,** 1000–1008
15. Chen, L., Tian, L., MacDonald, S. H., McClafferty, H., Hammond, M. S., Huibant, J. M., Ruth, P., Knaus, H. G., and Shipston, M. J. (2005) *J. Biol. Chem.* **280,** 33599–33609
16. Kwon, S. H., and Guggino, W. B. (2004) *Proc. Natl. Acad. Sci. U.S.A.* **101,** 15237–15242
17. Davies, K. P., Zhao, W., Tar, M., Figueroa, J. C., Desai, P., Verselis, V. K., Kronengold, J., Wang, H. Z., Melman, A., and Christ, G. J. (2007) *Eur. Urol.* **52,** 1229–1237
18. Lee, J. H., Kim, H. J., Kim, H. D., Lee, B. C., Chun, J. S., and Park, C. S. (2009) *Biophys. J.* **97,** 730–737
19. Tian, L., Jeffries, O., McClafferty, H., Molyvdas, A., Rowe, I. C., Saleem, F., Chen, L., Greaves, J., Chamberlain, L. H., Knaus, H. G., Ruth, P., and Shipston, M. J. (2008) *Proc. Natl. Acad. Sci. U.S.A.* **105,** 21006–21011
20. Tian, L., Coghill, L. S., McClafferty, H., MacDonald, S. H., Antoni, F. A., Ruth, P., Knaus, H. G., and Shipston, M. J. (2004) *Proc. Natl. Acad. Sci. U.S.A.* **101,** 11897–11902
21. Tian, L., Duncan, R. R., Hammond, M. S., Coghill, L. S., Wen, H., Rusinova, R., Clark, A. G., Levitan, I. B., and Shipston, M. J. (2001) *J. Biol. Chem.* **276,** 7717–7720
22. Ma, D., Zerangue, N., Lin, Y. F., Collins, A., Yu, M., Jan, Y. N., and Jan, L. Y. (2001) *Science* **291,** 316–319
23. Rickman, C., Medine, C. N., Bergmann, A., and Duncan, R. R. (2007) *J. Biol. Chem.* **282,** 12097–12103
24. Saleem, F., Rowe, I. C., and Shipston, M. J. (2009) *Br. J. Pharmacol.* **156,** 143–152
25. Yusifov, T., Savalli, N., Gandhi, C. S., Ottolia, M., and Olcese, R. (2008) *Proc. Natl. Acad. Sci. U.S.A.* **105,** 376–381
26. Xu, W., Liu, Y., Wang, S., McDonald, T., Van Eyk, J. E., Sidor, A., and O'Rourke, B. (2002) *Science* **298,** 1029–1033
27. Zarei, M. M., Zhu, N., Alioua, A., Eghbali, M., Stefani, E., and Toro, L. (2001) *J. Biol. Chem.* **276,** 16232–16239
28. Bonifacino, J. S., and Traub, L. M. (2003) *Annu. Rev. Biochem.* **72,** 395–447
29. Sandoval, I. V., Martinez-Arca, S., Valdueza, J., Palacios, S., and Holman, G. D. (2000) *J. Biol. Chem.* **275,** 39874–39885
30. Madrid, R., Le Maout, S., Barrault, M. B., Janvier, K., Benichou, S., and Mérot, J. (2001) *EMBO J.* **20,** 7008–7021
31. Ma, D., Zerangue, N., Raab-Graham, K., Fried, S. R., Jan, Y. N., and Jan, L. Y. (2002) *Neuron* **33,** 715–729
32. Mikosch, M., Käberich, K., and Homann, U. (2009) *Traffic* **10,** 1481–1487
33. Taneja, T. K., Mankouri, J., Karnik, R., Kannan, S., Smith, A. J., Munsey, T., Christesen, H. B., Beech, D. J., and Sivaprasadarao, A. (2009) *Hum. Mol. Gen.* **18,** 2400–2413
34. Zuzarte, M., Rinné, S., Schlichthörl, G., Schubert, A., Daut, J., and Preisig-Müller, R. (2007) *Traffic* **8,** 1093–1100
35. Sevier, C. S., Weisz, O. A., Davis, M., and Machamer, C. E. (2000) *Mol. Biol. Cell* **11,** 13–22

⌘ *Author's Choice*

THE JOURNAL OF BIOLOGICAL CHEMISTRY VOL. 285, NO. 31, pp. 23954–23962, July 30, 2010

Multiple Palmitoyltransferases Are Required for Palmitoylation-dependent Regulation of Large Conductance Calcium- and Voltage-activated Potassium Channels*

Received for publication, April 24, 2010, and in revised form, May 26, 2010 Published, JBC Papers in Press, May 27, 2010, DOI 10.1074/jbc.M110.137802

Lijun Tian, Heather McClafferty, Owen Jeffries[1], and Michael J. Shipston[2]

From the Centre for Integrative Physiology, College of Medicine & Veterinary Medicine, University of Edinburgh, Edinburgh EH89XD, Scotland, United Kingdom

Palmitoylation is emerging as an important and dynamic regulator of ion channel function; however, the specificity with which the large family of acyl palmitoyltransferases (zinc finger Asp-His-His-Cys type-containing acyl palmitoyltransferase (DHHCs)) control channel palmitoylation is poorly understood. We have previously demonstrated that the alternatively spliced stress-regulated exon (STREX) variant of the intracellular C-terminal domain of the large conductance calcium- and voltage-activated potassium (BK) channels is palmitoylated and targets the STREX domain to the plasma membrane. Using a combined imaging, biochemical, and functional approach coupled with loss-of-function (small interfering RNA knockdown of endogenous DHHCs) and gain-of-function (overexpression of recombinant DHHCs) assays, we demonstrate that multiple DHHCs control palmitoylation of the C terminus of STREX channels, the association of the STREX domain with the plasma membrane, and functional channel regulation. Cysteine residues 12 and 13 within the STREX insert were the only endogenously palmitoylated residues in the entire C terminus of the STREX channel. Palmitoylation of this dicysteine motif was controlled by DHHCs 3, 5, 7, 9, and 17, although DHHC17 showed the greatest specificity for this site upon overexpression of the cognate DHHC. DHHCs that palmitoylated the channel also co-assembled with the channel in co-immunoprecipitation experiments, and knockdown of any of these DHHCs blocked regulation of the channel by protein kinase A-dependent phosphorylation. Taken together our data reveal that a subset of DHHCs controls STREX palmitoylation and function and suggest that DHHC17 may preferentially target cysteine-rich domains. Finally, our approach may prove useful in elucidating the specificity of DHHC palmitoylation of intracellular domains of other ion channels and transmembrane proteins.

S-Palmitoylation, the reversible addition of 16-carbon saturated palmitic acid to intracellular cysteine residues through a labile thioester linkage (1–5), is emerging as an important dynamic and potent determinant of ion channel function. Palmitoylation controls cell surface expression and regulation of many ligand-gated ion channels, including α-amino-3-hydroxyl-5-methyl-4-isoxazole-propionate (6), *N*-methyl-D-aspartate (7), Kainate (8), P2X7 (9), and γ-aminobutyric acid, type A (10–12). Palmitoylation also controls the function of voltage-gated calcium (13–15), sodium (16), and potassium (17–19) as well as other channels such as AQP4 (20). For example, in Kv1.1 potassium channels palmitoylation controls voltage dependence (18), and in the stress-regulated exon (STREX)[3] splice variant of large conductance calcium- and voltage-activated potassium (BK) channels, palmitoylation determines channel regulation by protein phosphorylation (19). However, although functional insights into ion channel regulation by protein palmitoylation are beginning to emerge, the control of channel palmitoylation is poorly understood, as for other palmitoylated proteins (21).

Protein palmitoylation is controlled by the balance of palmitoyl acyltransferases and palmitoyl thioesterases (1–5). Recently the zinc finger DHHC (Asp-His-His-Cys) type-containing protein family has emerged as a large family of palmitoyl acyltransferases with 23 members in the mouse and human genomes (22, 23). Previous studies have implicated the relatively promiscuous palmitoyltransferase DHHC3 (also known as Golgi-specific DHHC zinc finger protein, GODZ) in palmitoylating some ligand-gated ion channels (6, 7, 10, 12). However, the role of DHHC3 or other DHHCs in controlling palmitoylation of other ion channels, including BK channels, is not known. Furthermore, whether different DHHCs display specificity for palmitoylating individual ion channels has not been examined systematically. Elucidation of such DHHC-substrate relationships would provide significant insight into both the functional role of ion channel palmitoylation and the specificity of DHHCs for diverse target proteins.

We have previously demonstrated that a dicysteine motif (Cys^{12}-Cys^{13}) within the alternatively spliced STREX insert of the intracellular C terminus of BK channels (see Fig. 1) is palmitoylated and targets the C terminus to the plasma membrane in the absence of the transmembrane domains (19). In this manuscript, we have thus asked which DHHCs are responsible for palmitoylation of the STREX domain of the BK channel. We

* This work was supported by the Wellcome Trust.
⌘ *Author's Choice*—Final version full access.
[1] Recipient of a Biotechnology and Biological Sciences Research Council Ph.D. studentship.
[2] To whom correspondence should be addressed. Tel.: 44-131-6503253; Fax: 44-131-6506523; E-mail: mike.shipston@ed.ac.uk.

[3] The abbreviations used are: STREX, stress-regulated exon; BK channel, large conductance calcium- and voltage-activated potassium channel; DHHC, zinc finger Asp-His-His-Cys type-containing acyl palmitoyltransferase; HEK293, human embryonic kidney 293 cell; qRT, quantitative real time; siRNA, small interfering RNA; PKA, protein kinase A; PKAc, catalytic subunit of PKA; DMEM, Dulbecco's modified Eagle's medium; PBS, phosphate-buffered saline; HA, hemagglutinin; GFP, green fluorescent protein; YFP, yellow fluorescent protein; CRD, cysteine-rich domain.

took advantage of the robust endogenous palmitoylation of STREX channels in human embryonic kidney 293 (HEK293) cells as an assay system to systematically exploit both loss and gain of function approaches, through siRNA-mediated knockdown of endogenous DHHCs and overexpression of murine recombinant DHHCs, respectively, to interrogate the role of individual DHHCs in controlling STREX palmitoylation. In initial assays we exploited an imaging screen based on the palmitoylation-dependent plasma membrane localization of the intracellular STREX domain of the BK channel in HEK293 cells (19). Our data represent the first systematic analysis of the contribution of individual DHHCs in controlling palmitoylation of a voltage-gated ion channel. These studies reveal that multiple endogenous DHHCs control palmitoylation of STREX and that DHHC17 has the highest selectivity for the STREX Cys^{12}-Cys^{13} motif. Furthermore, we demonstrate that the DHHCs that regulate STREX palmitoylation can also assemble as a complex with the channel and determine the regulation of STREX channels by protein kinase A (PKA) phosphorylation.

EXPERIMENTAL PROCEDURES

Channel Constructs—The generation of full-length, C-terminal, and CRD epitope-tagged constructs of the STREX and ZERO variants of the murine BK channel has been described (19). All mutagenesis was performed using QuikChange mutagenesis (Stratagene) with constructs fully sequenced on both strands to verify sequence integrity.

Cell Culture, Transfection, and RNA Extraction—HEK293 cells were maintained in DMEM containing 10% fetal calf serum in a humidified atmosphere of 95% air, 5% CO_2 at 37 °C. The cells were passaged every 3–7 days using 0.25% trypsin in Hanks' buffered salt solution containing 0.1% EDTA. For RNA extraction or biochemical studies, the cells were grown in 24- or 6-well plates, respectively. For electrophysiological or imaging assays, the cells were plated on glass coverslips within 6-well plates. Twenty-four hours prior to the experiment, the cells were washed, and medium was replaced with DMEM containing ITS serum replacement (Sigma). The cells were transiently transfected at 40–60% confluence using Lipofectamine 2000 (Invitrogen) or FuGENE-HD (Roche Applied Science). For RNA interference, siRNAs were predesigned and supplied by Qiagen. The knockdown of DHHCs was performed in HEK293 cells by using two siRNAs (10–20 nM of each siRNA) for each gene. siRNA transfection was performed using HiperFect (Qiagen), essentially as described by the manufacturer. The respective cDNA was transfected 30 min after the completion of siRNA transfection. RNA extraction was carried out 48–72 h post-siRNA transfection using a High Pure RNA isolation kit (Roche Applied Science) according to the manufacturer's protocols. In all of the imaging and biochemical assays siRNA knockdown of DHHCs was monitored in parallel in each independent experiment. Independent experiments were conducted a minimum of three times in triplicate. The palmitoylation inhibitor 2-bromopalmitate (Sigma) was made as a fresh 100 mM stock in Me_2SO and applied at a final concentration of 100 μM overnight.

Quantitative Real Time PCR—cDNA was synthesized from the total mRNA of each DHHC knockdown sample using a Transcriptor High Fidelity cDNA synthesis kit (Roche Applied Science) as described by the manufacturer. The efficiency of knockdown of each DHHC at the mRNA level was analyzed using SYBR Green JumpStart Taq Ready Mix (Sigma) in a 25-μl total volume reaction on an ABIPrism 7000 real time PCR machine. Approximately 50–75 ng of cDNA was used per reaction with primers at 0.2 μM final concentrations. The internal reference control was endogenous β-actin detected using Qiagen primer set AT01680476. All of the reactions were performed in triplicate. Cycling conditions were 50 °C for 2 min, 95 °C for 10 min, followed by 40 cycles of 95 °C for 15 s, and then 60 °C for 1 min. All of the primers were previously validated with efficiencies calculated to be within 0.1 of the control using the equation $e = 10^{(1/\text{slope})} - 1$. The percentage of mRNA remaining was calculated using the equation % mRNA remaining $= 2^{-\Delta\Delta C_t} \times 100$.

Imaging—Briefly, the cells were plated on glass coverslips, transfected as above, and fixed 48 h after transfection except for experiments in Fig. 4 where cells were fixed 24 h post-transfection. The cells were first washed twice with PBS (Invitrogen) and then fixed with ice-cold 4% paraformaldehyde in PBS for 15 min at room temperature. The cells were washed three times with ice-cold PBS and quenched with 50 mM NH_4Cl in PBS for 10 min. The cells were washed three times in ice-cold PBS before mounting on microscope slides using Mowiol. The cells were initially analyzed under epifluorescence using an inverted Nikon Eclipse 2000 microscope using a 100× oil objective lens. High power confocal images were acquired on a Zeiss LSM510 laser scanning microscope, using a 63× oil Plan Apochromat (NA = 1.4) objective lens, in multi-tracking mode to minimize channel cross-talk. For each independent cell transfection, three or four coverslips/6-well cluster plate were analyzed for each construct. For each coverslip three to five random fields of view were analyzed to determine the number of transfected cells with plasma membrane localization of the respective fusion protein. The average percentage of transfected cells from each well was then determined for each independent transfection (experiment) and normalized to the corresponding wild type STREX control (membrane expression was typically observed in > 95% of transfected wild type STREX fusion proteins). The majority of experiments were performed blind. In addition, a random subset of cells was also analyzed by quantifying the relative peripheral membrane expression compared with the "intracellular" (cytoplasm + nucleus) expression using ImageJ. The ratio of membrane/intracellular fluorescence was determined and normalized to control treated cells assayed in the same experiment under identical conditions. There was no qualitative difference between these approaches. As such all of the data are expressed as percentages of the respective control means ± S.E. for N independent experiments, where n = minimum total number of cells analyzed across experiments for each construct/treatment.

Palmitoylation Assays, Pulldowns, and Western Blotting—CSS-palm prediction was performed using the published CSS-palm v2.0 palmitoylation algorithm (24).

[^{3}H]Palmitic Acid Incorporation—HEK293 cells were transiently transfected in 6-well cluster dishes (~ 3×10^6 cells/well) with the HA-tagged constructs as indicated in the respective figure legends. Forty-eight hours post-transfection, the cells were washed, and 1 ml of fresh DMEM containing 10 mg/ml

fatty acid free bovine serum albumin was added for 30 min at 37 °C. The cells were incubated in DMEM/bovine serum albumin containing 0.5 mCi/ml [^{3}H]palmitic acid (PerkinElmer Life Sciences) for 4 h at 37 °C, and then the medium containing the free label was removed. The cells were lysed in 150 mM NaCl, 50 mM Tris-Cl, 1% Triton X-100, pH 8.0, and centrifuged, and channel fusion proteins were captured using magnetic microbeads coupled to HA/GFP antibody (μMACS^{TM} epitope tag isolation kits; Miltenyi Biotech). After washing columns with 150 mM NaCl, 1% Nonidet P-40, 0.5% deoxycholate, 0.1% SDS, 50 mM Tris-Cl, pH 8.0, followed by washes with 50 mM Tris-Cl, pH 7.5, the captured proteins were eluted in SDS-PAGE sample buffer (50 mM Tris-Cl, pH 6.8, 5 mM dithiothreitol, 1% SDS, 1 mM EDTA, 0.005% bromphenol blue, 10% glycerol) prewarmed to 95 °C. The recovered samples were separated by SDS-PAGE, transferred to nitrocellulose membranes, and probed with either a monoclonal GFP antibody (Clontech; 1:3000) or polyclonal HA antibody (Zymed Laboratories Inc.; 1:1000). A duplicate membrane was dried and exposed to light-sensitive film at −80 °C using a Kodak Biomax transcreen LE (Amersham Biosciences). Co-immunoprecipitation experiments were performed essentially as described using the magnetic microbeads and antibodies as above.

Electrophysiological Assays—Single channel current recordings were performed in the inside-out configuration of the patch clamp technique at room temperature (20–24 °C). The pipette solution (extracellular) contained 140 mM NaCl, 5 mM KCl, 1 mM $CaCl_2$, 2 mM $MgCl_2$, 20 mM glucose, 10 mM HEPES, pH 7.4. The bath solution (intracellular) contained 140 mM KCl, 5 mM NaCl, 2 mM $MgCl_2$, 1 mM 1,2-bis(*o*-aminophenoxy)ethane-*N*,*N*,*N*′,*N*′-tetraacetic acid, 30 mM glucose, 10 mM HEPES, 1 mM ATP, pH 7.3, with free calcium $[Ca^{2+}]_i$ buffered to 0.1 μM, unless indicated otherwise. Channel activity was determined during 60-s depolarizations to +40 mV. Data acquisition and voltage protocols were controlled by an Axopatch 200B amplifier and pCLAMP9 software (Axon Instruments Inc., Foster City, CA). All of the recordings were sampled at 10 kHz and filtered at 2 kHz. Channel activity was allowed to stabilize for at least 10 min after patch excision before the addition of drugs. The catalytic subunit of PKA (PKAc) was from Promega (Madison, WI). Single-channel open probability (P_o) was derived from single-channel analysis using WINEDR (version 2.3.9; Dempster, J., University of Strathclyde, Strathclyde, UK). To determine the mean percentage of change in channel activity after a treatment, mean P_o or N^*P_o was measured immediately before and 10 min after the respective drug application. The effect of cAMP and/or PKAc on channel activity was typically maximal by ~5 min and remained stable over the next 10–30 min following application to inside-out patches. The effect of PKA-mediated phosphorylation was abolished in the absence of Mg-ATP and prevented using the PKA inhibitor PKI_{5-24} (data not shown and see Refs. 19 and 25–27).

Statistical Analysis—All of the data are presented as the means ± S.E. with N = number of independent experiments and n = number of individual cells analyzed in imaging assays. The data were analyzed by analysis of variance with post-hoc Dunnett's test or using a nonparametric Kruskal-Wallis test as appropriate with the significance set at $p < 0.05$.

RESULTS

Cysteine Residues within STREX Are the Only Endogenously Palmitoylated Residues in the Entire C Terminus of BK Channels—Expression of the entire intracellular C-terminal domain of the STREX splice variant of the murine BK channel as a HA- or GFP epitope-tagged construct (STREX-Cterm; Fig. 1*a*) in HEK293 cells resulted in robust palmitoylation (Fig. 1*b*) by endogenous palmitoyltransferases (DHHCs) and expression at the plasma membrane in the absence of the transmembrane domains (Fig. 1, *c* and *d*). We have previously demonstrated that the di-cysteine motif at amino acid positions 12 and 13 within the STREX insert is essential for this membrane localization and can be conferred by expression of the cysteine-rich domain (CRD) alone, which includes STREX and the immediately upstream heme-binding domain (19). In accordance with this, mutation of both cysteines to alanine (C12A/C13A) abolished palmitoylation of STREX-Cterm by endogenous DHHCs (Fig. 1*b*) as well as plasma membrane localization (Fig. 1*d*). In the C12A/C13A palmitoylation-deficient mutants, the fusion protein was robustly expressed as for wild type (Fig. 1*b*) but displayed a largely nuclear and/or cytoplasmic cellular distribution (Fig. 1*c*). Plasma membrane localization of the STREX C terminus, or CRD, was also abolished by preincubation of cells with the palmitoylation inhibitor 2-bromopalmitate (28, 29) (Fig. 1*d*). Furthermore, expression of the ZERO variant C terminus (ZERO-Cterm) that is identical to STREX-Cterm except with the exclusion of the STREX insert (19, 25, 27), was not palmitoylated by endogenous DHHCs in HEK293 cells and displayed a largely cytoplasmic distribution (Fig. 1, *b* and c). Taken together, these data demonstrate that the only cysteine residues within the entire C terminus of the STREX variant of the BK channel that are endogenously palmitoylated in HEK293 cells are cysteine residues 12 and 13 within the STREX insert.

Multiple Endogenous DHHCs Control Membrane Expression of the STREX Domain—In an attempt to address which DHHCs regulate palmitoylation of the STREX insert, we first examined the mRNA expression of endogenous DHHCs in our HEK293 cells. Using quantitative real time PCR (qRT-PCR) revealed expression of all 23 human DHHCs at the mRNA level (Fig. 2, *a* and *b*). In HEK293 cells DHHC4 mRNA was expressed at the highest level with most other DHHC mRNAs expressed at levels between 5 and 20% of DHHC4.

Based on this mRNA expression profile, we exploited multiple siRNAs against each DHHC isoform to allow us to screen the effect of knocking down DHHC isoforms on membrane localization of the STREX domain. For the majority of DHHCs, we could reliably achieve >80% knockdown (*i.e.* <20% mRNA remaining) of mRNA as determined by qRT-PCR, using two siRNAs/DHHC (Fig. 1*c*). In a few cases (*e.g.* DHHC 11 and 19), even using multiple distinct siRNA combinations, we were unable to achieve mRNA knockdown above 50%. Because antibodies are not available to reliably detect most DHHC isoforms, we were unable to monitor DHHC protein levels. Thus to monitor for knockdown efficiency in this system, we transfected siRNA against GFP to knock down expression of the STREX-Cterm-GFP fusion protein. Under our transfection conditions, typically >75% of all cells express the transfected fusion con-

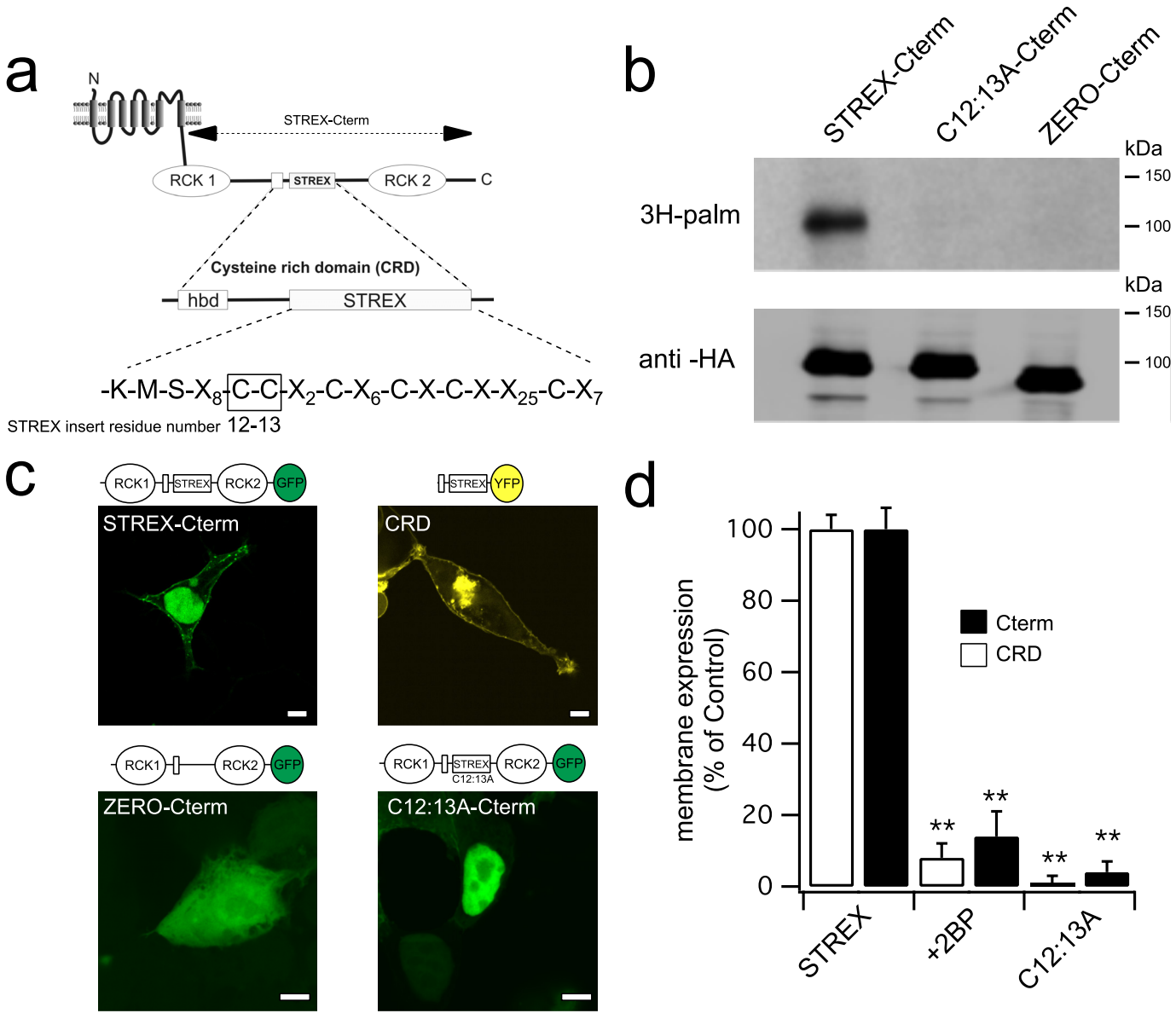

FIGURE 1. **Endogenous palmitoylation of the BK channel C terminus in HEK293 cells is only conferred by cysteine residues 12 and 13 in the alternatively spliced STREX insert.** *a*, schematic illustrating a single pore-forming α-subunit of the STREX splice variant of the BK channel. The STREX splice insert is localized in the intracellular linker between the two regulator of potassium conductance (RCK) domains. The STREX insert together with the upstream heme-binding domain represent the CRD of the linker. Amino acid numbering of the STREX insert starts with the first lysine residue, and cysteine residues 12 and 13 are predicted to be palmitoylated. *b*, fluorograph (*upper panel*) and corresponding Western blot (*lower panel*) of HA-tagged C-terminal constructs of the BK channel expressed in HEK293 cells. The cells were labeled with [^{3}H]palmitate (*3H-palm*) for 4 h, and the constructs were immunoprecipitated using anti-HA magnetic microbeads. *c*, representative single confocal sections and schematics of GFP C-terminal or YFP CRD constructs expressed in HEK293 cells. The *scale bars* are 5 μm. *d*, quantification of construct expression at the plasma membrane expressed as percentages of the membrane expression of the respective STREX-Cterm or CRD fusion protein. Cells treated with the palmitoyltransferase inhibitor 2-bromopalmitate (*2BP*) were exposed to 100 μM overnight. The data are the means $\pm$ S.E. where $N > 5$ and $n > 400$ for each construct/condition. **, $p < 0.01$, compared with respective STREX construct by analysis of variance with post-hoc Dunnett's test.

struct. In the presence of GFP siRNA, less than 2% of all cells displayed significant GFP expression, indicating that the efficiency of GFP knockdown was >97%.

By exploiting this siRNA screen in conjunction with expression of the CRD-YFP construct (to maximize signal/noise ratio), we first assayed the contribution of individual DHHCs to regulate the plasma membrane expression of the CRD-YFP construct in imaging assays. Individual knockdown of DHHCs 3, 5, 7, 9, and 17, but none of the other DHHCs in which high efficiency knockdown could be achieved resulted in a significant reduction in plasma membrane expression of the CRD-YFP fusion protein in HEK293 cells compared with the control (scrambled siRNA) alone (Fig. 2*d*), implicating these DHHCs in STREX palmitoylation. However, combinatorial knockdown of these DHHCs did not result in additive effects beyond those seen with the largest decrease in membrane expression of the CRD-YFP fusion protein with siRNA against DHHC9 (data not shown). Combinatorial knockdown was limited by the reduced efficiency of knockdown using multiple siRNAs and was limited by total siRNA concentrations >100 nM being toxic to cells. In contrast, inhibition of palmitoyltransferase activity using

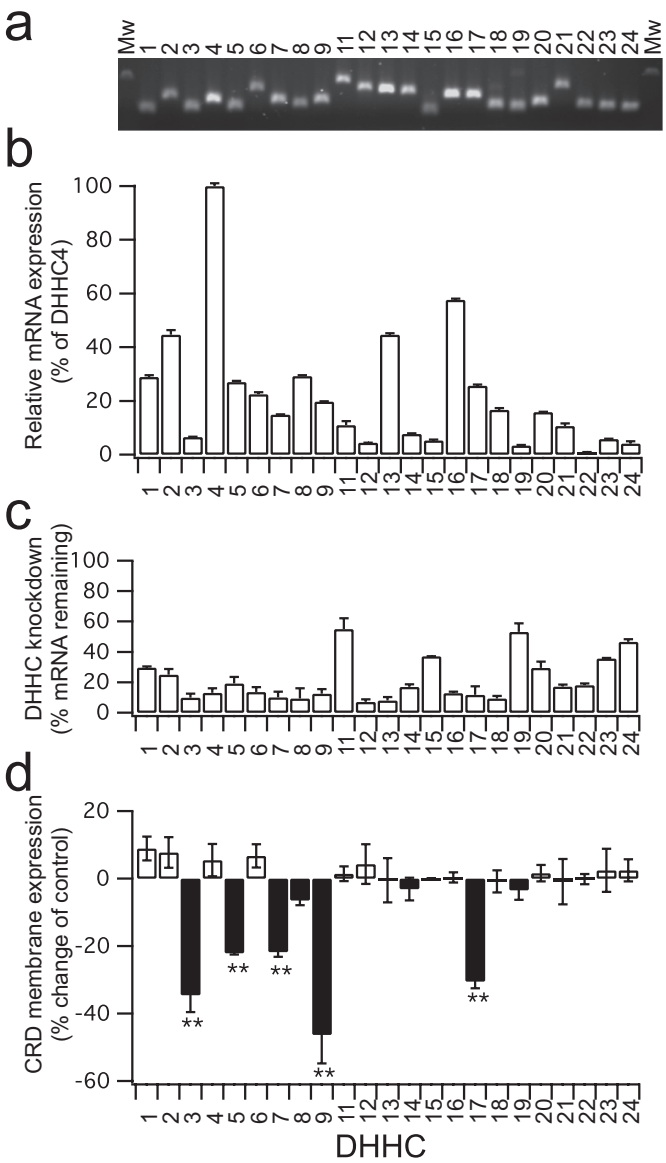

FIGURE 2. **Multiple endogenous DHHCs control membrane localization of the STREX domain.** *a*, representative agarose gel of Sybr-safe-stained PCR amplicons from real time qRT-PCR assays of DHHCs expressed in HEK293 cells (note numbering according to human DHHC convention, thus no DHHC10). *Mw*, molecular weight marker. *b*, relative mRNA expression of each DHHC expressed as a percentage of DHHC4. *c*, efficiency of siRNA-mediated knockdown of each DHHC using two independent siRNAs/DHHC. mRNA levels were quantified by qRT-PCR, and the mRNA expression remaining, following siRNA-mediated knockdown of the cognate DHHC, was expressed as a percentage of the respective control mRNA level for each DHHC. qRT-PCR assays were performed in parallel with the imaging assays in *d*. *d*, effect of DHHC knockdown on membrane expression of the CRD-YFP construct expressed in HEK293 cells. The data are expressed as the percentage of change in membrane expression compared with the CRD-YFP construct in the presence of the scrambled siRNA. The data are the means ± S.E. where $N > 3$ and $n > 350$ for each siRNA knockdown. **, $p < 0.01$, compared with CRD-YFP construct with scrambled siRNA by nonparametric Kruskal Wallis test with post-hoc test.

2-bromopalmitate reduced membrane expression of the CRD-YFP fusion protein to <10% of control (Fig. 1*d*).

Knockdown of DHHCs 3, 5, 7, 9, and 17 also significantly reduced plasma membrane expression of the STREX-Cterm-GFP fusion protein by ~50% (Fig. 3, *a* and *b*) compared with the scrambled siRNA control. To test whether siRNA knockdown of DHHCs 3, 5, 7, 9, and 17 in fact regulated palmitoylation status of the STREX domain, we assayed [^{3}H]palmitate incorporation into the STREX-Cterm construct. Importantly, siRNA knockdown of these DHHCs also significantly reduced but did not completely abolish palmitoylation of the STREX-Cterm fusion protein (Fig. 3, *c* and *d*). Similar reductions in both membrane expression and palmitoylation were observed when each individual DHHC was knocked down by siRNA. One possible explanation is that knockdown of any one of these DHHCs results in a compensatory reduction in expression of a common DHHC. For example, does knockdown of DHHC 3, 5, 7, or 9 also give a reduced DHHC17 expression? However, at least at the mRNA level, we saw no significant down-regulation of a common DHHC mRNA upon knocking down individual DHHCs (data not shown). Taken together these data suggest that the endogenous DHHCs 3, 5, 7, 9, and 17 are important determinants of the palmitoylation status of the STREX domain.

DHHC Overexpression Enhances Membrane Expression of the STREX C Terminus—If endogenous DHHCs 3, 5, 7, 9, and 17 control palmitoylation of the STREX domain, we hypothesized that overexpression of these DHHCs should enhance plasma membrane localization of the STREX C terminus. We thus co-expressed the STREX-Cterm-GFP construct with HA-tagged murine DHHCs (22) and examined the plasma membrane localization of STREX-Cterm-GFP in HEK-293 cells co-expressing both fusion proteins. To facilitate analysis we co-expressed constructs and imaged expression 24 h after expression. Under these conditions STREX-Cterm-GFP membrane localization is typically ~25% (Fig. 4*a*) of that seen under normal conditions when imaging is performed 48 h after transfection as in Figs. 1 and 3. Under these conditions, overexpression of DHHCs 3, 5, 7, 9, and 17 significantly increased (more than 2-fold) plasma membrane localization of the STREX-Cterm fusion protein (Fig. 4*b*). This stimulatory effect was not observed in the presence of the palmitoyltransferase inhibitor 2-bromopalmitate (data not shown).

In contrast, overexpression of DHHCs identified in our siRNA screen because not being involved in endogenous palmitoylation of the STREX domain, including those such as DHHCs 11, 19, and 24 in which siRNA knockdown was <70%, had no significant effect on STREX-Cterm-GFP expression at the plasma membrane (Fig. 4*c*). Furthermore, co-expression of the catalytically inactive palmitoyltransferase mutants DHHS3 or DHHS7 (22) had no effect on membrane expression, demonstrating that the palmitoyltransferase activity of the DHHCs is required rather than an effect via a possible chaperone function (Fig. 4*c*). To verify that the effect of DHHC overexpression was dependent upon palmitoylation of the STREX domain itself, we analyzed the effect of DHHCs 3, 5, 7, 9, and 17 on the C12A/C13A mutant of the STREX-Cterm fusion protein that is an absolute requirement for palmitoylation by endogenous DHHCs and expression at the plasma membrane (Fig. 1, *b*–*d*). Under these conditions membrane expression of the C12A/C13A fusion alone is almost undetectable (Fig. 4*d*). Surprisingly, overexpression of DHHCs 3, 5, 7, or 9 also significantly enhanced membrane expression of the C12A/C13A fusion protein to levels that in fact approached that observed upon co-expression with the wild-type STREX-Cterm-GFP (Fig. 4*d*). In contrast, although there was a small effect of DHHC17 to

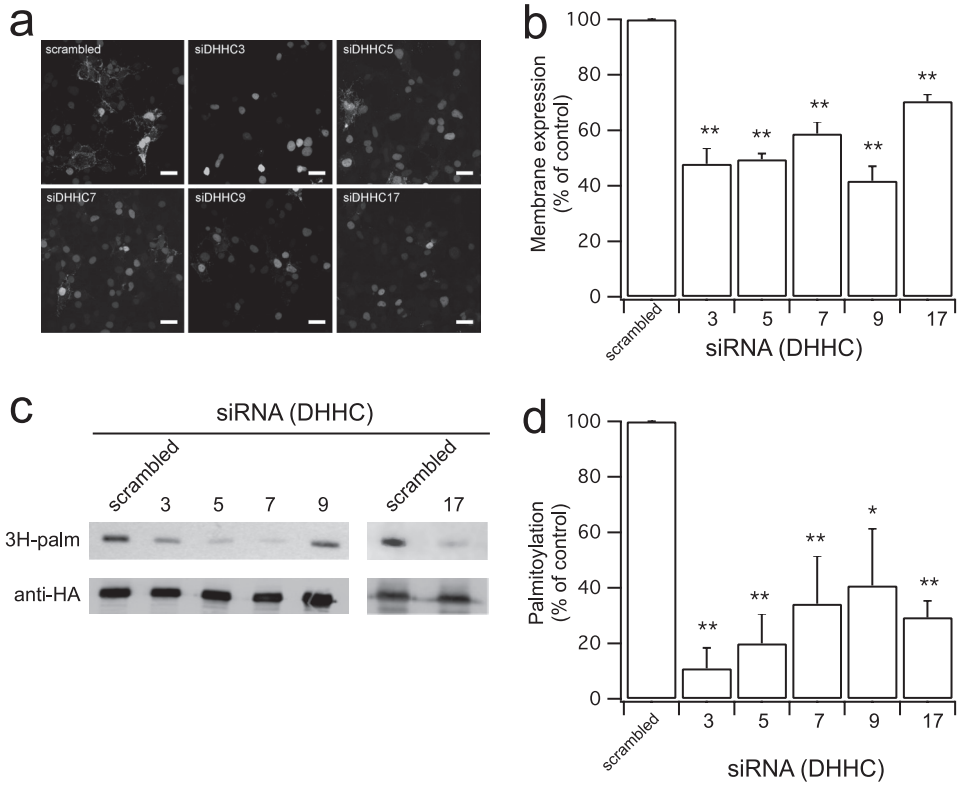

FIGURE 3. **DHHCs 3, 5, 7, 9, and 17 control STREX palmitoylation and membrane association.** *a*, representative low power confocal sections of HEK293 cells expressing the STREX-Cterm-GFP fusion protein and transfected with siRNA against the indicated DHHC. The *scale bars* are 20 μm. *b*, quantification of STREX-Cterm-GFP membrane localization, expressed as a percentage of the membrane localization with the scrambled siRNA, following the respective DHHC knockdown. The data are the means ± S.E. where $N > 4$ and $n > 350$ for each siRNA knockdown. *c*, fluorograph (*upper panel*) and corresponding Western blot (*lower panel*) of HA-tagged C-terminal constructs of the BK channel expressed in HEK293 cells. The cells were labeled with [^{3}H]palmitate (*3H-palm*) for 4 h, and the constructs were immunoprecipitated using anti-HA magnetic microbeads. *d*, quantification of STREX-Cterm palmitoylation following siRNA knockdown of DHHCs by siRNA as in *c*. The data are expressed as percentages of palmitate incorporation in the STREX-Cterm construct in scrambled siRNA-treated cells. The data are the means ± S.E., $N = 3–4$. *, $p < 0.05$; **, $p < 0.01$, compared with respective scrambled control group by analysis of variance with post-hoc Dunnett's test.

increase membrane expression of the C12A/C13A mutant, expression was still significantly lower (<40%) than that seen with the STREX-Cterm alone. These data imply that DHHC 17 is likely the most selective DHHC for palmitoylation of cysteines 12 and 13 in the STREX domain but also suggest that additional palmitoylation sites can be engaged by overexpression of DHHCs to control membrane expression of the C terminus of the STREX BK channel.

Intriguingly, the cysteine residue (Cys^{16}) immediately downstream of cysteines 12 and 13 within the STREX domain is also predicted to be palmitoylated using the CSS-PALM v2.0 algorithm (24). To address whether Cys^{16} may be a target for overexpressed DHHCs, we made the triple mutant C12A/C13A/C16A, in which all three cysteines are mutated to alanine. The construct was robustly expressed in HEK293 cells but failed to be located at the plasma membrane as predicted (Fig. 4*e*). However, co-expression of any DHHC now failed to enhance plasma membrane localization of the C12A/C13A/C16A construct (Fig. 4*e*). Taken together, these data suggest that DHHC17 is most selective for cysteines 12 and 13 within STREX but that exogenous overexpression of DHHCs 3, 5, 7, or 9 can also regulate palmitoylation status and membrane localization via Cys^{16}.

DHHCs Co-immunoprecipitate with STREX BK Channels—Previous studies have suggested that a number of palmitoylated proteins can assemble with their cognate DHHCs (2, 12, 21, 30). Because multiple DHHCs are able to control the palmitoylation status of the STREX domain, we asked whether DHHCs may be able to assemble in a complex with the full-length BK channel. In these studies full-length STREX channels with a C-terminal GFP fusion were co-expressed with HA-tagged DHHCs in HEK293 cells and subjected to reciprocal co-immunoprecipitation assays. Pulldown using anti-HA antibodies resulted in robust immunoprecipitation of DHHCs 3, 5, 7, 9, and 17. Immunoprecipitates were probed for the GFP tag on the BK channel, revealing co-immunoprecipitation with each DHHC (Fig. 5*a*). Immunoprecipitation controls including cells expressing STREX-GFP channel alone (Fig. 5, *control*) or beads alone (not shown) did not result in co-immunoprecipitation. Similar results were observed with the reciprocal pulldown in which channels were immunoprecipitated with anti-GFP and probing for the HA tag on the respective GFP (Fig. 5*b*), except that under these conditions we could not reliably co-immunoprecipitate DHHC5.

Knockdown of DHHC3, 5, 7, 9, or 17 Prevents PKA-mediated Inhibition of the STREX Channel—To address the functional relevance of STREX domain palmitoylation controlled by DHHC3, 5, 7, 9, and 17, we examined the functional cross-talk between the palmitoylation and PKA-dependent phosphorylation of the STREX channel reported previously (19). Phosphorylation of the STREX domain by PKA leads to channel inhibition; however, this inhibition is conditional on the STREX domain being palmitoylated and associated with the plasma membrane (19).

In cells treated with the scrambled siRNA, application of cAMP to the intracellular face of inside-out patches from HEK293 cells expressing the full-length STREX channel resulted in robust inhibition of STREX channel activity that is entirely dependent upon endogenous PKA activity closely associated with the channel (19, 25, 27), as reported previously in control conditions (Fig. 6). However, in cells in which DHHCs 3, 5, 7, 9, or 17 were individually knocked down by siRNA, cAMP-mediated inhibition of the channel was completely abolished (Fig. 6). To validate that the lack of cAMP-mediated inhibition of STREX channel activity in cells in which these DHHCs have been knocked down does not result from disruption of cAMP-dependent activation of PKA, we also analyzed the effect of applying the PKAc to the intracellular face of the patch. Under these conditions application of PKAc in control siRNA

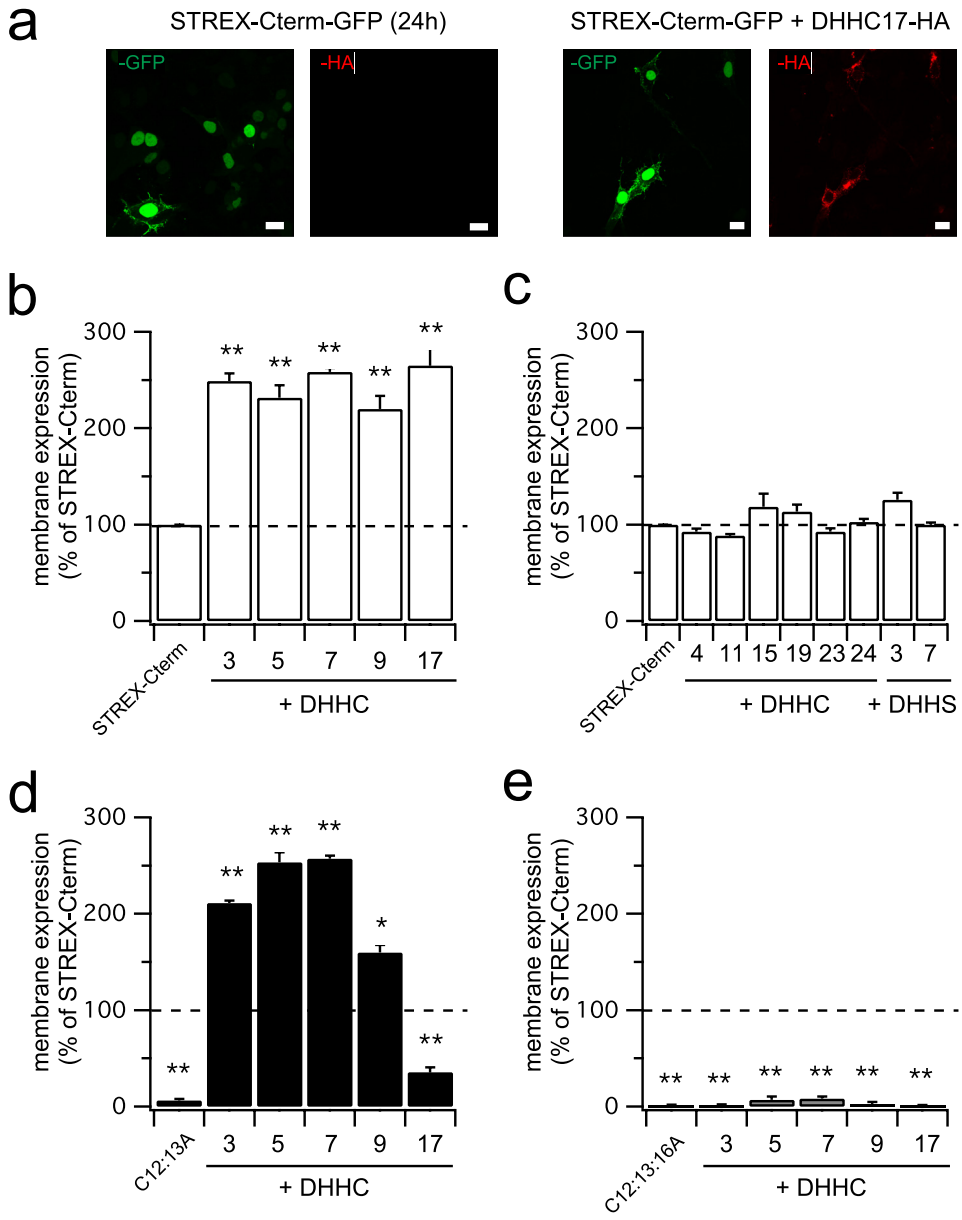

FIGURE 4. **DHHC overexpression enhances membrane localization of STREX-Cterm.** *a*, representative low power confocal sections of HEK293 cells 24 h after transfection with STREX-Cterm-GFP (*left-hand panels*) or co-transfected with DHHC17 (*right-hand panels*). Under each condition the STREX-Cterm-GFP localization and HA tag image planes are shown. The *scale bars* are 10 μm. *b* and *c*, quantification of STREX-Cterm-GFP. *d* and *e*, C12A/C13A (*d*) and C12A/C13A/C16A (*e*) membrane localization in cells co-expressing the corresponding DHHC, or the inactive mutant (DHHS). In *b–e*, the data are expressed as percentages of STREX-Cterm-GFP membrane localization observed in the absence of overexpressed palmitoyltransferase (100%, *dashed line*). The data are the means ± S.E. where $N > 5$ and $n > 400$ for each group. *, p 0.05; **, $p < 0.01$, compared with the STREX-Cterm-GFP construct in the absence of overexpressed palmitoyltransferase by analysis of variance with post-hoc Dunnett's test.

transfected cells inhibited STREX channel activity by 68 ± 8%, $n = 7$. In contrast, in cells in which DHHC17 was knocked down by siRNA, no significant change in activity was observed (mean change in activity was 10.8 ± 8.3%, $n = 5$). Thus knockdown of any of the DHHCs implicated in regulating palmitoylation of the STREX domain also controls the regulation of STREX channels by PKA-mediated phosphorylation.

DISCUSSION

Our data provide the first systematic analysis of the role of individual DHHC palmitoyltransferases in the palmitoylation and regulation of a voltage-gated ion channel. We demonstrate that the intracellular alternatively spliced STREX domain of BK channels is endogenously palmitoylated by multiple palmitoyltransferases (DHHCs). Using siRNA knockdown, DHHCs 3, 5, 7, 9, and 17 were all shown to control STREX domain palmitoylation and association of the STREX C terminus with the plasma membrane. Importantly, knockdown of these DHHCs also controlled PKA-dependent inhibition of the STREX BK channel that we have previously shown to be the major functional effect of palmitoylation of STREX in BK channels (19).

Previous analysis of ligand-gated ion channels has revealed an important role for DHHC3 (also known as GODZ) in controlling channel palmitoylation (6, 7, 10, 12, 30). DHHC3 is rather promiscuous in its palmitoylation of target proteins (21, 22, 31), and DHHC3 controlled palmitoylation of STREX. DHHC7, which may heteromultimerize with DHHC3 (10), was also implicated in STREX palmitoylation. In addition DHHC9, DHHC5, and DHHC17 also controlled STREX palmitoylation and function. The regulation of STREX by DHHC17 is particularly intriguing because DHHC17 is also reported to palmitoylate other cysteine-rich proteins including SNAP25 (32), cysteine string protein (33), and huntingtin (34). Overexpression assays suggested that DHHC17 has the highest selectivity for the palmitoylated dicysteine motif of STREX (cysteines 12 and 13 in STREX). Taken together, because Cys^{12}-Cys^{13} falls within a cysteine-rich domain, as a result of inclusion of the alternatively spliced STREX exon, this may suggest that DHHC17 may preferentially palmitoylate cysteine residues within internal cysteine-rich domains of proteins.

The ability of multiple DHHCs to target the same protein appears to be a general recurring theme in protein palmitoylation. However, it is somewhat surprising that knockdown of any one of these DHHCs (3, 5, 7, 9 or 17) has very similar effects on palmitoylation status, membrane association, and the ability to prevent PKA-mediated inhibition of STREX channels. Indeed, although our attempts to simultaneously knock down all of these DHHCs was unsuccessful, there was no significant addi-

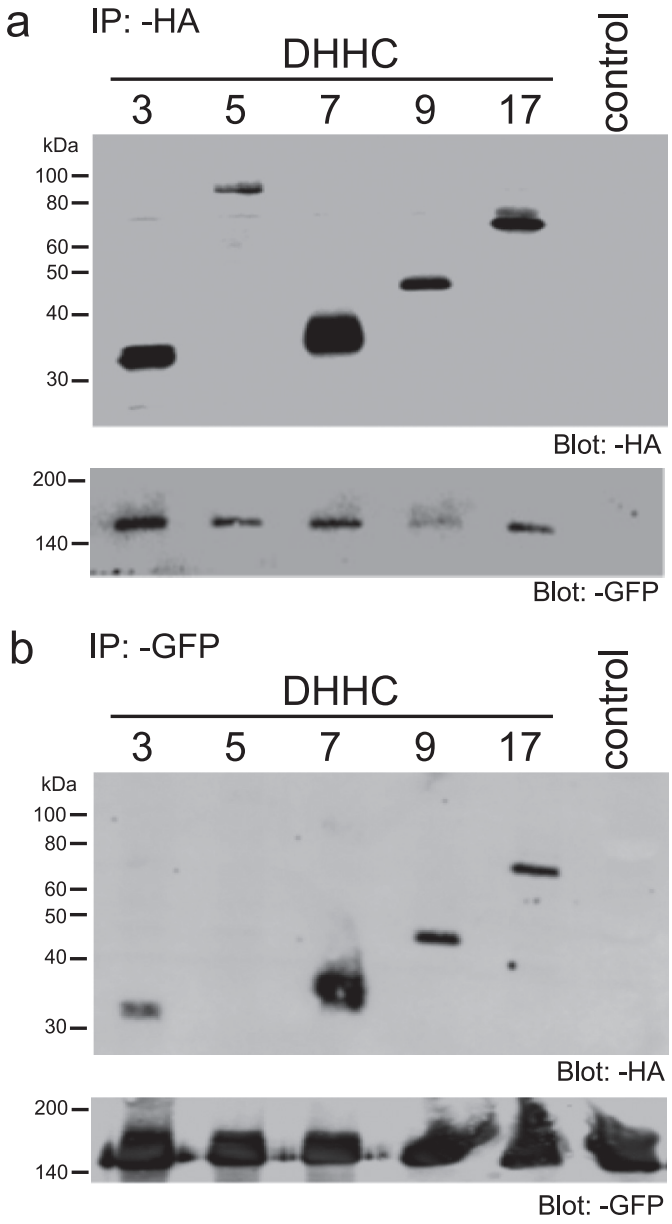

FIGURE 5. **DHHCs 3, 5, 7, 9, and 17 co-immunoprecipitate with full-length STREX BK channel.** Western blots of co-immunoprecipitated HA-tagged DHHCs with GFP-tagged full-length STREX BK channels expressed in HEK293 cells. In *a*, DHHCs were immunoprecipitated (*IP*) with anti-HA magnetic microbeads, and in *b*, channels were immunoprecipitated using anti-GFP magnetic microbeads, and immunoprecipitates were subjected to SDS-PAGE and transferred to polyvinylidene difluoride. The immobilon and the respective tag were probed and detected by enhanced chemiluminescence.

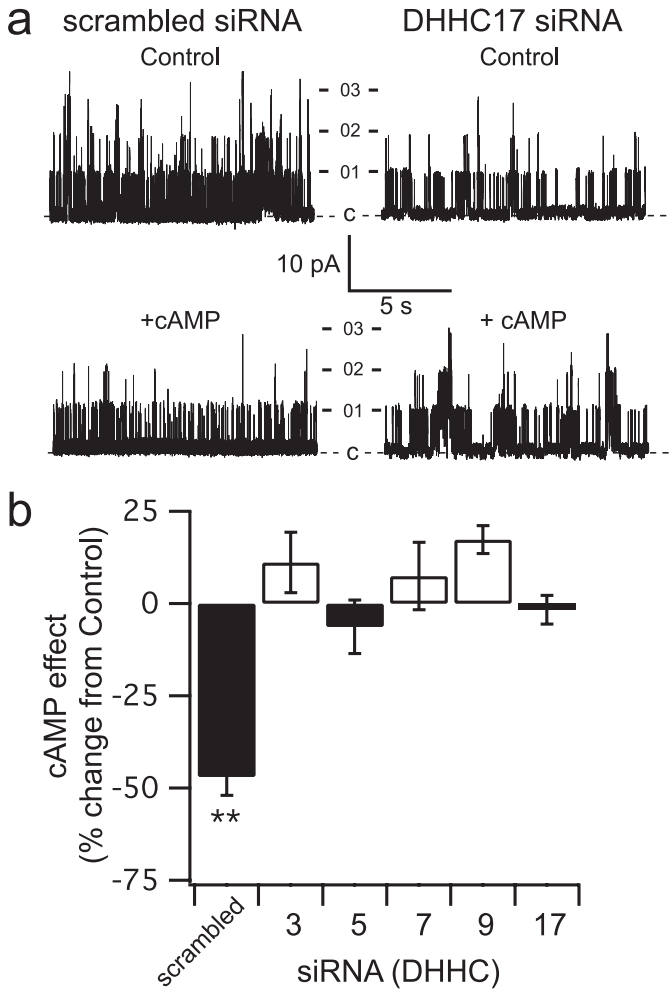

FIGURE 6. **DHHC knockdown prevents PKA-mediated inhibition of STREX channels.** *a*, representative single channel traces from excised inside-out patches of HEK293 cells expressing full-length STREX BK channels before and 5 min after exposure to cAMP. *Left-* and *right-hand panels* are from cells co-transfected with scrambled and DHHC17 siRNA, respectively. Patches were held at +40 mV in physiological potassium gradients with intracellular free calcium buffered to 0.1 μM in the presence of 2 mM Mg-ATP. *b*, summary bar chart of the effect of cAMP on STREX single channel open probability (P_o) expressed as the percentage of change in activity from pre-cAMP control under each condition. The data are the means ± S.E., $N = 6–10$/group. **, $p < 0.01$, compared with the scrambled siRNA group by nonparametric Kruskal Wallis test with post-hoc test.

tive effect on multiplexing siRNA knockdown. Multiple distinct mechanisms may be involved in this effect, resulting in each DHHC having an effect in controlling palmitoylation and function, as has been suggested with other proteins. For example, it may simply reflect that the normal cellular expression of each of these DHHCs is required for efficient palmitoylation as the channel traffics to the plasma membrane. It may also reflect potential different localization of specific DHHC substrate interactions occurring within the trafficking pathway. This may be particularly important for tetrameric proteins like BK channels such that a combinatorial code of palmitoylation on multiple sites across multiple subunits is important for the overall palmitoylation status and functional effect. For example, eight cysteine residues (*i.e.* 4× Cys^{12} and Cys^{13} in STREX) would be available for palmitoylation in the tetrameric homomeric channel. Although the majority of DHHCs that control STREX palmitoylation are thought to be Golgi/endoplasmic reticulum-localized upon overexpression (23), the localization of endogenous DHHCs and their potential trafficking is poorly understood because of the lack of available antibodies to characterize many of the endogenous DHHC proteins. Additional mechanisms may also exist. As already discussed, heteromultimerization of DHHCs may occur as previously demonstrated using overexpressed DHHC3 and DHHC7 (10), or the activity/localization of DHHCs may themselves be controlled by palmitoylation as has been shown for autopalmitoylation of some DHHCs (2). However, the extent to which other DHHCs heteromultimerize, the role of heteromultimerization, and the

functional effect of DHHC palmitoylation in native systems are largely unknown.

An additional factor that may also be important is the stoichiometry of BK channel palmitoylation that is required for the functional effects of palmitoylation to be manifest. In this regard, we have previously shown that phosphorylation of only a single STREX domain in the channel tetramer is important for functional regulation (25). Whether this is also the case for palmitoylation remains to be determined.

Increasing evidence suggests that DHHCs may assemble with their target substrates. For example, DHHC3 and 17 assemble with SNAP25 (21), whereas DHHC3 has been shown to form a complex with γ-aminobutyric acid, type A and α-amino-3-hydroxyl-5-methyl-4-isoxazole-propionate receptors (12, 30). Our data reveal that, at least in overexpression systems, the cognate DHHCs that palmitoylate the STREX domain also can assemble as a complex with the channel. Clearly whether the interaction is direct or results from assembly as a much larger macromolecular complex in native systems warrants further investigation. Furthermore, whether cycles of palmitoylation/depalmitoylation are required as the channels traverse different stages in the pathway leading to delivery to the cell surface remains to be explored.

Intriguingly, overexpression of DHHCs that endogenously control STREX palmitoylation (apart from DHHC17) also allowed access of these DHHCs to a cysteine residue (Cys^{16}) immediately downstream of the Cys^{12}-Cys^{13} site. This implies that Cys^{16} may also be a target for palmitoylation in some cell types in which these DHHCs have access to the site, thus extending the potential repertoire by which STREX channels may be regulated by palmitoylation. However, no other cysteine residues within the entire C terminus of the channel were targets for palmitoylation in HEK293 cells because mutation of Cys^{12}-Cys^{13} completely abolished palmitate incorporation by endogenous DHHCs.

In conclusion, our work reveals that DHHCs 3, 5, 7, 9, and 17 are important determinants of STREX BK channel palmitoylation, STREX domain interaction with the plasma membrane, and functional regulation. Our approach thus represents the first systematic analysis of ion channel palmitoylation by the multimember DHHC family of palmitoyltransferases. Our strategy employing both loss and gain of function strategies and utilizing fluorescent fusion proteins to screen for the effects of palmitoylation of plasma membrane expression of palmitoylated domains of transmembrane proteins may serve as an approach to further interrogate the specificity and role of DHHCs in controlling ion channel and other plasma membrane transmembrane protein regulation by protein palmitoylation.

Acknowledgments—We are grateful to Dr. Trudi Gillespie (IMPACT imaging facility, Centre for Integrative Physiology) for assistance in confocal imaging. We are grateful to Dr. Masaki Fukata for the generous gifts of the murine DHHC constructs and Dr. Luke Chamberlain for advice and DHHS3 and 7 constructs.

REFERENCES

1. el-Husseini, Ael-D, and Bredt, D. S. (2002) *Nat. Rev. Neurosci.* **3,** 791–802
2. Fukata, Y., and Fukata, M. (2010) *Nat. Rev. Neurosci.* **11,** 161–175
3. Kang, R., Wan, J., Arstikaitis, P., Takahashi, H., Huang, K., Bailey, A. O., Thompson, J. X., Roth, A. F., Drisdel, R. C., Mastro, R., Green, W. N., Yates, J. R., 3rd, Davis, N. G., and El-Husseini, A. (2008) *Nature* **456,** 904–909
4. Linder, M. E., and Deschenes, R. J. (2007) *Nat. Rev. Mol. Cell Biol.* **8,** 74–84
5. Resh, M. D. (2006) *Nat. Chem. Biol.* **2,** 584–590
6. Hayashi, T., Rumbaugh, G., and Huganir, R. L. (2005) *Neuron* **47,** 709–723
7. Hayashi, T., Thomas, G. M., and Huganir, R. L. (2009) *Neuron* **64,** 213–226
8. Pickering, D. S., Taverna, F. A., Salter, M. W., and Hampson, D. R. (1995) *Proc. Natl. Acad. Sci. U.S.A.* **92,** 12090–12094
9. Gonnord, P., Delarasse, C., Auger, R., Benihoud, K., Prigent, M., Cuif, M. H., Lamaze, C., and Kanellopoulos, J. M. (2009) *FASEB J.* **23,** 795–805
10. Fang, C., Deng, L., Keller, C. A., Fukata, M., Fukata, Y., Chen, G., and Lüscher, B. (2006) *J. Neurosci.* **26,** 12758–12768
11. Rathenberg, J., Kittler, J. T., and Moss, S. J. (2004) *Mol. Cell Neurosci.* **26,** 251–257
12. Keller, C. A., Yuan, X., Panzanelli, P., Martin, M. L., Alldred, M., Sassoè-Pognetto, M., and Lüscher, B. (2004) *J. Neurosci.* **24,** 5881–5891
13. Chan, A. W., Owens, S., Tung, C., and Stanley, E. F. (2007) *Cell Calcium* **42,** 419–425
14. Chien, A. J., Carr, K. M., Shirokov, R. E., Rios, E., and Hosey, M. M. (1996) *J. Biol. Chem.* **271,** 26465–26468
15. Hurley, J. H., Cahill, A. L., Currie, K. P., and Fox, A. P. (2000) *Proc. Natl. Acad. Sci. U.S.A.* **97,** 9293–9298
16. Schmidt, J. W., and Catterall, W. A. (1987) *J. Biol. Chem.* **262,** 13713–13723
17. Jindal, H. K., Folco, E. J., Liu, G. X., and Koren, G. (2008) *Am. J. Physiol.* **294,** H2012–H2021
18. Gubitosi-Klug, R. A., Mancuso, D. J., and Gross, R. W. (2005) *Proc. Natl. Acad. Sci. U.S.A.* **102,** 5964–5968
19. Tian, L., Jeffries, O., McClafferty, H., Molyvdas, A., Rowe, I. C., Saleem, F., Chen, L., Greaves, J., Chamberlain, L. H., Knaus, H. G., Ruth, P., and Shipston, M. J. (2008) *Proc. Natl. Acad. Sci. U.S.A.* **105,** 21006–21011
20. Suzuki, H., Nishikawa, K., Hiroaki, Y., and Fujiyoshi, Y. (2008) *Biochim. Biophys. Acta* **1778,** 1181–1189
21. Huang, K., Sanders, S., Singaraja, R., Orban, P., Cijsouw, T., Arstikaitis, P., Yanai, A., Hayden, M. R., and El-Husseini, A. (2009) *FASEB J.* **23,** 2605–2615
22. Fukata, M., Fukata, Y., Adesnik, H., Nicoll, R. A., and Bredt, D. S. (2004) *Neuron* **44,** 987–996
23. Ohno, Y., Kihara, A., Sano, T., and Igarashi, Y. (2006) *Biochim. Biophys. Acta* **1761,** 474–483
24. Ren, J., Wen, L., Gao, X., Jin, C., Xue, Y., and Yao, X. (2008) *Protein Eng. Des. Sel.* **21,** 639–644
25. Tian, L., Coghill, L. S., McClafferty, H., MacDonald, S. H., Antoni, F. A., Ruth, P., Knaus, H. G., and Shipston, M. J. (2004) *Proc. Natl. Acad. Sci. U.S.A.* **101,** 11897–11902
26. Tian, L., Coghill, L. S., MacDonald, S. H., Armstrong, D. L., and Shipston, M. J. (2003) *J. Biol. Chem.* **278,** 8669–8677
27. Tian, L., Duncan, R. R., Hammond, M. S., Coghill, L. S., Wen, H., Rusinova, R., Clark, A. G., Levitan, I. B., and Shipston, M. J. (2001) *J. Biol. Chem.* **276,** 7717–7720
28. Jennings, B. C., Nadolski, M. J., Ling, Y., Baker, M. B., Harrison, M. L., Deschenes, R. J., and Linder, M. E. (2009) *J. Lipid Res.* **50,** 233–242
29. Resh, M. D. (2006) *Methods* **40,** 191–197
30. Uemura, T., Mori, H., and Mishina, M. (2002) *Biochem. Biophys. Res. Commun.* **296,** 492–496
31. Fukata, Y., Iwanaga, T., and Fukata, M. (2006) *Methods* **40,** 177–182
32. Greaves, J., Prescott, G., Fukata, Y., Fukata, M., Salaun, C., and Chamberlain, L. (2009) *Mol. Biol. Cell* **20,** 1845–1854
33. Greaves, J., Salaun, C., Fukata, Y., Fukata, M., and Chamberlain, L. H. (2008) *J. Biol. Chem.* **283,** 25014–25026
34. Yanai, A., Huang, K., Kang, R., Singaraja, R. R., Arstikaitis, P., Gan, L., Orban, P. C., Mullard, A., Cowan, C. M., Raymond, L. A., Drisdel, R. C., Green, W. N., Ravikumar, B., Rubinsztein, D. C., El-Husseini, A., and Hayden, M. R. (2006) *Nat. Neurosci.* **9,** 824–831

THE JOURNAL OF BIOLOGICAL CHEMISTRY VOL. 285, NO. ??, pp. 1–xxx, ???? ??, 2010

Palmitoylation of the S0-S1 Linker Regulates Cell Surface Expression of Voltage- and Calcium-activated Potassium (BK) Channels*

Received for publication, June 11, 2010, and in revised form, July 14, 2010 Published, JBC Papers in Press, August 6, 2010, DOI 10.1074/jbc.M110.153940

Owen Jeffries[‡1], Nina Geiger[‡§], Iain C. M. Rowe[‡], Lijun Tian[‡], Heather McClafferty[‡], Lie Chen[‡], Danlei Bi[‡], Hans Guenther Knaus[¶], Peter Ruth[§], and Michael J. Shipston[‡2]

From the [‡]Centre for Integrative Physiology, College of Medicine & Veterinary Medicine, Hugh Robson Building, University of Edinburgh, Edinburgh EH8 9XD, United Kingdom, the [¶]Division for Molecular and Cellular Pharmacology, Department of Medical Genetics, Molecular and Clinical Pharmacology, Medical University Innsbruck, Peter-Mayr Strasse 1, 6020 Innsbruck, Austria, and [§]Pharmacology and Toxicology, Institute of Pharmacy, University Tuebingen, 72076 Tuebingen, Germany

***S*-Palmitoylation is rapidly emerging as an important post-translational mechanism to regulate ion channels. We have previously demonstrated that large conductance calcium- and voltage-activated potassium (BK) channels are palmitoylated within an alternatively spliced (STREX) insert. However, these studies also revealed that additional site(s) for palmitoylation must exist outside of the STREX insert, although the identity or the functional significance of these palmitoylated cysteine residues are unknown. Here, we demonstrate that BK channels are palmitoylated at a cluster of evolutionary conserved cysteine residues (Cys-53, Cys-54, and Cys-56) within the intracellular linker between the S0 and S1 transmembrane domains. Mutation of Cys-53, Cys-54, and Cys-56 completely abolished palmitoylation of BK channels lacking the STREX insert (ZERO variant). Palmitoylation allows the S0-S1 linker to associate with the plasma membrane but has no effect on single channel conductance or the calcium/voltage sensitivity. Rather, S0-S1 linker palmitoylation is a critical determinant of cell surface expression of BK channels, as steady state surface expression levels are reduced by ~55% in the C53:54:56A mutant. STREX variant channels that could not be palmitoylated in the S0-S1 linker also displayed significantly reduced cell surface expression even though STREX insert palmitoylation was unaffected. Thus our work reveals the functional independence of two distinct palmitoylation-dependent membrane interaction domains within the same channel protein and demonstrates the critical role of S0-S1 linker palmitoylation in the control of BK channel cell surface expression.**

Large conductance calcium- and voltage-gated potassium (BK) channels play an important role in regulating diverse physiological processes from neuronal excitability (1, 2) to the control of blood flow (3, 4). Dysfunction of the BK channel has been implicated in a number of disorders including epilepsy (5, 6), cerebellar ataxia (2), hypertension (3, 4), incontinence (7), and tumor cell proliferation (8, 9).

* This work was supported by the Wellcome Trust.

[1] Recipient of a BBSRC PhD doctoral training award.
[2] To whom correspondence should be addressed: Centre for Integrative Physiology, Hugh Robson Bldg., University of Edinburgh, Edinburgh EH8 9XD, UK. Tel.: 44-131-6503253; Fax: 44-131-6506521; E-mail: mike.shipston@ed.ac.uk.

The BK channel pore-forming α-subunit, is encoded by a single gene KCNMA1 (10), and assembles as tetramers, forming a K^+-selective channel. Functional diversity of BK channels is achieved by association with β-subunits (3) and other proteins (11), alternative splicing (12–14), and post-translational modifications such as phosphorylation (15).

We have demonstrated previously that an alternatively spliced variant of the BK channel, the Stress-regulated exon (STREX),[3] is palmitoylated within the STREX insert and regulates protein kinase A-mediated inhibition of STREX channels (16). These studies also revealed that channels lacking the STREX insert (ZERO variant) could also be palmitoylated indicating that additional cysteine residues are targets for palmitoylation (16). Furthermore, BK channels were identified in a proteomic screen for palmitoylated proteins in adult rat brain, (17) a tissue with generally low level expression of STREX channels when compared with the ZERO channel variant (5, 18). Moreover, a protein palmitoylation prediction algorithm (CSS-Palm) (19, 20) indicates that the BK channel contains several evolutionary conserved cysteine residues in the intracellular linker that links the S0 and S1 transmembrane domains (S0-S1 linker) that can be palmitoylated (Fig. 1*A*). Whether these residues are in fact palmitoylated is not known and the functional role of palmitoylation of the BK channel outside of the STREX insert has not been addressed.

Increasing evidence points to an important role for palmitoylation in the dynamic control of function, assembly or trafficking of membrane proteins, including ion channels. Palmitoylation increases protein hydrophobicity by post-translational thioester linkage of a saturated 16-carbon palmitic acid to specific cysteine residues, a reversible process that is dependent on a large family of protein palmitoyltransferases (DHHCs) and thioesterases (21). Palmitoylation can play a diverse role in controlling ion channel function including: the modulation of voltage sensing in Kv1.1 channels (22); control of phosphorylation status of BK channels (16) and the GluR6 receptor (23); assembly of sodium channels (24); cell surface stability of $GABA_A$ receptors (25); and trafficking of AMPA and NMDA receptors (26, 27).

[3] The abbreviations used are: STREX, stress-regulated exon; HEK293, human embryonic kidney 293 cell.

Here, we have identified evolutionary conserved cysteine residues in the intracellular N-terminal S0-S1 linker of BK channels that can be palmitoylated and that allows the domain to associate with the plasma membrane modulating cell surface expression of the channel. Importantly, the functional role of S0-S1 linker palmitoylation is distinct from that conferred by palmitoylation of the previously characterized C-terminal alternatively spliced STREX insert (16). Thus our work demonstrates functionally distinct palmitoylation-dependent membrane interaction domains within the same channel protein and that palmitoylation of the BK channel S0-S1 linker is an important determinant of cell surface expression.

EXPERIMENTAL PROCEDURES

Channel Constructs and Expression—The subcloning and site directed mutagenesis was performed on the murine BK channel α-subunit as has been described previously (13, 28). All amino acid numbering in full-length channel constructs is based on the murine (mSlo) BK channel sequence with start methionine at MDALI., accession number: AF156674. The S0-S1 linker -YFP fusion constructs used in Fig. 2 (S0-S1-YFP) incorporated the entire intracellular linker between the two predicted transmembrane domains, S0 and S1, beginning at residue Arg-44 and ending at residue Arg-114 cloned into a pEYFP-N1 vector backbone. Extracellular N-terminal Flag tag and intracellular C- terminal HA tag constructs of full-length channels were created in pcDNA3.1 as described (13, 27). Site-directed mutations were generated by standard procedures using the QuikChange system (Stratagene).

HEK293 Cell Culture and Immunofluorescence—HEK293 cells were maintained and transfected as described (13, 28). Cell surface labeling of the N-terminal Flag tag epitope of BK channels in non-permeabilized HEK293 cells (28) was performed using mouse monoclonal anti-Flag M2 antibody (5 μg/μl, Sigma) and Alexa-594-conjugated anti-mouse rabbit IgG (Molecular Probes). Cells were then fixed in 4% paraformaldehyde, permeabilized with 0.3% Triton X-100 in phosphate buffered saline (PBS) for 10 min and blocked with 0.05% Triton X-100 in PBS containing 3% BSA for 30 min. The intracellular C-terminal HA epitope tag was detected using 1.25 mg/ml anti-HA polyclonal rabbit antibody (Zymed Laboratories Inc.) and Alexa-488-conjugated anti-rabbit chicken IgG (Molecular Probes) and cells mounted using Mowiol. Confocal images were acquired on a Zeiss LSM510 laser scanning microscope, using a 63× oil Plan Apochromat (NA = 1.4) objective lens, in multitracking mode (16). Quantification of Flag surface expression was done in two ways: (i) using a threshold method to detect total number of transfected cells that displayed Flag surface expression in each group; and (ii) using absolute measures based on ratios of surface Flag (extracellular) fluorescence to intracellular signal (HA) in a random subset of all cells analyzed using Image J. 1.42q (Wayne Rasband, NIH). Data were then normalized to the corresponding control group (100%) as indicated in the respective figure legend. In these experimental paradigms the data obtained for relative surface expression using the threshold method was quantitatively the same as using absolute ratio measures.

CSS-Palm Prediction—We used the published CSS-Palm palmitoylation algorithm (19, 20), to predict cysteine residues within the entire coding sequence of the murine BK channel α-subunit. Sequences were analyzed with the CSS-Palm v2.0 web interface. The palmitoylation prediction threshold was set to the highest cutoff.

[^{3}H]Palmitic Acid Incorporation—HEK293 cells were transiently transfected in 6-well cluster dishes (≈3 × 10^6 cells per well) with full-length channel constructs as previously described (16). Briefly, 48 h after transfection, cells were washed and 1 ml of fresh DMEM containing 10 mg/ml fatty acid-free BSA was added for 30 min at 37 °C. Cells were incubated in DMEM/BSA containing 0.5 mCi/ml [^{3}H]palmitic acid for 4 h at 37 °C, and then the medium containing the free label was removed. Cells were lysed in 150 mM NaCl, 50 mM Tris-Cl, 1% Triton X-100 (pH 8.0), and channel fusion proteins were captured by using magnetic microbeads coupled to HA/GFP antibody (μMACS epitope tag isolation kits, Miltenyi Biotec). Captured proteins were eluted in SDS/PAGE sample buffer (50 mM Tris-HCl, pH 6.8, 5 mM DTT, 1% SDS, 1 mM EDTA, 0.005% bromphenol blue, 10% glycerol) prewarmed to 95 °C. The recovered samples were separated by SDS/PAGE, transferred to nitrocellulose membranes, and probed with a polyclonal HA antibody (1:1,000; Zymed Laboratories Inc.). A duplicate membrane was dried, sprayed with En^{3}hance fluorographic spray (PerkinElmer-Cetus), and exposed to light-sensitive film at −80 °C by using a Kodak Biomax transcreen LE (Amersham Biosciences).

Cell Surface Biotinylation Assay—Plasmids expressing HA-tagged BK channels were transiently transfected into HEK293 cells with Exgen 500 (Fermentas). 48 h post-transfection, cells were washed 3× with Hank's buffered salt solution (HBSS), and incubated on ice for 2 h in the presence of 5 μg/ml of Sulfo-NHS-LC-biotin (Pierce). Cells were lysed in NLB buffer with a protease inhibitor mixture after washing in ice-cold 100 mM glycine in HBSS (Roche, Germany). Biotinylated cell lysates were incubated with streptavidin-immobilized beads (Pierce) overnight at 4 °C and washed 3× with cold HBSS and once with water. The biotinylated membrane BK channel proteins were removed from the beads by incubating at 45 °C for 15 min in 2× Laemmli protein sample buffer, separated by SDS-PAGE and detected with anti-HA antibody using Western blotting. Parallel control biotinylation assays were conducted with mock transfected cells.

Electrophysiology—Single channel recordings and macropatch recordings were performed in the excised inside-out configuration of the patch-clamp technique at room temperature. The pipette solution (extracellular) contained 140 mM NaCl, 5 mM KCl, 0.1 mM $CaCl_2$, 1 mM $MgCl_2$, 20 mM glucose, 10 mM Hepes (pH 7.3). The bath solution (intracellular) contained 140 mM KCl, 5 mM NaCl, 1 mM $MgCl_2$, 1 mM BAPTA, 20 mM glucose, 10 mM Hepes, (pH 7.3) with free calcium $[Ca^{2+}]_i$ buffered from 0.33 to 10 μM, as indicated. Channel activity was determined during 100 ms depolarizations over a voltage range from −120 mV to +120 mV in 20 mV increments from a holding potential of −80 mV. Tail currents were then examined and normalized to the peak current (100%) in 1 μM Ca^{2+} and plotted as G/G_{MAX} corresponding to channel activity. Voltage sen-

sitivity was determined by a logarithmic transformation linearizing the activating component of the normalized (G/G_{MAX}) curves in 1 μM Ca^{2+}. Data acquisition and voltage protocols were controlled by an Axopatch 200 B amplifier and pCLAMP9 software (Axon Instruments). All recordings were sampled at 10 kHz and filtered at 2 kHz. Channel activity was allowed to stabilize for at least 10 min after patch excision before recording.

Fluorescent Membrane Potential Assay—Membrane potential assays were performed in transfected HEK293 cells incubated with FLIPR® Membrane Potential Blue Dye (Molecular Devices, Sunnyvale, CA) as described (29). Briefly, cells were plated in black walled, clear bottom 96-well plates and loaded with dye for 30 min at 37 °C to allow dye loading into the cell membrane. Assays were performed as room temperature using the Flexstation R II system (Molecular Devices) and channels activated by 1 μM ionomycin (a calcium ionophore), 16 s after measurement began. Fluorescent changes were read over a period of 3 min as relative fluorescent units (RFU). An increase in BK channel activity caused a hyperpolarization which was detected as a decrease in fluorescence. To compare between mutants the RFU were determined at $t = 70$ s, and the response of each channel mutant was then isolated by subtracting the control HEK depolarizing response and normalizing the hyperpolarization of the wild-type ZERO or STREX channel to 100%.

Statistics—All statistical analysis was performed using GraphPad Prism using 1-way ANOVA with Tukey *post hoc* test for significance between groups.

RESULTS

The S0-S1 Linker Is Palmitoylated in BK Channels—Using a palmitoylation prediction algorithm (CSS-Palm) (19, 20), the murine ZERO BK channel variant sequence revealed three cysteine residues, Cys-53, Cys-54, and Cys-56 that scored highly as predicted palmitoylation sites within the BK channel, scoring, 1.54, 1.48, and 0.92, respectively (Fig. 1*A*).

Sequence alignment of the three cysteine residues in the S0-S1 linker (Cys-53, Cys-54, and Cys-56) indicate strong evolutionary conservation across vertebrates with conservation of double cysteines (Cys-53 and Cys-54) extending across *Drosophila* and *Caenorhabditis elegans*, suggesting that this region may be of functional significance to the channel (Fig. 1*A*).

To directly assess whether the S0-S1 linker is in fact palmitoylated in the ZERO channel we assayed [^{3}H]palmitate incorporation into full-length channel proteins in HEK293 cells (Fig. 1*B*). Full-length ZERO channels were robustly palmitoylated by endogenous palmitoyltransferases. Importantly, mutation of all three cysteine residues in the S0-S1 linker to alanine (ZERO C53:54:56A) completely abolished [^{3}H]palmitate incorporation. Individual point mutation of cysteine residues demonstrated a reduced [^{3}H]palmitate incorporation but did not abolish it, thus suggesting that the triple cysteine mutant (ZERO C53:54:56A) is the key determinant for palmitoylation of the ZERO channel. Robust expression in Western blot analysis suggested that a change in palmitoylation status of the channels was not the result of decreased synthesis or degradation of channel protein (Fig. 1*B*). Together these data suggest that C53:54:56 is the only site that is palmitoylated in the ZERO channel.

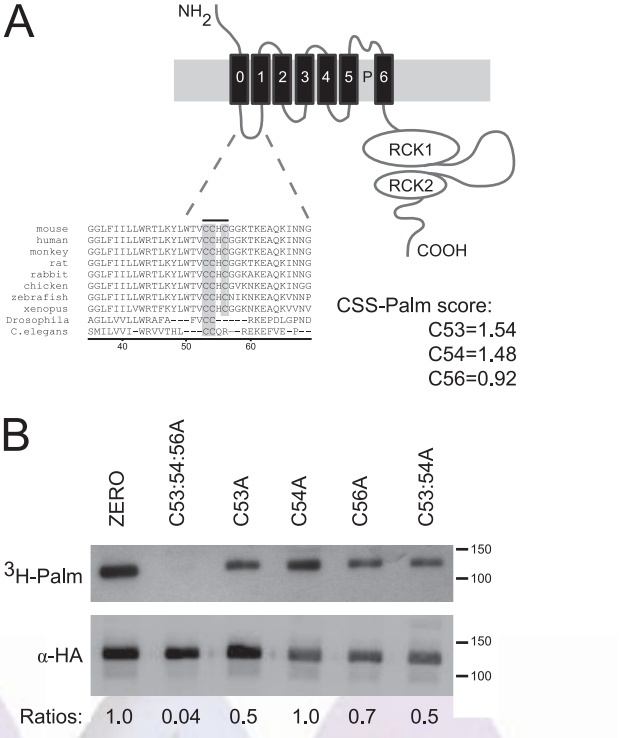

FIGURE 1. **The S0-S1 linker is palmitoylated in BK channels.** *A*, schematic illustrating the topology of the BK channel pore-forming α-subunit. Sequence alignments of cysteine residues in the S0-S1 linker indicate evolutionary conservation (*gray box*) across vertebrates, *Drosophila* and *C. elegans*. Murine sequence numbered starting from the initiation methionine (MDALI), accession number: AF156674. CSS-Palm prediction scores were determined with the CSS-Palm v2.0 platform. *B*, representative fluorographs (*upper*) and Western blots (*lower*) of full-length ZERO-HA channels and ZERO channels with mutation of key cysteine residues in the S0-S1 linker, expressed in HEK293 cells. Constructs were labeled with [^{3}H]palmitate for 4 h and immunoprecipitated (*IP*) by using α-HA magnetic microbeads and detected by fluorography. Ratios (normalized to the wild-type ZERO channel) of [^{3}H]palmitate detection in comparison to total protein expression are included.

Palmitoylation Targets the S0-S1 linker to the Plasma Membrane—Palmitoylation increases the hydrophobicity of a protein facilitating interaction with the intracellular plasma membrane. To examine whether the S0-S1 linker alone may target to the plasma membrane, constructs that incorporated the 70 amino acid S0-S1 linker fused in-frame with YFP (S0-S1-YFP construct, Fig. 2*A*) were created to determine the functional contribution of each cysteine residue within the identified region. Transient expression of the S0-S1 linker constructs in HEK293 cells resulted in robust expression at the plasma membrane as well as fusion protein trapped in intracellular compartments (Fig. 2*A*). Site-directed mutagenesis of the cysteine residues predicted to be palmitoylated in the S0-S1 linker to alanine resulted in significantly decreased expression at the plasma membrane. Mutation of individual cysteine residues resulted in significantly decreased plasma membrane targeting of between ~40–70% in relation to the S0-S1-YFP linker construct. Mutation of the double cysteines, conserved from human to *C. elegans*, also significantly decreased expression at the plasma membrane. Mutation of all three cysteine residues (S0-S1 C53:54:56A-YFP construct) resulted in near abolition (>90% decrease) of membrane targeting of the S0-S1 linker fusion protein (Fig. 2*B*).

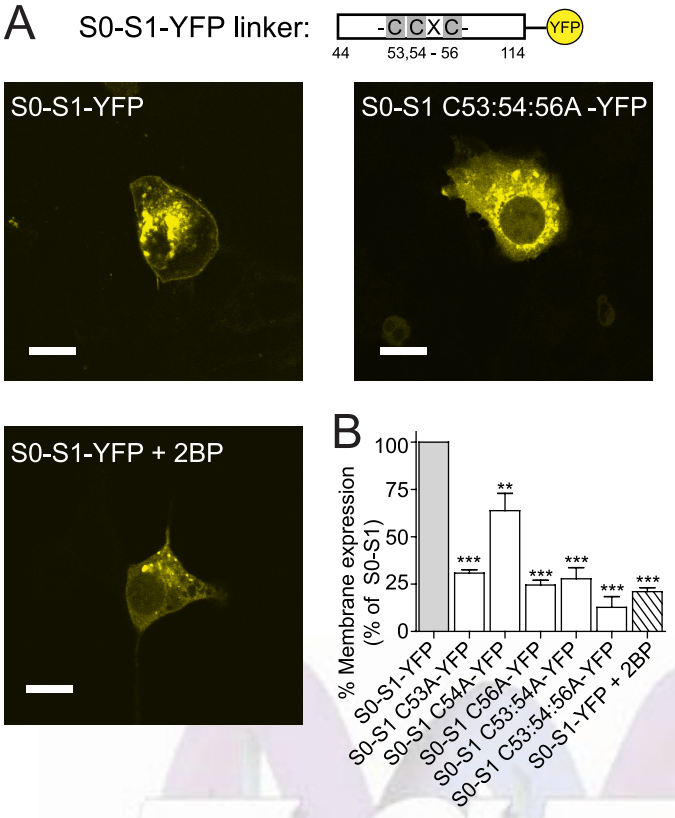

FIGURE 2. **Palmitoylation targets the S0-S1 linker to the plasma membrane.** A schematic of the short S0-S1 linker YFP fusion construct (S0-S1-YFP), that encodes the 70 amino acid intracellular S0-S1 linker between amino acids Arg-44 and Arg-11 fused in-frame with YFP, and relative position of the palmitoylated cysteine residues. *A*, representative single cell confocal images of the S0-S1-YFP linker, S0-S1 C53:54:56A-YFP linker, and the S0-S1-YFP linker fusion proteins after incubation with the palmitoylation inhibitor 2BP (100 μM) for 24 h, expressed in HEK293 cells (scale bars: 10 μm). *B*, summary bar graph illustrates the effect of site-directed mutagenesis of cysteine residues in the S0-S1 linker on localization of the respective S0-S1-YFP fusion protein at the plasma membrane expressed as a percentage of the wild-type S0-S1-YFP fusion protein (where wild-type S0-S1-YFP membrane expression is normalized to 100%). (For all S0-S1 linker constructs, N>3, n>330 cells analyzed). **, $p < 0.01$; ***, $p < 0.001$ compared with wild-type S0-S1 (ANOVA with Tukey *post hoc* test).

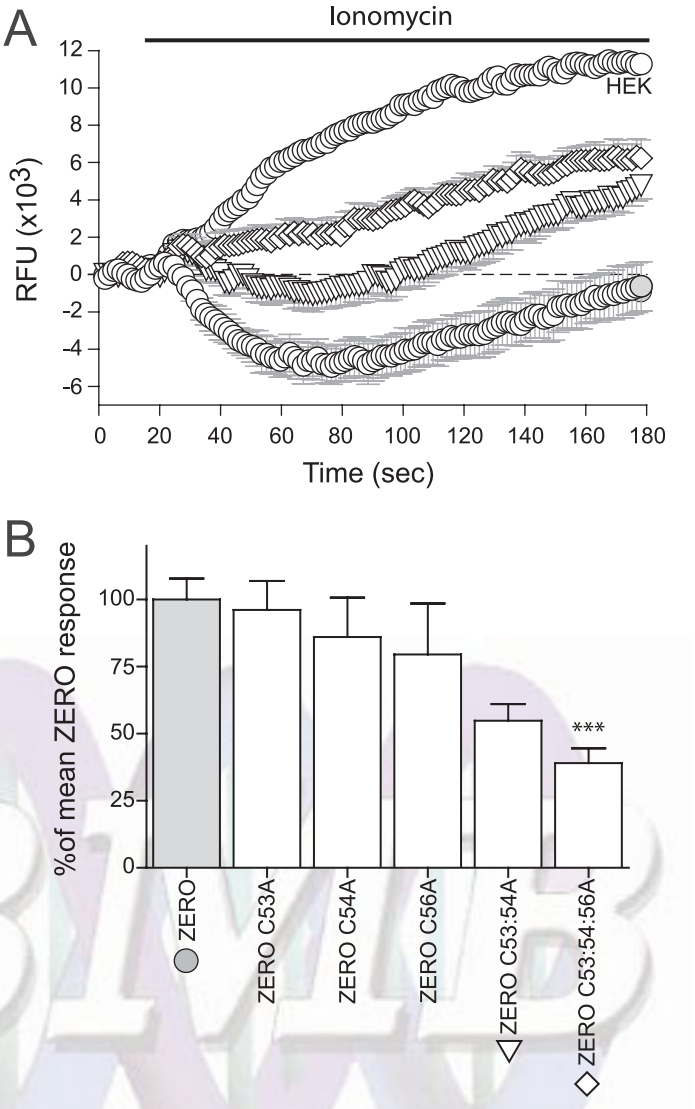

FIGURE 3. **Ionomycin-driven activation of BK channels is attenuated in S0-S1 mutant channels.** *A*, representative time course plots of mean change in relative fluorescence units (*RFU*) of the FLIPR-blue membrane potential dye in HEK293 cells expressing ZERO (*closed gray circles*, ●), ZERO C53:54A (*inverted triangles*,▽), ZERO C53:54:56A (*diamonds*, ◇), and mock-transfected HEK293 (*open circles*,○), in response to calcium influx induced by 1 μM ionomycin. *B*, summary bar chart of the membrane potential change for each construct expressed as a percentage of the maximal hyperpolarization, following subtraction of the HEK293 response, in the ZERO (*gray*) variant (where the ZERO response is normalized to 100%). Data were determined at the maximum hyperpolarizing response in the wild-type ZERO channel ($t = 70$ s) in the time course plots in *A*. All data are means ± S.E. ($n = 3$, n>24), ***, $p < 0.001$, compared with ZERO (ANOVA with Tukey *post hoc* test).

We demonstrated previously that palmitoylation-dependent membrane association of C-terminal constructs containing the alternatively spliced STREX insert of the BK channel could be controlled by phosphorylation of neighboring consensus phosphorylation sites (16). Phosphoproteomic analysis of BK channels has demonstrated that serine residues Ser-70 and Ser-71, that are immediately downstream of the S0-S1 palmitoylated cysteine residues, are phosphorylated *in vivo* (30). However, site-directed mutagenesis of these residues to either phosphomimetic (S70:71E) or phosphornull (S70:71A) had no significant effect on membrane association of the S0-S1-YFP fusion protein at the cell surface (3 ± 6.4% and 3 ± 9.5% reduction of wild-type S0-S1 membrane expression, respectively). This suggests that the phosphorylation status of these residues does not determine S0-S1 linker membrane association.

The effect of inhibition of endogenous palmitoylation on localization of the S0-S1 linker at the plasma membrane was examined with cells incubated with a palmitoylation inhibitor, 2-bromopalmitate (2-BP, 100 μM) for 24 h. This reduced association of the S0-S1 linker at the plasma membrane by ~80% (Fig. 2*B*). Together these data support the mutagenesis studies that targeting of the S0-S1 linker to the plasma membrane is controlled through palmitoylation of key cysteine residues.

S0-S1 Palmitoylation Has No Effect on Intrinsic Channel Activity—To determine whether palmitoylation of S0-S1 cysteine residues influences channel function we used a membrane-potential assay that has been previously shown to discriminate between BK channel splice variants with different calcium sensitivities (29). In this assay, BK channel activity is driven by ionomycin-induced calcium influx and is reported by movement of a fluorescent voltage-sensitive dye across the cell membrane in response to changes in cell membrane potential.

balt3/zbc-bc/zbc-bc/zbc04410/zbc3465-10z ZSUBMIT 8 xppws S=1 26/8/10 10:51 **4/Color Figure(s) F2,5,7** ARTNO: M110.153940

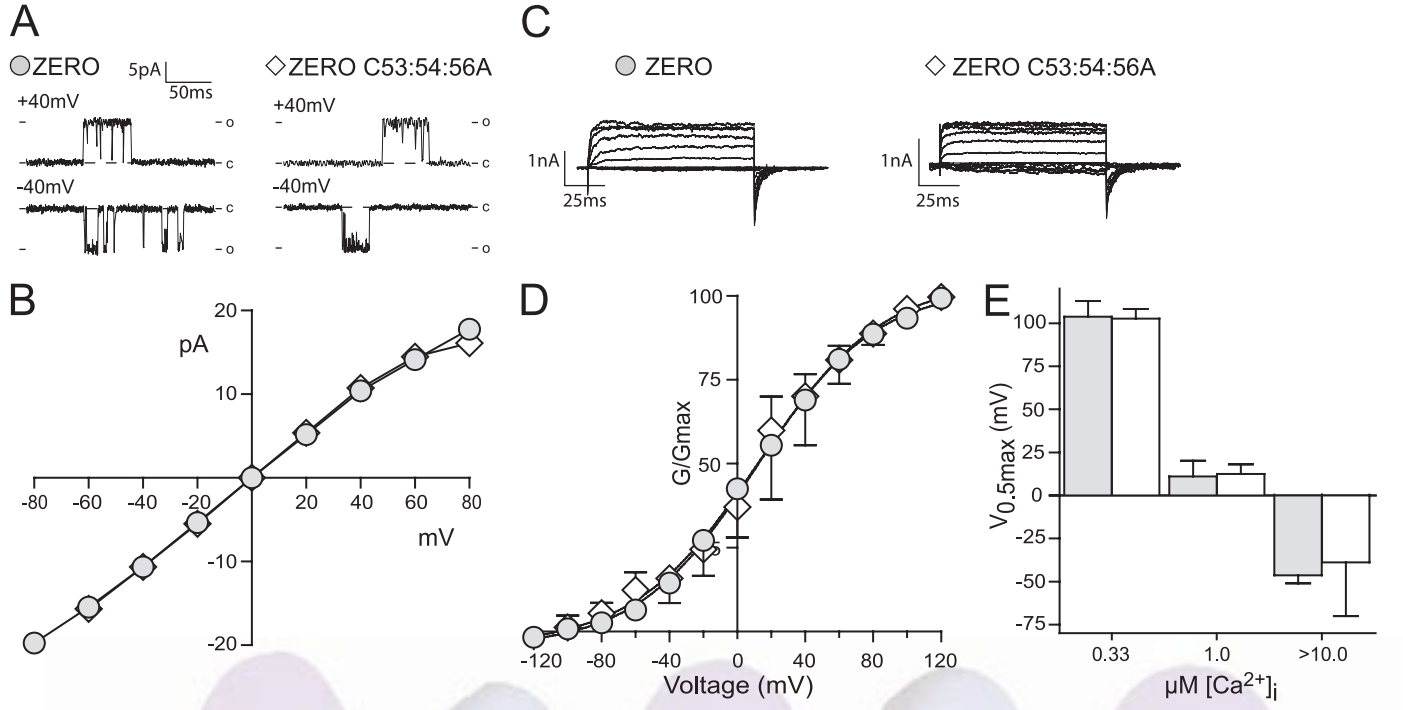

FIGURE 4. **The intrinsic channel properties are un-affected in de-palmitoylated BK channels.** *A*, representative single channel conductance recordings of excised inside-out patches at +40 and −40 mV in 0.33 μM Ca^{2+}. *B*, current (pA) voltage (*V*) plot for ZERO channels (*closed gray circles*, ●) and ZERO C53:54:56A (*diamonds*, ◇), showing that single channel conductance is unaffected in 0.33 μM Ca^{2+} ($n = 3$). *C*, representative macropatch recordings traces showing BK currents in response to a depolarizing voltage step protocol (−120 mV to +120 mV) from a holding potential of −80mV from excised inside-out patch recordings in equimolar potassium gradients and 1 μM free Ca^{2+} (scale bars: 1 pA/25 ms). *D*, G/G_{MAX} conductance curves show no change in channel activation at 1 μM free Ca^{2+} between ZERO (*closed gray circles*, ●) and ZERO C53:54:56A (*diamonds*, ◇). *E*, summary bar graph illustrates no significant changes in $V_{0.5max}$ across the physiological calcium range 0.33–10 μM free calcium. All data are means ± S.E. (n >3).

Activation of BK channels results in membrane hyperpolarization revealed by a decrease in relative fluorescence. We used full-length ZERO variant channels with cysteine mutations in the S0-S1 linker. The peak wild-type ZERO channel response at the 70 s time point was taken as 100%, to which mutant channels could then be compared (Fig. 3*A*). Mutation of the triple (C53:54:56A) cysteine residues within the identified palmitoylation site, significantly attenuated the activation driven by ionomycin of mutant channels by ~60% when compared with the wild-type ZERO channel (Fig. 3*B*). Mutation of individual and double cysteine residues (C53A, C54A, C56A, C53:54A) had no significant effect.

The membrane potential assay cannot discriminate between: shifts in the calcium/voltage sensitivity of the channel; altered channel conductance; or changes in expression of functional channels at the plasma membrane. As the C53:54:56A mutant channel showed the greatest change in membrane potential, palmitoylation incorporation, and in the imaging assays, the functional impact of the ZERO C53:54:56A mutant channel was compared with that of the wild-type ZERO variant channel hereafter.

Single channel slope conductance in excised inside-out patches was unchanged between ZERO and ZERO C53:54:56A channels (ZERO, 231 ± 3.9 pS and ZERO C53:54:56A, 227 ± 5.4 pS) determined in symmetrical potassium gradients (Fig. 4, *A* and *B*). Macropatch recordings over a range of calcium (0.33–10 μM $[Ca^{2+}]_i$) showed no significant difference in the half maximal voltage for activation of the channel (Fig. 4, *C–E*) and voltage dependence of the ZERO C53:54:56A channel was not significantly changed from wild-type ZERO channels (data not shown). These data suggest that neither changes in single channel conductance nor channel voltage and calcium sensitivity underlie the significantly reduced channel activity of the C53:54:56A mutant channels observed in the membrane potential assays. However, we noted that there appeared to be fewer mutant channels (ZERO C53:54:56A channels were reduced by ~70%, $n = 26$) at the plasma membrane compared with wild-type ZERO channels ($n = 12$) in our electrophysiology assays (data not shown). Therefore, we examined cell surface expression of the ZERO channel and the mutant (ZERO C53:54:56A) channel in quantitative immunofluorescence and cell surface biotinylation assays.

Palmitoylation Is an Important Determinant of BK Channel Cell Surface Expression—Mutation of the C53:C54:56 palmitoylation site in the S0-S1 linker of the BK channel might disrupt normal expression at the plasma membrane. Channel constructs were created with extracellular N-terminal FLAG tag epitopes that enabled detection on the extracellular surface of transfected HEK293 cells and with intracellular C-terminal HA tag epitopes, to determine total protein expression. In non-permeabilized cells, ZERO channels could be detected at the plasma membrane however, in the palmitoylation-deficient channels (ZERO C53:54:56A) surface expression was significantly reduced despite total protein expression being unaffected. Quantitative immunofluorescence analysis of N-terminal Flag-tagged ZERO C53:54:56A mutant channels, showed a significant ~55% decrease in cell surface expression in relation to the ZERO channel (Fig. 5, *A* and *B*). A similar reduction in

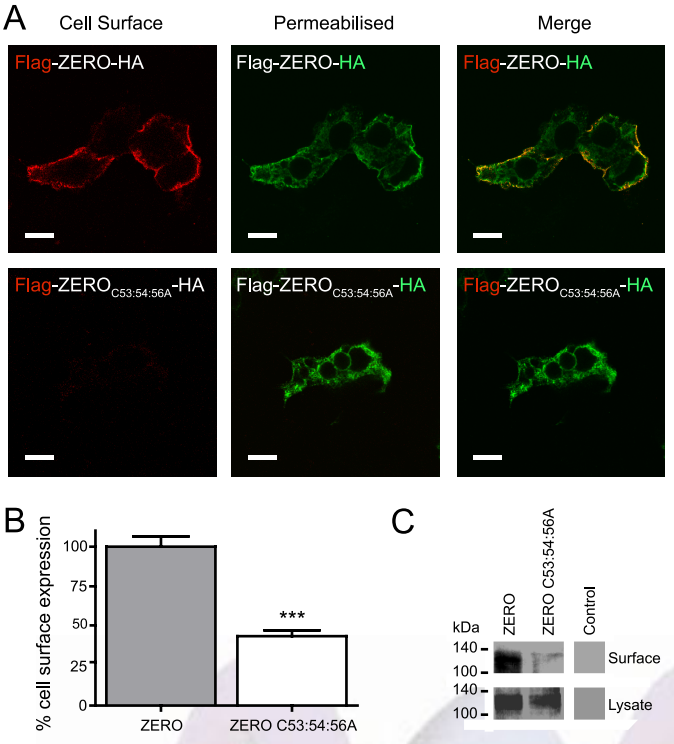

FIGURE 5. **Palmitoylation of the S0-S1 linker regulates cell surface expression of BK channels.** *A*, representative confocal images of HEK293 cells expressing Flag-ZERO-HA (*top panels*), and Flag-ZERO C53:54:56A-HA (*bottom panels*). The extracellular Flag epitope was labeled (*red*) under non-permeabilized conditions (cell surface) with the C-terminal HA epitope tag (*green*) labeled following cell permeabilization. Flag and HA labeling from the same cell are then overlaid (merge) (scale bars: 10 μm). *B*, quantification of cell surface expression between ZERO (*gray bars*) and ZERO C53:54:56A (*white bars*). Data are means ± S.E. ($n > 3$). **, $p < 0.01$, ANOVA with *post hoc* Tukey test compared with Flag-ZERO-HA construct. *C*, representative Western blots of HA immunoreactivity from cell surface biotinylation assays (*top panels*) and corresponding whole cell lysates (*bottom panels*) in HEK293 cells expressing ZERO-HA and ZERO C53:54:56A-HA channels and control mock transfected cells.

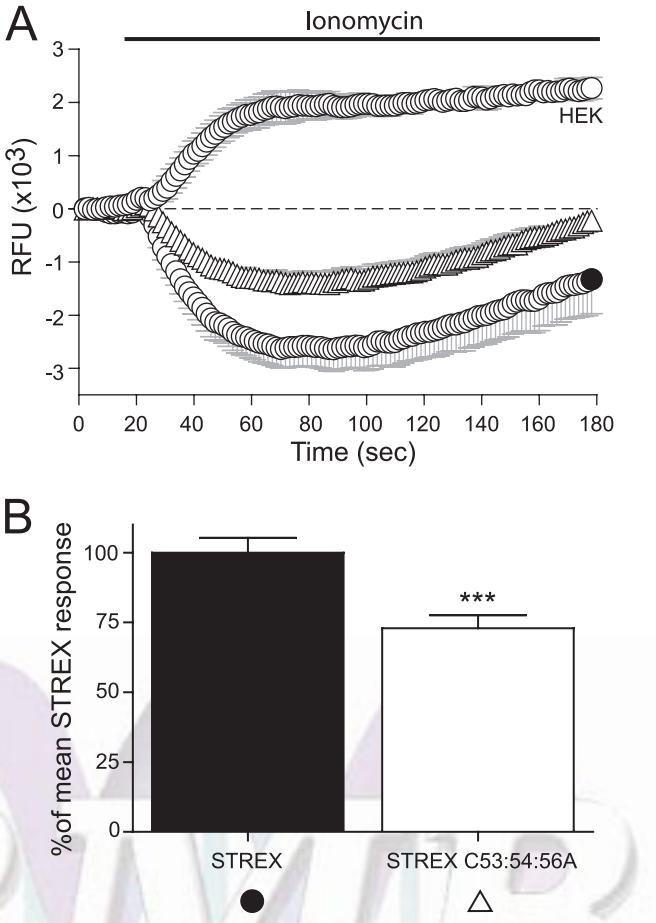

FIGURE 6. **Disruption of the S0-S1 linker palmitoylation site in STREX splice variant channels also attenuates the ionomycin-driven channel activation.** *A*, representative time course plots of mean change in relative fluorescence units (*RFU*) of the FLIPR-blue membrane potential dye in HEK293 cells expressing STREX (*closed black circles*, ●), STREX C53:54:56A (*upright triangles*, △), and mock-transfected HEK293 (*open circles*, ○), in response to calcium influx induced by 1 μM ionomycin. *B*, summary bar chart of the membrane potential change for each construct expressed as a percentage of the maximal hyperpolarization, following subtraction of the HEK293 response, in the STREX (*black*) variant (where the STREX response is normalized to 100%). Data were determined at the maximum hyperpolarizing response in STREX ($t = 70$ s) in the time course plots in *A*. All data are means ± S.E. ($n = 3$, $n > 24$), ***, $p < 0.001$, compared with STREX (ANOVA with Tukey *post hoc* test).

cell surface expression of the C53:54:56A mutant channels was also observed using cell surface biotinylation assays (Fig. 5*C*).

To investigate whether palmitoylation of the S0-S1 linker controls cell surface expression in channels that are also palmitoylated at the distinct C-terminal alternatively spliced STREX insert (16), STREX channels were also examined with mutations in the S0-S1 palmitoylation site. Firstly, we examined the S0-S1 linker mutation (C53:54:56A) in the STREX channel using the membrane-potential assay as before. Mutation of the S0-S1 palmitoylation site in STREX channel showed a ~30% attenuation of the ionomycin-induced activation of the channels, similar to that observed for the ZERO channel (Fig. 6, *A* and *B*). Therefore, to determine whether the S0-S1 linker palmitoylation site also controls cell surface expression of the STREX splice variant of the BK channel quantitative immunofluorescence analysis was performed. N-terminal Flag-tagged STREX C53:54:56A mutant channels also showed a significant reduction in channel surface expression of ~55% when compared with wild-type STREX channels (Fig. 7, *A* and *B*). STREX channels that could not be palmitoylated at the S0-S1 linker (STREX C53:54:56A) could still be palmitoylated via the STREX insert as predicted (Fig. 7*C*). The reduction in cell surface expression was further recapitulated in cell surface biotinylation assays (data not shown). Taken together, these data suggest that the S0-S1 linker palmitoylation site functions independently of the C-terminal palmitoylation site in the STREX insert and that the palmitoylation status of the S0-S1 linker is a critical determinant of cell surface channel expression irrespective of C-terminal splice variation.

DISCUSSION

We have identified an evolutionary conserved palmitoylation site within the intracellular N-terminal S0-S1 linker of BK channels that plays a critical role in the control of channel cell surface expression. Palmitoylation of the S0-S1 linker allowed the association of this N-terminal intracellular domain with the plasma membrane and controlled surface expression even in channel variants that express an additional palmitoylation-dependent membrane association domain (STREX) in the intracellular C terminus of the channel (16). As STREX palmitoyla-

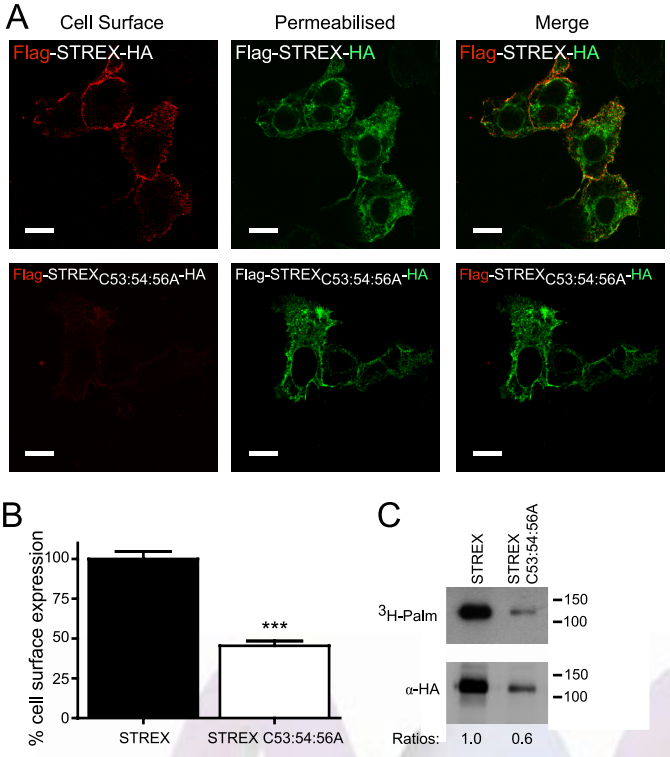

FIGURE 7. **S0-S1 palmitoylation site functions independently of additional STREX splice variant palmitoylation site to control BK channel surface expression.** *A*, representative confocal images of HEK293 cells expressing Flag-STREX-HA (*top panels*), and Flag- STREX C53:54:56A -HA (*bottom panels*). The extracellular Flag epitope was labeled (*red*) under non-permeabilized conditions (cell surface) with the C-terminal HA epitope tag (*green*) labeled following cell permeabilization. Flag and HA labeling from the same cell are then overlaid (merge) (scale bars: 10 μm). *B*, quantification of cell surface expression between STREX (*black bars*) and STREX C53:54:56A (*white bars*). Data are means $\pm$ S.E. (n $>$3). *, $p < 0.05$, ANOVA with *post hoc* Tukey test compared with Flag-STREX-HA construct. *C*, representative fluorographs (*upper*) and Western blots (*lower*) of full-length STREX-HA channels and STREX C53:54:56A channels expressed in HEK293 cells. Constructs were labeled with [^{3}H]palmitate for 4 h and immunoprecipitated (*IP*) by using α-HA magnetic microbeads and detected by fluorography. In this particular experiment protein expression of the two constructs was not equivalent; however, the C53:54:56A mutations do not compromise STREX expression *per se*. These data reveal the residual palmitoylation of the channel mediated via the STREX insert in contrast to the ZERO variant (see Fig. 1). Ratios (normalized to the wild-type STREX channel) of palmitate incorporation relative to total protein expression are included.

tion controls channel regulation by phosphorylation (16), rather than surface expression, as demonstrated here for the S0-S1 linker, our work demonstrates functionally distinct palmitoylation-dependent membrane interaction domains within the same channel protein.

The identified triple cysteine palmitoylation residues in the S0-S1 linker (C53:54:56) are conserved across the vertebrate phylum and are largely conserved in *Drosophila* and *C. elegans*, suggesting evolutionary retention of a functionally important region. This site would therefore be present in all functionally expressed BK channel proteins and is not predicted to be excluded by alternative splicing events. Indeed, proteomic screens identified BK channels as palmitoylated in the adult rat brain (17), a tissue in which the only other known site for BK channel palmitoylation is located within the STREX insert, which is expressed at relatively low levels. As protein palmitoylation is a highly dynamic and reversible process this would suggest that palmitoylation of the S0-S1 linker may be an important determinant in controlling BK channel cell surface expression under different physiological demands. For example, cell surface expression of BK channels is modified in aging coronary arteries (31), in smooth muscle cells of the uterus during pregnancy (32), colonic epithelia in response to aldosterone (33), and during malignant glioma tumor cell proliferation (9). While multiple mechanisms may control steady state surface expression the control of BK channel expression at the plasma membrane by palmitoylation may be an important determinant of a wide range of physiological functions.

Palmitoylation of the S0-S1 linker could modulate surface expression by multiple mechanisms including: (i) facilitation of channel assembly or ER export, (ii) stabilization at the plasma membrane, (iii) reduced retrieval from the plasma membrane, (iv) increased recycling, or (v) reduced channel degradation. Examination of the role of palmitoylation in each of these mechanisms warrants further investigation. Importantly, the S0-S1 linker *per se* appears to play an important role in controlling channel cell surface expression as revealed from analysis of alternative splice variants that may be included in this region. For example, a human splice variant of the BK channel called mk44, introduces a 44 amino acid sequence immediately downstream of the C53:C54:C56 palmitoylation site in the S0-S1 intracellular linker (34). This mk44 splice variant introduces a motif for endoproteolytic digestion and a site for *N*-myristoylation. *N*-Myristoylation of mk44 results in trapping of the channel in the ER. However, endoproteolytic cleavage allows the S0 transmembrane domain to traffic independently of the rest of the transmembrane and C-terminal domain of the channel to the plasma membrane (34). Another splice variant in the human BK channel, SV1, has been implicated in ER retention. The SV1 splice variant introduces 33 amino acids to the end of the S0-S1 linker introducing an ER retention-retrieval motif, CVLF (35). Although inclusion of these splice variants is not predicted, using the CSS-Palm algorithm, to significantly reduce palmitoylation of the C53:54:56 site,[4] whether these inserts disrupt palmitoylation of S0-S1 linker or its functional regulation of channel cell surface expression remains to be explored. The S0 transmembrane domain of BK channels is also an important determinant of BK channel α-subunit assembly with the regulatory β-subunits (36–40). Indeed, recent structural studies examining intra-α subunit di-sulfide cross-linking has demonstrated that the S0 transmembrane domain is located outside of the voltage sensing S1-S4 domains (36) and can form a major contact with the transmembrane domain 2 (TM2) of regulatory β1 (36) and β4 (40) subunits. Co-expression studies have also suggested a role for β-subunits in controlling BK channel cell surface expression. Indeed, β1-subunits have been suggested to decrease surface expression (41), and the β2-subunit also appears to modulate BK surface expression via a similar mechanism (42). Therefore, increasing evidence supports an important role for the S0-S1 linker and surrounding transmembrane domains in controlling BK channel cell surface expression.

[4] O. Jeffries and M. J. Shipston, unpublished data.

Palmitoylation of the BK S0-S1 Linker

Palmitoylation of the S0-S1 linker had no significant effect on the intrinsic single channel conductance or calcium/voltage sensitivity of BK channels. Moreover, mutation of the S0-S1 linker cysteines C53:54:56 to alanine also reduced cell surface expression of the STREX variant of the BK channel. We have previously demonstrated that the C terminus alternatively spliced STREX insert is palmitoylated and targets the STREX insert to the plasma membrane (16). Palmitoylation status of the STREX insert has no significant effect on channel cell surface expression however, it affects the calcium/voltage sensitivity of the channel and more importantly determines whether the STREX channel is inhibited by protein kinase A (PKA)-dependent phosphorylation (16). In the latter case, PKA phosphorylation dissociates the STREX domain from the plasma membrane through phosphorylation of an upstream serine residue. In contrast, phosphomimetic or phosphornull mutations of the S0-S1 linker at a tandem serine motif, shown to be phosphorylated *in vivo* (30), immediately downstream of the palmitoylated cysteine residues, have no effect of S0-S1 linker interaction with the plasma membrane. Taken together, these data demonstrate that BK channels may express two functionally distinct palmitoylation-dependent membrane interaction domains: the C-terminal alternatively spliced STREX insert and the constitutively expressed S0-S1 linker. The distinct functional consequence of the palmitoylation status of these two separate palmitoylated domains within the same channel protein also suggests that palmitoylation of S0-S1 and STREX may be independently regulated.

Acknowledgments—We thank Trudi Gillespie and the IMPACT imaging facility for assistance in confocal imaging assays.

REFERENCES

1. Raffaelli, G., Saviane, C., Mohajerani, M. H., Pedarzani, P., and Cherubini, E. (2004) *J. Physiol.* **557,** 147–157
2. Sausbier, M., Hu, H., Arntz, C., Feil, S., Kamm, S., Adelsberger, H., Sausbier, U., Sailer, C. A., Feil, R., Hofmann, F., Korth, M., Shipston, M. J., Knaus, H. G., Wolfer, D. P., Pedroarena, C. M., Storm, J. F., and Ruth, P. (2004) *Proc. Natl. Acad. Sci. U.S.A.* **101,** 9474–9478
3. Brenner, R., Peréz, G. J., Bonev, A. D., Eckman, D. M., Kosek, J. C., Wiler, S. W., Patterson, A. J., Nelson, M. T., and Aldrich, R. W. (2000) *Nature* **407,** 870–876
4. Sausbier, M., Arntz, C., Bucurenciu, I., Zhao, H., Zhou, X. B., Sausbier, U., Feil, S., Kamm, S., Essin, K., Sailer, C. A., Abdullah, U., Krippeit-Drews, P., Feil, R., Hofmann, F., Knaus, H. G., Kenyon, C., Shipston, M. J., Storm, J. F., Neuhuber, W., Korth, M., Schubert, R., Gollasch, M., and Ruth, P. (2005) *Circulation* **112,** 60–68
5. Brenner, R., Chen, Q. H., Vilaythong, A., Toney, G. M., Noebels, J. L., and Aldrich, R. W. (2005) *Nat. Neurosci.* **8,** 1752–1759
6. Du, W., Bautista, J. F., Yang, H., Diez-Sampedro, A., You, S. A., Wang, L., Kotagal, P., Lüders, H. O., Shi, J., Cui, J., Richerson, G. B., and Wang, Q. K. (2005) *Nat. Genet.* **37,** 733–738
7. Meredith, A. L., Thorneloe, K. S., Werner, M. E., Nelson, M. T., and Aldrich, R. W. (2004) *J. Biol. Chem.* **279,** 36746–36752
8. Bloch, M., Ousingsawat, J., Simon, R., Schraml, P., Gasser, T. C., Mihatsch, M. J., Kunzelmann, K., and Bubendorf, L. (2007) *Oncogene* **26,** 2525–2534
9. Weaver, A. K., Liu, X., and Sontheimer, H. (2004) *J. Neurosci. Res.* **78,** 224–234
10. Butler, A., Tsunoda, S., McCobb, D. P., Wei, A., and Salkoff, L. (1993) *Science* **261,** 221–224
11. Tian, L., Chen, L., McClafferty, H., Sailer, C. A., Ruth, P., Knaus, H. G., and Shipston, M. J. (2006) *Faseb. J.* **20,** 2588–2590
12. Shipston, M. J. (2001) *Trends Cell Biol.* **11,** 353–358
13. Tian, L., Duncan, R. R., Hammond, M. S., Coghill, L. S., Wen, H., Rusinova, R., Clark, A. G., Levitan, I. B., and Shipston, M. J. (2001) *J. Biol. Chem.* **276,** 7717–7720
14. Xie, J., and McCobb, D. P. (1998) *Science* **280,** 443–446
15. Tian, L., Coghill, L. S., McClafferty, H., MacDonald, S. H., Antoni, F. A., Ruth, P., Knaus, H. G., and Shipston, M. J. (2004) *Proc. Natl. Acad. Sci. U.S.A.* **101,** 11897–11902
16. Tian, L., Jeffries, O., McClafferty, H., Molyvdas, A., Rowe, I. C., Saleem, F., Chen, L., Greaves, J., Chamberlain, L. H., Knaus, H. G., Ruth, P., and Shipston, M. J. (2008) *Proc. Natl. Acad. Sci. U.S.A.* **105,** 21006–21011
17. Kang, R., Wan, J., Arstikaitis, P., Takahashi, H., Huang, K., Bailey, A. O., Thompson, J. X., Roth, A. F., Drisdel, R. C., Mastro, R., Green, W. N., Yates, J. R., 3rd, Davis, N. G., and El-Husseini, A. (2008) *Nature* **456,** 904–909
18. MacDonald, S. H., Ruth, P., Knaus, H. G., and Shipston, M. J. (2006) *BMC Dev. Biol.* **6,** 37
19. Ren, J., Wen, L., Gao, X., Jin, C., Xue, Y., and Yao, X. (2008) *Protein Eng. Des. Sel.* **21,** 639–644
20. Zhou, F., Xue, Y., Yao, X., and Xu, Y. (2006) *Bioinformatics* **22,** 894–896
21. Fukata, Y., Iwanaga, T., and Fukata, M. (2006) *Methods* **40,** 177–182
22. Gubitosi-Klug, R. A., Mancuso, D. J., and Gross, R. W. (2005) *Proc. Natl. Acad. Sci. U.S.A.* **102,** 5964–5968
23. Pickering, D. S., Taverna, F. A., Salter, M. W., and Hampson, D. R. (1995) *Proc. Natl. Acad. Sci. U.S.A.* **92,** 12090–12094
24. Schmidt, J. W., and Catterall, W. A. (1987) *J. Biol. Chem.* **262,** 13713–13723
25. Rathenberg, J., Kittler, J. T., and Moss, S. J. (2004) *Mol. Cell Neurosci.* **26,** 251–257
26. Hayashi, T., Thomas, G. M., and Huganir, R. L. (2009) *Neuron* **64,** 213–226
27. Hayashi, T., Rumbaugh, G., and Huganir, R. L. (2005) *Neuron* **47,** 709–723
28. Chen, L., Tian, L., MacDonald, S. H., McClafferty, H., Hammond, M. S., Huibant, J. M., Ruth, P., Knaus, H. G., and Shipston, M. J. (2005) *J. Biol. Chem.* **280,** 33599–33609
29. Saleem, F., Rowe, I. C., and Shipston, M. J. (2009) *Br. J. Pharmacol.* **156,** 143–152
30. Yan, J., Olsen, J. V., Park, K. S., Li, W., Bildl, W., Schulte, U., Aldrich, R. W., Fakler, B., and Trimmer, J. S. (2008) *Mol. Cell Proteomics* **7,** 2188–2198
31. Marijic, J., Li, Q., Song, M., Nishimaru, K., Stefani, E., and Toro, L. (2001) *Circ. Res.* **88,** 210–216
32. Song, M., Zhu, N., Olcese, R., Barila, B., Toro, L., and Stefani, E. (1999) *FEBS Lett.* **460,** 427–432
33. Sørensen, M. V., Matos, J. E., Sausbier, M., Sausbier, U., Ruth, P., Praetorius, H. A., and Leipziger, J. (2008) *J. Physiol.* **586,** 4251–4264
34. Korovkina, V. P., Fergus, D. J., Holdiman, A. J., and England, S. K. (2001) *Am. J. Physiol. Cell Physiol.* **281,** C361–C367
35. Zarei, M. M., Eghbali, M., Alioua, A., Song, M., Knaus, H. G., Stefani, E., and Toro, L. (2004) *Proc. Natl. Acad. Sci. U.S.A.* **101,** 10072–10077
36. Liu, G., Niu, X., Wu, R. S., Chudasama, N., Yao, Y., Jin, X., Weinberg, R., Zakharov, S. I., Motoike, H., Marx, S. O., and Karlin, A. (2010) *J. Gen. Physiol.* **135,** 449–459
37. Liu, G., Zakharov, S. I., Yang, L., Deng, S. X., Landry, D. W., Karlin, A., and Marx, S. O. (2008) *J. Gen. Physiol.* **131,** 537–548
38. Meera, P., Wallner, M., Song, M., and Toro, L. (1997) *Proc. Natl. Acad. Sci. U.S.A.* **94,** 14066–14071
39. Wallner, M., Meera, P., and Toro, L. (1996) *Proc. Natl. Acad. Sci. U.S.A.* **93,** 14922–14927
40. Wu, R. S., Chudasama, N., Zakharov, S. I., Doshi, D., Motoike, H., Liu, G., Yao, Y., Niu, X., Deng, S. X., Landry, D. W., Karlin, A., and Marx, S. O. (2009) *J. Neurosci.* **29,** 8321–8328
41. Toro, B., Cox, N., Wilson, R. J., Garrido-Sanabria, E., Stefani, E., Toro, L., and Zarei, M. M. (2006) *Neuroscience* **142,** 661–669
42. Zarei, M. M., Song, M., Wilson, R. J., Cox, N., Colom, L. V., Knaus, H. G., Stefani, E., and Toro, L. (2007) *Neuroscience* **147,** 80–89